

Technical Report

TR-01-11

Project Deep Drilling KLX02 – Phase 2

Methods, scope of activities and results Summary report

Compiled by Lennart Ekman
GEOSIGMA AB/LE Geokonsult AB

April 2001

Svensk Kärnbränslehantering AB

Swedish Nuclear Fuel
and Waste Management Co
Box 5864
SE-102 40 Stockholm Sweden
Tel 08-459 84 00
+46 8 459 84 00
Fax 08-661 57 19
+46 8 661 57 19



Project Deep Drilling KLX02 – Phase 2

Methods, scope of activities and results Summary report

Compiled by Lennart Ekman
GEOSIGMA AB/LE Geokonsult AB

April 2001

Keywords: deep drilling, core borehole, borehole investigations, geoscientific parameters.

This report concerns a study which was conducted for SKB. The conclusions and viewpoints presented in the report are those of the author(s) and do not necessarily coincide with those of the client.

Foreword

During the autumn 1992 a 1700 m deep, \varnothing 76 mm core borehole was drilled at Laxemar, Oskarshamn, south-eastern Sweden. At the time being, this was the deepest core borehole drilled in crystalline rock in Scandinavia. The aim of the borehole was to test drilling technique and to enable investigations of the bedrock beyond 1000 m, which was the approximate depth limit in SKB's previous geoscientific investigations. Two extensive borehole investigation programs were applied. A preliminary survey during and immediately after the drilling operations was succeeded by a five year period of extended investigations. The two investigation programs, named Phase 1 respectively Phase 2 of Project Deep Drilling KLX02, resulted in a large number of reports. The purpose of the present report is to provide a summary of the investigations performed in borehole KLX02 during Phase 2. In order to make different geoscientific conditions within the Laxemar area more understandable, selected results from Phase 1 and from geoscientific investigations previously (before Phase 1) and later (after Phase 2) performed within the Laxemar area are also presented.

Lennart Ekman, LE Geokonsult (previously GEOSIGMA), was main author and editor of the report, Jan-Erik Ludvigson, GEOSIGMA, wrote Chapter 6 and Marcus Laaksuharju, GeoPoint (previously INTERA), was co-writer of Chapter 7.

Uppsala April 2001

Lennart Ekman

Abstract

Geoscientific investigations performed by SKB, including those at the Äspö Hard Rock Laboratory, have so far comprised the bedrock horizon down to about 1000 m. The primary purposes with the c. 1700 m deep, \varnothing 76 mm, subvertical core borehole KLX02, drilled during the autumn 1992 at Laxemar, Oskarshamn, south-eastern Sweden, was to test core drilling technique at large depths and with a relatively large diameter and to enable geoscientific investigations beyond 1000 m. Drilling of borehole KLX02 was fulfilled very successfully. Results of the drilling commission and the borehole investigations conducted in conjunction with drilling have been reported earlier.

The present report provides a summary of the investigations made during a five year period after completion of drilling. Results as well as methods applied are described. A variety of geoscientific investigations to depths exceeding 1600 m were successfully performed. However, the investigations were not entirely problem-free. For example, borehole equipment got stuck in the borehole at a several occasions. Special investigations, among them a fracture study, were initiated in order to reveal the mechanisms behind this problem. Different explanations seem possible, e.g. breakouts from the borehole wall, which may be a specific problem related to the stress situation in deep boreholes.

The investigation approach for borehole KLX02 followed, in general outline, the SKB model for site investigations, where a number of key issues for site characterization are studied. For each of those, a number of geoscientific parameters are investigated and determined. One important aim is to erect a lithological-structural model of the site, which constitutes the basic requirement for modelling mechanical stability, thermal properties, groundwater flow, groundwater chemistry and transport of solutes.

The investigations in borehole KLX02 resulted in a thorough lithological-structural characterization of the rock volume near the borehole. In order to attain a structural model valid for larger volumes of rock, different authors also included some results covering investigations performed in other parts of the Laxemar area.

Rock mechanical investigations were conducted to depths exceeding 1300 m and the normal, horizontal and vertical stress magnitudes and orientations were determined as functions with depth. In connection with the stress measurements, a hydromechanical study was performed. By temperature logging of the water column in the borehole, also thermal properties of the bedrock were, to some extent, studied.

A hydrogeological test programme was applied, including single-hole measurements in borehole KLX02 as well as an interference test between this borehole and another deep (1078 m) borehole, KLX01, in the Laxemar area.

Finally, extensive hydrogeochemical investigations were performed in borehole KLX02. Ensuing from advanced sampling, analysis and evaluation technique, the groundwater prevailing at different depths in and near the borehole was characterized regarding composition and evolution. For a better understanding of prevailing hydrogeochemical conditions in KLX02, also the flow regime in the open borehole was studied.

Abstract (in Swedish)

SKBs geovetenskapliga undersökningar, inklusive de vid Äspölaboratoriet, har i huvudsak avsett djup ner till en tänkt förvarsnivå vid ca 500 m. Ett fåtal undersökningsborrhål har nått drygt 1000 m. De viktigaste syftena med det ca 1700 m djupa, nästan vertikala kärnborrhålet KLX02, som under hösten 1992 borrades vid Laxemar, Oskarshamns kommun, var att möjliggöra geovetenskapliga undersökningar och test av borrhålsinstrument till större djup än 1000 m. Ett annat syfte var att undersöka möjligheterna att med befintlig kärnborrningsteknik utföra kärnborrhål med relativt grov diameter, \varnothing 76 mm, till större djup än 1000 m. Borrningsentreprenaden, som genomfördes mycket framgångsrikt, jämte borrhålsundersökningar utförda under borrningsfasen har tidigare avrapporterats.

I föreliggande rapport sammanfattas det undersökningsprogram som genomfördes under en femårsperiod efter avslutad borrning. Såväl metoder som resultat redovisas. Ett stort antal geovetenskapliga undersökningar till mer än 1600 m djup genomfördes framgångsrikt. Vissa problem uppkom dock. Exempelvis fastnade borrhålsutrustning i borrhålet vid olika tillfällen. Speciella undersökningar utfördes för att utröna orsaken till detta. Flera förklaringar är möjliga, t.ex. utfall från borrhålsväggen, vilket kan vara ett speciellt problem relaterat till spänningssituationen i djupa borrhål.

Undersökningsprogrammet följde i stora drag det koncept som SKB upprättat för platsundersökningar, där fokus inriktas på ett antal nyckelfaktorer. Var och en av dessa innefattar flera geovetenskapliga parametrar. Parameterbestämningen leder fram till en geovetenskaplig karaktärisering av undersökningsplatsen. I ett tidigt skede upprättas en litologisk-strukturgeologisk modell, som utgör huvudverktyget vid senare modellering av mekanisk stabilitet, termiska egenskaper, grundvattenflöde, grundvattenkemi och transport av lösta ämnen.

Undersökningarna i KLX02 resulterade i en noggrann litologisk och strukturgeologisk karaktärisering av bergvolymen närmast borrhålet. Genom att anknyta till undersökningar utförda i andra delar av Laxemarområdet har några författare gjort försök att upprätta preliminära strukturgeologiska modeller som innefattar en stor del av Laxemarområdet. Dessa modeller skiljer sig i vissa avseenden från varandra, främst beroende på vilket bakgrundsmaterial som varit tillgängligt vid olika tidpunkter.

Bergmekaniska mätningar utfördes i KLX02 till mer än 1300 m djup, varvid storleken liksom orienteringarna på normal-, horisontal- och vertikalspänningarna kunde bestämmas som funktioner mot djupet. I samband med spänningsmätningarna utfördes hydro-mekanisk sprickkaraktärisering. Genom temperaturloggning av vattenpelaren i borrhålet erhöles även viss kunskap om bergets termala förhållanden.

Det hydrogeologiska testprogram som applicerades i borrhål KLX02 omfattade såväl enhålsmätningar som en interferenstest mellan KLX02 och ett annat djupt (1078 m) borrhål, KLX01, i Laxemarområdet.

Slutligen utfördes omfattande hydrogeokemiska undersökningar, varvid grundvattnet på olika djup karaktäriserades med avseende på sammansättning och utvecklingshistoria. För att uppnå bättre förståelse av de hydrogeokemiska förhållandena i KLX02 undersöktes även flödesregimen i borrhålet.

Contents

1	Introduction	9
1.1	Background	9
1.2	The Laxemar area	11
1.3	Investigation programme and reporting	13
2	Sequence of activities and project organization	15
2.1	Sequence of activities	15
2.2	Project organization	15
3	Geology	19
3.1	Introduction	19
3.2	Regional and local geological setting	20
	3.2.1 Lithological conditions	20
	3.2.2 Deformation	22
3.3	Geological investigations in the Laxemar area during Phase 2	24
	3.3.1 Borehole design	25
	3.3.2 Petrological classification of drill cuttings	28
	3.3.3 Examination of thin sections	29
	3.3.4 Core logging	32
	3.3.5 Fission track studies	35
	3.3.6 Geophysical logging	38
	3.3.7 TV-logging	39
	3.3.8 Borehole radar measurements	40
	3.3.9 Summary of the geological conditions in connection with borehole KLX02	45
3.4	The structural character of the Laxemar area – studies performed during and after Phase 2	50
	3.4.1 Study of lineaments	50
	3.4.2 Correlation of radar reflectors between boreholes KLX01 and KLX02	57
	3.4.3 Interpretation of the connection between fractured sections in boreholes KLX01 and KLX02 and lineaments in the Laxemar-Simpevarp-Äspö area	62
	3.4.4 Method tests – ground geophysics	66
	3.4.5 Reflection seismics and VSP (Vertical Seismic Profiling)	69
4	Rock mechanics	73
4.1	Introduction	73
4.2	Rock stress measurements in borehole KLX02	74
	4.2.1 Background	74
	4.2.2 Measurement principles and scope of investigations	74
	4.2.3 Instrumentation	76
	4.2.4 Results	78
	4.2.5 Comments on the results	83
	4.2.6 Comparison with hydrofracturing stress measurements in boreholes KAS02 and KAS03 on Äspö	87

4.3	Hydromechanical characterization	90
4.3.1	Introduction	90
4.3.2	New development of the hydraulic fracturing equipment	91
4.3.3	Overview of field tests	92
4.3.4	Evaluation of <i>in situ</i> hydraulic and hydromechanical properties of rock fractures	94
4.3.5	Influence of fracture properties on the evaluation of stress from hydrofracturing	99
4.4	Borehole stability – investigation of fracture orientations in selected parts of KLX02 and comparison with fracture data from core boreholes on Äspö and preliminary investigations of borehole breakouts	101
4.4.1	Methods and scope of activities	101
4.4.2	Results	103
4.4.3	Discussion	110
4.4.4	Borehole breakouts	115
5	Thermal properties	117
5.1	Introduction	117
5.2	Thermal investigations at Laxemar	117
5.2.1	The thermal properties of the rock	117
5.2.2	Temperatures	118
6	Hydrogeology	121
6.1	Introduction	121
6.2	Hydraulic tests in borehole KLX02	122
6.2.1	Background	122
6.2.2	Objectives and Scope of Activities	122
6.2.3	Results	128
6.2.4	Hydraulic responses between KLX02 and KLX01 in relation to geological structures	133
7	Groundwater chemistry	135
7.1	Introduction	135
7.2	Sampling of groundwater and calcite fracture fillings in borehole KLX02	136
7.2.1	Objectives	136
7.2.2	Sampling in borehole KLX02	136
7.3	Analytical procedures	141
7.4	Representativity of groundwater samples	142
7.5	Results	143
7.5.1	Scatter plots	143
7.5.2	M3 groundwater modelling	143
7.6	Conclusions	148
7.7	Investigation of the flow regime in borehole KLX02	151
	Executive summary	159
	Acknowledgements	171
	References	173
	Appendices 1–3	181

1 Introduction

1.1 Background

A 1700.5 m long, near vertical, \varnothing 76 mm core borehole, KLX02, was drilled during the autumn 1992 at Laxemar, close to the nuclear power plant at Simpevarp, Oskarshamn, south-eastern Sweden (see overview map, Figure 1-1). The main objects of the drilling project, which was conducted by the Swedish Nuclear Fuel and Waste Management Co, SKB, was to test core drilling technique for \varnothing 76 mm to large depths and to enable investigations of several geoscientific parameters at larger depths than had been possible earlier in core drilled boreholes. Prior to drilling of borehole KLX02, borehole investigations performed by SKB were in general limited to maximally c. 1000 m. This restriction included the studies connected with pre-investigations, construction and performance of the Äspö Hard Rock Laboratory (Äspö HRL), situated close to Laxemar, see Figure 1-1. The most important of the parameters investigated in KLX02 were rock composition and structures, rock mechanical and hydromechanical parameters, hydrogeological conditions, groundwater flow paths near and at some distance from the borehole, and groundwater composition.

The length of borehole KLX02, 1700.5 m, corresponding to a vertical depth of about 1660 m, demanded special efforts during drilling and regarding the borehole investigations conducted subsequent to the drilling activities. Different types of down-hole equipment had to be adapted to the greater depths. The existence of borehole KLX02 also opened the prospect of testing down-hole technique in general for more extreme depths than before.

Borehole KLX02 also provided, and still provides, excellent possibilities for special geoscientific studies related to the unique depth for core drilled boreholes in crystalline bedrock. For example, rock stress measurements and hydro-mechanical experiments were performed in the borehole at depths exceeding all previous investigations in crystalline rock in Sweden, hence augmenting these topics with new and interesting information. Groundwater was sampled in KLX02 deeper than ever before in a cored borehole in Swedish crystalline rock, borehole radar measurements were performed to greater depths than before etc. However, the investigation programme designed for KLX02, which in general outline was implemented prior to drilling, and later on settled more in detail, was not focused primarily on studies of a very special sighting. Instead, such investigations were stressed, which provide information needed to accomplish a thorough geoscientific characterization of and a safety analysis for a site aimed as a future deep repository for spent nuclear fuel or other long-lived waste material.

Geoscientific parameters required for a site characterization have been identified in previous studies. For example, in /1-1/ the significance of geoscientific information for a deep repository is stated. The aim of /1-1/ is to describe how geoscientific properties and conditions in one way or the other are related to the safety aspects of the repository, to the construction and to the fundamental

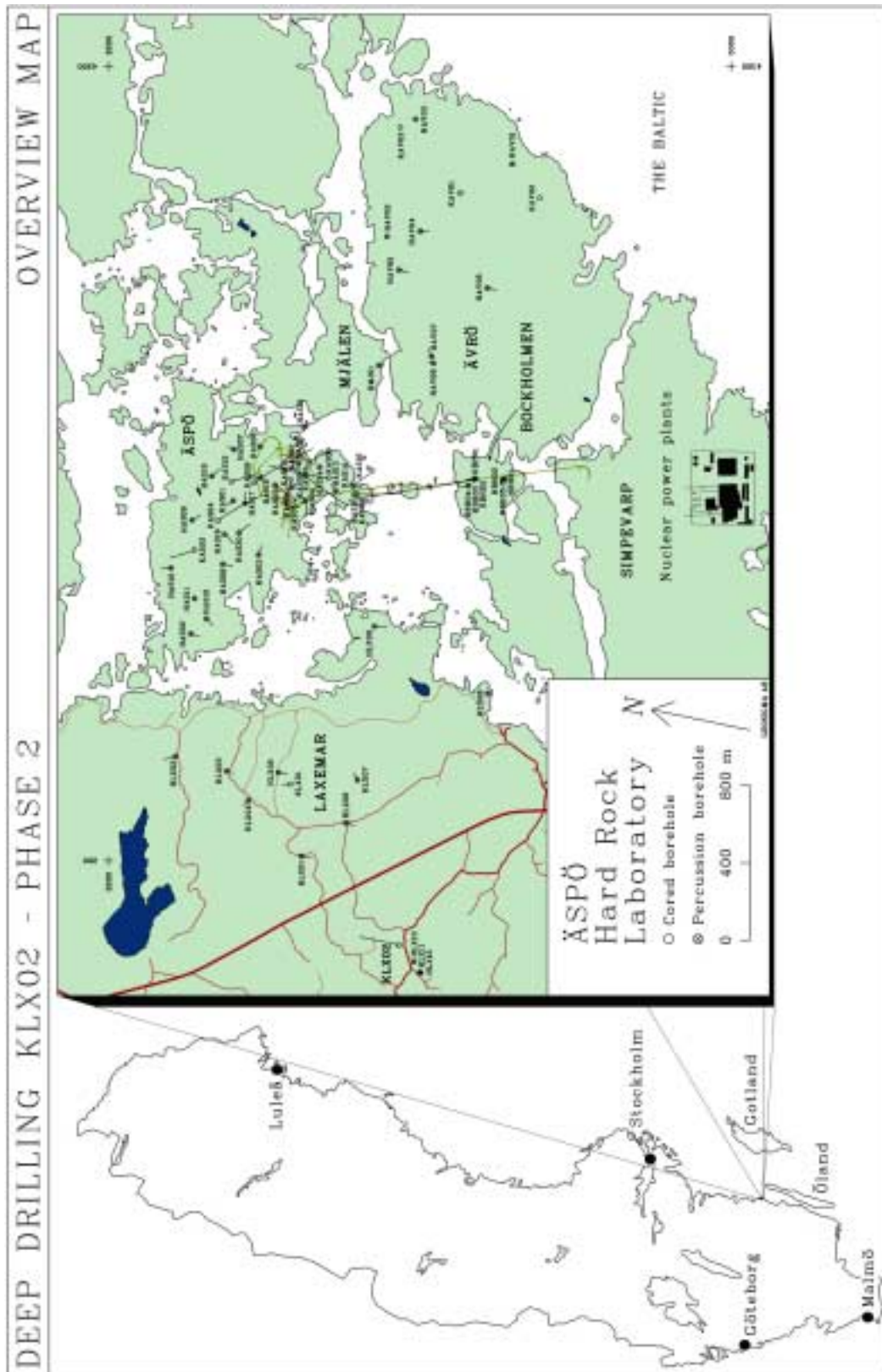


Figure 1-1. Overview of the Äspö Hard Rock Laboratory (Äspö HRL) site, including the Simpevarp area to the south and the Laxemar area to the west. The investigation boreholes drilled from the ground surface and the Äspö HRL tunnel are marked in the figure.

geoscientific comprehension. Although /1-1/ was not yet published at the commencement of the investigations in borehole KLX02, the framework for geoscientific investigations outlined by SKB since many years, and systematically described in /1-1/, served as a platform for the investigation programme applied for borehole KLX02. Six geoscientific parameters are in /1-1/ indicated as key issues for site characterization:

- Geology.
- Rock mechanics – mechanical stability.
- Thermal properties.
- Hydrogeology.
- Chemistry.
- Retention properties – radionuclide transport.

Investigations of retention properties have so far not been conducted in borehole KLX02. Otherwise, the investigations followed this structure, at least in rough outline. In the present report, one chapter is devoted to each of the five first items listed above. Each chapter includes an introduction, based mainly on /1-1/, with a brief outline of the parameters needed, methods for parameter identification and domains of parameter application.

The investigations performed in borehole KLX02 are in this report identified as “Project Deep Drilling KLX02 – Phase 2”. Within the frame of this project it has not been possible to fulfil all requirements for a site characterization. Considering the circumstance that (in principle) only one borehole was included in the study, this fact must be regarded as quite comprehensible. On the other hand, some special studies scoped beyond investigations for an ordinary site characterization.

Although heavily focused on Project Deep Drilling KLX02 – Phase 2, the investigation results presented in this report are not completely restricted to this project. In order to enhance the understanding of certain geoscientific conditions within the Laxemar area, for example regarding structural setting and hydro-geological character, selected results from investigations in borehole KLX02 as well as in other parts of the Laxemar area performed prior to and after Phase 2 are also included in the report.

1.2 The Laxemar area

The Laxemar area constitutes the mainland immediately to the west alongside the island of Äspö, see Figure 1-2. The predominant rock type is a medium-grained, reddish grey granitoid belonging to the Transscandinavian Igneous Belt (TIB). A large share of the bedrock is exposed. Moraine and peat are the dominating soils. The topography is slightly more accentuated compared to the conditions at Äspö with adjacent islands. The altitude slightly exceeds 22 m.a.s.l. in the southern part. Trenches divide the area into blocks.

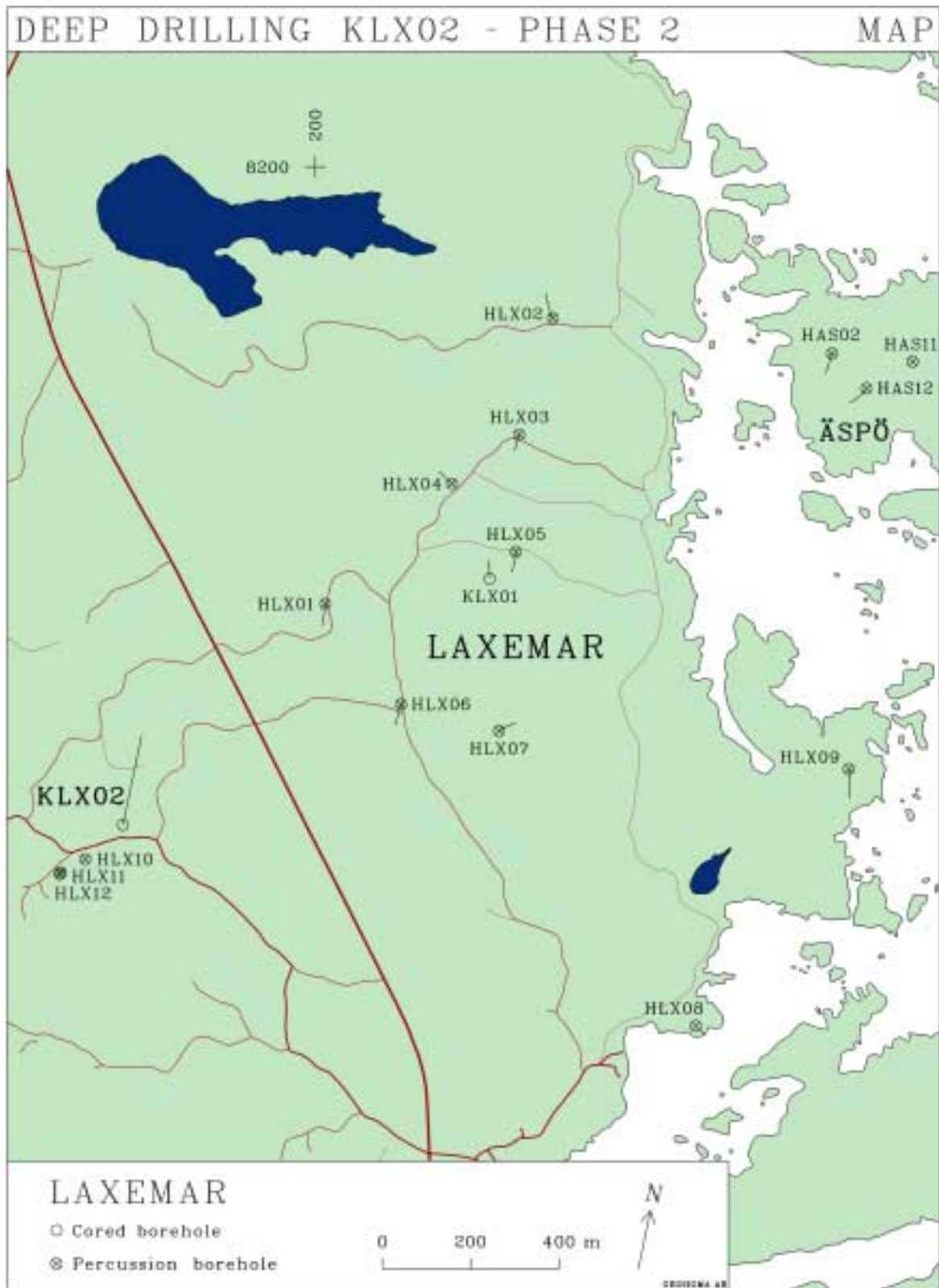


Figure 1-2. Overview of the Laxemar area with the location of investigation boreholes.

The drilling of KLX02, performed during the autumn 1992, was preceded by drilling of another cored borehole, KLX01, within the Laxemar area, the length of which reached 703 m at a first drilling effort in 1988. This borehole, situated about 1 km NE of borehole KLX02, see Figure 1-2, was in 1990 deepened to 1078 m. Hence, since 1992 two deep cored boreholes exist at Laxemar within a limited area, a fact which was used for structural and hydraulic correlation studies, see Chapters 3 and 6. Furthermore, twelve percussion drilled boreholes, HLX01-12, were produced within the Laxemar area to serve as flushwater wells during drilling of the core boreholes respectively as observation wells for long-term groundwater level studies. Some of those boreholes were drilled during the first drilling campaign in 1987, two in 1991, and three boreholes during a third campaign in 1992. Geometrical and administrative data for all SKB boreholes situated within the Laxemar area are presented in Appendix 1.

1.3 Investigation programme and reporting

Drilling of the new deep core borehole, denominated KLX02, was completed with a minimum of technical difficulties. The total length of the borehole became 1700.5 m. During the drilling process, a programme for geoscientific examinations and measurements in the borehole was accomplished, e.g. sampling of drill cuttings, registration of drilling parameters, deviation control, several types of hydraulic tests and groundwater sampling. The drilling activities with accompanying investigations, terminated in 1993, have been referred to as Phase 1 of Project Deep Drilling KLX02. The scope of activities and the results obtained within the frame of Phase 1 were reported 1994 in /1-2/.

After completion of Phase 1, a new research programme, “Project Deep Drilling KLX02 – Phase 2”, was initiated in 1993. The field activities included were in progress during the period 1993–early 1998. Several Technical Reports, Progress Reports, articles and other papers scoping a variety of topics were produced during the period of investigations. The present report provides a summary, based on the published material from the investigations accomplished within Phase 2. Besides the investigations restricted to the borehole itself, a few studies were made of the ground surface in the near vicinity of borehole KLX02, combined with analyses of previously performed aerial surveys. Also a hydraulic interference test between boreholes KLX02 and KLX01 was conducted. All types of investigations are included in this final report. As mentioned above, also some results derived from investigations performed before and after Phase 2 are comprised.

Chapter 2 of the report describes the outline of the investigation programme, including the sequence of performance of all activities as well as their duration. Also the project organization is presented. The succeeding five chapters, i.e. Chapters 3–7, are devoted to the investigations accomplished during Phase 2. Each chapter treats one of the five items geology, rock mechanics, thermal properties, hydrogeology and hydrochemistry. After a short introduction, the scope of activities, investigation methods applied as well as results obtained are described. Finally, to get a quick outline of the major findings, the Executive Summary (after Chapter 7) is recommended.

2 Sequence of activities and project organization

In this chapter a brief summary is given of the activities included in the investigation programme designed for Project Deep Drilling KLX02 – Phase 2, together with the timetable for their performance. Also the project organization is presented and the main Technical and Project Reports resulting from the project are listed, grouped according to geoscientific topics.

2.1 Sequence of activities

The activities conducted within Phase 2, the time requirement for each activity and the sequence of investigations are illustrated in Figure 2-1. As noticed, the duration of the complete programme was about 5 years. Also, the main reports produced during the course of Phase 2 are listed in the figure.

2.2 Project organization

The Project Organization for Project Deep Drilling KLX02 – Phase 2 is described in Figure 2-2. The organization was simple. A number of specialists/consultants were contracted directly by SKB for the performance of a variety of geoscientific studies according to the investigation programme. The field activities were planned in detail by the project manager and consultants at a series of project meetings and, later, the results discussed after completed investigations. Figure 2-2 also includes the main reports resulting from the different investigations during Phase 2. For the complete list of deliverables and background reports, it is referred to References.

Figure 2-1. Investigation Programme and Sequence of Activities for Project Deep Drilling KLX02 - Phase 2 (Red = field investigation, Blue = analysis and reporting).

PROJECT DEEP DRILLING KLX02 - PHASE 2	ACTIVITIES																					
	SEQUENCE OF ACTIVITIES AND REPORTS																					
	1993				1994				1995				1996				1997				1998	
	1	2	3	4	1	2	3	4	1	2	3	4	1	2	3	4	1	2	3	4	1	2
1. GEOLOGY																						
1.1 Sampling and analysis of drill cuttings from KLX02																						
1.2 Sampling and petrological classification of thin section samples from KLX02																						
1.3 Reporting of 1.1 and 1.2 (AR 94-50)																						
1.4 Detailed mapping of the drill core from KLX02																						
1.5 Geophysical logging in KLX02																						
1.6 Analysis and reporting of 1.1-1.5 (AR 95-37)																						
1.7 Borehole radar measurements in KLX02																						
1.8 Analysis and reporting of 1.7 (AR 93-43)																						
1.9 Analysis of radar reflectors between KLX01 and KLX02. Reporting (AR 94-28)																						
1.10 TV-logging in KLX02 (black&white)																						
1.11 BIPS TV-logging in KLX02																						
1.12 Surface mapping and lineament analysis near KLX02																						
1.13 Reporting of 1.12 (AR 94-23)																						
1.14 Fission track sampling on drill cores from KLX02																						
1.15 Analysis and reporting of 1.14 (GFF 118, 1996; article in Terra Nova no. 11, pp 210-215)																						
1.16 Structural analysis of the Laxemar area (pers. comm. R. Stanfors)																						
1.17 Ground geophysical measurements (bulk resistivity)																						
1.18 Analysis and reporting of 1.17 (PR D-98-01)																						
2. ROCK MECHANICS																						
2.1 Hydraulic fracturing stress measurements																						
2.2 Analysis and reporting of 2.1 (PR U-97-27)																						
2.3 Hydromechanical field measurements																						
2.4 Analysis and reporting of 2.3 (PR U-97-26)																						
2.5 Caliper-logging in KLX02																						
2.6 TV-logging in KLX02 (black & white)																						
2.7 Analysis and reporting of 2.5 and 2.6 (AR 95-38)																						
2.8 Special fracture study of KLX02, KAS02 and KAS03 (AR 95-44)																						
3. THERMAL PROPERTIES																						
3.1 Temperatur logging in KLX02 (see AR 95-37)																						
4. GEOHYDROLOGY																						
4.1 Single hole tests in KLX02																						
4.2 Interference tests KLX01-KLX02																						
4.3 Analysis and reporting of 4.1 and 4.2 (PR U-96-32)																						
5. GROUNDWATER AND CALCITE FILLING CHEMISTRY																						
5.1 First sampling with Tube sampler																						
5.2 Sampling with the SKB packer sampler																						
5.3 Analysis and reporting of 5.1 and 5.2 (TR 95-05)																						
5.4 Sampling of noble gases																						
5.5 Analysis and reporting of 5.4 (ICR 97-04)																						
5.6 Second sampling with Tube sampler																						
5.7 Analysis and reporting of 5.6 (AR in press)																						
5.8 Sampling of calcite fillings																						
5.9 Analysis and reporting of 5.8 (TR 95-06 and ICR 97-04)																						

DEEP DRILLING KLX02 - PHASE 2		ORGANIZATION
<div style="border: 1px solid black; padding: 5px; margin: 0 auto; width: 80%;"> <p>PROJECT MANAGEMENT SKB (Lars O Ericsson/Peter Wikberg)</p> </div> <div style="text-align: center; margin: 5px 0;"> </div> <div style="border: 1px solid black; padding: 5px; margin: 0 auto; width: 60%;"> <p>PROJECT CO-ORDINATION GEOSIGMA Co. (Lennart Ekman)</p> </div>		
TOPIC	PERFORMING ORGANIZATION	MAIN DELIVERABLES
GEOLOGY	GEOSIGMA Co. Scandiaconsult Bygg- och Industriteknik Co. MALÅ GeoScience Co. (field performance and data processing)/Roy Stanfors Consulting Co. (reporting) SGU Lund Terralogica Co. Roy Stanfors Consulting Co. SGU Uppsala/LTU	SKB AR 93-43 SKB AR 94-28 SKB AR 94-23 SKB AR 95-37 SKB AR 94-50 GFF 118, 1996 Article in Terra Nova, no 11, pp. 210-215 pers. comm. SKB PR D-98-01
ROCK MECHANICS-MECHANICAL STABILITY	MALÅ GeoScience Co. VATTENFALL HYDROPOWER Co. KTH/LBL GEOSIGMA Co.	SKB AR 95-38 SKB PR U-97-27 SKB PR U-97-26 SKB AR 95-44
THERMAL PROPERTIES	MALÅ GeoScience Co./ Roy Stanfors Consulting Co.	SKB AR 95-37
GEOHYDROLOGY	GEOSIGMA Co. (field performance)/Golder Associates Co. (reporting)	SKB PR U-96-32
GROUNDWATER CHEMISTRY	GeoPoint Co./Conterra Co./ KTH Intera Co./Terralogica Co. Geokema Co./GöU/KTH Intera Co./Geokema Co. Geokema Co.	SKB TR 95-05 SKB AR 99-09 SKB ICR 97-04 SKB TR 95-06

Figure 2-2. Organization Plan for Project Deep Drilling KLX02 – Phase 2 with main deliverables from the project.

3 Geology

3.1 Introduction

A basic requirement for meeting the needs of repository engineering and performance assessment is the development of a relevant lithological-structural model of the site in question. This model constitutes a simplified description of the rock composition and fracturing. The simplification process is one of the most crucial issues in site characterization, as this simplification provides the basis for design and modelling work for all other characterization key factors /3-1/. A description of the lithology and the main discontinuities is necessary to provide a framework for modelling of mechanical stability, thermal conditions, groundwater flow and groundwater chemistry.

The process of developing a reliable lithological-structural model of a site in fractured crystalline rock is often complex, demanding a huge amount of background data. The complications inherent in the characterization of a rock volume are, however, site specific and become enlarged with increasing site volume and geological heterogeneity. According to /1-1/ a thorough knowledge of the following lithological-structural parameters is required:

- Topography.
- Overburden, i.e. soil distribution.
- Rock distribution.
- Rock composition.
- Ductile structures.
- Brittle structures.

The lithological-structural features need to be characterized in a regional as well as in a detailed scale.

Relevant methods for a geological-structural characterization are /1-1/:

1. Digital elevation modelling.
2. Aerial geophysical surveys.
3. Ground geophysical measurements.
4. Geological mapping (bedrock composition, fractures, soils).
5. Core and percussion drilling.
6. Geological and geophysical borehole investigations.
7. Sampling and laboratory analyses of drill cores and drill cuttings.

Within the frame of Project Deep Drilling KLX02 – Phase 2 mainly studies according to items 6 and 7 were performed. However, prior to or subsequent to this project, also other investigations were made in the Laxemar area, covering essential aspects of items 1–5. Nevertheless, for erecting a complete lithological-structural model of the Laxemar area to serve the purpose of designing a deep repository for spent nuclear fuel, several additional deep investigation boreholes would be needed.

3.2 Regional and local geological setting

3.2.1 Lithological conditions

The municipality of Oskarshamn in south-eastern Sweden, see Figure 3-1, is situated in a region, which lithologically is dominated by rocks belonging to the c. 1850–1650 m.y. (million years) old Transscandinavian Igneous Belt (TIB). This belt is extending from south-eastern Sweden to south-eastern Norway and is dominated by a variety of plutonic rocks of different ages and compositions. The Oskarshamn area is almost devoid of ores and industrial minerals.

In the following text, the bedrock in the Oskarshamn region, see Figure 3-1, is briefly described. As can be seen in the figure, the geology of the sea bottom outside the coast is also included in the bedrock map, though less detailed due to sparse information.

The oldest rocks in the Oskarshamn area are c. 1900 m.y. metasedimentary rocks, including quartzite, which belong to the so-called Västervik formation (light blue and blue in Figure 3-1). Furthermore, metabasite, which is interpreted to be mainly of volcanic origin (dark green in Figure 3-1), and c. 1900 m.y. old felsic to intermediate, metavolcanic rocks occur (light green in Figure 3-1). The oldest intrusive rocks in the region are c. 1830 m.y. old (or older), usually slightly gneissic metagranitoids of granodioritic to tonalitic composition (beige with black dots in Figure 3-1) /3-2/.

The predominating rocks in the area are granite, granodiorite and monzonite to quartz monzodiorite belonging to the c. 1800 m.y. old generation of TIB rocks (different shades of soft red, with or without black dots in Figure 3-1). They are traditionally called “Småland granites” in this part of Sweden /3-2/. The different varieties are often intimately associated, and gradual transitions are common. The Småland granites in general are more or less isotropic, and large areas with rather homogeneous varieties exist. Mafic rocks of mainly gabbroid and dioritic composition (middle green in Figure 3-1) are associated with the Småland granites. Diorite and gabbro are relatively frequently occurring in an approximately east-west trending belt north of the city of Oskarshamn.

In certain parts of the region, e.g. in the Laxemar-Simpevarp-Äspö area (the black square in Figure 3-1), fine-grained, granitic dykes, related to the Småland granites, are frequently found.

Volcanic rocks (yellow in Figure 3-1) are closely related to the Småland granites, both regarding age and space. They are traditionally called “Småland porphyries” because of their commonly porphyritic texture. In the Oskarshamn region, the volcanic rocks mainly occur in a belt from the city of Oskarshamn and westwards, see Figure 3-1.

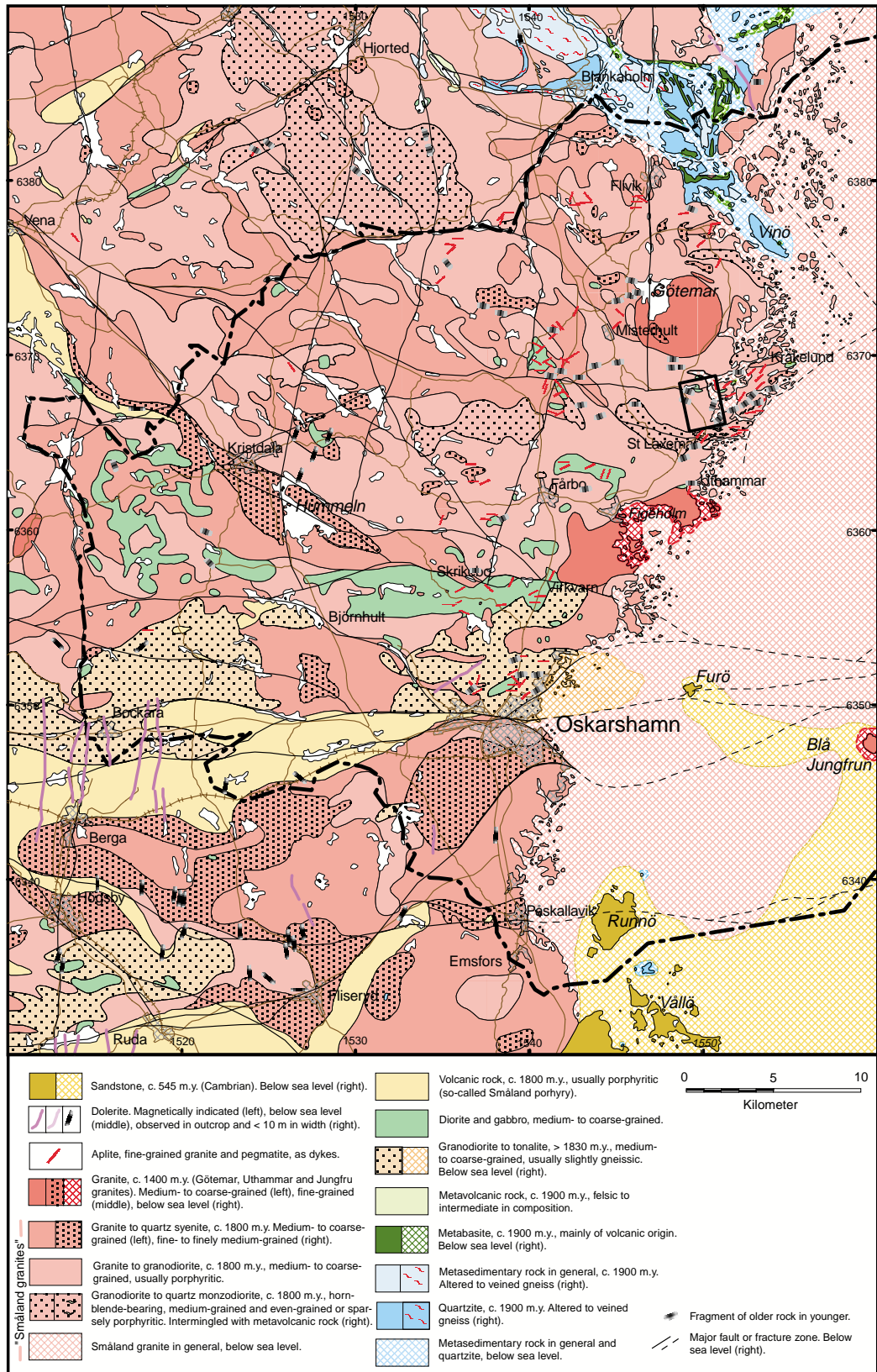


Figure 3-1. Geological map of the Oskarshamn region. The border of the municipality of Oskarshamn is represented by the fat black, dashed and dotted line. The Laxemar-Simpevarp-Äspö area is marked with a black square (after /3-2/).

The youngest plutonic rock in the area is a c. 1450–1400 m.y. old so-called anorogenic granite (dark red in Figure 3-1) /3-2, 3-3/. One of the occurrences, the Götemar granite, appears about two kilometres north of the Laxemar area. The other two localities are the Uthammar and Jungfru granites.

Dolerite (purple, lilac and black in Figure 3-1) represents a subordinate rock in this region. Two generations of dolerite occur, one of which is inferred to be related to the TIB rocks, while the other is interpreted to be much younger, about 900 m.y. old.

The youngest rock in the area is the c. 545 m.y. Cambrian sandstone (brown colour in Figure 3-1), which covers the Precambrian rocks along the coast south of Påskallavik and on the islands of e.g. Runnö and Furö.

Within the Laxemar-Simpevarp-Äspö area (the black square in Figure 3-1) the geological conditions were studied exhaustively in connection with the pre-investigations prior to construction of the nuclear power plant facilities at Simpevarp respectively the excavation of the Äspö HRL tunnel. Figure 3-2 is a detailed geological map of the western part of this area, here called the Laxemar area.

As appears from the map, the dominating rock is a greyish red to grey medium-grained, porphyritic (with 1–3 cm phenocrysts), granite to granodiorite, a variety of porphyritic Småland granite. South-east of borehole KLX02 and west of borehole HLX08 this rock type is characterized by somewhat smaller phenocrysts, about 1 cm in diameter /3-3/. This variety is called Ävrö granite.

To the north, a mafic rock with a dioritic to gabbroic composition is surrounded by a greyish-red to red medium-grained variety of Småland granite. Another mafic rock occupies the area south-east of lake Frisksjön. Xenolites of metabasites and other, unspecified rock types are common in the Laxemar area, especially south of lake Frisksjön.

An intermediate, reddish grey, finely medium-grained to medium-grained, usually sparsely porphyritic variety of Småland granitoid is rather common on the island of Äspö, and is usually called “Äspö diorite”. However, this variety is more correctly a quartz monzodiorite to quartzdiorite. It has also been encountered in drill cores from the Laxemar area, although not found on the surface. This points to the importance of a detailed geological mapping in order to investigate whether this rock type also exists on the surface. For further description of the rock types prevailing in the Laxemar-Simpevarp-Äspö area, see also Section 3.3.4.

3.2.2 Deformation

The area in Figure 3-1 has, during the geological history, been subjected to ductile as well as brittle deformation. The most important regional ductile shear zone is known as the Oskarshamn-Bockara zone. It belongs to a system of ductile shear zones that can be followed tens to hundreds of kilometres westwards from the city of Oskarshamn. These ductile shear zones are also inferred to continue eastwards below the island of Öland, where they, however, are covered by younger, Phanerozoic rocks.

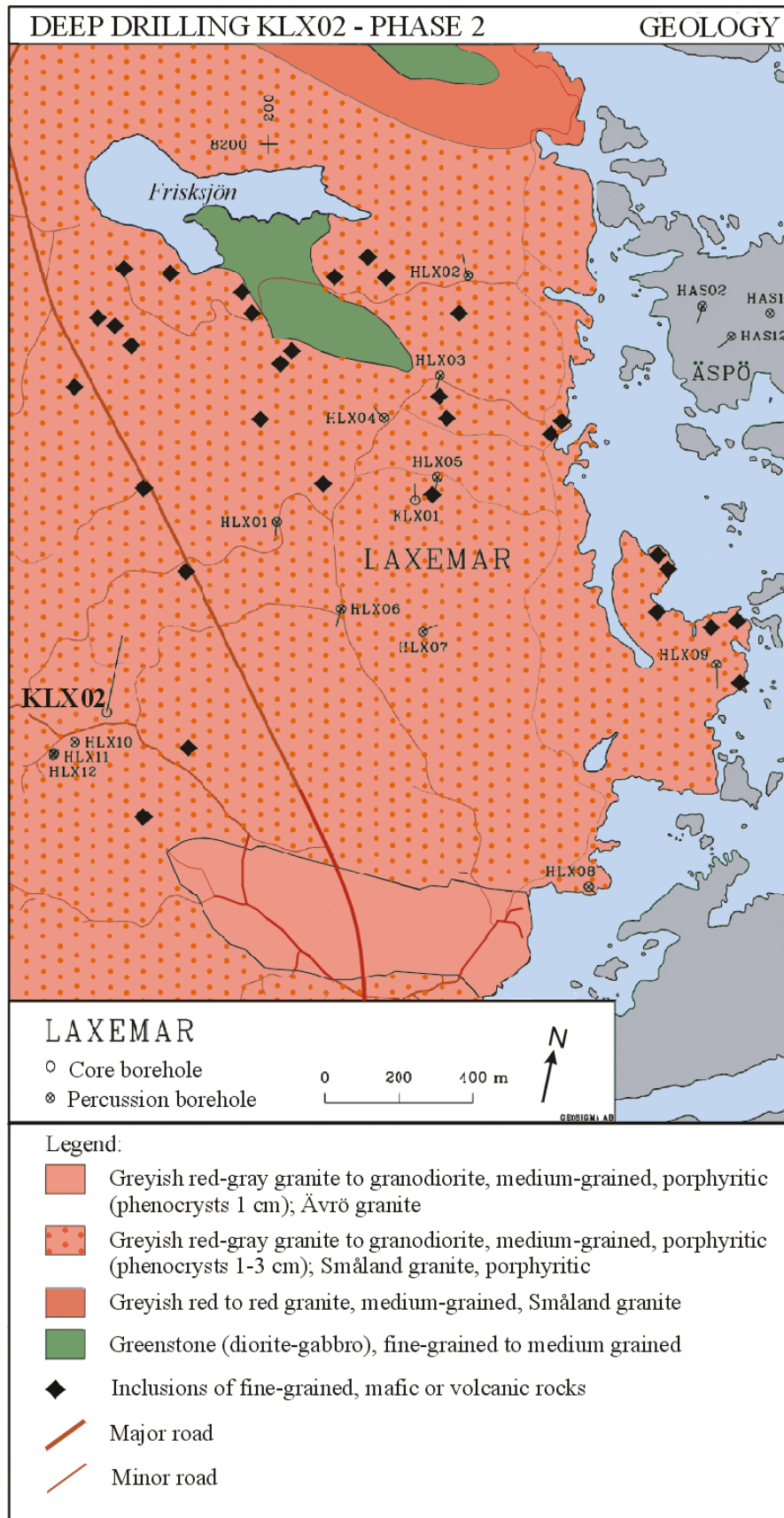


Figure 3-2. Bedrock map of the Laxemar area (modified after /3-3/).

The transition from ductile to brittle deformation occurred about 1700 m.y. ago /3-2/. The Oskarshamn-Bockara shear zone is accompanied by a system of brittle, regional deformation zones, i.e. fracture zones, which indicate that the ductile shear zone has been reactivated in a brittle, tectonic regime, see Figure 3-1. The rest of the area is characterized by a pattern of relatively evenly spaced, major fracture zones with dominating north-south and northwest-southeast orientations. The majority of the major fracture zones are probably faults. Besides these, a network of smaller, local, fracture zones divides the bedrock into irregular blocks with side lengths of a few kilometres.

The map in Figure 3-1 is essentially a planar projection of a three dimensional pattern of fracture zones. Therefore, horizontal or subhorizontal fracture zones may be underrepresented, since they are difficult to discover on the surface.

The Laxemar-Simpevarp-Äspö area is mainly characterized by brittle deformation. However, also a ductile shear zone, the so called Äspö shear zone, striking northwest-southeast, was encountered during the geological investigations on the island of Äspö. Two east-west trending, regional fracture zones can be followed from the coastline. They join each other a few kilometres west of Laxemar, see Figure 3-1. From there, they continue as one single zone farther westwards.

A third, north-south striking, regional fracture zone is traceable from the northern east-west trending zone northwards through the Götemar granite, see Figure 3-1. Furthermore, local fracture zones with different orientations intersect the Laxemar-Simpevarp-Äspö area.

3.3 Geological investigations in the Laxemar area during Phase 2

The expression “the Laxemar area” mentioned in this report is defined as a three dimensional (3D) rock volume, approximately delimited by the location of the twelve investigation boreholes, see Figures 1-2 and 3-2. The investigations performed in the Laxemar area, prior to and during Phase 1 and Phase 2 of Project Deep Drilling KLX02, were not focused on the issue of developing an elaborated 3D lithological-structural model of the site. However, attempts were made to arrive at a simplified model to be used as a tool for different interpretation tasks. Three different approaches to this challenge, with emphasis on the structural character, are presented in this report. Detailed descriptions of the rock composition are, though, limited to the nearest vicinity of borehole KLX02.

The geological investigations performed during Phase 2 of Project Deep Drilling KLX02 primarily included borehole investigations and a study of discontinuities in the area between boreholes KLX01 and KLX02. The geological/geophysical borehole investigations in KLX02 were:

- Petrological classification of drill cuttings and core samples.
- Modal analysis of thin sections.
- Chemical analysis of core samples.
- Core logging.
- Fission track-studies on core samples.
- Conventional geophysical borehole logging with nine methods.
- Borehole radar measurements with two antenna types (dipole and directional).
- Borehole TV-logging with two systems (black & white and colour).

The study of fracture zones in the area between the two deep boreholes KLX01 and KLX02 included a ground search and a scrutiny of earlier performed aerial surveys and digital elevation modelling. This, in combination with the study of borehole information from KLX01 and KLX02, aimed at identifying fracture zones connecting the two boreholes, thereby making the development of a simple structural model of this rock volume possible. With aid from experiences of the investigations at the Äspö HRL and of recent semi-regional ground geophysical surveys, this model has lately been further developed, cf. Sections 3.4.3, 3.4.4 and 3.4.5.

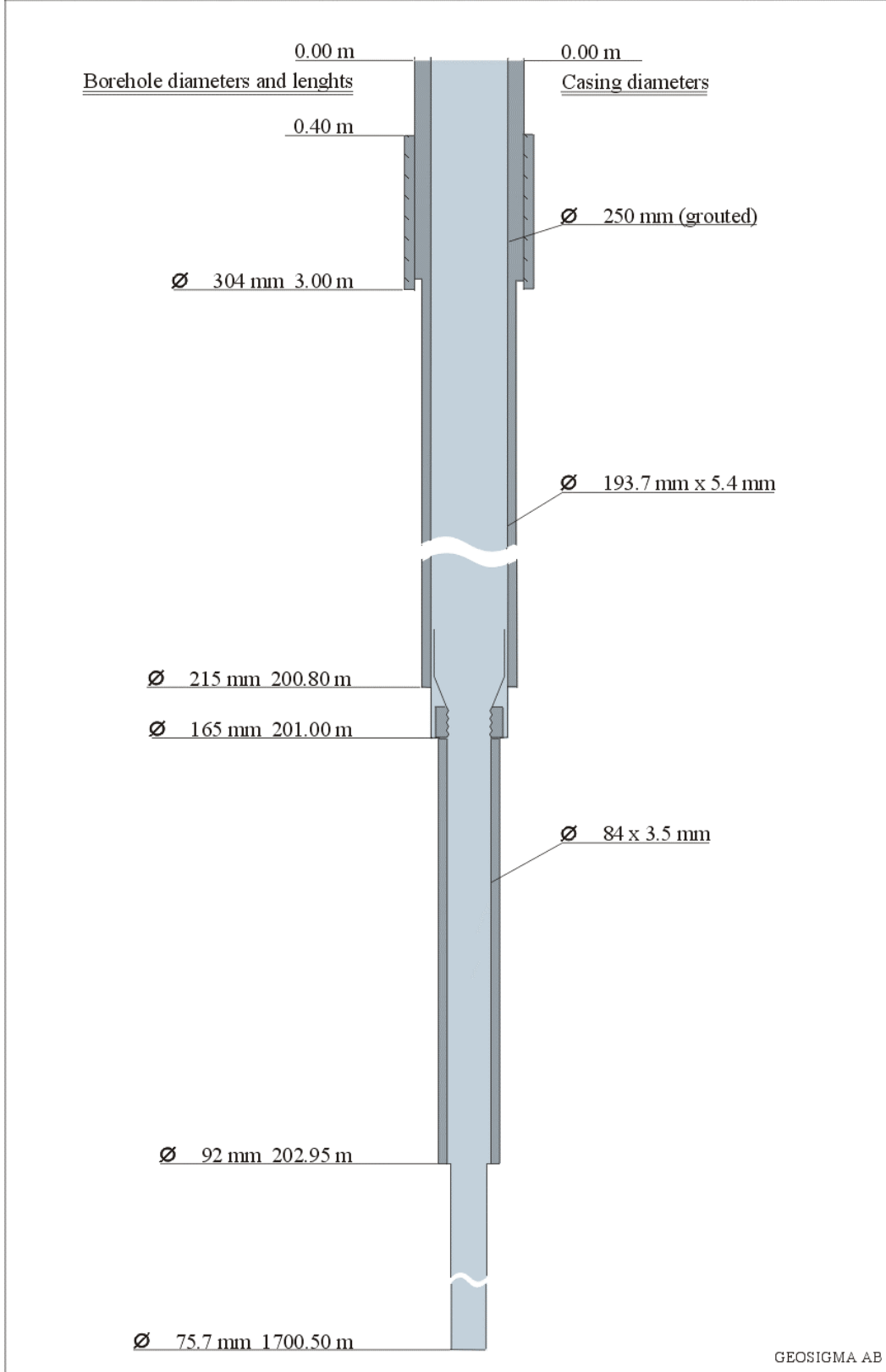
In the present section the geological investigations within and in the nearest vicinity of borehole KLX02 are presented. Section 3.4 is devoted to the studies of geological structures in the rock volume between boreholes KLX01 and KLX02.

3.3.1 Borehole design

Borehole KLX02 was drilled according to the so called telescope drilling technique. During drilling the borehole was air-lift pumped for retrieval of drilling water and drill cuttings. In order to enable a better understanding of the investigations performed in the borehole, a brief description of the borehole design is given below, cf. Figure 3-3.

The upper 201 m of the borehole were percussion drilled, in three steps /1-2/. Initially, a drill bit producing a \varnothing 165 mm pilot borehole was applied. In the second step, the borehole was reamed to \varnothing 215 mm with a reamer bit mounted on top of a pilot bit. However, prior to reaming, a \varnothing 250 mm conductor casing was set by drilling a 2.5 m deep, \varnothing 304 mm hole into the bedrock. The casing was sealed off against soil and rock by cement grouting. After reaming, a temporary double support casing was installed from top to bottom of the predrilled hole along with the support casing for air-lift pumping. A support casing is necessary for reducing vibrations in the drill string during drilling. The core drilling commenced from the bottom of the percussion drilled borehole. At the first two metres, between 201–202.95 m, a \varnothing 92 mm borehole was produced in order to permit installation of a stainless steel funnel between the percussion respectively the core drilled parts of the borehole.

From 202.95 m to the borehole bottom the borehole diameter is near 76 mm. After core drilling, the reamed part of the borehole, i.e. down to 200.8 m, was cased by a \varnothing 193.7 mm steel casing. No grouting was performed during this operation. The borehole configuration after completion is illustrated in Figure 3-3.



GEOSIGMA AB

Figure 3-3. Borehole KLX02. Configuration after completed drilling and casing installations.

Deviation measurements were performed after drilling. The results are illustrated in Figure 3-4. Borehole KLX02 is inclined 85° at the ground surface and the deviation is small. The difference between borehole length and vertical depth is therefore limited. The bottom of the borehole reaches some 1660 m below the ground surface, i.e. 2 % less deep than expected for an ideal, completely straight borehole inclined 85° with the borehole length 1700.5 m.

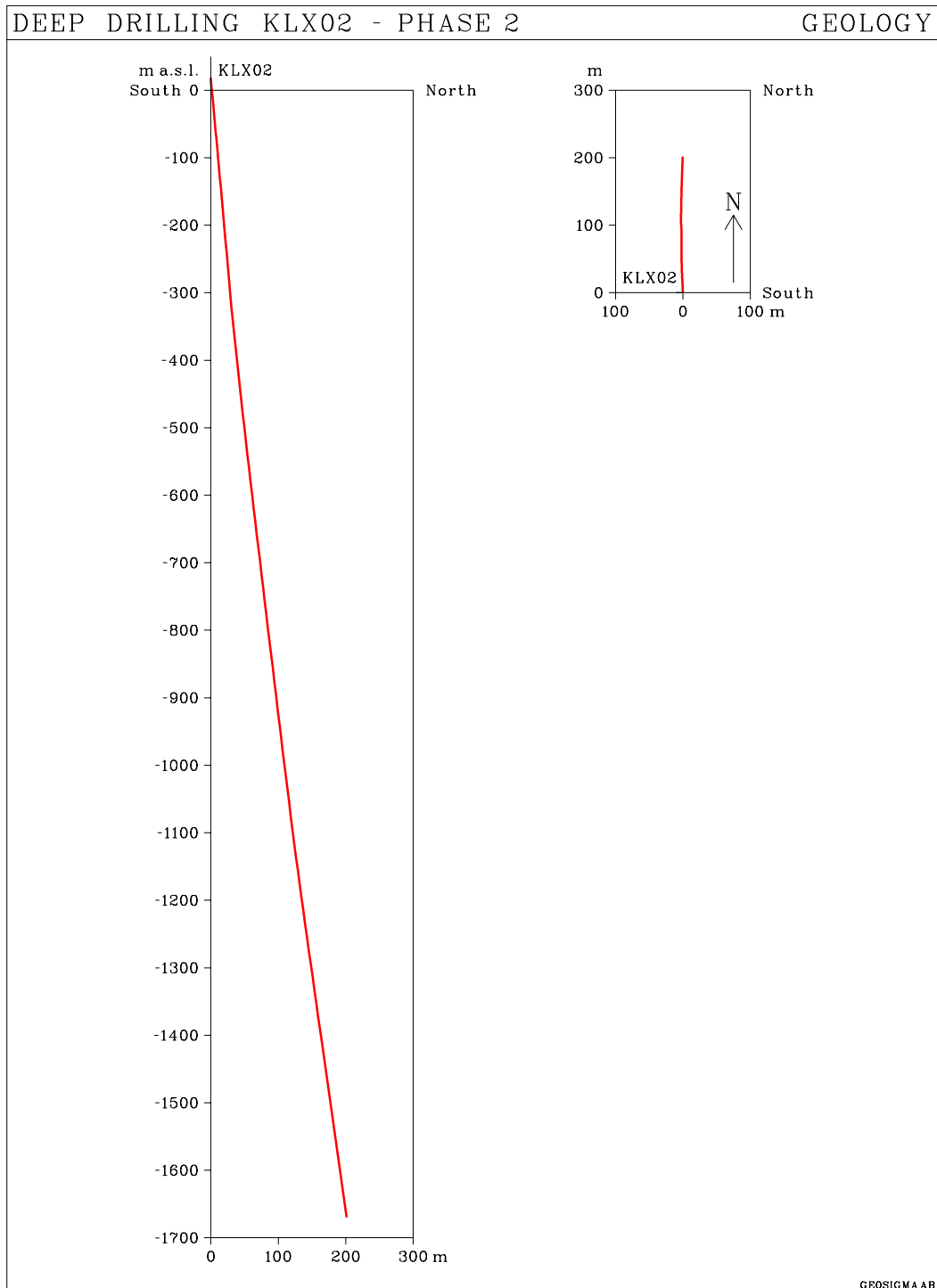


Figure 3-4. Deviation of borehole KLX02.

3.3.2 Petrological classification of drill cuttings

Since drill cores were not produced from the percussion drilled part of borehole KLX02, drill cuttings were sampled to provide data for petrological documentation of the upper 201 m of the bedrock. A sample was collected at every third metre in the borehole section 9–198 m. I.e. altogether 64 samples were collected and analysed /3-4, 3-5/, of which 20 were studied more thoroughly. Six rock types were identified from the analysis of drill cuttings. For an account of the age and regional context of each rock type, see Section 3.2.1. Sampling levels and the rock type connected to each sample are given in Table 3-1.

Table 3-1. Rock types within the interval 9–198 m in borehole KLX02 according to examination of drill cuttings. After /3-5/. Asterisk (*) indicates more closely examined samples. Underlines represent transitions between the rock groups indicated with capital letters. These are:

- A) Greenstone (greyish black, fine-grained)
- B) Diorite (dark grey, finely medium-grained)
- C) “Äspö diorite” (i.e. reddish grey, finely medium-grained to medium-grained granodiorite to quartz monzodiorite)
- D) Granite to granodiorite (greyish red, finely medium-grained to medium-grained)
- E) Granite (greyish red to red, finely medium-grained)
- F) Granite (red, fine-grained)

Sampling level (m)	Rock type	Sampling level (m)	Rock type	Sampling level (m)	Rock type
9 *	<u>F + A</u>	72 *	D	135	<u>D + C</u>
12	C + A	75	D	138 *	E
15	C	78 *	D + E	141	E
18	<u>C</u>	81	D + E	144	E
21 *	<u>F + A</u>	84	D	147	E
24	C	87	<u>D</u>	150 *	E
27	C	90	E + D	153	E
30	<u>C + F</u>	93	<u>E + D</u>	156	<u>E</u>
33	<u>A</u>	96	D	159 *	<u>E + A</u>
36 *	C	99 *	D	162	E + F
39	C	102	D	165 *	E + F
42	<u>C</u>	105	D	168 *	<u>E + F + A</u>
45 *	B	108 *	D	171	F + A
48	B + A	111	D	174	<u>F + A</u>
51	B	114	D	177	D
54	B	117 *	D	180 *	<u>D</u>
57 *	B + F	120	D	183	<u>E + F + A</u>
60	B + F	123	D	186	D
63	B	126	D	189	D
66	<u>B</u>	129	D	192	D + F
69	D	132	D	195	D
				198 *	D

Considering Table 3-1, the borehole section 9–198 m may be divided into intervals of different rock composition:

1. 9– 42 m. Dominated by rock group C with elements of groups A and F.
2. 42– 66 m. Group B prevails with dashes of A and F.
3. 66–135 m. Group D completely dominating, however with sparse elements of group E between 78 m and 93 m.
4. 135–156 m. Group E exclusively.
5. 156–174 m. This short interval is characterized by a mixture of A, E and F.
6. 174–198 m. Group D with few elements of A, E and F.

Detailed logging of the KLX02 drill core was conducted during Phase 2, cf. Section 3.3.4. The logging resulted in a rock type classification of the core in four major rock groups in accordance with a classification system developed at the Äspö HRL /3-6/:

- Småland granite.
- Äspö diorite.
- Greenstone.
- Fine-grained granite.

If the four-group system is selected, group B in Table 3-1 will be defined as belonging to group “Greenstone”, while groups D and E both are classified as “Småland granite”. In the remainder of this report, only the four-group classification will be used. Concerning the age and regional context of each rock type, see Section 3.2.1. An illustration of the rock composition based on the above four-group classification of borehole KLX02, including also the percussion drilled part, is presented in Figure 3-12 and in the core log in Appendix 3.

3.3.3 Examination of thin sections

As mentioned above, borehole KLX02 was core drilled below 203 m depth, producing a \varnothing 76 mm borehole. The core, which is preserved at the drillcore stores at CLAB, Simpevarp, was preliminary logged during Phase 1 and logged in detail during Phase 2, see Section 3.3.4. 27 thin sections sampled from the cores below 203 m were studied under the microscope /3-5/. Modal analysis of the samples was applied to provide a rock type classification of the drill core. Also chemical analysis was performed on seven of the samples (Appendix 2). The results of the modal analysis are displayed in Table 3-2 and in the triangular diagram of Figure 3-5. The classification of thin sections is illustrated up in Figure 3-6. When compared to the core log in Appendix 3 and Figure 3-12, a few discrepancies are observed. Three samples (at 335.80 m, 529.40 m, and at 995.90 m) were by the thin section analysis defined as Äspö diorite, whereas the core at these intervals was mapped as Småland granite. This illustrates the obvious difficulty to separate these two, very similar rock varieties from each other by pure ocular inspection. One of the thin section samples defined as Äspö diorite, at 724.80 m, is mapped as greenstone.

Table 3-2. Results of modal analysis (volume %) of core samples from borehole KLX02. After Table 2 in /3-5/.

Mineral distribution (volume %) in 27 core samples (thin sections) from KLX02																											
Minerals	Sample number																										
	1	2	3 #	4	5	6	7	8 #	9	10	11	12	13 #	14 #	15	16	17 #	18 #	19 #	20	21	22	23	24	25 #	26	27
Quartz	25	25	+	23	25	14	+	22	31	10	31	-	2	6	16	29	+	19	32	19	9	5	8	7	10	1	11
K-feldspar	38	15	+	26	27	17	12	32	23	16	42	11	+	+	16	46	-	35	32	28	1	3	3	37	3	-	7
Plagioclase	26	41	3	38	35	49	-	28	35	41	20	23	38	30	47	18	33	34	25	40	24	47	48	21	58	35	30
Biotite	5	14	35	-	10	11	+	10	3	8	-	-	-	23	5	-	4	6	-	7	36	18	20	+	14	36	33
Chlorite	-	-	5	6	+	-	17	1	3	-	4	7	7	-	5	2	+	1	5	-	-	-	-	4	+	-	-
Muscovite	-	-	-	+	-	-	-	+	-	-	1	-	+	-	+	1	-	-	2	1	-	-	-	23	+	-	+
Fluorite	-	-	-	-	-	-	-	-	-	-	+	-	-	-	-	+	-	+	+	+	-	-	-	-	-	-	-
Amphibole	-	-	55	-	-	+	56	-	-	19	-	50	45	26	3	-	56	-	-	+	10	20	9	-	5	13	2
Epidote	3	2	+	3	1	6	11	4	3	+	1	5	4	11	4	3	3	2	2	2	12	2	5	4	5	7	11
Allanite	-	-	-	-	-	+	-	+	-	-	+	-	+	+	-	+	-	-	-	-	-	-	-	-	-	-	-
Prehnite	+	-	+	1	+	-	-	+	+	-	+	+	+	1	+	-	+	+	+	+	+	+	2	-	+	-	-
Pumpellyite	+	-	-	-	-	+	-	-	+	-	-	-	-	-	-	-	-	-	+	-	-	-	+	-	-	-	-
Sphene	2	1	-	2	1	1	2	2	1	1	+	3	1	1	1	+	+	1	+	2	3	2	1	2	2	3	3
Calcite	+	+	-	-	-	+	-	+	+	-	+	-	+	-	+	-	-	-	+	-	-	+	-	+	+	-	+
Apatite	+	+	+	+	+	+	1	+	+	1	+	1	1	1	1	+	2	+	+	+	2	1	1	+	1	2	1
Zircon	+	+	-	-	+	+	+	+	+	+	+	-	+	+	+	+	+	+	+	+	+	+	+	+	+	-	+
Opauques	1	2	1	1	1	1	+	+	1	3	1	+	2	1	1	+	1	+	+	1	4	1	2	+	2	3	2

= chemically analysed sample; - = not detected; + = present in small quantities (< 0.5 %)

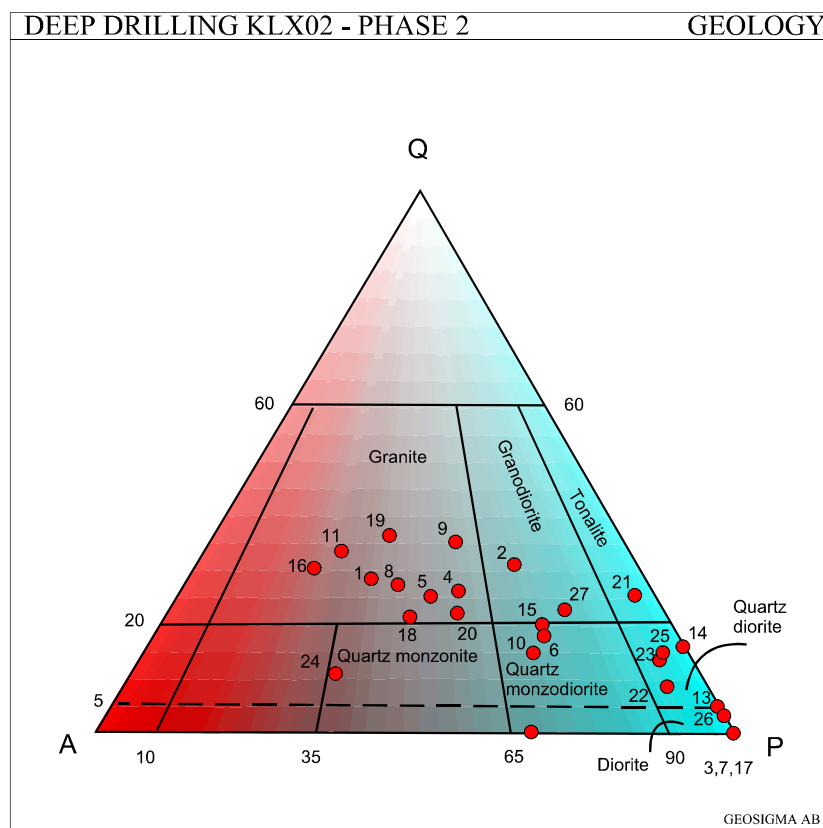


Figure 3-5. Modal classification of rock samples from KLX02 according to /3-7/. Modified after Figure 1 in /3-5/.

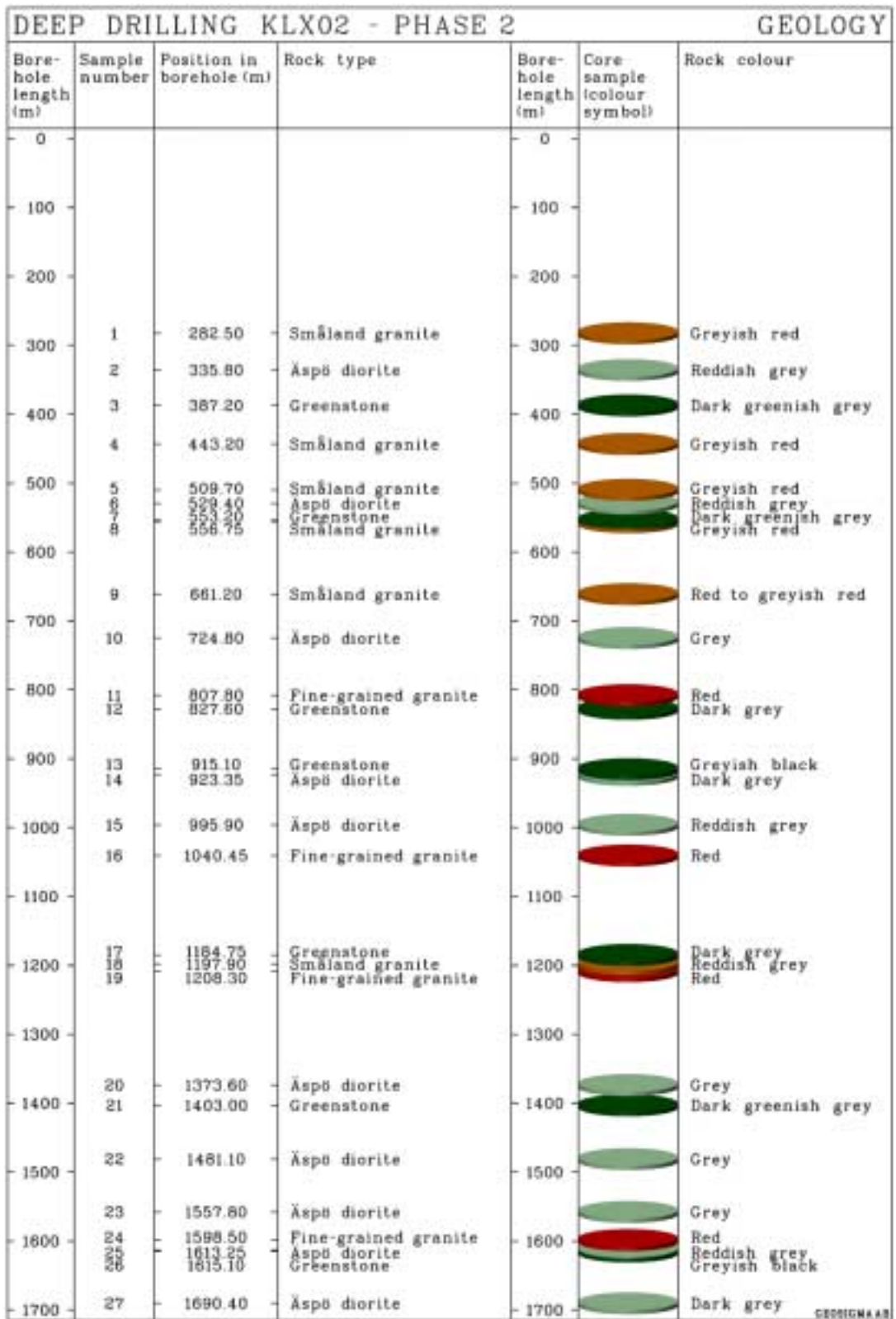


Figure 3-6. Rock type classification according to analysis of thin sections in borehole KLX02.

3.3.4 Core logging

Simultaneously with the drilling of borehole KLX02, a preliminary logging of the drillcore was performed. During Phase 2, detailed logging of the 1499.5 m long core (201–1700.5 m) was accomplished /3-4/ using the PetroCore core logging system (developed by SKB), following the standard procedures elaborated at the Äspö HRL /3-8/.

The core logging data is presented in Appendix 3 as composite diagrams including also geophysical logging and borehole radar results. A simplified and scale reduced core log is also presented in Figure 3-12 together with fracture frequency data and borehole radar results. The rock composition was classified according to the four-group system described in section 3.3.2 with Småland granite, Äspö diorite, greenstone and fine-grained granite as major rock types. In addition, pegmatite is frequently encountered as dikes in the core.

The petrological characteristics of the four rock groups are briefly summed up in the following description /3-6/.

Description of rock types prevailing in the Laxemar-Simpevarp-Äspö area

Småland granite

Småland granite is a traditional term covering several varieties of about 1800 m.y. old granitoids belonging to the Transscandinavian Igneous Belt (TIB). The Småland granite dominating on Äspö and in the Laxemar area is, as described in Section 3.2.1, a greyish red-grey, medium-grained granitoid (granite, granodiorite), generally with 1–3 cm phenocrysts of microcline.

A variety of Småland granite dominating the island of Ävrö, and thus assigned the name Ävrö granite, occurs also at the northern coast of Simpevarp, on the island of Bockholmen and in the southern part of the Laxemar area. It is very similar as the above described Småland granite, however with smaller, about 1 cm, phenocrysts. When referred to Småland granite below, no clear distinction is maintained between the varieties with larger or smaller phenocrysts.

Äspö diorite

Also the so called Äspö diorite is regarded as a variety, in this case of more mafic composition, of Småland granite. The Äspö diorite is a grey, medium-grained quartz monzodiorite-quartzdiorite, occasionally with red phenocrysts of microcline.

Greenstone

The greenstone appears in a couple of varieties. The origin of the first, a greyish black to dark-grey, fine-grained greenstone, is presumably a supracrustal of volcanic derivation. The modal and chemical composition corresponds to a basalt to andesite. This rock type generally emerges as remnants within the diorites and granitoids, and is thus older. However, the exact age is unknown, and it is not yet clarified whether

this variety of greenstone belongs to the older Svecofennian supracrustals or to the younger, postorogenic volcanics.

Another type of greenstone comprises dark-grey, fine medium-grained diorites. Occasionally they contain red, rather idiomorphic phenocrysts of microcline. At least some of those are metamorphic.

Fine-grained granite

During the geological investigations at the Äspö HRL, fine-grained granites were found as small massifs and dikes. This rock type is greyish red to dark red and fine-grained, often foliated or strongly fractured with cavities. The majority of the dikes at the ground surface are strongly deformed. This is also evident from the thin sections of fine-grained granites, which display not only parallel mylonitic structures, but also strong fracturing or crushing.

The fine-grained granites may be classified as true granites. The modal analysis (Table 3-2) and the triangular diagram (Figure 3-5) illustrate that they are rather rich in alkalis. This is also clear from the chemical analyses (Appendix 2).

The Småland granite and the fine-grained granite represent the “granite” field in the triangular diagram, the Äspö diorite the “granodiorite-quartz monzodiorite” and, finally, the greenstone the “quartzdiorite-diorite” fields.

Datings of the fine grained granite at Äspö have shown a similar age, close to 1800 m.y., as for the Äspö diorite (and other Småland granites).

Dominating rock types in the core of KLX02

Appendix 3 and the simplified core log in Figure 3-12 clearly demonstrate that the dominating rock type in KLX02 is Småland granite. Within a few sections the Småland granite is grading into the more mafic variety, the Äspö diorite. Below about 1450 m the Äspö diorite is the dominating rock.

5–10 m wide sections of greenstone occur frequently, especially between 600–950 m. In the Äspö HRL the same variety of greenstone has been observed as sheets, dikes and small massifs.

Fine-grained granite composes less than 2 % of the total core length. It appears in a few 1–5 m wide sections, probably representing the same type of veins or dikes frequently found in the Äspö HRL, there constituting about 15 % of the total rock mass.

Rock distribution and fracture frequency data from KLX02 are in Figure 3-7 compared to the same parameters for the 1078 m deep core borehole KLX01 at Laxemar and two core boreholes at the island of Äspö, KAS02 and KAS03, 924 m

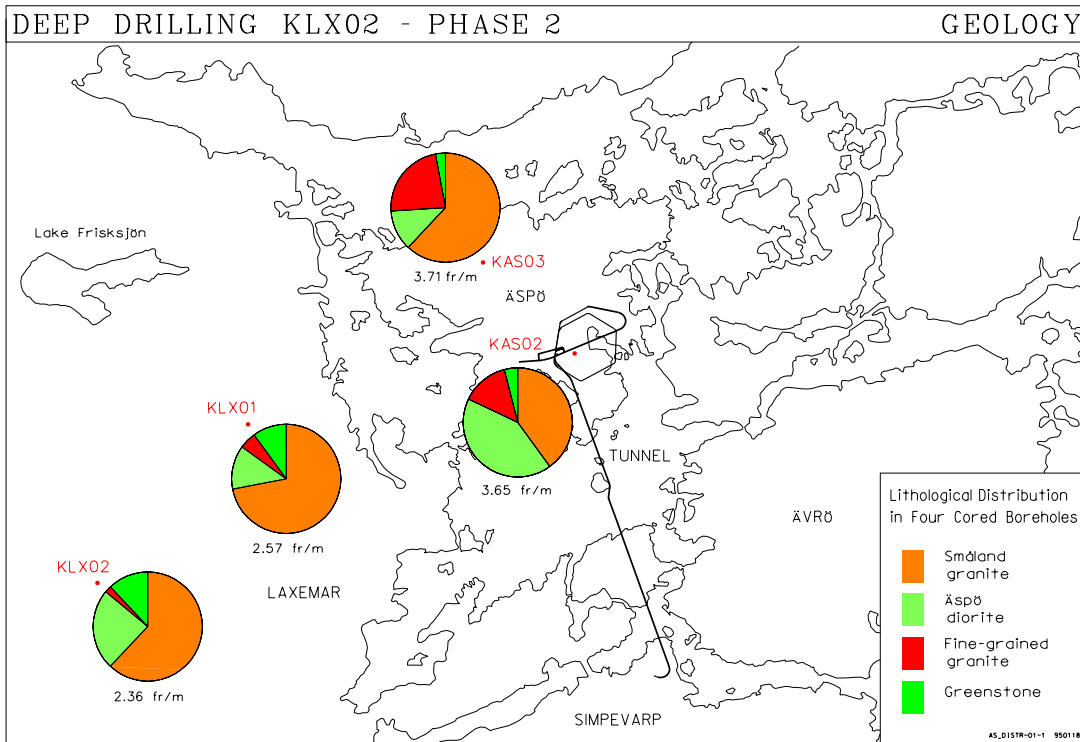


Figure 3-7. Distribution of main rock types and fracture frequency in the cored boreholes KLX01, KLX02 (Laxemar), KAS02 and KAS03 (Äspö). After Figure 3-1 in /3-2/.

respectively 1002 m long. Obviously, the fine-grained granite occupies smaller volumes of the drill cores in the Laxemar boreholes than in the two boreholes on Äspö, whereas the opposite situation is valid for greenstone. The fracture frequency is significantly lower in the Laxemar than in the Äspö boreholes.

Fracturing and alterations in the core

Besides the lithological description of the core, core logging with the PetroCore system comprehends the following parameters /3-8/:

- Fracture frequency (frequency of natural fractures, i.e. non-drill induced open fractures, either coated or non-coated).
- Location in the core (= borehole length), width and lithological character of crushed rock.
- Location, width and type of alteration of the rock.
- Location and type of fracture infillings.

The composite log in Appendix 3 illustrates that the core, regarding fracture frequency, may be divided into four intervals (cf. also the simplified core log in Figure 3-12):

- 1) 200– 730 m – normal fracture frequency
- 2) 730–1120 m – increased fracture frequency
- 3) 1130–1550 m – low fracture frequency
- 4) 1550–1700.5 m – highly fractured and altered interval

The fracture frequency of 3 fractures/m observed to a depth of 730 m is well in accordance with the fracturing observed in “normal” Småland granite and in Äspö diorite within the Äspö area. As a mean, one narrow (1–2 m wide) section with increased fracturing (>20 fractures/m) occurs at every 50 m. In these highly fractured parts of the core, epidote and oxidation are frequently occurring.

At about 730 m a pronounced increase in fracture frequency is observed. The increase culminates at about 1070–1120 m in a 50 m wide section with crushed and strongly weathered rock. It is assumed in /3-2/ that section 730–1120 m represents an intersection with one or two major discontinuities indicated by the aerogeophysical survey of the Simpevarp area /3-9/, but also other interpretations have been made, see Section 3.4.5.

The very low fracture frequency between 1120–1550 m is followed by an approximately 80 m long core section characterized by intense altering and high fracture frequency. This section and the last 20 m of the core probably represent major fracture zones /3-2/.

3.3.5 Fission track studies

Background and scope of activities

Fission tracks are known to be created in minerals by fission of ^{238}U . However, at high temperatures the tracks are annealed. The annealing temperature is mineral specific. E.g. for apatite, total annealing is considered to occur above 130 ± 20 °C and for titanite above 250 ± 20 °C. At lower temperatures, the fission tracks are partially annealed (partial annealing zone) or unaffected by annealing.

Fission track (FT) studies can be used to date when a certain mineral cooled below its annealing temperature and also to reveal its tectonothermal history. This entails that conclusions can be drawn about e.g. uplift and subsidence of the part of the crust included in this study. The technique for performance of FT-studies is, together with its application on thermotectonic events in central and southern Sweden, described in /3-10/.

With the purpose of determining the existence and magnitude of Phanerozoic paleo-loads on the present surface, a FT-study was initiated in 1994 by SKB at the Laxemar area. The drillcore from borehole KLX02 was sampled at the depths 3 m, 994 m and 1696 m. Apatites and titanites were concentrated from these samples and were used for the fission track analyses. The study is presented in /3-11, 3-12/.

Results

The results of the apatite FT-analyses are illustrated in Table 3-3, whereas the statistical parameters from the confined fission track length measurements are shown in Table 3-4.

Results of inverse modelling techniques applied on apatite fission track (AFT) data, using the method of Lutz and Omar /3-13/, are presented in Figure 3-8. The AFT-ages for the three samples are significantly different from each other at the 95 %-level, in contrast to titanite fission track ages (not displayed here).

The modelling reveals that the surface sample (from 3 m depth) passed into the zone of partial annealing 410±20 m.y. ago, which represents the age of the oldest modelled fission track. This means that today's surface has been buried to a depth equivalent to the total annealing, and that all information about the time before 410 m.y. ago has been erased.

Table 3-3. Results from fission track length measurements on apatite samples from the drill core of borehole KLX02.

Sample no	No of grains	$\rho_s \times 10^6$ track cm ⁻²	$\rho_i \times 10^6$ track cm ⁻²	$\rho_{std} \times 10^6$ track cm ⁻²	χ^2 %	Age (m.y.)	1 σ (m.y.)	Corrected age (m.y.), i.e. the oldest track
KLX02 (3 m)	33	3.28	2.85	1.93	89	340	1±8	410±20
KLX02 (994 m)	12	3.52	3.93	1.93	99	264	1±8	347±20
KLX02 (1696 m)	16	3.01	4.38	1.93	94	206	1±6	295±16

ρ_s , ρ_i , ρ_{std} = density of spontaneous, induced and dosimeter tracks (tracks/cm²); χ^2 = result of χ^2 -test (a value < 5 % implies mixed ages; Age = the pooled apparent fission-track age; σ = standard deviation.

Table 3-4. Statistical parameters from confined fission track length measurements on apatite samples from the drill core of borehole KLX02.

Sample nr	Mean (μm)	Std. Error	Std. Dev.	Variance	Point	Min	Max
KLX02 (3 m)	13.16	0.10	1.86	3.44	333	6.55	16.80
KLX02 (994 m)	12.17	0.10	1.81	3.28	308	6.30	16.15
KLX02 (1696 m)	11.30	0.15	1.99	3.94	177	5.18	15.58

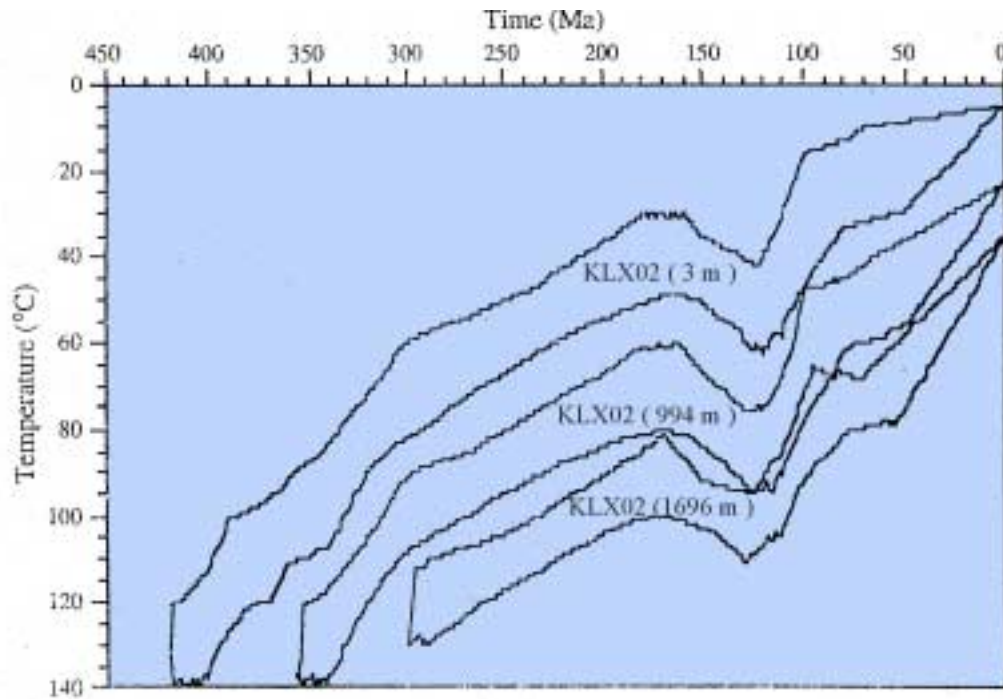


Figure 3-8. Results of inverse modelling using the method of Lutz and Omar (1991), /3-13/, of apatite fission track (AFT) data. Cf. /3-11, 3-12/.

The sample from 994 m cooled from the total annealing into the partial annealing zone at 347 ± 20 m.y. The deepest sample, from 1696 m, displays an age of 295 ± 16 m.y. for the oldest track. The track lengths in the apatites versus standard deviation indicate that the samples were thermally disturbed some time after they had passed the zone of partial annealing. The modelling also demonstrated that a thermal event happened in Mid-Jurassic to Late Cretaceous time, during which the temperature increased in the order of 20 to 30 °C, /3-11, 3-12 and 3-14/.

Conclusions

Figure 3-8 demonstrates that the thermal spectras are nearly identical for all three samples. An assumed thermal gradient of 30 °C/km indicates a total uplift in the order of 3 to 4 km since Late Silurian.

Since today's surface roughly corresponds to the surface exposed 570 m.y. ago (the Subcambrian peneplain), the area must have been heated due to burial. It is well known that the area was covered by Cambro-Silurian sediments. These were, though, thinner than about 500 m and cannot alone be responsible for the high temperatures recorded at the cover/basement contact (the present surface). In contrast, the results are consistent with an uplift and erosion during the Upper Paleozoic of hitherto unknown amounts of sediments. These must have been some 3–4 km thick and were dominantly Devonian sediments, most likely eroded from the uplifted Caledonides.

The apatite fission track data documents a complex thermal history from Late Silurian/Early Devonian to present. The surface sample cooled into the partial annealing zone 410 ± 20 m.y. ago at the 95 % significance level and was exposed to continuous uplift until the Middle Jurassic. During Late Jurassic and Early Cretaceous, a new episode of subsidence took place before the final uplift and erosion, that was completed during the Tertiary.

The results from the fission track analyses were, together with earlier published radiometric datings of rocks in south-eastern Sweden, used to reveal the history of uplift and subsidence for the Äspö region, since the granitoids of the area were formed 1800 m.y. ago /3-11, 3-12/.

3.3.6 Geophysical logging

Nine geophysical logging methods were applied in borehole KLX02 /3-4/:

- Gamma Ray
- Density
- Susceptibility
- Normal resistivity, 0.4 m
- Neutron
- Sonic
- Caliper
- Flow (UCM)
- Deviation

The borehole was also TV-logged at several occasions, see Section 3.3.7, and a borehole radar survey, described in section 3.3.8, was performed as well.

Most geophysical logging methods were conducted to borehole length 1440 m, however, the flow logging as far as to 1650 m. The reason why the lowermost part of the borehole was excluded from the geophysical logging, was an obstacle at 1448 m which fell out from the borehole wall after the flow logging and obstructed passage of borehole probes thereafter.

The selected methods provided additional support for lithological interpretation and fracture determination and enabled analysis of radioactive, magnetic, geometrical and geohydrological characteristics. The flow logging is also commented in Chapter 6.

A detailed description of the geophysical logging methods and instruments used is presented in /3-4/.

The results of the geophysical logging in KLX02 are, together with core logging data, illustrated in the composite diagrams in Appendix 3. Comparison of the geophysical logging data with the PetroCore data reveals a very clear correlation concerning rock type, alteration and fracturing. The following examples may be accentuated:

- Density log. Very distinct density peaks corresponding to greenstone at e.g. 350 m, 390 m, 605 m, 665 m and at 1180 m.
- Sonic log. Evident sonic anomalies correlating with fractured sections at e.g. 380 m, 470 m, 800 m, 870 m and at 1080–1100 m.
- Susceptibility log. Good correlation between altered and crushed sections and low susceptibility at e.g. 430 m, 470 m and 1060–1110 m.
- Normal 0.4 m log. Distinct low resistivity anomalies corresponding to increased fracturing and alteration at e.g. 270 m, 340 m, 390 m, 620 m, 660 m and 1050–1110 m.
- Caliper log. Pronounced anomalies coinciding with fractured sections at e.g. 385 m, 435 m, 800 m and at 815 m.

The flow log, which detects changes in flow rate versus borehole length during pumping (or injection) in the borehole, demonstrated particularly big inflows (> 25 l/min) at 210 m and 249 m and distinct, however minor (1–9 l/min), inflows at 270 m, 314 m, 335 m, 430 m, 797 m, 860 m, 1090 m and 1155 m. The majority of the flow anomalies correspond to increased fracture frequencies, see Appendix 3.

3.3.7 TV-logging

TV-logging was performed in borehole KLX02 at several occasions. Two TV-systems were applied:

- The black & white SKB CCD-camera, described in /3-15/.
- The SKB BIP-system (colour-TV), described in /3-16/.

The TV-inspections of borehole KLX02, conducted at six occasions during 1993–1997, were initiated for several reasons, e.g. for instrument tests and for inspection of the borehole fluid and borehole walls in connection with trapping of down-hole equipment /3-15/. The SKB BIP-system was used (besides for tests of the system itself) for the study of the borehole walls, especially concerning fracturing. For this purpose the BIP-system was involved as a special fracture detecting and orientation tool at the hydrofracturing stress measurements and at the hydromechanical studies performed in KLX02, see Chapter 4. The only separately reported TV-survey was the black & white TV-investigation carried out in connection with problems with borehole equipment getting stuck in the borehole /3-15/. BIPS-investigations performed as an aid for the hydrofracturing operations were reported in /4-1/ and /4-6/.

3.3.8 Borehole radar measurements

Single hole directional and dipole antenna reflection radar measurements were performed in KLX02 with the RAMAC[®]-system and 45–50 MHz antennas /3-17/. The borehole radar survey started with dipole antenna measurements in the borehole interval 209.55–1405.5 m. An obstacle in the borehole at about 1448 m, encountered in connection with earlier investigations (cf. Section 3.3.6), entailed that the measurements could not be continued much beyond 1400 m. The preliminary field results from the dipole antenna survey indicated, that the prospects for successful directional antenna measurements below a borehole length of about 1000 m were limited, mainly due to a very increased salinity of the groundwater below this depth. Saline groundwater causes damping of the radar pulse, hence deteriorating the possibilities to detect radar reflectors. The salinity in KLX02 below 1000 m exceeds a level where radar measurements in general are regarded as meaningful. However, the last visible reflector in the dipole antenna survey is situated at 1392 m. The directional antenna survey was restricted to the interval 209.55–1034.55 m.

The primary objective of the borehole radar measurements was to gain information about the bedrock in the proximity of borehole KLX02 concerning lithological contacts and structural character, including orientation of encountered geological structures.

The radar data is presented as grey scale filtered radar maps /3-17/. One example from the directional antenna survey is given in Figure 3-9.

The dipole as well as the directional antenna mode enabled the study of structures at distances of about 30 m outside the borehole. The amplitude of the direct pulse between transmitter and receiver was used as a support for the interpretation of structures in the borehole, which is based on the fact that in most parts where the radar pulse is damped, the dielectric permittivity is increased. This may indicate a high water or clay mineral content, a factor often related to increased fracturing of the rock.

The directional antenna measurements permitted orientation of several structures intersecting the borehole. All reflectors identified from directional antenna reflection maps are listed in Table 3-5. The table includes:

- a reflection identification number,
- the interpreted location (borehole length) of the intersection in the borehole,
- the angle of intersection between the reflector plane and the borehole axis,
- magnetic azimuth,
- an estimate of the intensity and orientation of the reflector,
- dip/strike,
- the location of and a brief comment on the lithological character of corresponding structures close to or at the point of intersection of the radar reflector, as revealed from the detailed core log.

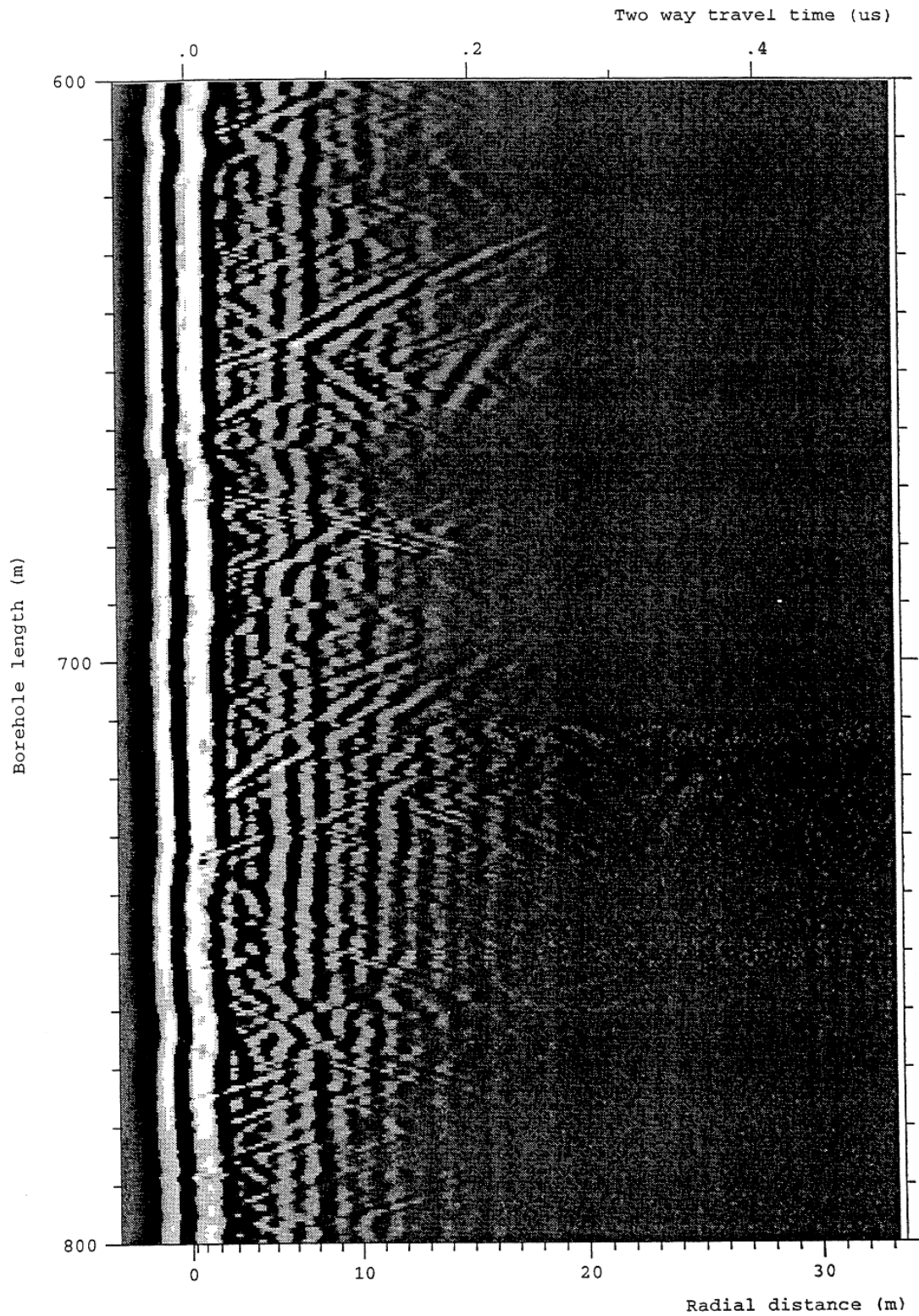


Figure 3-9. Example of a radar reflection map from the directional antenna survey in borehole KLX02. Section 600–800 m, 45–50 MHz antenna, bandpass filtered data, dipole component. After Figure 4.3 in /3-17/.

Table 3-5. Reflectors identified from directional antenna measurements in borehole KLX02. After Table 4.1 in /3-17/.

Reflector (ID-no.)	Position (m)	Angle to borehole axis (Degr.)	Magnetic azimuth T(0)=180 (Degr.)	Strength 1= Weak 2= Medium 3= Strong U=Uncertain	Orientation Dip/Strike	Position of corresponding structure (m)	Geological character
1	51	5	350	2	88/260		In casing
2	195	9	110	1	79/199		In casing
3	197	30	30	1	66/118		In casing
4	212	16	260	1	73/352	208– 212	Oxidized fractures
5	251	38	90	2	53/175	252– 253	Crushed and fractured granite
6	262	34	200	2	49/292		Weak tectonization
7	269	35	200	3	48/292	266– 269	Crushed and fractured granite
8	271	23	150	3	61/238	266– 269	Crushed and fractured granite
9	280	19	210	1	65/301		
10	296	19	270	2	72/002		
11	341	59	180	3	24/270	338– 340	Crushed and fractured granite
12	367	59	200	1	24/295	355– 358	Greenstone
13	388	61	270	2	30/012	384– 389	Crushed and fractured greenstone
14	394	57	310	2	38/047	384– 389	Crushed and fractured greenstone
15	396	44	310	1	51/045	384– 389	Crushed and fractured greenstone
16	422	36	180	2	47/270		
17	423	46	200	1	37/293		
18	446	36	210	2	48/303	430– 444	Oxidized zone, partly crushed
19	457	6	240	1	81/331	455– 470	Oxidized zone, partly crushed
21	465	13	150	2	71/239	455– 470	Crushed, fractured, oxidized
20	472	31	210	3	53/302	466– 468	Crushed
22	491	38	230	1	48/325	490– 491	Sealed vein?
23	515	26	210	2	58/302	515– 517	Crushed, fractured, oxidized zone
24	529	47	220	2	38/316	530– 531	Fractured granite
25	541	7	190	1	76/280	540– 554	Greenstone
26	546	29	290	1	64/023	540– 554	Greenstone
27	566	32	200	2	52/292	559– 563	Oxidized zone
64	602	31	130	1	55/216	596– 601	Oxidized zone
28	605	11	240	3	76/331	604– 609	Greenstone
29	620	29	220	2	56/313	623– 624	Crushed granite
30	628	13	180	1	70/270	630– 632	Greenstone
31	628	23	260	2	66/353	630– 632	Greenstone
32	644	35	230	2	51/324		
33	655	47	210	3	37/304	659– 666	Fractured, crushed greenstone
34	660	49	210	1	35/305	659– 666	Fractured, crushed greenstone
35	662	26	210	3	58/302	659– 666	Fractured, crushed greenstone
36	667	64	250	2	24/355	659– 666	Fractured, crushed greenstone
37	702	21	230	1	65/322	700– 707	Greenstone
38	706	40	220	1	45/314	700– 707	Greenstone
39	716	43	210	2	41/304	709– 727	Greenstone
40	729	11	230	2	75/321	724– 733	Fractured greenstone
41	732	26	250	2	62/343	724– 733	Fractured greenstone
42	739	17	0	2	81/180	738– 740	Oxidized zone
43	741	36	270	1	53/005	738– 740	Oxidized zone
44	753	47	350	1	50/081	755– 759	Crushed, fractured greenstone
45	778	51	240	2	36/338	773– 775	Greenstone
46	784	46	260	2	43/357	778– 780	Crushed, fractured greenstone
47	792	44	240	2	43/336	786– 788	Crushed, fractured greenstone
48	809	45	70	1	48/154	807– 808	Crushed, fractured, fine-grained granite
49	818	40	220	2	45/314	801– 855	Crushed, fractured greenstone
50	825	34	220	2	51/314	801– 855	Crushed, fractured greenstone
51	838	30	130	1	56/217	801– 855	Crushed, fractured greenstone
52	853	46	220	1	39/315	801– 855	Crushed, fractured greenstone
53	862	36	240	2	51/335	860– 868	Crushed, fractured granite
54	867	36	240	1	51/335	860– 868	Crushed, fractured granite
55	887	38	270	1	52/005	880– 902	Crushed, chloritised greenstone
56	908	37	280	1	55/015	903– 920	Crushed, chloritised greenstone
57	917	45	270	1	45/007	903– 920	Fractured greenstone
58	925	44	260	2	45/357	920– 928	Fractured Äspö diorite
59	954	48	260	1	41/358	949– 959	Fractured, epidotised greenstone
60	983	34	240	1	53/335	978– 979	Narrow, crushed zone
61	992	30	260	1	59/354	1002–1006	Narrow, crushed zones
62	1005	57	260	1	32/001	1002–1006	Epidotised, crushed zones
63	1027	50	260	1	39/358	1027–1028	Crushed greenstone

Some sections in borehole KLX02 exhibit a low amplitude of the direct pulse in the directional antenna measurements. These sections are presented in Table 3-6, each with one or several references to the corresponding reflector(s) and to the location of and lithological character of any adjacent structure.

The dipole antenna reflectors, described in detail in /3-17/, are in this report illustrated only for borehole section 1035–1405.5 m, see Figure 3-12, where directional antenna measurements were not performed.

The agreement between reflectors experienced in the directional respectively the dipole antenna measurements is good, and the locations of 48 out of a total of 64 directional antenna reflectors correspond to the location of dipole antenna reflectors /3-17/.

Figure 3-10 is a Wulff-net plot of normals to all oriented radar reflectors in KLX02. A clustering of normals representing the strike $290-20^\circ$ (magnetic azimuth $T(0)=180^\circ$) is exposed in the plot, corresponding to dips towards the north-east and south-east. All oriented radar reflectors representing greenstone dikes and structures within the dikes can be studied in another Wulff-net plot, see Figure 3-11. The strike and dip of the dikes and of structures within them seem to be approximately the same as those of all radar reflectors, especially reflectors prevailing from about 800 m and downwards to the end of the directional radar survey at about 1035 m.

Table 3-6. Sections in borehole KLX02 exhibiting low amplitude of the direct pulse in the directional antenna measurements. After Table 4.2 in /3-17/.

Low amplitude (m)	Corresponding directional antenna (No.)	Position of structure (m)	Geological character
265– 274	7, 8	266– 269	Crushed and fractured granite
338– 345	11	338– 340	Crushed and fractured granite
384– 395	13, 14	384– 389	Crushed and fractured greenstone
430– 475	18, 19	430– 470	Oxidized zone, partly crushed
	21	455– 470	Crushed, fractured, oxidized
	20		Does not reach borehole
520– 545	24	530– 531	Fractured granite
	25	540– 554	Greenstone
663– 673	35, 36	659– 666	Fractured, crushed greenstone
687– 705	37, 38	700– 707	Greenstone
730– 747	40, 41	724– 733	Fractured greenstone
	42, 43	738– 740	Oxidized zone
752– 761	44	755– 759	Crushed and fractured greenstone
780– 785	46	778– 780	Crushed and fractured greenstone
801– 826	48, 49, 50	801– 855	Crushed and fractured greenstone
848– 874	52	801– 855	Crushed and fractured greenstone
	53, 54	860– 868	Crushed and fractured granite
884– 905	55	880– 902	Crushed, chloritized greenstone
913– 930	57	903– 920	Fractured greenstone
949– 963	59	949– 959	Fractured, epidotitized greenstone
990–1020	60, 61, 62	1002–1028	Narrow, crushed zones

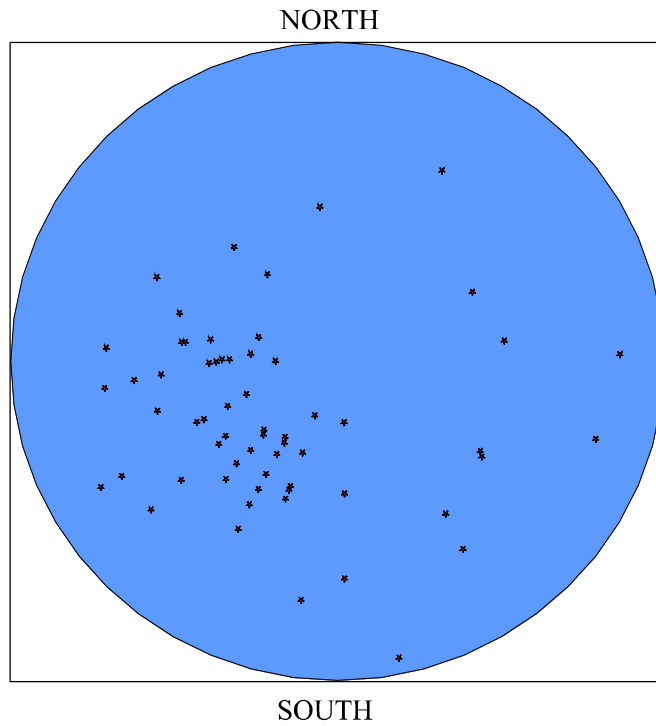


Figure 3-10. Wulff-net plot of normals to all oriented radar reflectors in borehole KLX02. After Figure 5.1 in /3-17/.

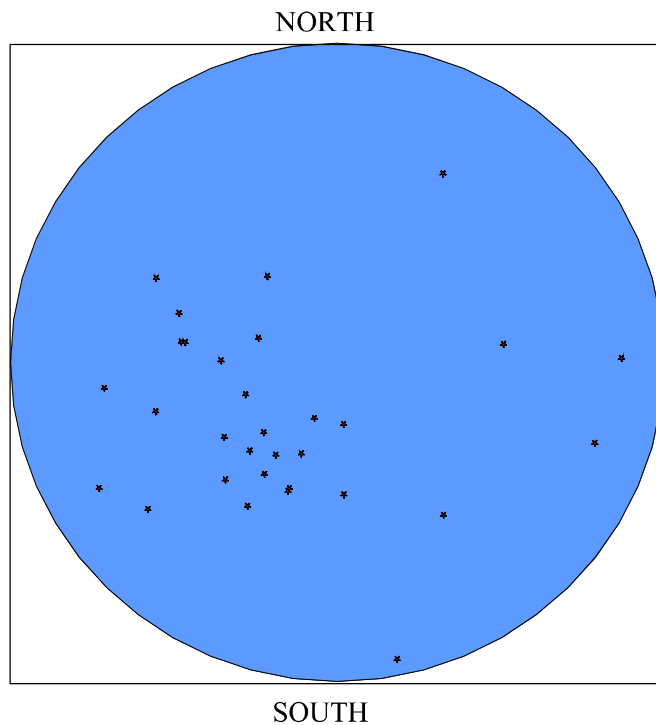


Figure 3-11. Wulff-net plot of normals to oriented radar reflectors representing greenstone dikes and structures within greenstone dikes in borehole KLX02. After Figure 5.2 in /3-17/.

Only a few narrow sections of fine-grained granite were discovered in the drill core from the part of the borehole where directional antenna measurements were performed. One of them, at 809 m, exhibits a reflector with the orientation 48/154 in the radar map. Also six relatively limited sections of Äspö diorite exist in this part of the borehole. Only one of them displays a radar reflection. The orientation is 45/357, i.e. sub-parallel to the orientation of the majority of greenstone dikes.

3.3.9 Summary of the geological conditions in connection with borehole KLX02

In Figure 3-12 a synthesis is presented of lithological and structural data of the bedrock at and close to borehole KLX02. Data is based on the PetroCore logging, analysis of drill cuttings and borehole radar measurements. Supporting data was supplied from the geophysical borehole logging and TV-logging. The lithological information from the drill core and from the sampling of drill cuttings, covering a total borehole length of 1700.5 m, is in the first column of Figure 3-12 compressed to a length of about 19 cm. In the next column the distribution along the core of the total number of natural fractures (however, crush zones excluded) is illustrated. (A more detailed information of these parameters is given in Appendix 3.) The location of all radar reflectors encountered at the directional antenna survey (below 1035 m the dipole antenna survey) is displayed in the third column. The fourth and fifth columns provide a graphical overview of the variation of dip and strike of the radar reflectors. For every 100 m of the directional antenna surveyed part of the borehole, each dip and strike direction is illustrated in a circle diagram.

Lithological conditions

The rock type dominating the drill core (and drill cuttings) of borehole KLX02 is Småland granite, which constitutes about 63 % of the total borehole length (cf. Figure 3-7). The following borehole sections are totally dominated by Småland granite:

- 65– 540 m (65–200 m refers to drill cuttings)
- 960–1375 m
- 1405–1450 m

About 25 % of the core length is composed of Äspö diorite. The following seven sections, most of them rather short, consist of this rock type:

- 10– 68 m (drill cuttings)
- 920– 928 m
- 1373–1380 m
- 1450–1532 m
- 1533–1590 m
- 1609–1613 m
- 1616–1700.5 m

Obviously, the Äspö diorite is the predominant rock type below 1450 m.

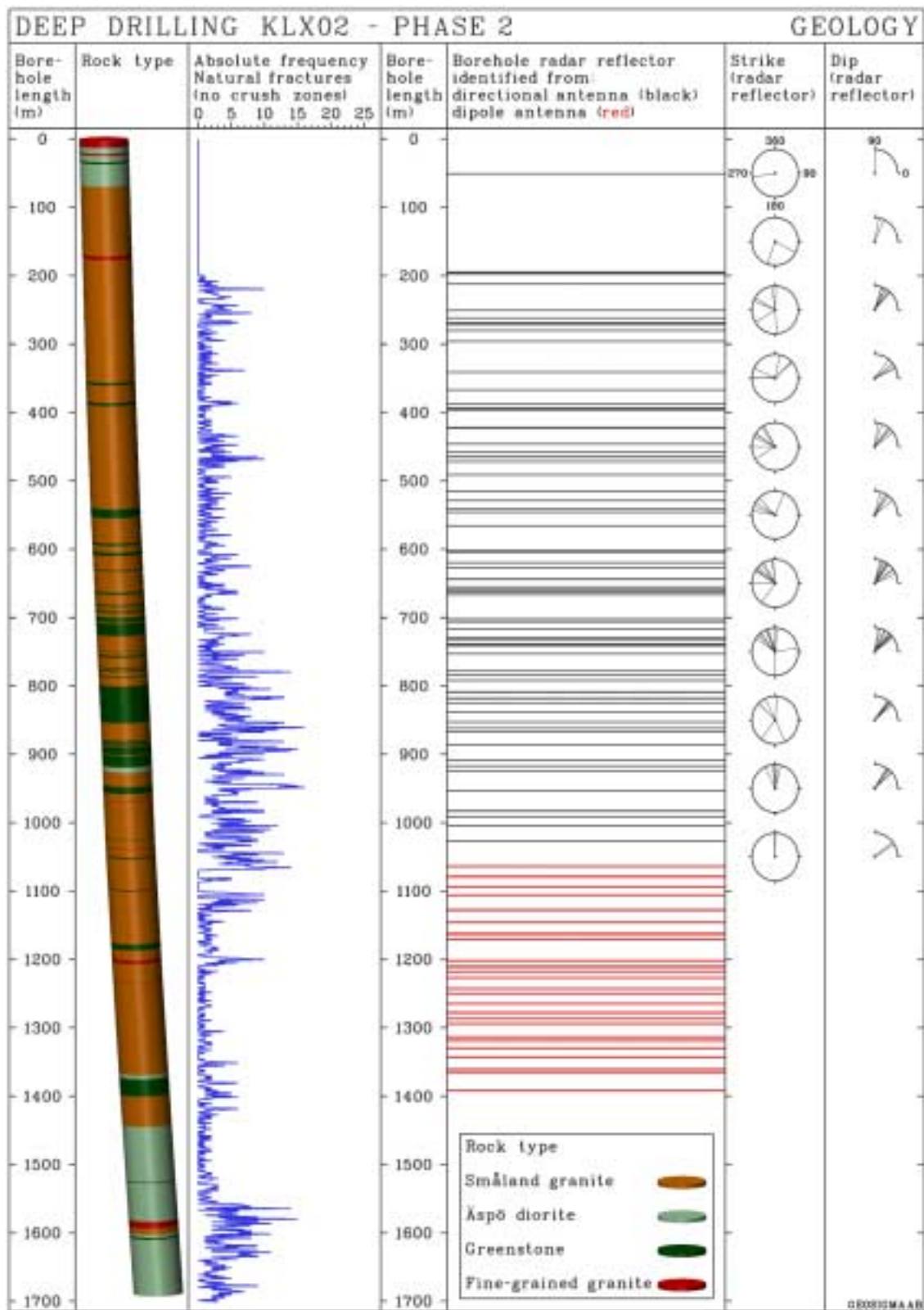


Figure 3-12. The lithological and structural characteristics of borehole KLX02.

Greenstone occurs in the core as a large number of 5–10 m wide dikes, found from top to bottom. A few of them are wider than 10 m, e.g. at 1380–1405 m. Especially in the more than 400 m long section 540–960 m the share of greenstone dikes is abundant. The section between 800 m and 855 m is totally dominated by this rock type. The deepest greenstone dike in the borehole is found at 1614–1616 m. In total, greenstone occupies about 10 % of the drill core.

Fine-grained granite constitutes less than 2 % of the total length of the drill core. It emerges in a few 1–10 m wide sections of which the most important are found at:

- 0– 10 m (drill cuttings)
- 19– 22 m (drill cuttings)
- 169– 175 m (drill cuttings)
- 1204–1210 m
- 1590–1600 m

Several minor veins of fine-grained granite were mapped in section 700–1040 m.

Fracturing

The mean fracturing of the drill core from KLX02 is 2.36 fractures/m (crushed sections excluded), which is a lower frequency than for the other deep borehole at Laxemar, KLX01 (2.57 fractures/m), and essentially lower than for the two deep boreholes at Äspö, KAS02 and KAS03 (3.65 respectively 3.71 fractures/m), see Figure 3-7.

In rough outline, the PetroCore logged part of borehole KLX02 (between about 203–1700.5 m) may, concerning fracture character, be divided into four sections:

- 203– 730 m
- 730–1120 m
- 1120–1550 m
- 1550–1700.5 m

Section 203–730 m

In general, the fracture frequency of this section is in the range of 1–3 fractures/m. As a mean, one 1–2 m wide section with increased fracturing, mainly due to crushed rock, occurs at every 50 m. The fracture frequency in these highly fractured parts of the core may exceed 20 fractures/m.

Section 203–730 m is dominated by Småland granite. However, two intervals of Äspö diorite, at 520–540 m and 708–727 m, occur, the first one and the lower part of the second displaying increased fracturing. Inclusions of greenstone veins appear, especially between 550 m and 730 m. Epidote is a common mineral in the highly fractured parts of the core, where also oxidation is frequent.

The number of radar reflectors from the directional antenna survey is, as a mean, 7.2 per 100 m borehole length. The mean distance between radar reflectors is 13.9 m (range of variation 0–45 m). The corresponding figures for the dipole antenna

survey is 7.4, 13.5 m and 1–65 m. 37 % of the directional reflectors expose a dip in the range of 46–60° and 29 % in the range 61–75°, i.e. middle-steep and steep reflectors dominate. The same conclusion can be drawn from the dipole survey. 11 % of the reflectors are displayed in the sector 16–30°.

The strike of 50 % of all directional reflectors down to 730 m borehole length is found in the sector 270–315°, and 24 % in the sector 315–360°. Hence, a strike dominance between west and north (74 %) is prevailing. Other important directions are 0–45° (11 %) and 225–270° (8 %).

Section 730–1120

The fracture frequency increases at about 730 m and maintains a high level, in general 3–10 fractures/m, however with frequent peaks much exceeding 10 fractures/m, as far as to about 1120 m. However, sections of low fracture frequency (< 3 fractures/m) exist also in this part of the borehole, although the total length of those is small.

Compared to the lithology of the previous, relatively homogeneous section, this part of the borehole exhibits a different, lithologically more heterogeneous character. Slightly less than 50 % of the total core length is composed of Småland granite. Greenstone dikes constitute nearly 30 % and Äspö diorite more than 20 %. According to /3-4/, borehole KLX02 probably intersects one or even two of the major discontinuities indicated by the aerogeophysical survey of the Simpevarp area. The interval 730–1120 m may represent this intersection, which would explain the increased fracture frequency. An alternative interpretation is presented in /3-33/, cf. Section 3.4.

The type of mineral alteration is diversified. Between 730 m and 910 m oxidation occurs frequently. In minor parts of the core, mainly between 910 m and 1068 m, also epidote and chlorite is found. Section 1068–1087 m is strongly weathered. Finally, in section 1105–1111 m the core is again characterized by oxidation.

The number of dipole radar reflectors per 100 m borehole length in section 730–1120 m (the directional antenna survey ended at 1035 m), is 7.7, a slight increase compared to the previous section. The mean distance between reflectors is 13.0 m (range of variation 1–37 m). 48 % of the directional antenna reflectors in section 730–1035 m are dipping in the range of 46–60° and 43 % in the range 31–45°. In other words, middle-steep dips strongly dominate. The dipole survey gives, concerning dips, the same impression. No reflectors flatter than 30° were encountered in the directional survey.

Data from the directional antenna survey between 730 m and 1035 m indicates a strong strike dominance in the sectors 316–360° (48 %) and 270–315° (13 %). Hence, strike directions between west and north are the most frequent also in this section, although a tendency of increased frequency of northerly directions is obvious. This is confirmed by the fact that many radar reflectors also strike in the range 0–15° (22 %). The radar reflector strikes described in this and the previous borehole section may be compared to the Wulff-net plot in Figure 3-10, in which the same set of radar data is described in an alternative way.

Section 1120–1550 m

Below 1120 m the fracture frequency decreases significantly, and section 1120–1550 m displays the most low-fractured part of the borehole. Here, the fracture frequency falls below 2 fractures/m over long distances. Three crushed zones occur, separated by a distance of respectively 135 m and 110 m.

In the upper 330 m of this borehole section, Småland granite constitutes about 85 % of the drill core. The share of greenstone is 8 %, while the rest of the core is composed of about similar proportions of Äspö diorite and fine-grained granite. Äspö diorite occupies the lower 100 m, except for a 1.5 m wide greenstone dike at 1532 m.

Alteration of the rock is very uncommon, although signs of oxidization and epidotization are present.

Directional radar measurements were not performed in this section. The dipole radar survey ended at 1405.5 m. The last reflector was identified at 1392 m, before the attenuation caused by increased salinity was too strong. The average number of radar reflectors per 100 m borehole length is 8.5 in section 1120–1392 m. The mean distance between reflectors is 11.8 m (range of variation 1–15 m). Thus, in spite of a significant decrease of fracture frequency, an increase in radar reflector frequency is observed in the radar measured part of the section. 57 % of the radar reflectors from the dipole antenna survey display an angle towards the borehole axis (which is dipping 5° from the vertical plane) in the span of 46–60° and 30 % an even steeper angle. 13 % of the structures may be regarded as horizontal or sub-horizontal (0–45°).

Section 1550–1700.50 m

Finally, the deepest parts of borehole KLX02, especially between 1550–1640 m and from 1667 m to the borehole bottom, are again exposed to increased fracture frequency. The amplitudes resemble those encountered in the borehole interval 725–1120 m. The short section 1640–1667 m, though, exhibits a “normal” fracture frequency, below 4 fractures/m. According to /3-4/ the highly fractured parts may be interpreted as representing major fracture zones.

As mentioned before, the bottom part of borehole KLX02 is totally dominated by Äspö diorite, interspersed only by a thin vein of greenstone at 1532 m and a section of about 26 m length at 1590–1616 m, where fine-grained granite, Småland granite, Äspö diorite and greenstone are alternating.

Radar data are lacking from this part of the borehole, since the deepest borehole radar survey (dipole antenna) was concluded at 1405.5 m.

3.4 The structural character of the Laxemar area – studies performed during and after Phase 2

The significance of a good lithological-structural description of a site in order to provide a framework for modelling mechanical stability, thermal properties, groundwater flow, groundwater chemistry and transport of solutes was stressed at the beginning of this chapter. The background information needed to obtain a reliable lithological-structural description of the Laxemar area is far from complete. However, the existing structural data has been thoroughly analysed, and attempts have been made to present at least simplified lithological-structural models of the site. Four studies aiming at erecting such models (with emphasis on the structural character) will be presented below:

- A lineament study reported in /3-18/.
- A study of radar reflectors in boreholes KLX01 and KLX02 reported in /3-19/.
- A lineament study combined with aerial and ground geophysical data (Roy Stanfors, pers. communication).
- A reflection seismic survey and a VSP-study (Vertical Seismic Profiling) performed in borehole KLX02 /3-33/.

Method tests of half-regional resistivity measurements, electrical soundings and transient electromagnetic soundings, presented in Section 3.4.4, also gave contributions to the structural interpretations.

During drilling of borehole KLX02, hydraulic responses were observed in borehole KLX01 using the monitoring system previously installed in this borehole, /3-20, 3-21/, situated approximately 1 km NE of KLX02, see Figure 1-2. Therefore, an interference test between the two boreholes under more controlled conditions was regarded as a task of great interest for the hydro-geological test programme within Phase 2 (see Chapter 6). Interpretation of hydraulic interference tests in fractured rock is one example of a situation when a structural model is required for analysis of the test results. The first two of the studies mentioned above were initiated with the specific aim to provide a simple structural model of the rock volume between boreholes KLX01 and KLX02, to serve as a tool for interpretation of the interference test. The third, later performed study, is another contribution to this issue, based on more extensive background material. The goals for the reflection seismic survey, performed still later and not focused primarily on the interference test, are described in Section 3.4.5. The VSP-measurements provided some support for the reflection seismic survey.

3.4.1 Study of lineaments

The strategy for the lineament study reported in /3-18/ implied investigations and/or analysis and synthesis according to the following four items:

1. Study of the drill core from KLX02.
2. Analysis of digital elevation modelling (DEM) data and airborne geophysical measurements (magnetic and VLF).

3. Field survey including an inventory and characterization of topographical lineaments.
4. Analysis of borehole radar reflectors from the directional radar antenna survey in borehole KLX02.

Certain investigations of the drill core of borehole KLX02, focused on fracturing and the occurrence of greenstone and mylonites, was regarded necessary, since the lineament study later reported in /3-18/ was performed at a stage, when the detailed core mapping was not yet completed. Nor were the results of the radar surveys performed in borehole KLX02 yet published. However, results from the radar surveys were available by personal communication with the responsible geophysicist.

Digital elevation modelling (DEM) and aeromagnetic analyses performed prior to Phase 2 revealed lineaments of mainly four orientations: N-S, NE-SW, NW-SE and E-W /3-9/, /3-22/, /3-23/ and /3-24/. The correlation between steep topographic gradients and aeromagnetic anomalies is generally good /3-24/. Assuming that such lineaments constitute the intersection of fracture zones with the ground surface, six higher order candidates appropriate for intersection with KLX01 and KLX02 are, according to /3-18/, present in the study area, see Figure 3-13.

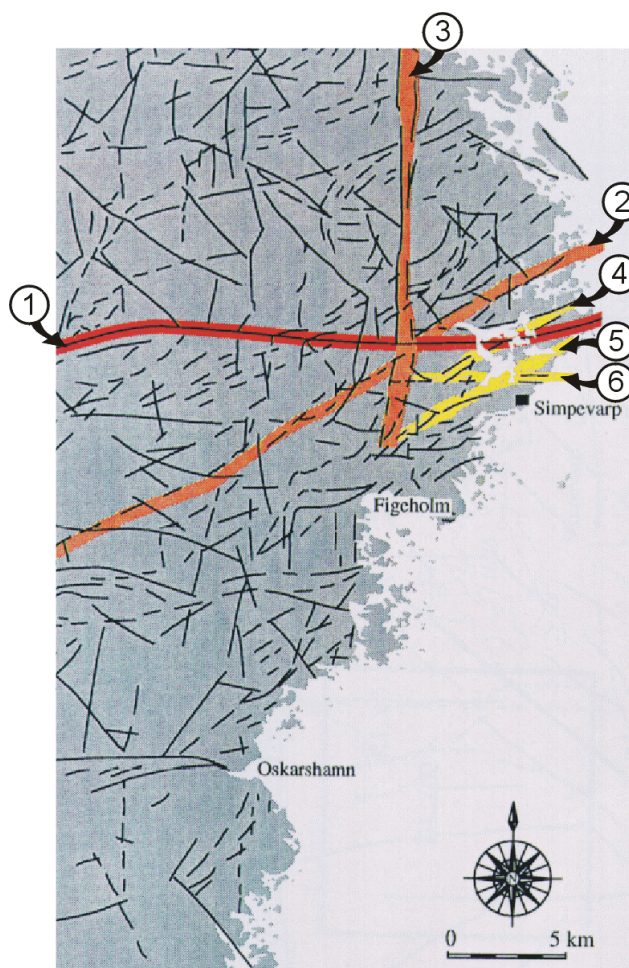


Figure 3-13. Overview of high and low order lineaments in the Laxemar-Simpevarp-Äspö area. Modified after Figure 3 in /3-18/.

The most prominent of these six structures, no. 1 in Figure 3-13, is trending E-W across the Laxemar area and continues across the island of Äspö. Inferred from surface investigations on Äspö, where a trench has been excavated across the structure, the dip of the structure is steep, in the range of 75°N–90°. Two lineaments, trending NE-SW respectively N-S close to the Laxemar area (no. 2 and 3), are less continuous, but equally prominent. The dip of the first structure is basically unknown. However, surface outcroppings of NE striking mylonites (locality 2 in Figure 3-15) confirm the existence of such a structure. The dip of the mylonite structures is 80–85°. Finally, the high order lineament trending N-S (no. 3) is well exposed in some of the quarries around the Götemar granite found a few km north of the Laxemar area. Where exposed, it consists of steep sub-parallel faults and joints with a large (> 50 m) lateral extent.

In a figure of larger scale, e.g. Figure 3-14, the higher resolution reveals that the NE trending structures, e.g. no. 4, are relatively persistent, while the large N-S striking lineaments (no. 3) exhibits a more diffuse and discontinuous character. This figure also reveals several lower order lineaments.

During the ground search performed within the frame of the investigation reported in /3-18/, an attempt was made to locate and characterize some of the major and minor lineaments illustrated in Figure 3-15 (of which several correspond to lineaments in Figures 3-13 and 3-14). One significant experience from the tunnel excavation at the Äspö HRL is that large scale structures, such as the high order structure trending E-W across the Laxemar area, can be relatively dry, whereas seemingly insignificant structures such as the short NE striking structure immediately south of Äspö (better known in the Äspö-literature as zone NE-1, see Figure 3-14) may be very permeable and fractured. This emphasizes the fact that identification and characterization also of lower order lineaments may be of importance in order to erect a structural model of a site as a basis for hydro-geological interpretations.

Although the degree of bedrock exposure is high in the Laxemar area, erosion processes have effected most fracture zones to such a degree that they are inaccessible for observation /3-18/. A few exceptions (localities 2, 3 and 4 in Figure 3-15), though, confirm the presence of structures of interest for the study presented in /3-18/. A complicating factor for the interpretation is, however, the fact that also other structures, equally prominent on the surface, but not detected by aeromagnetic survey or digital modelling, were discovered.

Finally, the reflectors from the directional antenna survey described in section 3.3.8 were analysed. Three of the strongest radar reflectors in borehole KLX02 were projected to the ground surface, see Figure 3-15. An attempt was made to match the reflectors with observed geophysical and topographical anomalies. The three reflectors were selected through personal communication with the performer of the radar survey, before the interpretation of the radar investigation was concluded. In the final list of radar reflectors from the directional antenna survey presented in Table 3-5 only one reflector seems to fit the selection made in /3-18/. This is reflector no. 2, striking 199°, corresponding to the projected reflector no. 1 in Figure 3-15. The second and third projected radar reflectors must be regarded as more unreliable.

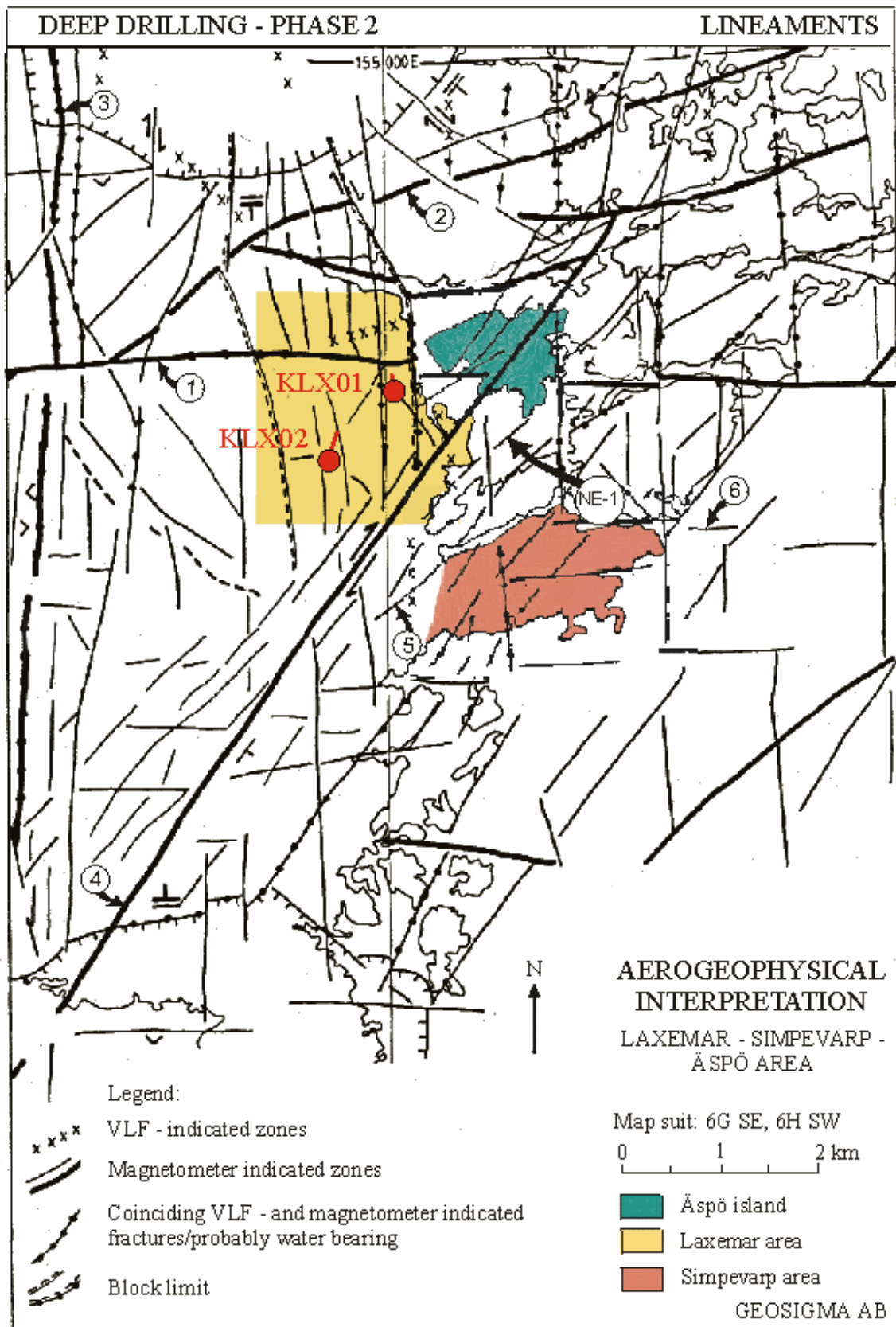
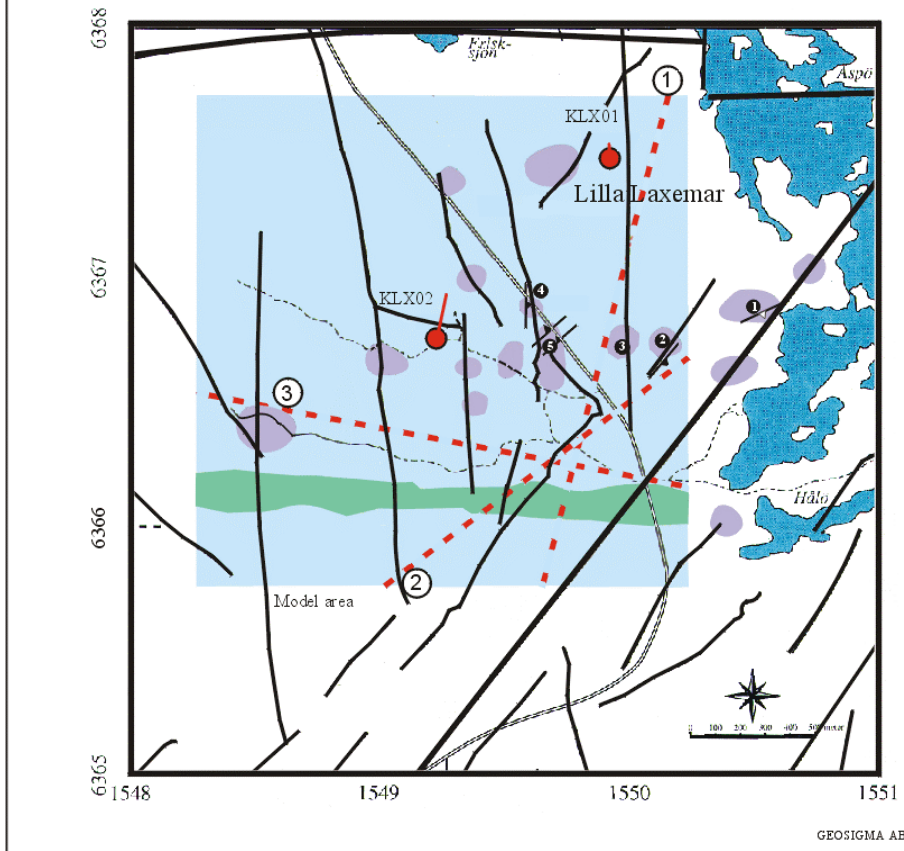


Figure 3-14. Aerogeophysical interpretation of the Äspö-Simpevarp-Laxemar area with surroundings. Modified after Figure 6.2 in /3-9/. A variety of this figure is found in /3-18/ (Figure 4). The lineaments numbered 1, 2...6, correspond to the numbered lineaments in Figure 3-13.








LEGEND	
	= major lineament (from DEM - analysis)
	= minor lineament (from DEM - analysis)
	= radar reflector found in KLX02 projected to the ground surface. (Munier, 1993)
	= field checked localities
	= greenstone dikes encountered in KLX02 and projected to the ground surface. (Munier, 1993)

Figure 3-15. Map of major and minor lineaments in the Laxemar area and localities investigated during the study presented in /3-18/. Structures projected from the drill core of KLX02 (greenstone dikes) and three radar reflectors projected from directional radar measurements in borehole KLX02 are also marked in the figure. Modified after Figure 5 in /3-18/.

It was concluded that the match between radar reflectors and geomagnetic and topographic lineaments is scanty. Even if an error of $\pm 10^\circ$ in the determination of orientation of the radar reflectors, and a natural variability of strike and dip of 15° is assumed, the reflector striking NNE (projection no. 1), which seems to match the geophysical lineaments relatively well, fits poorly with dips observed on outcrops. The unreliable reflector striking WNW (no. 3) could not be matched at all with any geophysical lineament. The uncertain projection no. 2, striking NE, fitted, like was the case with no. 1, inadequately with dips observed on outcrops.

In the synthesis presented in /3-18/ all available information is combined in order to infer a 3D-geometry of geological structures. The starting-point for erecting a 3D-model was the directional radar survey in KLX02, since this method permits the study of the lateral extent of geological structures several tenths of metres from the borehole. However, boreholes KLX01 and KLX02 are separated from each other by a distance of about 1000 m. This is therefore the minimum size of any structure intersecting both boreholes. The three intense radar reflectors mentioned above were therefore assigned the shape and size of a flat circular disc with a radius of 1.5 km. The projection of these reflectors on the ground match observed aeromagnetic or topographic lineaments very crudely, as demonstrated above. Several different explanations to this fact are conceivable. In /3-18/ several arguments are advocated to support the explanation that the extensions of the three reflectors in question are overestimated, implying that the reflectors are not able to intersect both boreholes.

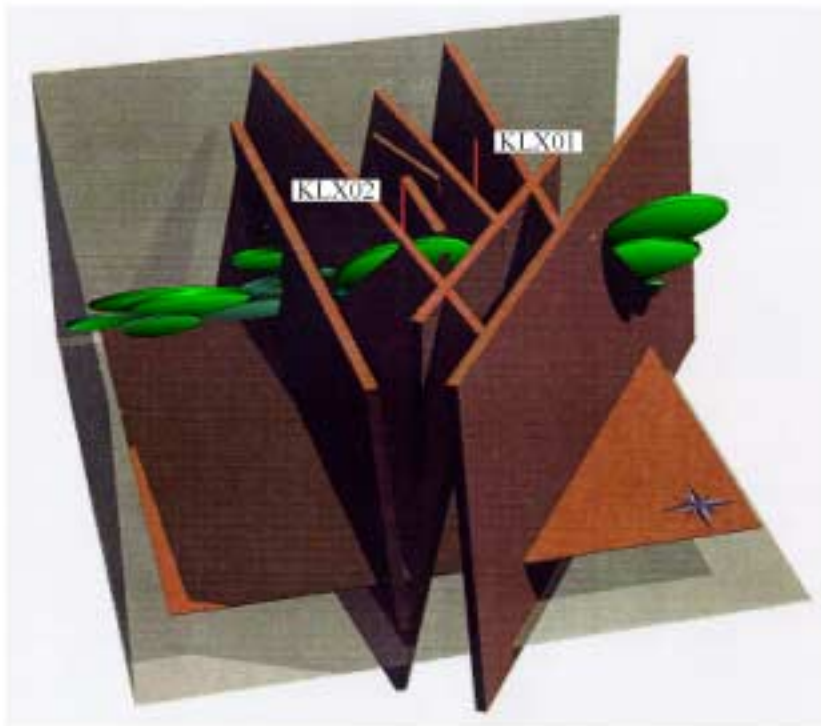
However, a few possibilities are in /3-18/ still regarded as left open for a direct hydraulic communication between the two boreholes. As pointed out above, directional radar measurements in KLX02 were limited to a borehole length of about 1035 m. Several sections of increased fracturing exist from 1035 m to the bottom of the borehole (see Section 3.3.9). They may well represent intersections of fracture zones, and it cannot be excluded that the lateral extent and dip of one or several of them is such, that they (it) intersect(s) both boreholes. Available data does not, however, permit the confirmation of such a conclusion.

A second possibility is represented by an assumed sub-horizontal fault (dip $\pm 15^\circ$) encountered at 1602 m in the drill core of KLX02. With a sufficient lateral extent, this structure would have the potential of intersecting also borehole KLX01. With a less extent, it may still be feasible for this structure to connect steep fracture zones intersecting KLX01, thus indirectly connecting boreholes KLX01 and KLX02. (Among the reflectors observed from the reflection seismic survey, see Section 3.4.5, reflector F is subhorizontal. The extension is limited, but intersects, if extrapolated, borehole KLX02 at c. 1600 m borehole length.)

A third structure with a potential of intersecting both boreholes and the ground surface is constituted by the swarms of greenstone sheets observed in the drill core of KLX02, striking approximately E-W and dipping N, as revealed in /3-17/. It is regarded as improbable that the lateral extent of a single sheet is such that it may intersect both boreholes. Hypothetically, these sheets may, however, be components of a larger structure with the potential of intersecting both the surface and the boreholes. A structure of this nature would constitute some kind of a semi-direct connection between the boreholes. A surface projection of such a structure, based on a number of encountered greenstone sheets in KLX02, is suggested in Figure 3-15. The projection does not correspond to aeromagnetic- and VLF-lineaments. The digital element modelling did, however, show a weak topographic lineament with the appropriate strike and location.

Figure 3-16 is a graphical condensation of the hypotheses presented in the study of /3-18/. Available aeromagnetic lineaments, surface and sub-surface information is here combined and modelled in 3D-space. The synthesis postulates that no single structure is responsible for hydraulic responses detected in borehole

KLX01 during pumping in KLX02. Instead, fracture zones of various orientations interact with swarms of fractured meta-volcanic sheets to form a network of conductors indirectly connecting boreholes KLX01 and KLX02.



GEOBOMA AB

Figure 3-16. A 3D-model of geological structures in the Laxemar area. Modified after Figure 7 in /3-18/.

3.4.2 Correlation of radar reflectors between boreholes KLX01 and KLX02

Radar measurements with the RAMAC[®]-system were performed in borehole KLX01 prior to Phase 2 using the dipole antenna equipment /3-25/ and during Phase 2 in (part of) borehole KLX02 with both dipole and directional antennas /3-17/, see section 3.3.8. The results were used in a special study aiming at correlation of radar reflectors between boreholes KLX01 and KLX02 /3-19/. The attempt to do this was accomplished with support from the computer programme CROSHOLE, which is part of the RAMAC[®] software. With this programme, extrapolation of radar reflectors encountered in a specific borehole to an arbitrary number of other boreholes is possible. The programme hereby calculates the positions of intersection and the intersection angles. Correlation of radar reflectors between boreholes situated relatively close to each other, i.e. some tenths of metres up to almost 100 m, has previously been performed successfully several times, see for example /3-26/. The considerable distance, c. 1000 m, between boreholes KLX01 and KLX02 renders the possibilities for a successful result more difficult. The method was, however, judged as worth trying, partly for the reason of testing the method limitations concerning distances between the involved boreholes.

The radar reflectors from the directional antenna survey in KLX02 served as a starting-point for the correlation study. Only radar reflectors in KLX02 fulfilling one or several of the following criteria were regarded as suitable for the correlation attempt:

- reflectors with strong and persistent character,
- reflectors occurring at sections with a low radar amplitude of the direct pulse,
- reflectors obtained at spinner measurement anomalies.

A low radar amplitude indicates a prominent section with increased fracture frequency. Spinner measurements represent, as described in section 3.3.6, a method for indicating water flow out from or into a borehole versus depth during pumping from, respectively injection of water into the borehole.

The following procedure was applied for the correlation attempt. Data assigned to each selected reflector in borehole KLX02 was punched into the CROSHOLE calculation programme in the following order: ID-number of the reflector, depth of intersection of the reflector with the radar measured borehole, and dip/strike of the reflector. After input of the geometrical data for borehole KLX01, it was possible to calculate the intersection depth and the radar angle in this borehole.

The next step was to check borehole KLX01 at the intersection depth received from the CROSHOLE programme regarding reflectors with radar angles (angles to the borehole axis) satisfying the calculated angles. The fitness between calculated radar angles and such obtained from the radar survey in KLX01 was considered important in the correlation procedure. If no reflector with a suitable radar angle existed at the calculated intersection depth, the radar diagram was searched upwards and downwards for about 100 m, in order to, if possible, locate a reflector displaying a suitable radar angle.

When matching reflectors were discovered in both boreholes, the geological character of the two intersections were compared. If the resemblance in geological character and of geometric parameters between the boreholes was satisfying, the correlation was classified as “good”. As mentioned above, it should though be emphasized, that the large distance between the two boreholes implies a high degree of uncertainty in the correlation process.

A total number of 59 radar reflectors were selected for the correlation process according to the three selection criteria. 20 of those two or three criteria coincided, which means that the number of reflectors included in the study was reduced to 39. The distribution of the directional radar reflectors in KLX02 according to the three mentioned selection criteria were the following:

- 15 reflectors with strong and persistent character,
- 25 reflectors associated with low radar amplitude sections (9 coincident with the point above),
- 19 reflectors falling together with spinner anomalies (7 coincident with the first point, 4 with the second point).

Seven of the selected 39 radar reflectors in KLX02 were regarded as possible to correlate between boreholes KLX01 and KLX02 according to the method depicted. In Table 3-7 these reflectors are listed and described concerning geological character. Also the candidate reflectors in KLX01 possible for correlation with KLX02 are listed and described. The locations of these reflectors projected to the ground surface are illustrated in Figure 3-17, and a vertical cross section between the boreholes is presented in Figure 3-18. The seven correlated reflectors are briefly commented on below.

Two reflectors, no. 8 and 36, embodied all three selection criteria. The correlation of no. 8 was, though, not convincing, and no. 36 was interpreted to intersect at a deep section in KLX01, where radar measurements have not been performed. However, the agreement of geological character of this reflector between the boreholes was good. Reflector no. 36 exhibits a flat dip (24°) and the projected position at the ground surface hits far away from borehole KLX02, see Figure 3-17.

Reflector no. 11 was selected from criteria no. 1 and 3 (strong and persistent character and congruent with a spinner measurement anomaly). The correlation of the reflector was considered as “good”.

The correlation of reflector no. 14, which was selected from criteria no. 1 and 2, was not persuasive due to disagreement of geological character between the boreholes.

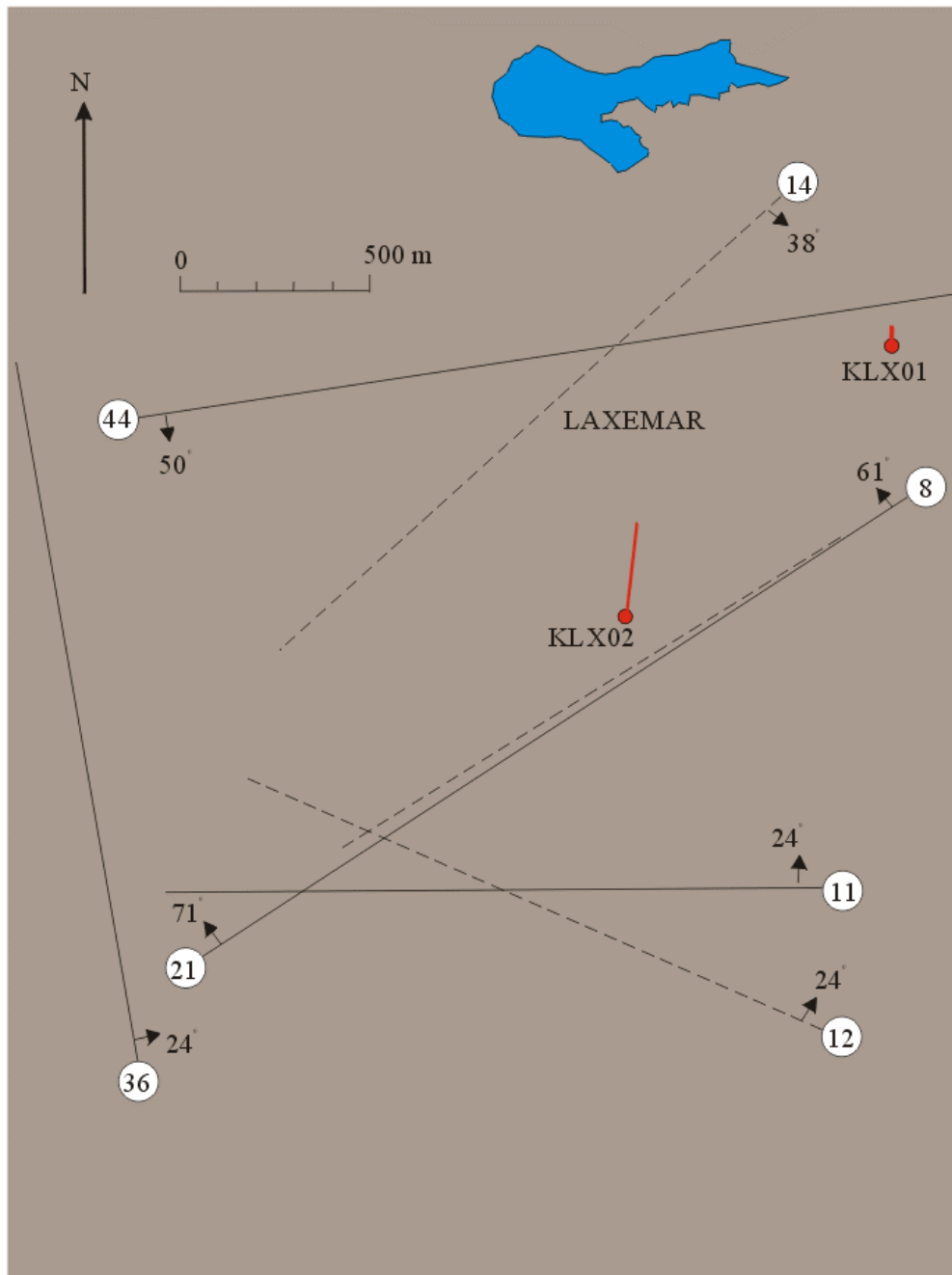
Finally, reflectors no. 12, 21 and 44 coincide with spinner anomalies. The resemblance regarding geological character, calculated geometry of radar angle and intersection depth was considered as “good” for no. 21 and 44, whereas no. 12 was judged as “possible”. Reflectors no. 11 and 12 are sub-parallel and appear very close to each other, within the boreholes as well as at the surface.

**Table 3-7. Compilation of radar reflectors correlated between KLX01 and KLX02.
After Table 4.1 in /3-19/.**

Reflector in KLX02 in KLX02 (ID-no.)	Position in KLX02 (m)	Orientation of reflector (dip/strike)	Geological character in KLX02	Possible candidate in KLX01 (ID-no.)	Position of candidate in KLX01 (m)	Geological character in KLX01	Estimation of the correlation	Correlation conditions		
								Strong and persistent	Low radar amplitude	Spinner anomaly
8	271	61/238	Crushed, fractured, oxidized	21	231	Greenstone	Not good	X	X	X
11	341	24/270	Crushed, fractured	28 56	339 623	Grst,apl,grt Oxidized, crushed	Unsure Good	X		X
12	367	24/295	Grst partly oxidized	62	693	Crushed, oxidized	Possible			X
14	394	38/047	Crushed, fractured grst	48	455	Oxidized	Unsure	X	X	
			crushed	41	461	Oxidized,	Unsure			
21	465	71/239	Crushed, fractured, oxidized	38	409	Fractured, oxidized	Good			X
36	667	24/355	Fractured, crushed grst	39	427	"	Good			
			-	-	1000-1017	Crushed,	No radar meas. but possible	X	X	X
			-		1031-1034	Greenstone	"			
			-		1043-1045	Greenstone	"			
44	753	50/081	Crushed,	23	324	Grst,apl,grt	Good			X

Explanation of used abbreviations:
grt=Småland granite
grst=Greenstone
apl=Aplite

If the results from the lineament study presented in Figure 3-15 is compared with the results from the radar correlation study, a very scanty match between the structural features identified and discussed in the respective studies is noticed. However, the ground projection of reflector no. 11 seems to coincide relatively well with the greenstone structure discussed in /3-18/, although the dip of the structure diverges between the two studies. The remaining six projected radar reflectors regarded as possible to correlate between boreholes KLX01 and KLX02 do not correspond to any structure discussed in the lineament study presented in /3-18/.



GEOSIGMA AB

Figure 3-17. Plan map illustrating calculated intersections with the ground surface of radar reflectors correlated between boreholes KLX02 and KLX01. Solid lines indicate reflectors with a correlation considered as “good”, while dashed lines symbolize reflectors with a correlation judged as “possible” or “uncertain”. After Figure 4.1 in /3-19/.

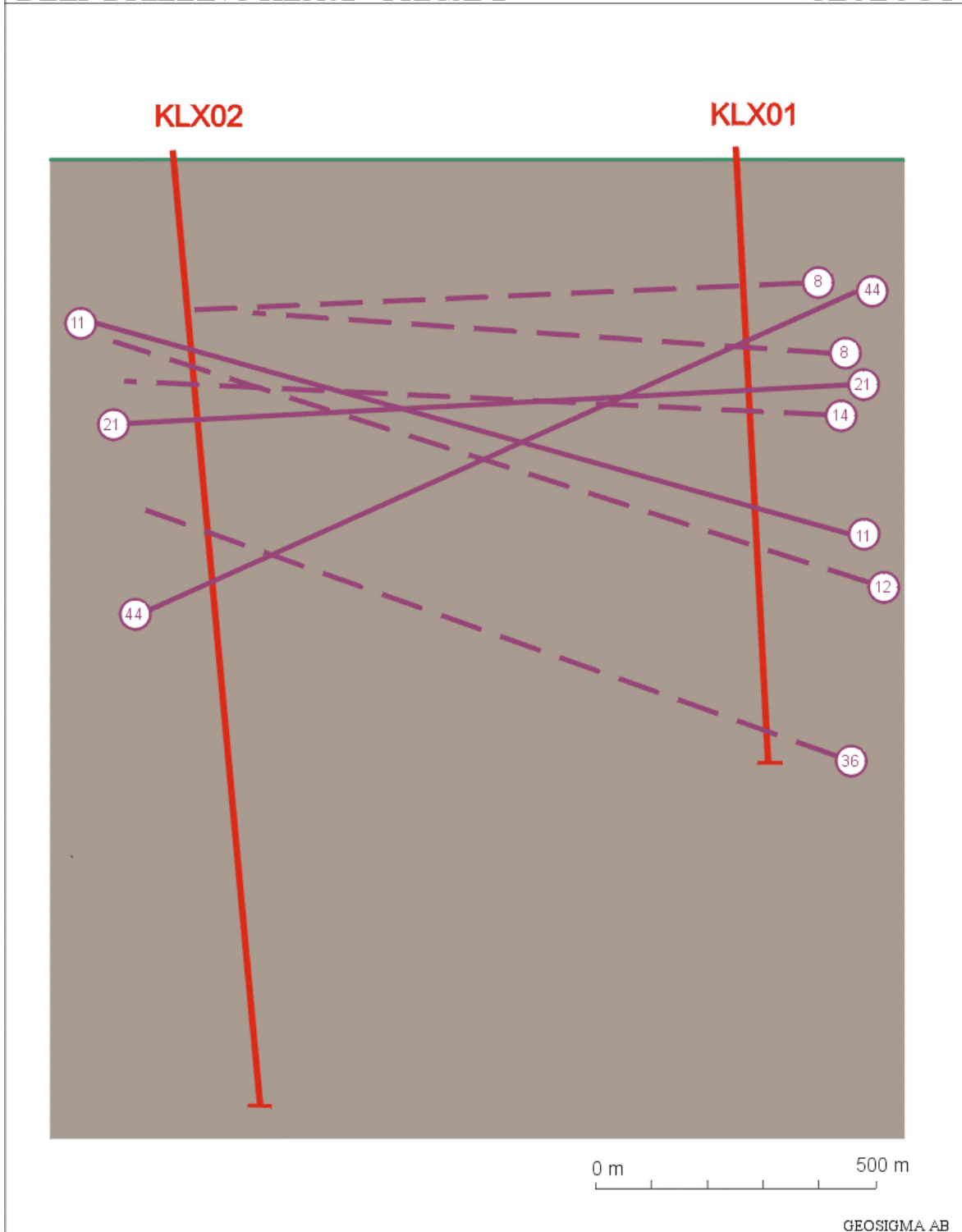


Figure 3-18. Vertical cross section between boreholes KLX01 and KLX02 displaying correlated radar reflectors. The boreholes are projected on the plane connecting the starting points of the respective boreholes. Solid lines indicate reflectors with a correlation considered as “good”, while dashed lines symbolize reflectors with a correlation judged as “possible” or “uncertain”. For reflector no. 8 two possible solutions are presented. After Figure 4.2 in /3-19/.

3.4.3 Interpretation of the connection between fractured sections in boreholes KLX01 and KLX02 and lineaments in the Laxemar-Simpevarp-Äspö area

A regional structural model has been developed for the Simpevarp area, including the islands of Äspö and Ävrö, the peninsula of Simpevarp and the Laxemar area with the nearest surroundings /3-1/. The middle-eastern part of this model is illustrated in Figure 3-19. The model is primarily based on aerogeophysical investigations /3-9/, topographical lineament interpretation /3-22/ and VLF anomalies /3-27/. The regional model exhibits a number of major discontinuities striking predominantly NE-ENE /3-28/. Geological observations and geophysical ground measurements along a large number of profiles perpendicular or semi-perpendicular to the discontinuities /3-29/ reveal that they are often characterized by a 100–200 m wide oxidized zone with a slightly increased fracture frequency /3-30/.

Some of the major discontinuities have been penetrated by boreholes at the island of Äspö or have been traversed by the Äspö tunnel, thereby being exposed to more detailed studies. The regional structural model in combination with experiences of discontinuities from i.a. the Äspö HRL investigations and the results of borehole investigations in KLX01 and KLX02 framed the basis for the

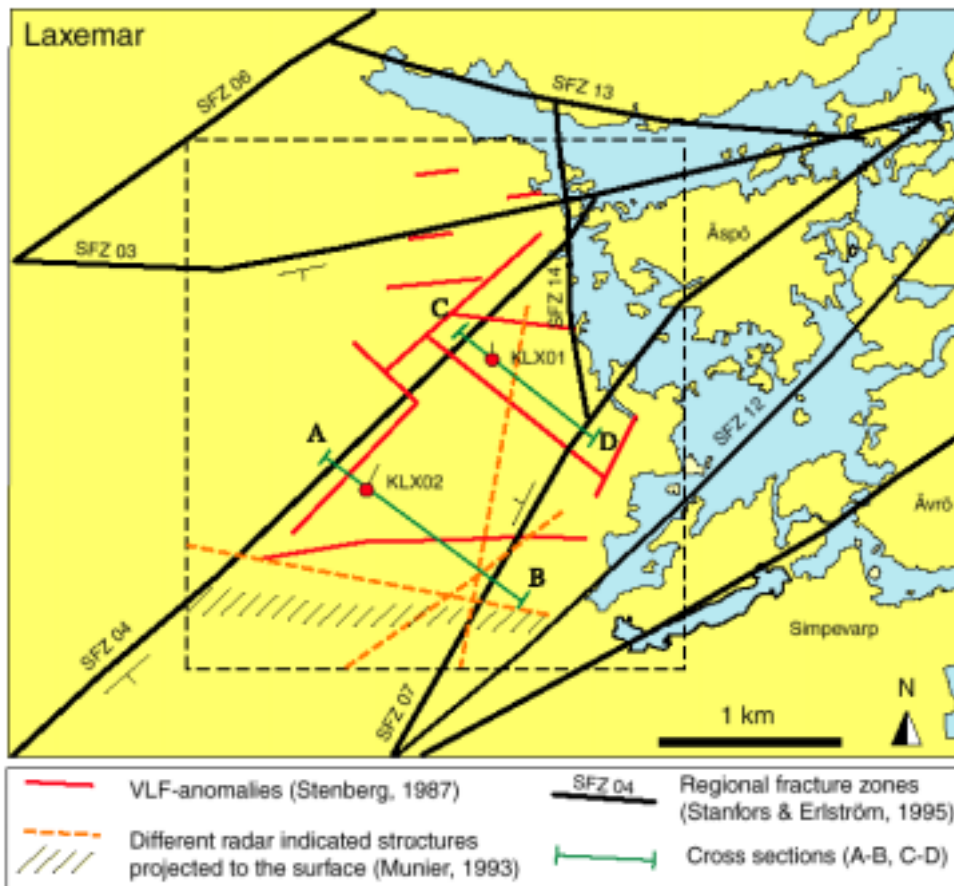


Figure 3-19. Part of the regional structural model of the Simpevarp area. Modified after (part of) Figure 2 in /3-1/. Roy Stanfors pers. comm.

interpretation of the major structural features within the Laxemar area presented in this section (Roy Stanfors, pers. comm.). This local structural model should, however, not be regarded as the final interpretation of the structural character of the Laxemar area, but rather be looked upon as one of several possible solutions. Results from i.a. reflection seismics performed later in the Laxemar area (see Section 3.4.5) have added new information, which may motivate modifications of the interpretations presented here of the structural setting of the Laxemar area.

Investigations of discontinuities by drilling or tunnel excavation have frequently demonstrated a central core of the discontinuity with a high fracture frequency, often water bearing, alternatively with heavily crushed and clay altered rock. The experiences from i.a. the Äspö HRL also indicate, that regional zones of this kind in general are composed of a number of branches, which, regarding strike, dip and character, alternate considerably, both laterally and vertically (Roy Stanfors pers. comm.). Figures 3-20 and 3-21 illustrate a number of sections in boreholes KLX01 and KLX02 which may be related to the major discontinuities SFZ04 and SFZ07, see Figure 3-19 (SFZ07 is in the Äspö HRL-reports, e.g. /3-1/, known as zone EW-1). Assumptions about the dip of these zones, SE respectively NW, are essentially based on geophysical data /3-9, 3-31/. In KLX02 the fracture frequency, as described in Section 3.3.9, is increased in almost the entire 390 m long interval 730–1120 m. The fracturing is especially intensive within section 800–1100, where also a substantial element of greenstone dikes are encountered between 800–900 m.

A transection along the profile A-B, see Figures 3-19 and 3-20, explains how the fractured section, according to this interpretation, may be associated with, primarily, zone SFZ04. The long fractured interval in KLX02 indicates that this borehole intersects a relatively wide zone (SFZ04) at a steep angle. A contribution from one or several branches of SFZ07, with a less steep dip, is also regarded as feasible. The corresponding interpretation for borehole KLX01 is presented in Figure 3-21.

To conclude, in this preliminary structural model, certain fractured intervals in boreholes KLX01 and KLX02 are connected with the major (regional) discontinuities SFZ04 and SFZ07. Experiences from primarily the Äspö HRL, argue that the major discontinuities are linked together by a large number of minor, often water bearing fracture zones with the dominating strikes NW-NNW and ENE /3-32/.

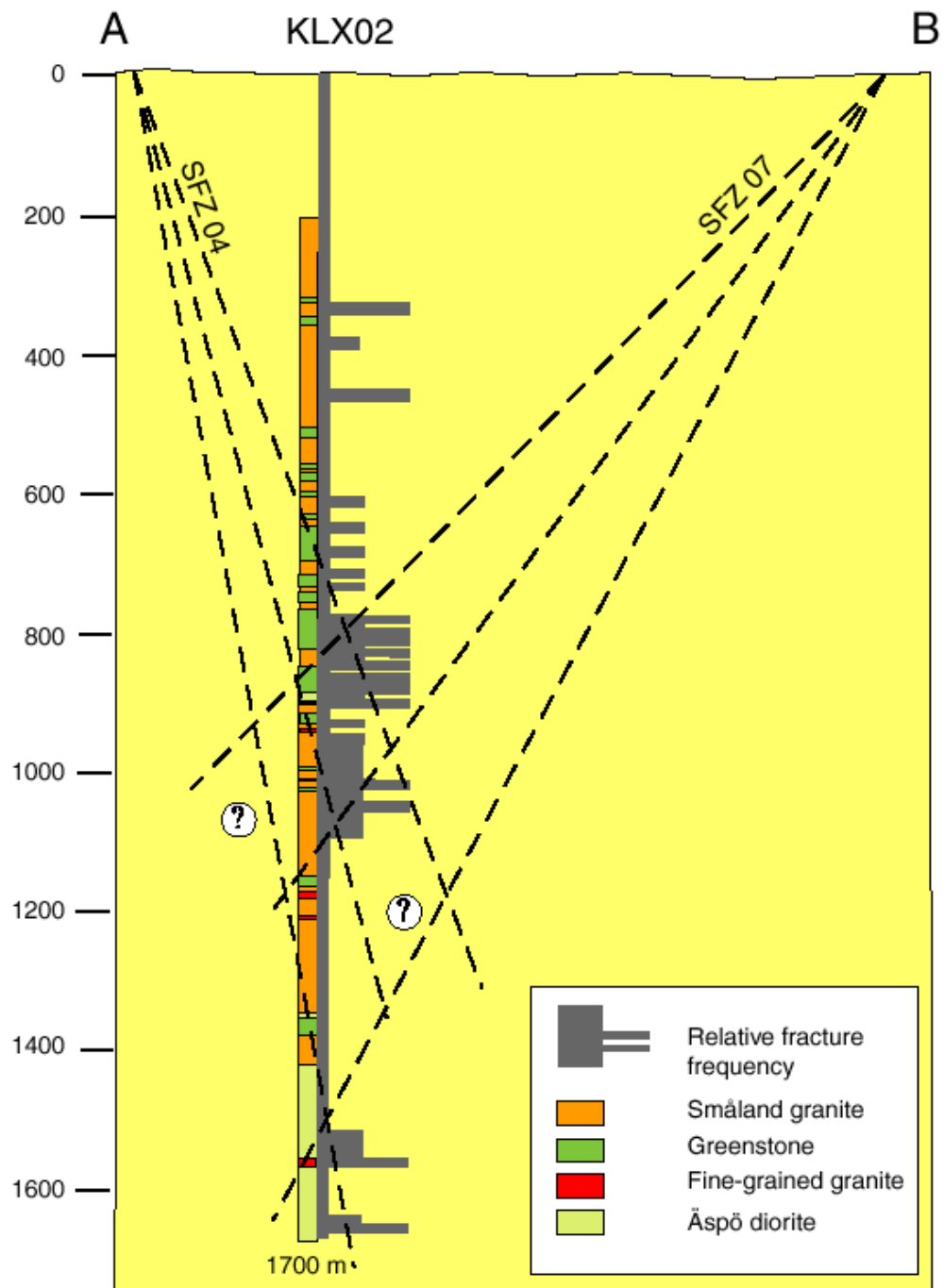


Figure 3-20. Borehole KLX02. Interpretation of possible connections between fractured sections in the borehole and surface indicated discontinuities. Roy Stanfors pers. comm.

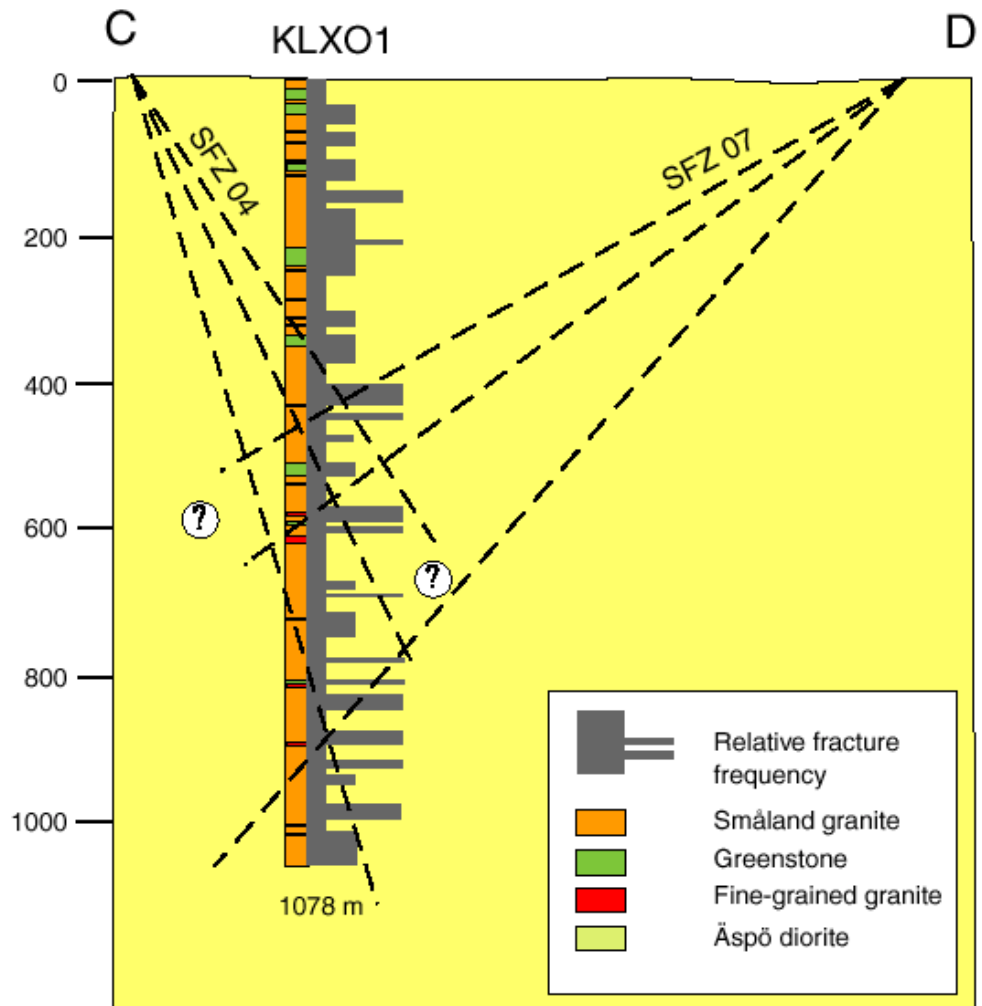


Figure 3-21. Borehole KLX01. Interpretation of possible connections between fractured sections in the borehole and surface indicated discontinuities. Roy Stanfors pers. comm.

3.4.4 Method tests – ground geophysics

Ground geophysical measurements with three methods were performed in the Laxemar and Götömar areas during late 1996 and early 1997 /3-31/. The investigations add further information to the lithological and structural conditions in these areas, which was used i.a. in the study presented in Section 3.4.3.

Three different geophysical methods were tested:

- Half-regional resistivity measurements (HRR).
- Electrical soundings (VES).
- Transient electromagnetic soundings (TEM).

All three methods were used for determination of the electrical resistivity of the bedrock.

The HRR-measurements revealed the bulk-resistivity of the bedrock, which is displayed as shades in a surface map, see Figure 3-22. Within the Laxemar area, the bulk-resistivity of the Småland granite exposes values in the interval 3 000–10 000 Ωm . The intrusion of Götömar granite exhibits a higher bulk-resistivity, 14 000–30 000 Ωm . The difference between the two geological units may be explained by different fracturing, where the lower bulk-resistivity of the Småland granite is pointing at an increased fracture frequency compared to the Götömar granite.

The depth to saline groundwater is provided mainly from the interpretation of TEM-soundings. These measurements indicate a depth of about 900 m as an average for the entire investigated area, see Figure 3-23. Minor deviations from this value were observed in part of the investigated area. These may, however, be explained by influence from near sited low-resistive fracture zones, alternatively a locally increased fracture frequency of the rock mass.

Low-resistive discontinuities are mainly indicated by HRR-measurements as anomalies characterized by a short wave-length, superposing long-waved anomalies displaying the bulk-resistivity and influence of saline groundwater. Several steep low-resistive zones are indicated within the Laxemar area by the HRR-investigations. The location of these are in good agreement with the zones described in the regional structural model presented in Section 3.4.3, cf. Figure 3-19. E.g the discontinuities SFZ03, SFZ04 and SFZ07 are all indicated as low-resistive zones, see Figure 3-23. Due to disturbances from a power line, measurements across SFZ04 failed. However, it is believed that the same structure was encountered at TEM-soundings further north. These soundings indicate a dip of SFZ04 towards SE, exactly as stated in the regional model.

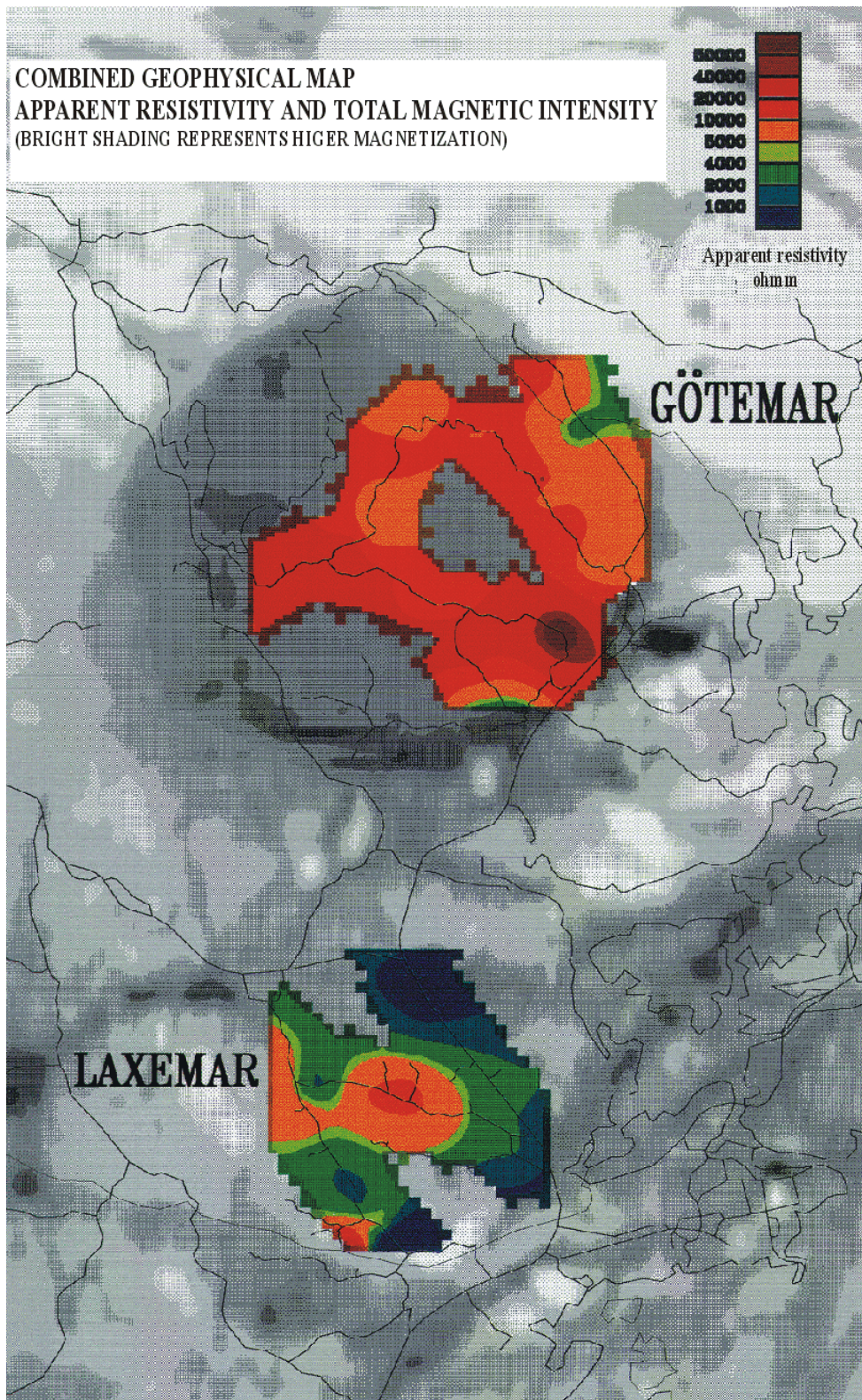


Figure 3-22. Results from half-regional resistivity measurements (HRR) in the Laxemar-Götemar region. Apparent resistivity towards a background of magnetic total intensity. After /3-31/.

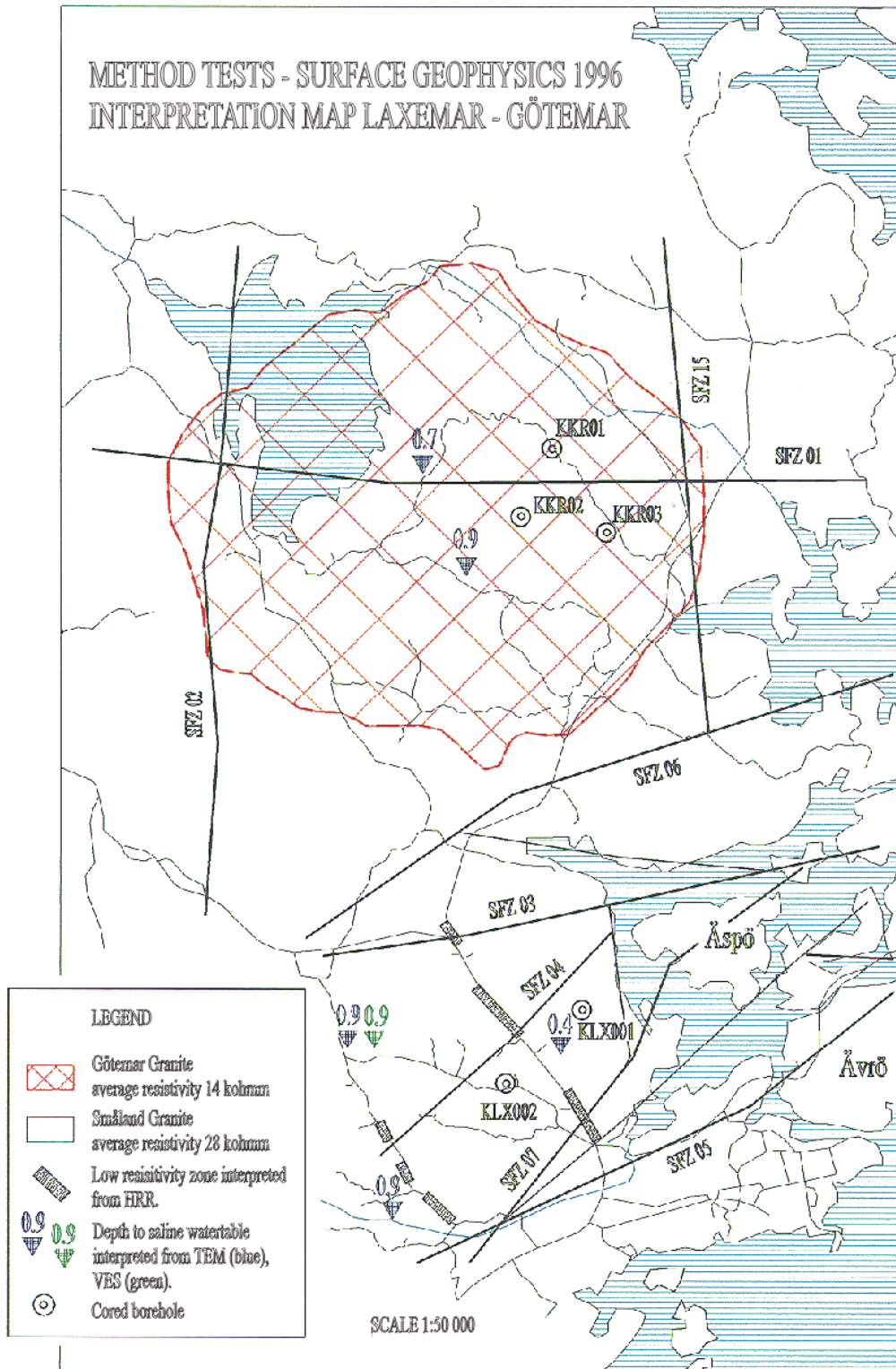


Figure 3-23. Results from half-regional resistivity measurements (HRR), electric soundings (VES) and transient electromagnetic soundings (TEM) in the Laxemar-Götemar region. Indications of low-resistive zones interpreted from HRR and depth to the transition between freshwater and saline water interpreted from TEM (blue) and from VES (green). After /3-31.

3.4.5 Reflection seismics and VSP (Vertical Seismic Profiling)

A reflection seismic study was conducted along two c. 2 km long crossing lines at Laxemar in December 1999 /3-33/. The crossing was located at the interception of borehole KLX02 with the ground surface, see Figure 3-24. The main goal of the reflection seismic investigation was to perform a full-scale test of newly developed methods with use of small shotholes and small explosive charges.

A second goal was to identify fracture zones in the investigated area, primarily zones that might correlate with water bearing fracture zones previously identified in boreholes, e.g. borehole KLX02.

Both lines had a 10-metre separation between geophones and charge holes. Shot sizes were 15-gram plastic explosives for shots in rock and 75-gram explosives for shots in loose sediments and till. The results from the measurements demonstrate that the small shothole technique with small charges works well for rock investigations to a depth of 3–4 km. The seismic signal penetrates at least to c. 1500 m along both lines. Over some parts of the lines the signal penetrates to c. 6000 m /3-33/.

Shallow, middle-steep reflectors

Five middle-steep (30–50°) shallow reflectors were identified in the Laxemar area, see Figure 3-24 and 3-25. Three of these, A, C and D, can be projected to the surface on both seismic lines and, hence, their 3D-characteristics be determined.

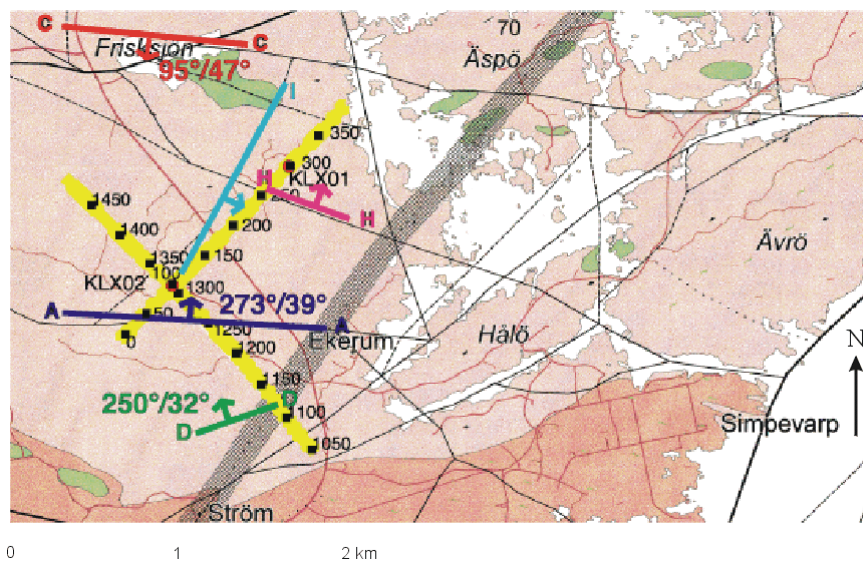


Figure 3-24. Geological map with the shot seismic lines in yellow and surface projections of reflectors A, C and D as well as probable positions of reflectors I and H. Modified after /3-33/.

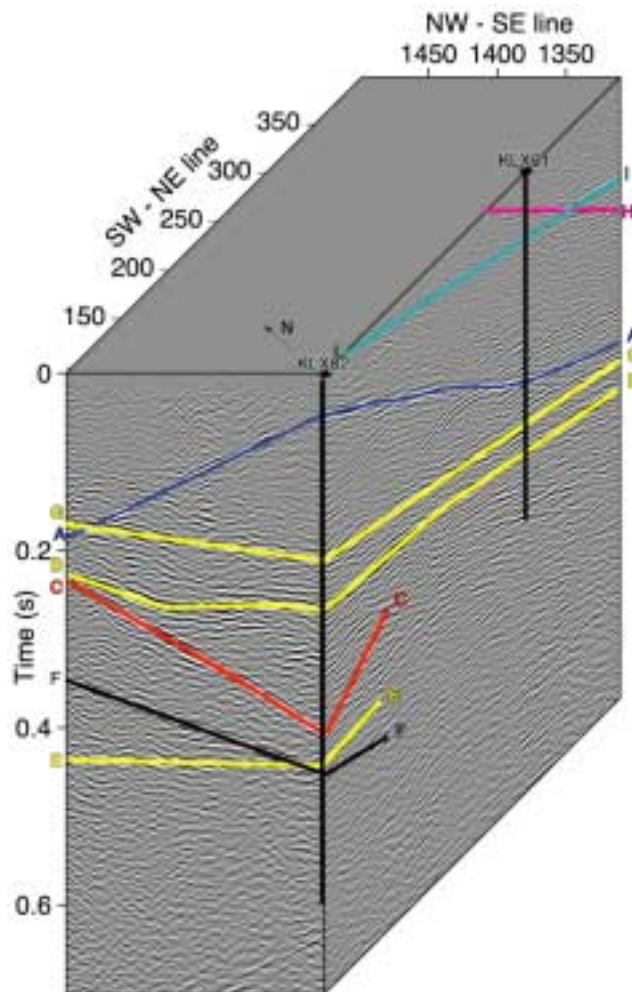


Figure 3-25. The two reflection seismic profiles merged at their crossing at borehole KLX02. Reflectors visible on both sides of the crossing (A, B, C, E, F and G) can be assigned a 3D-interpretation. Reflectors visible only on one side (H and I) must correlate with a structure on the ground surface in order to be interpreted three-dimensionally. The reflector crossing points with the boreholes are not the true crossing points for the dipping reflectors. Modified after Figure 3-4 in /3-33/.

These reflectors also coincide with topographical depressions. The two other middle-step reflectors are visible only on one line. However, since they are assumed to correlate with topographical depressions, they may still be assigned a three-dimensional orientation. Four of the five mentioned reflectors also correlate with previously mapped fracture zones, see Figure 3-24. The map in this figure is an enlarged detail from a geological-structural map produced by the Geological Survey of Sweden and presented in /3-34/. The same map, although in a smaller scale, and hence less detailed, is presented in Figure 3-1. The interpreted lineaments in Figure 3-24 display a relatively good, although not complete correspondence with the lineaments in Figure 3-14.

Strike, dip and interceptions with the ground surface and deep boreholes in the Laxemar area is given in Table 3-8.

The heavily fractured zone in borehole KLX02 at 1550–1700.5 m does not correspond to a distinct reflection seismic reflector close to the borehole. This may be due to this zone being subhorizontal but not reflective, or too steep to be followed all the way to borehole KLX02 on the two relatively short seismic profiles in question. In /3-33/ the second alternative is regarded as most probable, and it is supposed that reflector C (more distinct further away from KLX02) may be correlated with the highly fractured interval. The intersection with KLX02 at 1400 m (at a dip of 48° towards S) given in Table 3-8 is just one of several possible interpretations. Assuming a somewhat larger seismic velocity would increase the dip, entailing an intersection at a larger depth in KLX02.

Shallow, flat reflectors

A zone of increased subhorizontal reflectivity, delimited by reflectors B and G, was encountered at 650–900 m depth in borehole KLX02, see Figure 3-25. This zone is gently dipping towards east and can be correlated with greenstones and associated fracture zones in KLX02. The zone continues in direction towards borehole KLX01, but becomes here less distinct. It is notable, that the zone of increased reflectivity does not include the entire interval of increased fracture frequency, c. 730–1120 m, in KLX02. The subhorizontal zone interpreted from the reflection seismics may explain the hydraulic responses observed between boreholes KLX02 and KLX01 (cf. Chapter 6).

Reflector E at c. 1200 m depth in KLX02 dips around 9° towards the north and would reach the surface c. 10 km south of Laxemar, if it is planar.

Table 3-8. Geometry of five shallow, middle-steep reflectors identified from the reflection seismic survey performed in the Laxemar area /3-33/.

Reflector	Strike	Dip	Intersection with ground surface	Intersection with KLX02	Intersection with KLX01
A	273°	39°	c. 200 m S KLX02	c. 200 m	c. 650 m
C	95°	48°	c. 1325 m N KLX02	c. 1400 m	c. 650 m
D	250°	32°	c. 800 m SSE KLX02	c. 500 m	c. 830 m
H	293° ?	44° ?	c. 850 m NE KLX02	–	c. 200 m
I	20° ?	44° ?	c. 240 m WNW KLX01	–	c. 300 m

The extension of reflector F is limited, and the reflector is not visible either at borehole KLX02 or at KLX01. If the visible reflector is extrapolated towards the boreholes, the extensions intersect KLX02 at approximately 1600 m, which coincides with the highly fractured interval at 1550–1700 m, and KLX01 still deeper, i.e. much below the bottom of the borehole.

Deep reflectors

Strong reflectors were observed at c. 3 km depth. They probably emerge from the same zone as earlier interpreted from Ävrö data /3-34/. This zone dips 9° towards north and intersects, if planar, the ground surface about 10 km south of Laxemar.

VSP (Vertical Seismic Profiling)

VSP-measurements were performed during the autumn 2000. The results have not yet been reported. However, it may be stated that one reflector from the VSP-measurements seems to correspond well with reflector A from the reflection seismic survey (Christopher Juhlin pers. comm.).

4 Rock mechanics

4.1 Introduction

Mechanical stability is one of the fundamental safety-related functions of the rock mass. The significance of mechanical stability in this context involves primarily the function of the buffer and the canisters, which are not allowed to alter due to rock movements. Neither should new fractures modify the groundwater flow around the repository to such extent that the retention properties are substantially impaired /1-1/.

The interpretation of mechanical stability may be divided into different scales and different time aspects, for different weights of overburden:

- *Repository scale.* The potential consequences of e.g. thermal changes, variation of dynamic loads or large scale changes in the weight of overburden will be analysed and the *long-term* mechanical influence on the groundwater flow estimated.
- *Detailed scale (scale of tunnels, shafts and canister boreholes).* The mechanical stability must be assessed for construction design and operation, and is also fundamental for the long-term function of the repository.

The fulfilment of a rock mechanical analysis related to the design and construction of a deep repository for nuclear waste requires appropriate modelling tools and a range of input parameters. These parameters are in /1-1/ identified as:

- Geometry of discontinuities.
- Mechanical properties of fractures.
- Mechanical properties of intact rock.
- Mechanical properties of the rock mass (intact rock and fractures).
- Density and thermal properties.
- Boundary conditions and supporting data.

Adequate methods for determination of these parameters are also given in /1-1/. They include i.a. core logging, laboratory tests on drill cores, geophysical field measurements, rock stress measurements and analysis of the lithological/structural model from a rock mechanical perspective.

A complete site characterization programme related to the topic of rock mechanics is relatively comprehensive. The investigations performed within Project Deep Drilling KLX02 – Phase 2 covered only certain aspects of such a programme. If extended investigations would be considered, the already performed studies will serve as a proper basis.

Three main studies related to rock mechanics were performed within Phase 2:

- Stress measurements applying the hydraulic fracturing method /4-1/.
- Determination of hydromechanical properties (in connection with the stress measurements) /4-6/.
- A special study of the stability of borehole KLX02 related to problems with jamming of equipment used for down-hole investigations /4-16/.

Sections 4.2, 4.3 and 4.4 provide comprehensive presentations of the respective studies.

4.2 Rock stress measurements in borehole KLX02

4.2.1 Background

Two methods have been practised for *in situ* rock stress measurements at the Äspö HRL investigations, overcoring and hydrofracturing. Overcoring has to be performed in connection with drilling of a borehole, while hydrofracturing is conducted in existing boreholes. The exposition of methods and results of the stress measurements in borehole KLX02 at Laxemar, where only hydrofracturing was applied, is based on /4-1/.

4.2.2 Measurement principles and scope of investigations

The hydraulic fracturing method has been presented by several authors, see e.g. /4-2/ and /4-3/. The method is based on the principle of counteracting forces.

A borehole section, normally less than 1 m in length, is sealed off with a straddle packer. The sealed off section is then slowly pressurized with a fluid, usually water, which will generate tensile stresses at the borehole wall. Pressurization is continued until the borehole wall ruptures through tensile failure, and a hydrofracture is initiated.

The resisting stresses, that have to be exceeded in order to initiate failure, are exerted by 1) the tensile strength of the rock and 2) the *in situ* stresses. Hence, by recording the pressure at failure, the effect of the *in situ* stresses is obtained, provided that the tensile strength is known. More information about the rock stresses is obtained by propagating the hydrofracture further out into the rock. Once failure has occurred, water from the sealed off borehole section penetrates into the fracture, thereby exposing the fracture surfaces to normal stress from the pressurized water. The pressure required to propagate the hydrofracture will balance the normal stress acting across the fracture plane.

The initiated fracture is normally parallel to the borehole axis, and two fractures are initiated simultaneously in diametrically opposite positions on the borehole periphery. Obviously, the hydrofracture will be initiated at the point and

propagate in the direction offering least confinement. The fracture will therefore develop in a direction perpendicular to the minimum rock stress, and hence stress directions can be resolved by determining fracture orientation, see Figure 4-1.

Theory and interpretation technique for hydrofracturing, which are thoroughly described in e.g. /4-2/ and /4-3/, are excluded in this report.

The rock stress measurements presented in this chapter were performed by SwedPower Co. (at the time of performance Vattenfall Hydropower Co.). The overall objective was to obtain information on the stress conditions of the bedrock at KLX02, and especially at depths exceeding 500 m. More specifically, the purpose of the hydrofracturing stress measurements was to determine the horizontal stress field (magnitudes and orientations) within the interval 200–1430 m borehole length. Prior to these tests, no rock stress measurements had been conducted below 1000 m depth in Sweden.

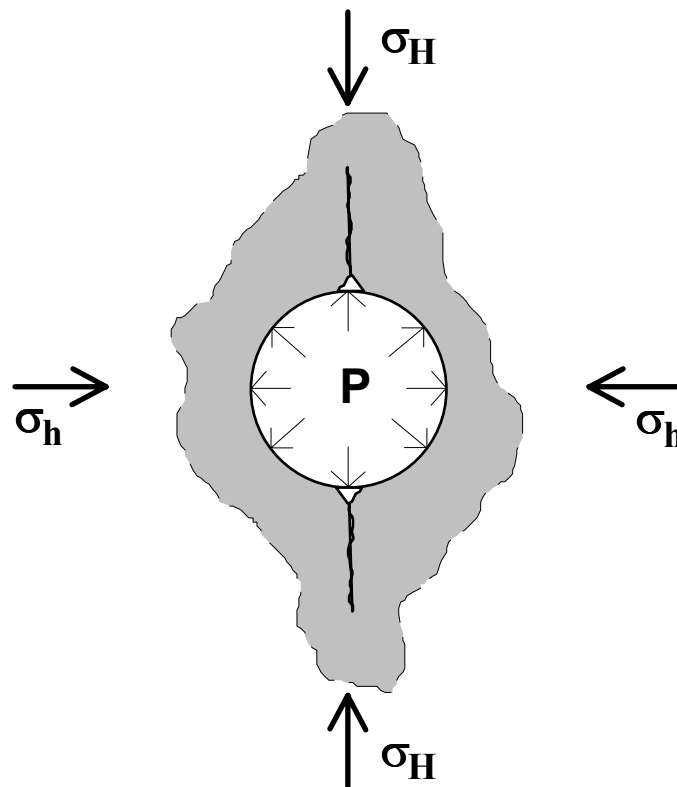
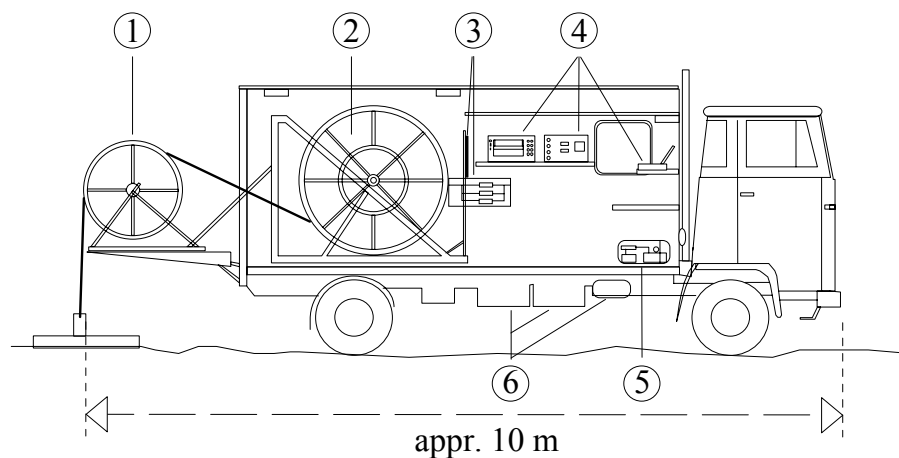


Figure 4-1. Schematic cross section of a borehole, illustrating the hydraulic fracturing method. If the borehole is vertical, σ_H and σ_h are the maximum and minimum horizontal stresses respectively. After Figure 2-1 in /4-1/.

4.2.3 Instrumentation

SwedPower Co. has at its disposal a mobile instrumentation unit for hydraulic fracturing stress measurements, see Figure 4-2. This equipment, here denominated the Mobile Hydrofracturing Equipment, was developed at the Luleå University of Technology with financial support from SKB and is described in detail in /4-4/. The measurement unit is permanently installed on a truck and has a 850 m multihose cable connected to a down-hole tool for hydrofracturing and injection testing. This tool includes a straddle packer with a separation of c. 0.6 m. In 1993, a specially designed valve was added above the packer section to allow for pressure pulse testing, see Section 4.3.2.

Since the Mobile Hydrofracturing Equipment at the time of the stress measurements admitted testing only to 850 m borehole length, an alternative test strategy had to be applied. The best option appeared to be the use of a pipe string as the carrier of the straddle packer and with the hydraulic hoses clamped against the pipes. The best fitted equipment unit for this purpose was the SKB Pipe String Equipment, normally used for different types of hydraulic testing, see Figure 4-3. All parts of this unit are mounted or stored in a steel container. One major disadvantage with this system compared to the Mobile Hydrofracturing Equipment with its multihose, is that down- and up-hoisting of the down-hole tool is essentially more time- and manpower consuming.



- 1 Guidewheel for multihose on adjustable working platform.
- 2 Drum for 1000 m multihose.
- 3 Flow meter manifold and manifold for control of fracturing flow and packer pressure.
- 4 Data registration equipment, signal amplifier, chart recorder and portable PC.
- 5 High pressure water pump.
- 6 400 l diesel fuel tanks, hydraulic pump and -tank.

Figure 4-2. Cross section of the Mobile Hydrofracturing Equipment with 850 m multihose cable. After Figure 3 in /4-3/.

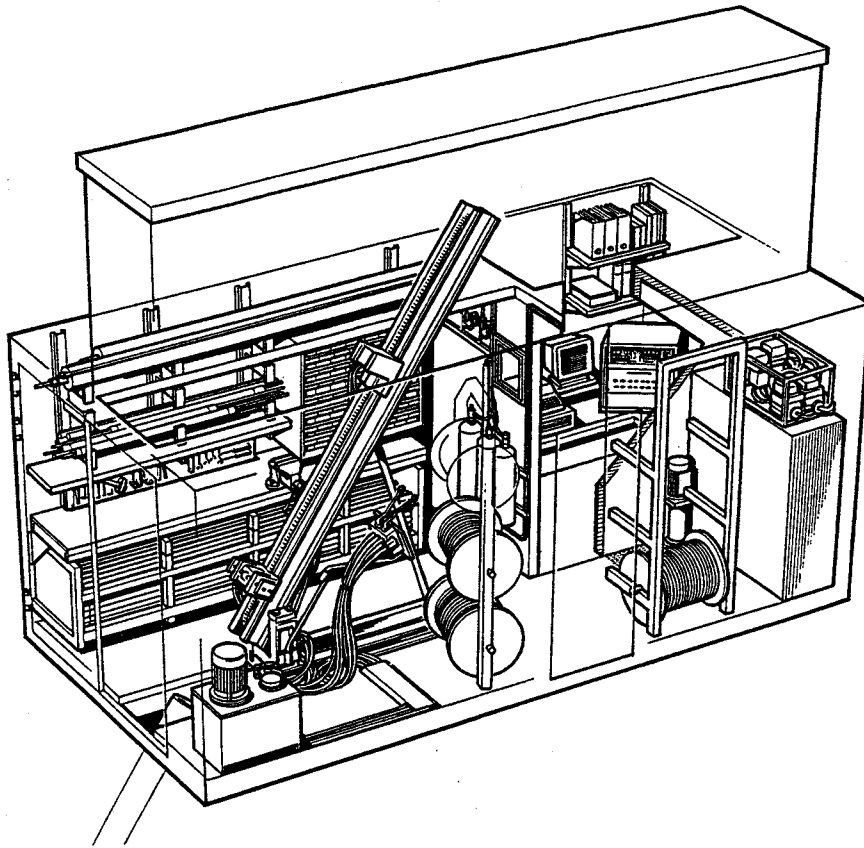


Figure 4-3. Schematic illustration of the SKB Pipe String Equipment used during the deep hydraulic fracturing rock stress measurements in borehole KLX02. After Figure 7.12 in /4-5/.

All measurements above borehole length 850 m were conducted with the Mobile Hydrofracturing Equipment using the multihose, the ordinary straddle packer and a down-hole pressure gauge. For tests below 850 m, the Pipe String Equipment was engaged. However, the high pressure pump, manifold for test control, gauges and recording electronics etc of the Mobile Hydrofracturing Equipment were all necessary for performance of the hydrofracturing measurements. These parts were therefore connected to the Pipe String Equipment during testing below 850 m.

For orientation of the induced hydrofractures, an impression packer is normally used. During the measurements in KLX02, this packer was used for all measurements above 850 m. Below 850 m, where the Pipe String Equipment was applied for hydrofracturing, the down- and up-hoisting of the impression packer was considered as unacceptably time consuming. Instead, the BIP-system (see Section 3.3.7) was used for orientation. Since the fracturing was operated by a pipe string and the BIP-measurements with a cable, a slight divergence in the length determination may prevail between the two methods. To avoid missing the exact location of the test points, the BIP-measurements were started 5 m above each estimated test point and ended 5 m below this point.

4.2.4 Results

In all, 43 hydraulic fracturing stress measurements were accomplished in borehole KLX02. 21 of these were performed with the Mobile Hydrofracturing Equipment and 22 with the Pipe String Equipment. Of the latter, 17 were located deeper than 1000 m below ground surface. Interpretation of the 43 conducted tests revealed that 35 of them could be regarded as successful. Table 4-1 presents position data and rock type for all test points and, for each unsuccessful test, a comment on the possible reason for the test failure.

For the 21 test points between 207.2 m and 756.8 m the impression packer was used for orientation, while the fractures from the 22 deeper test points were oriented with the BIP-system.

Stress magnitudes

The interpretation of the hydrofracturing measurements resulted in three different stress components:

- 1) Fracture normal stress.
- 2) Maximum horizontal stress.
- 3) Minimum horizontal stress.

Magnitudes of the measured stresses are presented in Figures 4-4 and 4-5. Figure 4-4 illustrates the fracture normal stresses from the 41 tests where a complete test cycle could be fulfilled. The normal stress is the stress acting across the pressurized fracture plane. The fracture may either be induced by the hydrofracturing or pre-existing, i.e. reopened during the fracturing. The data in Figure 4-4 therefore represent stresses acting across coaxial as well as inclined fractures. No horizontal or sub-horizontal fractures were obtained during the measurements.

For 35 of the test points, coaxial fracturing was observed or interpreted to have occurred. The stress magnitudes for those points are presented in Table 4-2. However, concerning 20 of the deep tests, where the BIP-system was applied for fracture orientation, some uncertainty prevails, whether all tests were successful.

Figure 4-5 illustrates the evaluated maximum and minimum horizontal stress magnitudes, σ_H and σ_h , as a function of vertical depth. For comparison, the theoretical vertical stress, σ_v , is indicated by a solid line in the figure. A polynome trend/regression line of fourth order has been added for the maximum/minimum horizontal stresses respectively. The results are commented on later in this section.

Table 4-1. Background data for all hydraulic fracturing test points in borehole KLX02. After Table 3-1 in /4-1/.

Borehole length (m)	Vertical depth (m)	Rock type	Comments
207.2	206.4	Småland granite	
273.5	272.5	Småland granite	Inclined fracture
289.3	288.2	Småland granite	Inclined fracture
297.2	296.1	Småland granite	
307.0	305.8	Småland granite	
348.0	346.7	Småland granite	
354.0	352.7	Greenstone	
360.9	359.5	Småland granite	No imprint taken
375.9	374.5	Småland granite	
429.0	427.4	Småland granite	
489.6	487.7	Småland granite	Inclined fracture
506.0	504.1	Småland granite	
542.6	540.5	Greenstone	
557.8	555.7	Småland granite	
581.7	579.7	Småland granite	
603.5	601.2	Småland granite	
644.3	641.8	Småland granite	Inclined fracture
696.8	694.1	Småland granite	
707.5	704.8	Greenstone	
712.9	710.2	Greenstone	Packer failure
756.8	753.9	Greenstone	
871.5	868.2	Småland granite	
873.3	870.0	Småland granite	
879.6	876.2	Småland granite	
965.0	962.7	Småland granite	Pre-existing fracture?
990.6	986.8	Småland granite	
1075.0	1068.9	Småland granite	Hose failure
1133.0	1128.7	Småland granite	
1174.0	1169.5	Småland granite	
1194.5	1190.0	Småland granite	
1212.0	1207.4	Småland granite	
1224.0	1219.3	Småland granite	
1227.0	1222.3	Småland granite	
1230.0	1225.3	Fine-grained granite	
1275.0	1270.1	Småland granite	
1287.5	1282.6	Småland granite	
1293.0	1288.1	Småland granite	
1296.0	1291.1	Småland granite	
1300.0	1295.0	Småland granite	
1329.5	1324.4	Småland granite	
1336.0	1330.9	Småland granite	
1339.0	1333.9	Småland granite	
1342.0	1336.9	Småland granite	

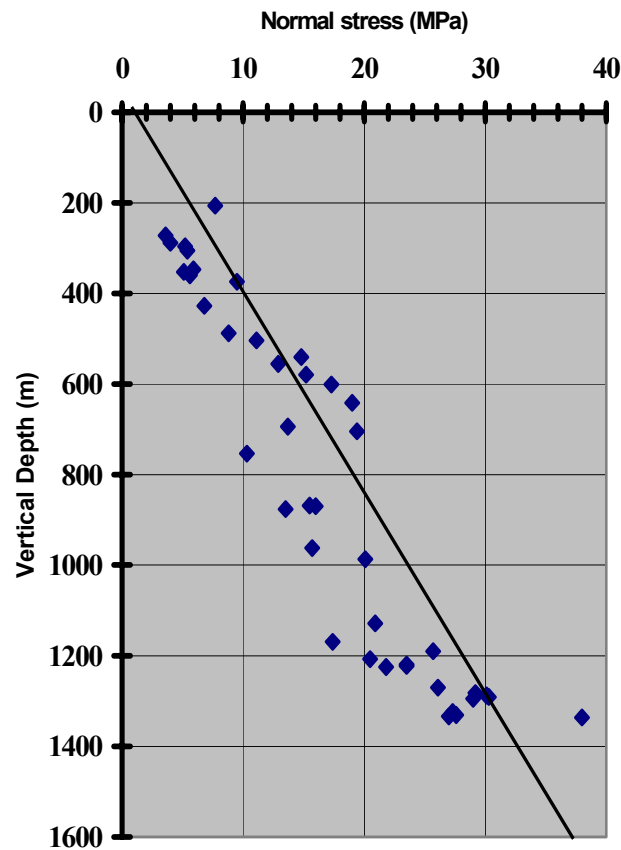


Figure 4-4. Fracture normal stress in borehole KLX02 as a function of depth. Solid line represents the theoretical vertical stress. After Figure 3-1 in /4-1/.

Orientations

As mentioned previously, the test points between 207.2 m and 756.8 m borehole length were oriented using a conventional impression packer and a single shot unit with a magnetic compass. All test points below 756.8 m were scanned using the SKB BIP-system. The application of this system for orientation of fractures induced by hydrofracturing was tested for the first time in borehole KLX02. A few comments are given below on the outcome of this new approach.

The BIP-system creates a digital colour image of the complete borehole wall. In the present study the highest resolution of 0.25 mm in length distance between each 360° scanning was applied. Each such scanning includes a total of 360 pixels, and the resulting image (i.e. picture of the wall) is normally, with clear borehole water and clear borehole walls, of very high quality. Even mineral grain boundaries are clearly detectable (cf. /3-16/).

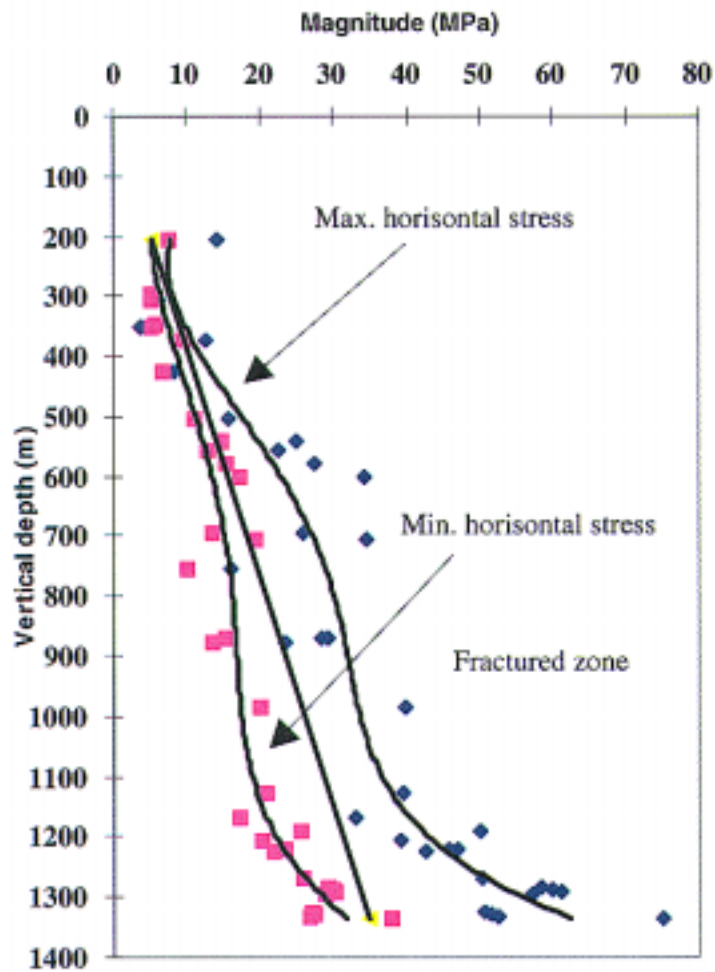


Figure 4-5. Vertical and horizontal stresses in borehole KLX02 as a function of depth. The straight solid line represents the theoretical vertical stress. Polynome trendlines are fitted to the horizontal stresses. After Figure 4-1 in /4-1/.

Shortly after drilling of borehole KLX02, it was observed that a dark discolouring started to build up on the borehole wall within the interval c. 800–1200 m borehole length. The explanation of this phenomenon is not fully recognized. However, it is reasonable to believe, that the dark stain is an effect of the short-circuit between fracture systems with different pressure potential induced by the drilling, enabling vertical flow to occur along the borehole. By this mechanism, groundwater of different chemical composition may be mixed, possibly resulting in different chemical reactions, e.g. chemical precipitation (cf. Chapter 7).

Within the discoloured interval, the texture of the rock is very difficult to identify from the BIP-images. The smudge, however, had the advantage of preserving imprints from the position of the straddle packer during hydrofracturing. Hence, this phenomenon offered a method to identify the exact location of each test point within the discoloured interval. The difference in length determination between

Table 4-2. Calculated rock stresses from hydraulic fracturing measurements in borehole KLX02. σ_v = vertical stress, σ_H = maximum horizontal stress, σ_h = minimum horizontal stress. After Table 3-2 in /4-1/.

Borehole length (m)	Vertical depth (m)	σ_v (MPa)	σ_H (MPa)	σ_h (MPa)
207.2	206.4	5.4	14.1	7.7
297.2	296.1	7.7	5.3	5.2
307.0	305.8	8.0	6.2	5.4
348.0	346.7	9.0	6.3	5.9
354.0	352.7	9.2	(3.8)	5.4
375.9	374.5	9.7	12.7	9.5
429.0	427.4	11.1	8.4	6.8
506.0	504.1	13.1	15.9	11.1
542.6	540.5	14.1	25.0	14.8
557.8	555.7	14.4	22.5	12.9
581.7	579.7	15.1	27.6	15.3
603.5	601.2	15.6	34.3	17.3
696.8	694.1	18.0	26.0	13.7
707.5	704.8	18.3	34.7	19.4
756.8	753.9	19.6	16.1	10.3
871.5	868.2	22.6	29.4	15.5
873.3	870.0	22.6	28.5	16.0
879.6	876.2	22.8	23.4	13.5
990.6	986.8	25.7	39.9	20.1
1133.0	1128.7	29.3	39.6	20.9
1174.0	1169.5	30.4	32.9	17.4
1194.5	1190.0	30.9	49.9	25.7
1212.0	1207.4	31.4	39.2	20.5
1224.0	1219.3	31.7	47.0	23.5
1227.0	1222.3	31.8	45.8	23.5
1230.0	1225.3	31.8	42.7	21.8
1275.0	1270.1	33.0	50.5	26.1
1287.5	1282.6	33.3	58.5	29.2
1293.0	1288.1	33.5	59.9	30.1
1296.0	1291.1	33.6	61.1	30.3
1300.0	1295.0	33.7	57.2	29.0
1329.5	1324.4	34.4	50.6	27.3
1336.0	1330.9	34.6	51.5	27.6
1339.0	1333.9	34.7	52.5	27.0
1342.0	1336.9	34.8	75.1	38.0

the pipe string used during hydrofracturing and the BIP-cable used for fracture orientation could also be estimated with aid from the packer imprints. The estimate could then be used to locate test points outside the stained interval.

It should be emphasized, that although the exact locations of the test sections below 850 m could easily be identified, it was very difficult to discover the induced fractures. The probable cause of this is, that the induced tensile fractures close very tightly after completion of the testing, especially at large depths, where high normal stresses prevail. For the majority of the identified fractures below

850 m, there remains a degree of uncertainty regarding orientation. Only in one case, at borehole length 1342.0 m, the induced fracture was identified without hesitation, due to the fact that a white stain had been created around the fracture.

Contrary to the orientation problems accompanying the induced fractures, the pre-existing fractures, either unsealed or sealed, were clearly visible on the BIP-images. No such fractures were, however, discovered within the straddled hydro-fracturing test intervals.

The interpreted orientations of the induced hydrofractures are presented in Table 4-3 with a comment on the fractures impossible or difficult to discover. A graphical presentation of the orientation of the maximum horizontal stress as a function of vertical depth is given in Figure 4-6. In the figure, the upper and lower boundaries for the interval with increased fracturing illustrated in Figure 3-12 have been included. This fractured interval has, as mentioned in Chapter 3, been interpreted to represent a major fracture zone.

4.2.5 Comments on the results

Stress magnitudes

The results of the stress measurements in borehole KLX02 presented in Table 4-2 and Figure 4-4 clearly demonstrate that the stress magnitude versus depth does not follow a linear relationship. Instead, the stress curves are characterized by several gradient shifts versus depth. Four intervals of different stress gradients are identified for both the maximum and minimum stresses:

- 1) 200– 350 m – small to moderate gradient
- 2) 350– 700 m – large gradient
- 3) 700–1100 m – gradient close to zero
- 4) 1100–1342 m – large gradient

The core log and the geophysical logs may provide a plausible explanation for this gradient profile, see Chapter 3 and Appendix 3. In Figure 4-7 the lithology and fracturing of the drill core is illustrated together with the magnitude of maximum and minimum horizontal stresses versus depth, the theoretical vertical stress and the orientation of the maximum horizontal stresses versus depth. At about 730 m borehole length, a significant increase in fracture frequency is observed. The high fracture frequency prevails to about 1120 m. During earlier attempts to elucidate the structural setting of the Laxemar site, this borehole interval (or part of it) has been interpreted as a major fracture zone, possibly of regional extension, either with a middle-steep or a subhorizontal dip, see Section 3.4.3 and Section 3.4.5. Obviously, the interval close to zero-gradient coincides with the (possible) fracture zone. The prominent gradients above and below the fractured interval may be explained by stress redistribution in association with the fracture zone. Figure 4-4 illustrates that the stresses at about 1300–1350 m have regained the magnitudes lost within the fracture zone. The stress field is, in other words,

not only disturbed within the zone itself but also several hundred metres above and below the zone. With the stress magnitude recovery below the fracture zone in mind, it seems probable that the gradient for the stress magnitude versus depth below 1342 m (the deepest measured point) is smaller than in the interval of stress recovery, i.e. between 1100–1350 m.

Table 4-3. Orientation of induced fractures from hydraulic fracturing tests in borehole KLX02. After Table 3-3 in /4-1/.

Borehole length (m)	Vertical depth (m)	Orientation of maximum horizontal stress, σ_H (°)	Remarks
207.2	206.4	171	
297.2	296.1	158	
307.0	305.8	14	
348.0	346.7	132	
354.0	352.7	137	
375.9	374.5	167	
429.0	427.4	151	
506.0	504.1	135	
542.6	540.5	147	
557.8	555.7	30	
581.7	579.7	159	
603.5	601.2	28	
696.8	694.1	99	
707.5	704.8	150	
756.8	753.9	22	
871.5	868.2	–	Not identified
873.3	870.0	150 (155–165)	
879.6	876.2	143 (129–157)	
990.6	986.8	–	Not identified
1133.0	1128.7	165 (160–170)	
1174.0	1169.5	?	
1194.5	1190.0	(115)	Great uncertainty
1212.0	1207.4	145 (140–150)	
1224.0	1219.3	120 (115–125)	Great uncertainty
1227.0	1222.3	130 (125–135)	
1230.0	1225.3	?	
1275.0	1270.1	–	Not identified
1287.5	1282.6	128 (120–135)	
1293.0	1288.1	90 (85–95)	
1296.0	1291.1	98 (95–100)	
1300.0	1295.0	90 (85–95)	
1329.5	1324.4	95 (90–100)	
1336.0	1330.9	90 (80–100)	
1339.0	1333.9	–	Not identified
1342.0	1336.9	60 (55–65)	

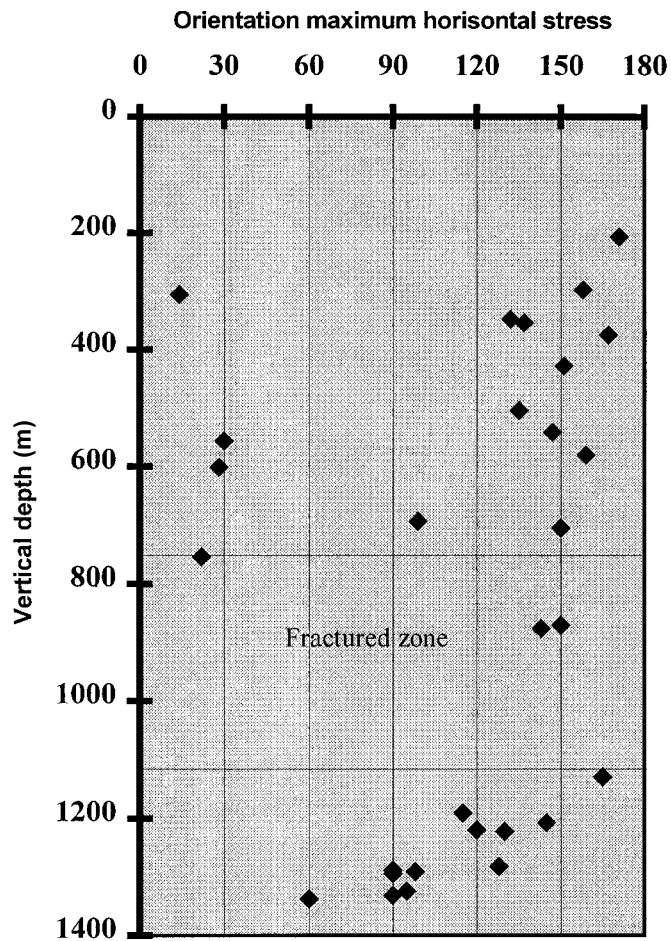


Figure 4-6. The orientation of the maximum horizontal stress as a function of depth. The figure includes the boundaries for the borehole interval of more intense fracturing. After Figure 4-2 in /4-1/.

The minimum horizontal stress, which between 200 m and 750 m is of the same order as the theoretical vertical stress, falls clearly below the vertical stress from 750 m to the end of the measurements at 1342 m. This fact indicates strike-slip faulting conditions in the interval 750–1342 m.

The average linear stress increase between 207 m and 1340 m borehole length is 0.045 MPa/m for the maximum horizontal stress respectively 0.021 MPa/m for the minimum horizontal stress. This is in good agreement with the general trend observed from a large number of stress measurements in Sweden.

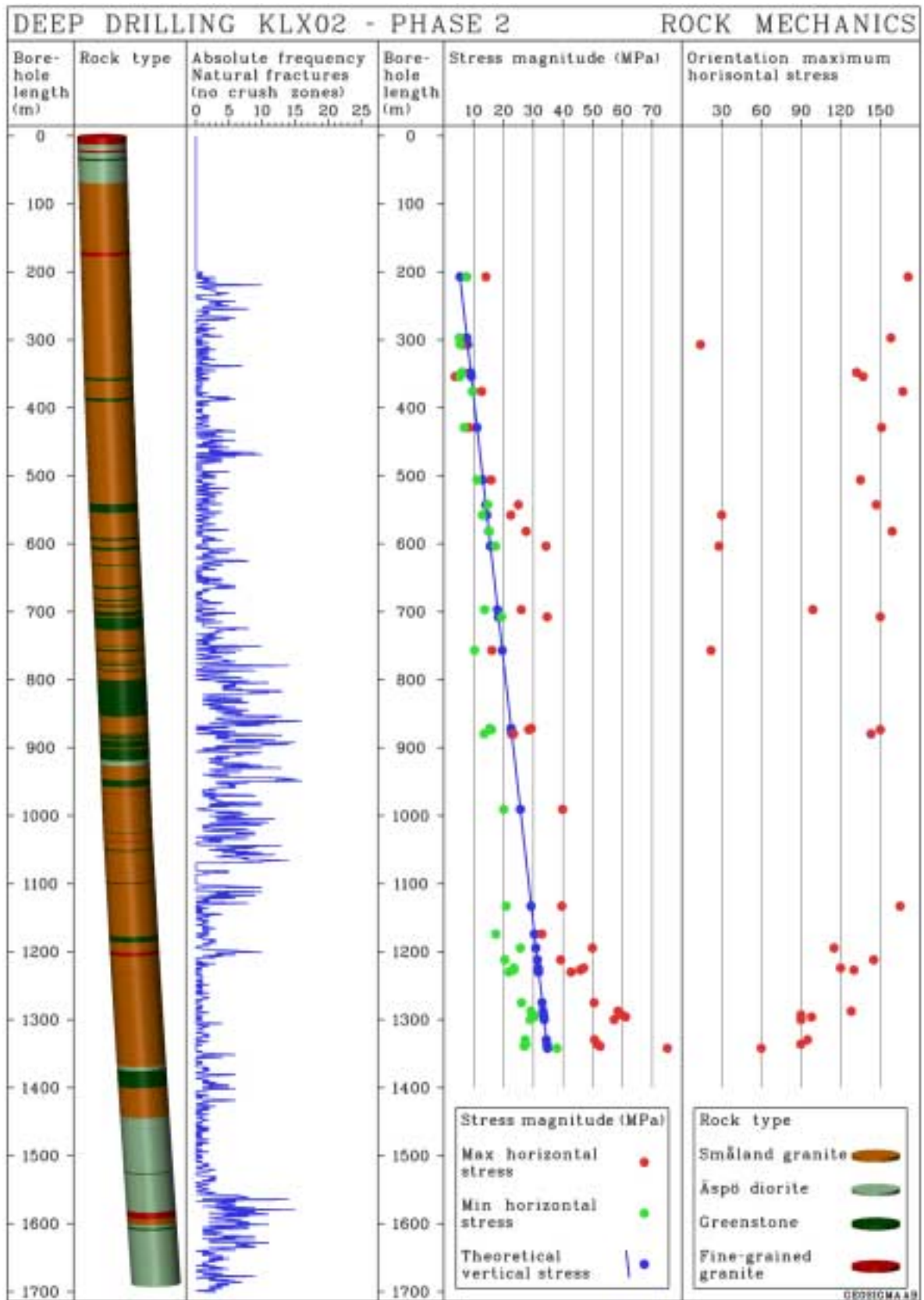


Figure 4-7. Lithology, fracturing, stress magnitudes and orientations versus depth in borehole KLX02.

Stress orientations

The orientation of the maximum horizontal stress as observed from Table 4-3 and Figure 4-6 exhibits a rather stable value to approximately 1100 m borehole length. However, five outliers are identified between 207 m and 1100 m, four of which have yielded orientations between N15°E–N30°E and the fifth the orientation N9°W. These orientations cannot be explained by measurement errors. If the mentioned outliers are ignored, a mean orientation for the maximum horizontal stress within the depth interval 207–1133 m of N29°W prevails (151° clockwise from magnetic north). This orientation agrees well with other stress measurements performed in the area, e.g. those from the Äspö tunnel and the hydrofracturing measurements in KAS02 and KAS03 at the island of Äspö. (cf. Section 4.2.6). Below approximately 1100 m depth, a drastic reorientation of the maximum horizontal stress is indicated. The orientation gradually changes from NW to a NE-direction at 1340 m. A constant orientation for the deepest measurements can, however, not be identified. The graph in Figure 4-6 clearly illustrates that the start of the reorientation corresponds to the lower boundary of the highly fractured borehole interval. This fact supports the previously stated suggestion, that the stress field is disturbed within this interval.

4.2.6 Comparison with hydrofracturing stress measurements in boreholes KAS02 and KAS03 on Äspö

Hydraulic fracturing rock stress measurements were performed during 1988 and 1989 in two nearly vertical boreholes, KAS02 and KAS03, on the island of Äspö, see Figure 1-1. In KAS02 the measurements were conducted in the interval 113–737 m (borehole length) and in KAS03 between 131–963 m.

An interesting feature discovered in the results from KAS02 and KAS03 is that in both boreholes, zones are indicated within which the gradient of the stress magnitude is very low, or even close to zero. As described in the previous section, a corresponding result was obtained for borehole KLX02 at Laxemar.

The magnitudes of the minimum horizontal stress from the three boreholes are illustrated in Figure 4-8. A similar magnitude for all three boreholes is indicated for the interval between the start of the measurements to about 500 m borehole length (approximately = vertical depth). Below that level, however, a significant discrepancy of the magnitudes is exposed. All three boreholes display an interval of almost constant stress magnitude versus depth. In KAS02 this interval is found at 600–750 m, in KAS03 at 500–700 m and in KLX02 at 750–1100 m. The disturbance of the stress field above respectively below the supposed fracture zone observed in KLX02 is recognized also above and below the interval of low stress gradient in KAS03. A similar disorder is seen above the corresponding interval in KAS02. In this case the borehole ends right within this interval.

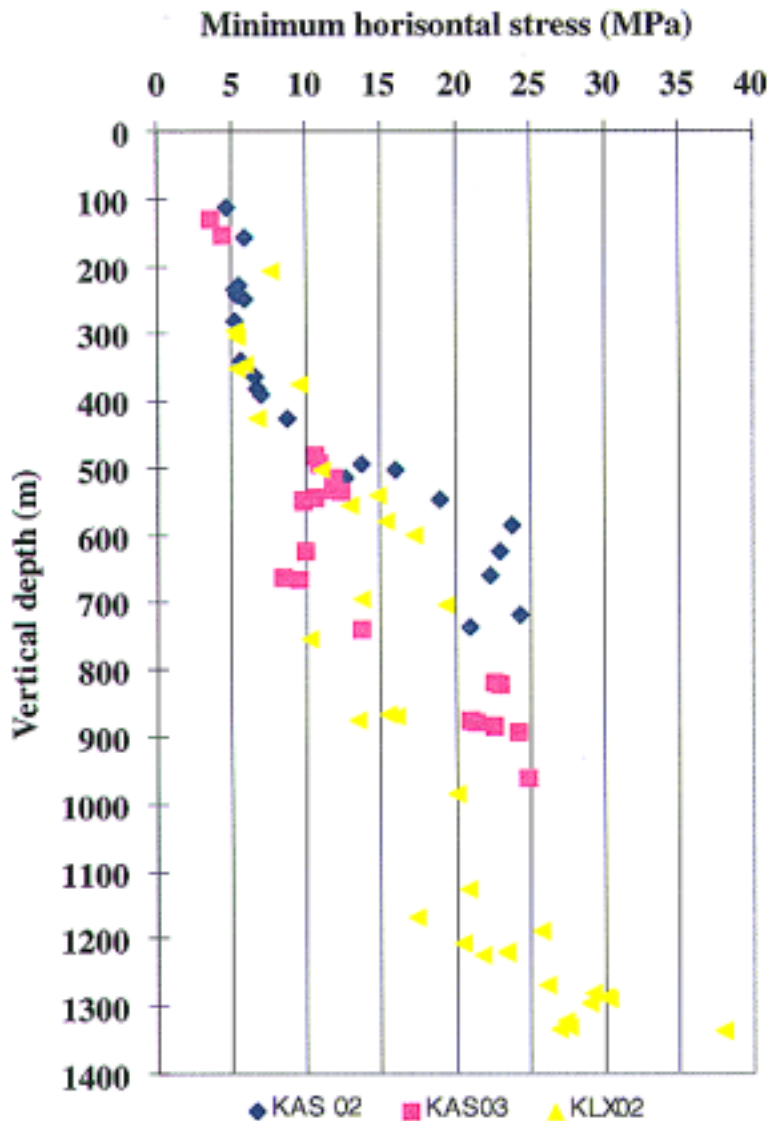


Figure 4-8. The minimum horizontal stress as a function of depth as measured from hydraulic fracturing rock stress measurements in boreholes KAS02, KAS03 and KLX02. After Figure 5-1 in /4-1/.

The orientations of the maximum horizontal stress in the three boreholes, which can be studied in Figure 4-9, are in good agreement between the three boreholes, which supports the idea of a NW-SE trend for the maximum horizontal stress in the uppermost part of the crust within this region.

A renewed analysis of stress indicators in borehole KLX02 performed after the completion of Phase 2 suggested that the orientation of the maximum horizontal stress above and below the interval 700–1100 m vertical depth is NW-SE /4-6/. However, within this interval, an ENE-WSW orientation was proposed. These analyses were below 870 m (like the analyses in /4-1/) based on BIPS-images, a method associated with great uncertainties. In /4-6/ it is therefore pointed out that further research should be conducted to confirm the true orientation of the maximum horizontal stress at great depth in KLX02.

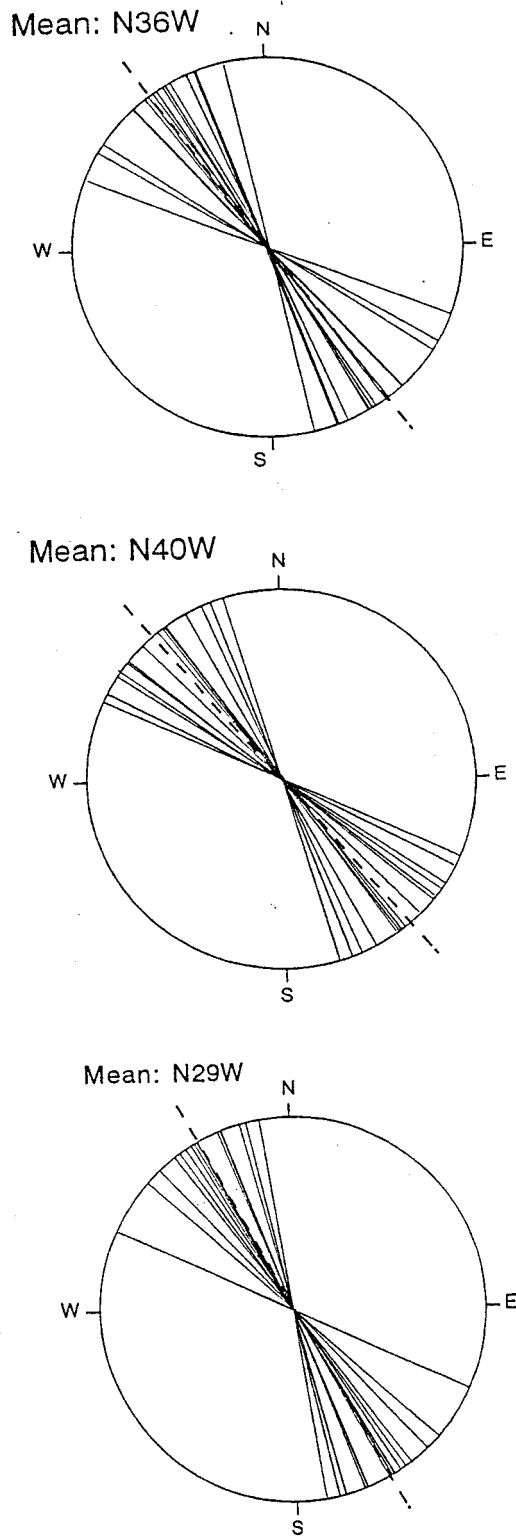


Figure 4-9. Orientation of the maximum horizontal stress determined from hydraulic fracturing rock stress measurements in boreholes KAS02 (top), KAS03 (middle) and KLX02, interval 200–1100 m, outliers excluded (lower). After Figure 5-2 in /4-1/.

4.3 Hydromechanical characterization

The presentation given in this section is in all essentials based on report /4-7/.

4.3.1 Introduction

Fractures and fracture zones are the dominating features for flow and contaminant transport in crystalline bedrock. Hydromechanical fracture properties such as geometry, aperture, roughness and stiffness have a strong influence on the flow and transport behaviour /4-8/. Previous studies have demonstrated also the dependency of fluid flow along fractures on the prevailing *in situ* stress field through a sensitive aperture and flow rate relationship. Many field studies have witnessed that the hydraulic conductivity in general decreases with depth, mainly because increased stress compresses the open fractures to a smaller aperture. Thus, the fluid flow and transport of dissolved constituents are dependent on both the hydromechanical properties and the *in situ* stress field.

Hydromechanical properties have to be determined in an experiment that involves both fluid flow and mechanical deformation. In the laboratory, drill cores from a borehole intersecting fractures can be tested for stress versus transmissivity. However, a drill core sample represents only a single point in the fracture plane, which may not be representative of the entire *in situ* fracture plane behaviour. Furthermore, the fracture is to some extent disturbed during the process of drilling and preparation of a laboratory sample. It is therefore preferable to test fractures under *in situ* conditions involving a larger area of the fracture surface.

The *in situ* stress field may be determined by a conventional hydraulic fracturing stress measurement. In such a test, the maximum principal stress is calculated from the reopening pressure determined in a constant rate injection test. It has been understood for many years that some deficiencies are inherent in the interpretation of reopening pressure, and that this pressure is dependent on the injection rate. This indicates that the reopening process is affected by residual fracture aperture and normal stiffness. A better understanding of the reopening process would serve to obtain a more reliable determination of the maximum principal stress.

The study reported in /4-7/ scopes the above mentioned two topics: 1) *in situ* hydromechanical properties of various types of fractures and 2) the reopening process during hydrofracturing stress measurements.

The succeeding part of this sections is devoted to the following issues:

- In Section 4.3.2 the development of a new component of the hydraulic fracturing equipment used for the field tests is described.
- In Section 4.3.3 an overview of all hydrofracturing field tests performed in borehole KLX02 is presented.
- Several types of injection tests together with numerical modelling were applied for determination of the *in situ* hydromechanical properties such as fracture aperture, fracture normal stiffness and normal stress. The results were reported in /4-9/, /4-10/ and /4-11/, all included in /4-7/. In section 4.3.4 a short summary with major findings is given.
- Finally, section 4.3.5 is treating the influence of fracture properties on the evaluation of stress from hydrofracturing. These studies are reported in /4-12/ and /4-13/, both included in /4-7/.

4.3.2 New development of the hydraulic fracturing equipment

The SKB Mobile Hydrofracturing Equipment is thoroughly described in /4-4/. In 1993, a specially designed valve was added above the packer section to allow for pressure pulse testing. The new system includes an electrical switch, an electromagnetic valve and another valve triggered by compressed air with aid of a piston (Figure 4-10). Compressed air is supplied through one of the three hydraulic hoses within the multihose system and the entire process is controlled by the electrical switch at the ground surface. The valve system has the capacity of creating pressure pulses of at least 20 MPa within a fraction of a second. With the new tool, a pressure pulse is created by opening and closure of the valve (Figure 4-10 c).

The rate of the pressure decay depends on the hydraulic properties of the rock and of the storage capacity of the sealed-off well section. If the storage capacity of the sealed volume is known, the hydraulic properties of the fracture can be evaluated through curve matching with an analytical solution. The effective well storage capacity depends on two parameters, the compressibility of the water and the compliance of the test equipment during pressurization. A recent laboratory test to determine the water storage capacity of the sealed-off test section is presented in /4-14/ (included in /4-7/). The results of the laboratory test demonstrate that the effective storage capacity S_e is:

$$S_e = 3.6 \cdot 10^{-9} \text{ m}^3/\text{m} \text{ for } 56 \text{ mm boreholes,}$$

$$S_e = 7.0 \cdot 10^{-9} \text{ m}^3/\text{m} \text{ for } 76 \text{ mm boreholes.}$$

These values should be used in the evaluation of pulse tests where the packer pressure is ≥ 10 MPa and the maximum pulse pressure is less than 4 MPa below the packer pressure.

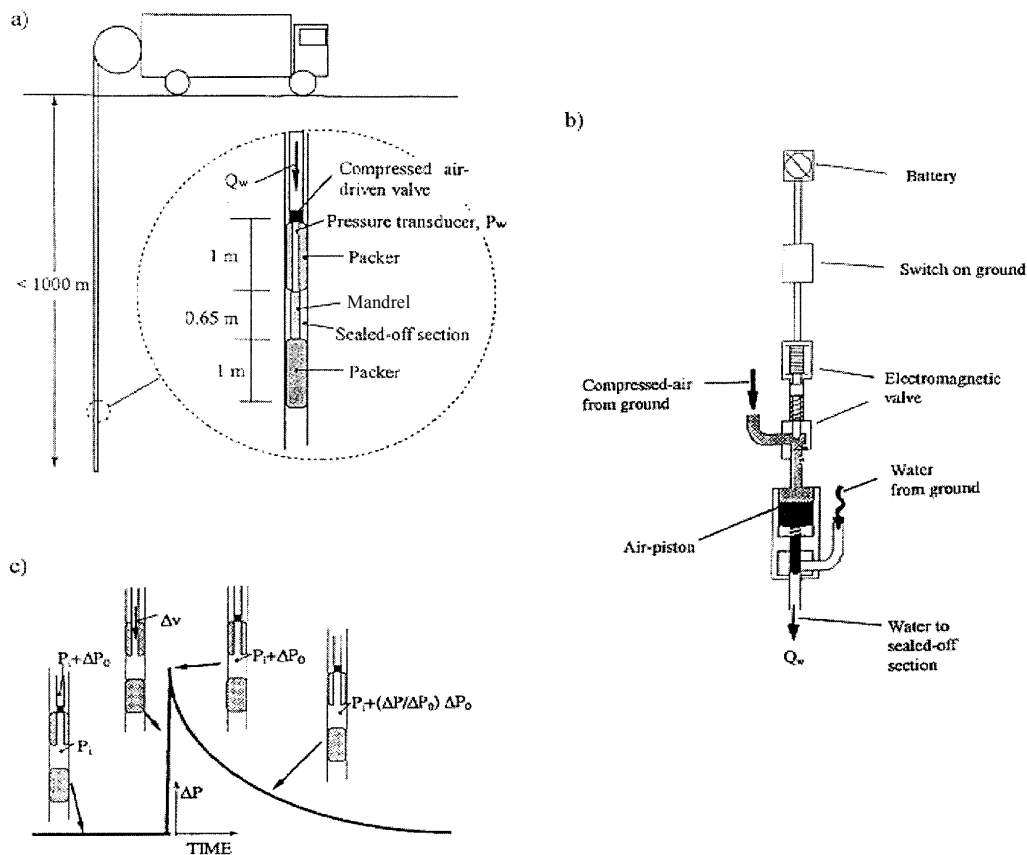


Figure 4-10. Equipment for conducting pulse tests: a) down-hole tool b) simplified picture of the down-hole shut-in system and c) principle of conducting a pulse test. After Figure 2-1 in the main document in /4-7/.

4.3.3 Overview of field tests

The field tests in borehole KLX02 at Laxemar for determination of hydro-mechanical parameters were conducted during the summer and autumn of 1996 in conjunction with the conventional hydrofracturing stress measurement program presented in Section 4.2. The field tests, aiming at determination of hydro-mechanical parameters, may be divided into:

- Measurements on existing fractures.
- Measurements on fractures induced by hydraulic fracturing.

The mobile equipment described in Section 4.2.3 was engaged for performance of all tests. A straddle-packer tool with a separation of c. 0.6 m was applied. After completion of the hydraulic testing, an impression packer was lowered into the borehole in order to determine the orientation of each fracture.

Existing fractures

The purpose of the tests performed on existing fractures in borehole KLX02 was to determine *in situ* hydromechanical properties. In a first attempt, injection tests were performed on fractures selected with aid from the PetroCore log and located at every 100 m between 250 m and 550 m borehole length. At each level, a borehole section of 5 m was covered with several pulse injection tests. Conductive fractures could be detected only at 250 m, despite the fact that the core log reports several fractures per m in all sections. Since the pulse test equipment is capable of measuring fracture apertures in the order of a few microns, it can be concluded that the fractures in the sections in question are sealed with mineral fillings. Hence, their hydraulic conductivity is not significant in relation to the overall hydraulic conductivity of the rock mass. This fact brought about a change in strategy. Pictures with the BIP-system (cf. Section 3.3.7) were consulted for location of open fractures. With this method three zones located at respectively 267 m, 315 m and 337 m borehole length were selected for extensive hydraulic testing, see Table 4-4. These zones appear as anomalies on the temperature and resistivity logs. Furthermore, the spinner log here indicates the highest hydraulic conductivities in the upper 700 m of the borehole, see Appendix 3. Table 4-4 gives a summary of the types of injection tests performed on existing fractures in borehole KLX02.

Induced fractures

The tests performed in KLX02 on induced fractures served to provide hydro-mechanical parameters essential during a reopening test in classical hydraulic stress measurements. In this case, borehole sections with no apparent fractures were selected. The applied test cycle followed the succession described in the head-line of Table 4-5, where it is also illustrated that the complete test cycle was adopted on all tested fractures. The first pulse test was conducted in order to

Table 4-4. Injection tests conducted in borehole KLX02 on existing fractures. After Table 3-1 in /4-7/.

Borehole length (m)	Pulse injection test	Constant pressure injection test	Shut-in test	Step-pressure injection (hydraulic jacking)	Fracture characteristics
250	X				Several conductive
267	X	X	X	X	Several conductive
315	X	X	X	X	One main conductive
337	X	X	X	X	No conductive
350	X				Several conductive
402	X				No conductive
424	X				No conductive
450	X				No conductive
550	X				No conductive

Table 4-5. Injection tests conducted in borehole KLX02 on fractures induced by hydraulic fracturing. After Table 3-2 in /4-7/.

Borehole length (m)	1 st Pulse test	Fracturing	2 nd Pulse test	Reopening and shut-in tests	Step-pressure injection (hydraulic jacking)
297	X	X	X	X	X
376	X	X	X	X	X
490	X	X	X	X	X
679	X	X	X	X	X

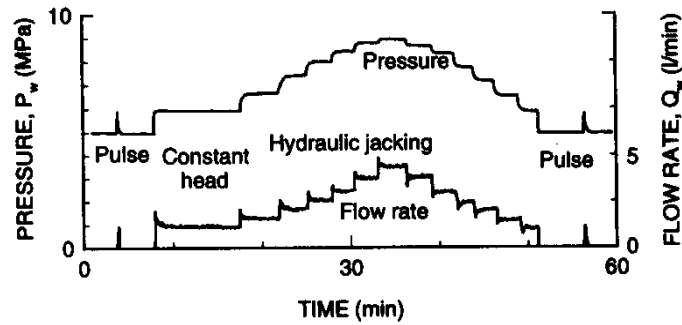
reassure that the selected rock section was intact, without hydraulic conductive fractures. A conventional hydraulic fracturing stress measurement operation was then performed including fracturing, reopening and shut-in tests. After fracturing, the second pulse test was performed in order to determine the hydraulic properties of the newly created fracture. The pulse injection tests and shut-in tests are interpreted and the results presented in /4-7/. For the matter of reopening and step-pressure tests, these are part of ongoing research for development of more accurate stress determination methods and were not yet completed at the day of printing report /4-7/.

4.3.4 Evaluation of *in situ* hydraulic and hydromechanical properties of rock fractures

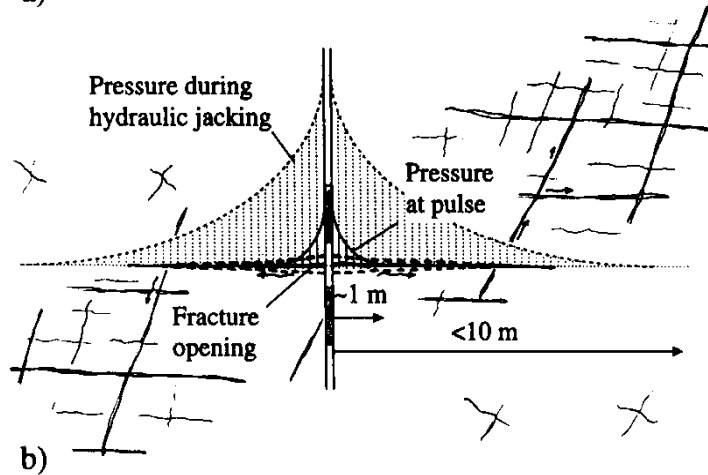
A number of existing fractures in three highly conductive zones intersecting borehole KLX02 at borehole lengths 267 m, 316 m respectively 337 m were tested. By analysis of these tests, the *in situ* hydromechanical fracture properties were determined. The results have been published in /4-8/ and /4-9/, scrutinizing the fracture parameters aperture, normal stiffness and normal stress, and in /4-10/, which is treating the parameter fracture storativity. These reports are also summarized in /4-7/.

Borehole KLX02 is at 267 m and 337 m borehole length intersected by fracture zones, each a few metres wide and dominated by a few open fractures. Several types of injection tests were performed on these according to the sequence presented in Figure 4-11 a. The purpose of the pulse tests respectively the constant head injection tests is to establish the initial hydraulic conditions before the start of the high pressure hydraulic jacking test, see Figure 4-11 b.

Hydraulic jacking tests are recognized by a step-wise increase in the fluid pressure and recording of the fluid pressure at the end of each step. During increase of the fluid pressure, the effective normal stress decreases, entailing opening of the fracture. The fracture opening results in an increased hydraulic conductivity of the



a)



b)

Figure 4-11. Hydraulic injection tests for coupled hydromechanical evaluation. a) Well pressure and well flow as a function of time. b) Radius of influence for various tests. After Figure 4-1 in the main document in /4-7/.

fracture, which will be detected as an increase in flow rate. During a high pressure injection test, the flow rate is strongly dependent on the fracture aperture and on the fracture normal stiffness in the vicinity of the borehole /4-11/. The domination of these parameters implies that they are possible to back-calculate from the pressure and flow responses without significant disturbing influence from other parameters.

Hydraulic aperture and fracture normal stiffness

The hydraulic aperture and the fracture normal stiffness were, as described in /4-7/ and /4-9/, back-calculated by coupled numerical modelling of the multiple pressure injection tests according to /4-8/. The numerical model used is the coupled hydromechanical finite element code ROCMAS /4-15/. During the process of model calibration, the input parameters are adjusted until the pressure and flow responses match the field measurements. The result of the evaluation is presented as fracture transmissivity versus depth in Figure 4-12.

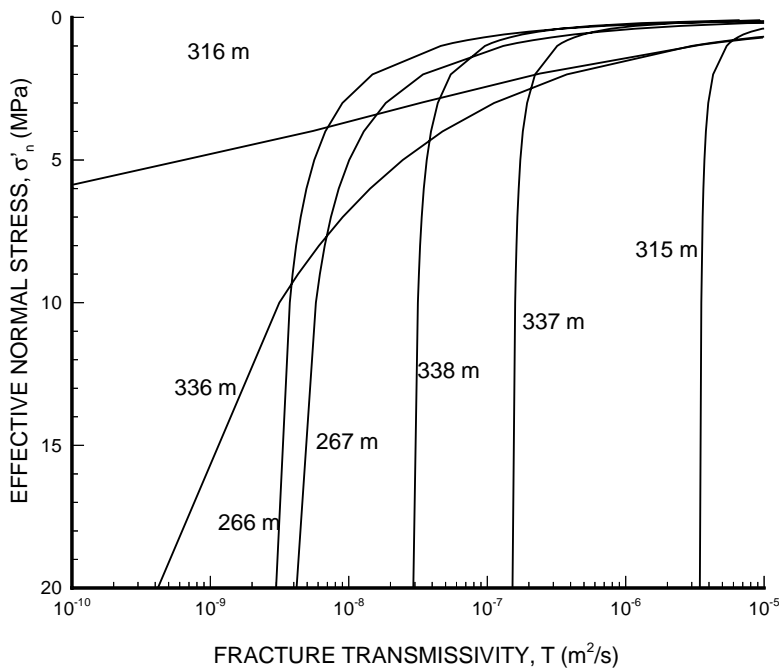


Figure 4-12. Hydraulic transmissivity versus effective normal stress for fractures in borehole KLX02. After Figure 4-2 in the main document in /4-7/.

The fractures at 316 m and 336 m display a major decrease in transmissivity with increasing normal stress, and would be practically closed if located at a depth of 500 m or more. These are examples of fractures with a low normal stiffness together with a relatively small residual aperture. In return, the remaining fractures included in this test represent another category of fractures, which is relatively insensitive to changes in normal stress. Even at high stresses and at great depths these fractures would, accordingly, be open and have a large hydraulic conductivity. On the borehole-TV images the fractures of the last category appear as open and unmated, probably due to previous shear displacement and dissolution of fracture filling materials, see Figure 4-13.

One important consequence of the results obtained is, that the hydraulic conductivity is more likely to depend on normal stress and depth in the upper few hundred metres of the bedrock. In this region both the mated joints in the more competent rock and fracture zones contribute to the overall hydraulic conductivity. However, at great depths, the mated joints will be closed, and the conductivity is dominated by relatively stress insensitive unmated fractures. The study reported in /4-7/ has clarified that the hydromechanical properties of rock fractures are strongly dependent on the current *in situ* state, which is affected by past shearing or other tectonics, and by cementation or dissolution of mineral filling. Fractures should therefore be tested *in situ*.

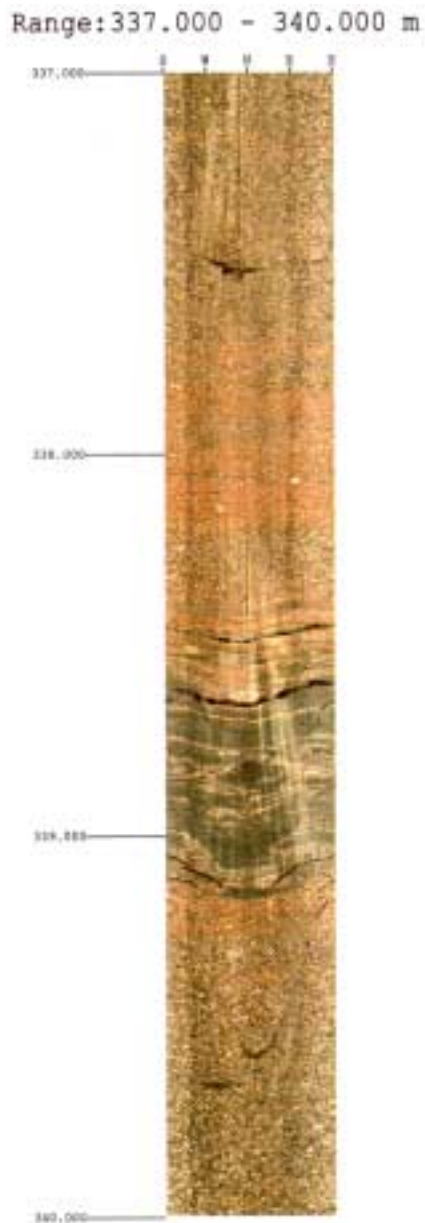


Figure 4-13. BIPS-image from section 337–340 m in borehole KLX02 with an open unmated fracture. After Figure 7.3c in /4-9/.

Fracture storativity

During water injection into a single fracture in hard rock, the storage of water is dominated by the normal deformation of the fracture, as demonstrated in /4-10/. In most cases the storativity will be entirely controlled by the combined stiffness of the fracture and the ambient rock mass. Early in the injection test, when the radius of influence is small, the storage is determined by the stiffness of the ambient rock mass. Later, when the radius of influence increases, the storage is controlled by

the fracture normal stiffness. Therefore, if the transmissivity is dictated by flow in planar fractures, the strong coupling to the stiffness implies, that the storage capacity can be derived from the pressure dependency of the fracture aperture in a high pressure injection test. Such an estimate may be performed in combination with conventional hydraulic tests as a method for independent determination of the storage capacity, enabling bounding of the curve matching within reasonable limits. This implies that other hydraulic properties can be determined more unambiguously.

The fracture storativity determined by high pressure injection tests versus effective normal stress is presented in Figure 4-14 together with data from previous measurements in granitic rocks at two other sites. A relation between storativity and effective normal stress is derived in a similar manner as for the transmissivity in Figure 4-12. It is obvious that the transmissivity varies more widely compared to the storativity at a certain stress level. This originates from the fact that the hydraulic aperture varies much more than the normal stiffness. The transmissivity is strongly affected by the current hydraulic aperture which depends on the previous shear and other tectonic history as well as on the cementation and dissolution of fracture fillings. Therefore, it is not readily correlated with the present normal stress. Storativity, on the other hand, with its strong dependency on the current normal stiffness, is better correlated to the prevailing normal stress.

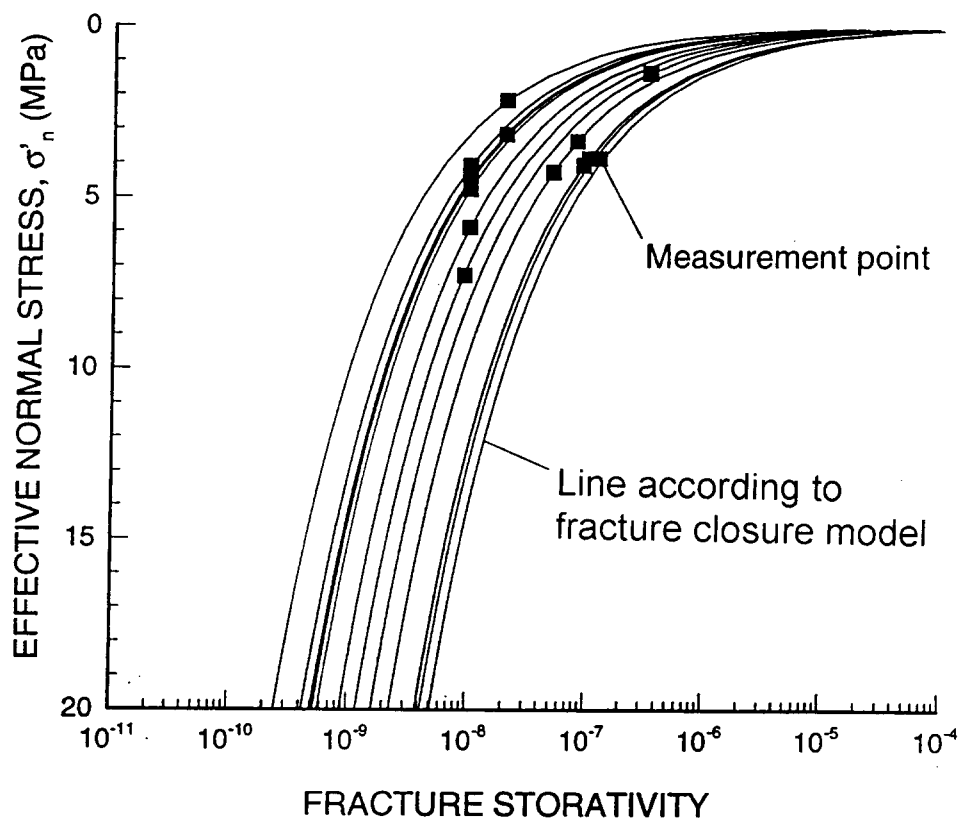


Figure 4-14. Storativity versus effective normal stress in borehole KLX02. After Figure 4-3 in the main document in /4-7/.

4.3.5 Influence of fracture properties on the evaluation of stress from hydrofracturing

/4-11/ and /4-12/ present research related to the determination of stress from the hydraulic fracturing data. In the study reported in /4-11/ the hydraulic conductivity was measured in borehole KLX02 by pulse injection at borehole lengths 297 m, 376 m, 490 m and 697 m. The tests were simulated and interpreted with a finite element model of the borehole and fracture system. The results of the pulse tests revealed a fracture aperture range of 3–15 μm . The evaluation also indicated that the fractures propagated to a radius less than one metre and that the fracture normal stiffness was $\leq 2000 \text{ GPa/m}$.

In /4-12/ a coupled hydromechanical modelling of a hydraulic fracturing reopening test is presented. The hydraulic aperture and the normal stiffness determined in /4-11/ served as reference data. The results of the modelling indicate that, after fracturing, the hydraulic fracture itself disturbs the stress field around the borehole, see Figure 4-15. The minimum tangential stress at the intersection of the borehole with the fracture is therefore smaller than predicted for a linear elastic, isotropic and homogeneous medium. During injection, fluid penetrates the fracture, which opens gradually as a function of the effective normal stress. At a sufficiently high flow rate, the reopening pressure and the maximum pressure become independent of the injection flow rate and equal to the minimum tangential stress at the borehole and fracture intersection, see Figure 4-16.

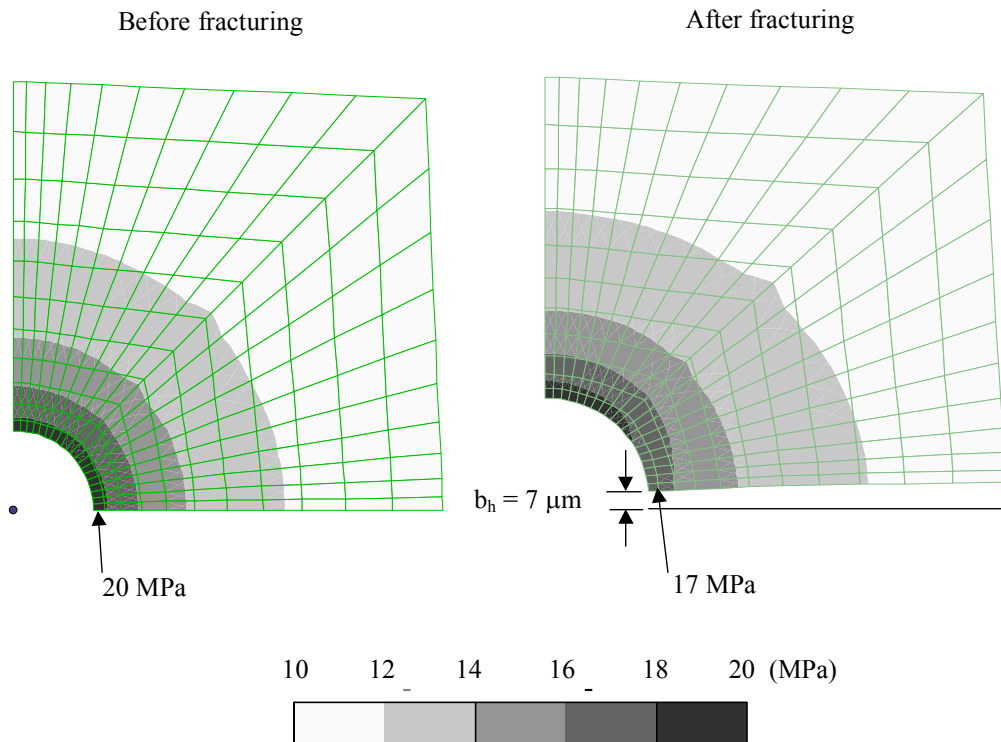


Figure 4-15. Modelling results of maximum principal stress before and after hydraulic fracturing in KLX02. After Figure 5-1 in the main document in /4-7/.

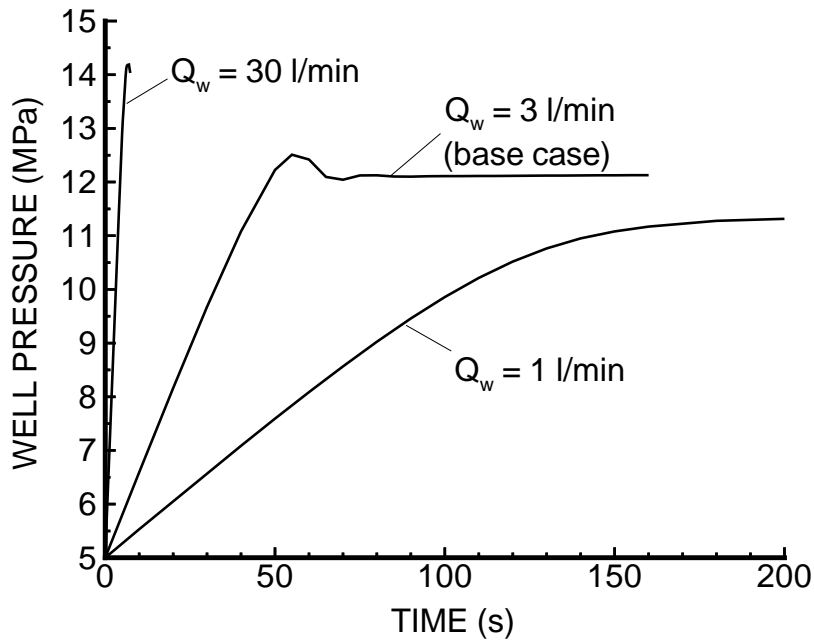


Figure 4-16. Results of modelling of a reopening test in KLX02 with variation of the injection rate Q_w . After Figure 5-2 in the main document in /4-7/.

However, this maximum pressure is still much lower than what would be predicted by the classical hydraulic fracturing theory. The reason is the above mentioned stress redistribution caused by the fracture itself. This indicates that in most cases, the maximum principal stress is underestimated in a conventional hydraulic fracturing stress measurement. In such a case, it may be necessary to compensate for the fracture normal stiffness in the calculation of the maximum principal stress.

4.4 Borehole stability – investigation of fracture orientations in selected parts of KLX02 and comparison with fracture data from core boreholes on Äspö and preliminary investigations of borehole breakouts

During investigations in borehole KLX02, down-hole equipment got caught in the borehole at several occasions. For example, such incidents occurred three times during the period September 1994 to September 1995. Due to this repeated problem, a special study was initiated in order to clarify to what extent the fracture character of the borehole affects the risk for down-hole equipment to get caught /3-15/ and /4-16/. The methods selected for this aim and the scope of activities are presented in Section 4.4.1. The main findings are presented in Section 4.4.2, and a discussion is held in Section 4.4.3, where also other possible explanations to this kind of problem are focused on. Finally, section 4.4.4 presents some results from /4-6/ concerning a study of the borehole wall performed with the BIP-system with focus on borehole breakouts, which is the term for a stress induced process, where rock particles of different sizes come loose from the borehole wall. However, this term is also often used to describe those parts of a borehole where breakouts have occurred and sometimes also referring to the loose particles falling down the borehole.

4.4.1 Methods and scope of activities

The following hypotheses were formulated prior to the investigations:

- A high fracture frequency may increase the risk of equipment jamming due to an uneven borehole wall.
- Fractures intersecting the borehole axis at a small angle (i.e. in this case steeply oriented fractures, since borehole KLX02 is subvertical) may increase the risk of equipment getting caught, either due to a barb effect, or due to an increased hazard of borehole washouts to occur. The term washouts is here defined as loose rock particles entering the borehole despite the underlying causes (stress, drilling, water etc. induced causes).

The aim of the special study reported in /3-15/ and /4-16/ was to test the validity of these hypotheses but also to search for other possible explanations to the actual problem.

Two different approaches were applied for the study. To begin with, borehole geophysical logging was conducted in 1995 with two logging methods: borehole-TV (black & white images) and a three arm caliper /3-15/. The purpose of the TV-logging was to inspect those parts of the borehole where down-hole equipment had got caught, in order to reveal obstacles, washouts etc. The caliper log monitors the borehole radius versus depth. Detection of discontinuities in the borehole wall is therefore possible with this method. The caliper logging performed in July 1995 was compared to a previous caliper logging accomplished

in 1993. The purpose of the comparison was to discover differences in the profile of the borehole wall, which might have turned up in the meantime, for example due to borehole washouts.

Secondly, three sections, where borehole equipment had got stuck in connection with up-hoisting, were selected for fracture investigations /4-16/. Each section has the length of 100 m or 110 m, starting some tenths of metres above, respectively ending some tenths of metres below, the point where the equipment got caught. These sections are:

1. Section 275–375 m (borehole geophysical probe caught at about 339 m).
2. Section 375–485 m (straddle packer caught at approximately 435–436 m).
3. Section 1035–1135 m (straddle packer caught at approximately 1087 m).

BIPS-images from these sections were examined and the absolute orientation (strike and dip) of all fractures (open and sealed) was calculated with the software included in the BIP-system. The angle of fracture intersection with the borehole, in this study denominated the α -angle, was calculated from the dip, using the formula α -angle = 90° -dip. This is a petty simplification, since strictly this formula is valid only for vertical boreholes, whereas borehole KLX02 is applied with a dip of 85° (towards N20°E). The maximum error in determination of strike/dip using the BIP-system is $\pm 5^\circ$, entailing a total maximum error of 10° in determination of the α -angle.

The α -angles were distributed into nine classes ($0-9^\circ$, $10-19^\circ$, ..., $80-90^\circ$). The fracture frequency for each class was plotted versus borehole length. So was the frequency of the total number of fractures versus borehole length. A stereogram of strike and dip, a so called Schmidt-net, was constructed for all fractures. Finally, the PetroCore log was consulted for determination of the lithological character of all investigated sections.

The fractures from sections 275–375 m and 375–485 m are clearly visible in the BIPS-images, supplying an easy method for determination of fracture orientation. However, in section 1035–1135 the borehole wall was covered with a dark chemical precipitation, which made determination of fracture orientation difficult or impossible.

For comparison with corresponding fracture parameters in other deep cored boreholes, two sections, comparative to sections 1 and 2 in borehole KLX02, were selected in each of the subvertical boreholes KAS02, KAS03 and KAS05 on the island of Äspö, see Figure 1-1. In these three boreholes sticking of down-hole equipment has been much less frequent. As far is known, an incident of that kind has occurred only once, in borehole KAS05 at 327 m borehole length. Because BIPS-images do not exist for these boreholes, PetroCore data was used for the fracture analysis. Since all four investigated boreholes have approximately the same dip, the *depths below the ground surface* for the investigated sections are comparable between the boreholes, although data is referred to borehole length.

The elevation of the ground surface at KLX02 is about 10 m higher than at the three boreholes on Äspö. This is also the approximate difference in *absolute level* between the sections in borehole KLX02 and those of the Äspö boreholes.

The α -angle for all natural fractures was determined and punched into the PetroCore file for boreholes KAS02, KAS03 and KAS05. In certain sections also strike and dip were measured and imported into the PetroCore file. In Table 4-6 those parts of boreholes KAS02, KAS03 and KAS05, where oriented fracture data is accessible within section 275–485 m (corresponding to sections 1 and 2 in borehole KLX02), is presented.

After concluded examination of each single borehole, fracture data from all boreholes was compared.

4.4.2 Results

TV-logging

The borehole camera used for this investigation provided black & white images. During a first attempt to inspect borehole KLX02, two elliptical objects attached to the borehole wall at approximately 339 m were discovered. The TV-inspection was thereby interrupted. A rinsing tool was fabricated and lowered into the borehole. The tool was down- and up-hoisted several times in order to clean the borehole wall from the objects discovered with the TV-camera.

After the borehole rinsing, the TV-inspection continued. The objects earlier observed at 339 m had now disappeared, and passing this part of the borehole during down-hoisting caused no further problem. At continued inspection during down-hoisting to 1400 m, the camera encountered two balls of electrical tape in the borehole. This kind of tape is used to attach cables and hoses to a pipe string during hydraulic borehole investigations. Fragments of tape may occasionally be left in the borehole in connection with down- or up-hoisting. The tape balls covered the camera lens, making further inspection of the borehole walls impossible. It was, however, observed at the end of the logging, that several tiny pieces of rock were adhered to one of the tape balls. These fragments, probably representing some kind of borehole washouts, may well be the cause of the problems with the down-hole equipment, taking into consideration that the space between the borehole wall and certain types of down-hole equipment is only a couple of millimetres.

Caliper logging

Figure 4-17 illustrates three sections of the three arm caliper logging performed in borehole KLX02 in 1993, i.e. prior to the period when major problems with caught down-hole equipment were faced, respectively in 1995, after three incidents. The three sections include those parts of the borehole where the equipment problems occurred: at 339 m, 435–436 m and at 1087 m.

Table 4-6. Borehole sections with oriented fracture data within section 275–485 m in boreholes KAS02, KAS03 and KAS05. After Table 2-1 in /4-16/.

Borehole	Section (m)	Sections with oriented fracture data (m)
KAS02	275 – 485	275.00 – 277.61
		283.19 – 284.55
		296.58 – 304.28
		304.36 – 312.24
		314.31 – 315.01
		316.77 – 322.89
		326.56 – 352.80
		353.15 – 370.44
		370.60 – 374.13
		375.35 – 405.04
		418.20 – 420.05
		424.30 – 438.23
		443.10 – 446.11
		450.82 – 485.00
		KAS03
289.30 – 290.56		
291.68 – 292.80		
293.36 – 294.70		
294.78 – 310.65		
333.45 – 337.75		
337.81 – 345.48		
345.53 – 351.01		
351.05 – 362.08		
363.98 – 371.07		
371.11 – 371.85		
371.89 – 379.99		
380.03 – 395.81		
396.09 – 396.64		
398.33 – 403.69		
404.68 – 407.66		
410.21 – 411.39		
411.45 – 417.23		
418.12 – 432.33		
437.17 – 448.54		
448.63 – 455.23		
455.29 – 466.10		
466.15 – 475.95		
477.05 – 485.00		
KAS05	275 – 485	340.80 – 353.80
		357.73 – 362.41
		363.28 – 388.96
		400.65 – 454.91
		462.61 – 465.51
		465.82 – 485.00

Some minor differences in the results between the two loggings were observed. These may, however, be caused by different positions of the caliper arms during logging. Some of the differences may be explained by parts of the borehole being oval-shaped. In order to detect such a feature, a caliper log with a minimum of four arms would be necessary /3-15/.

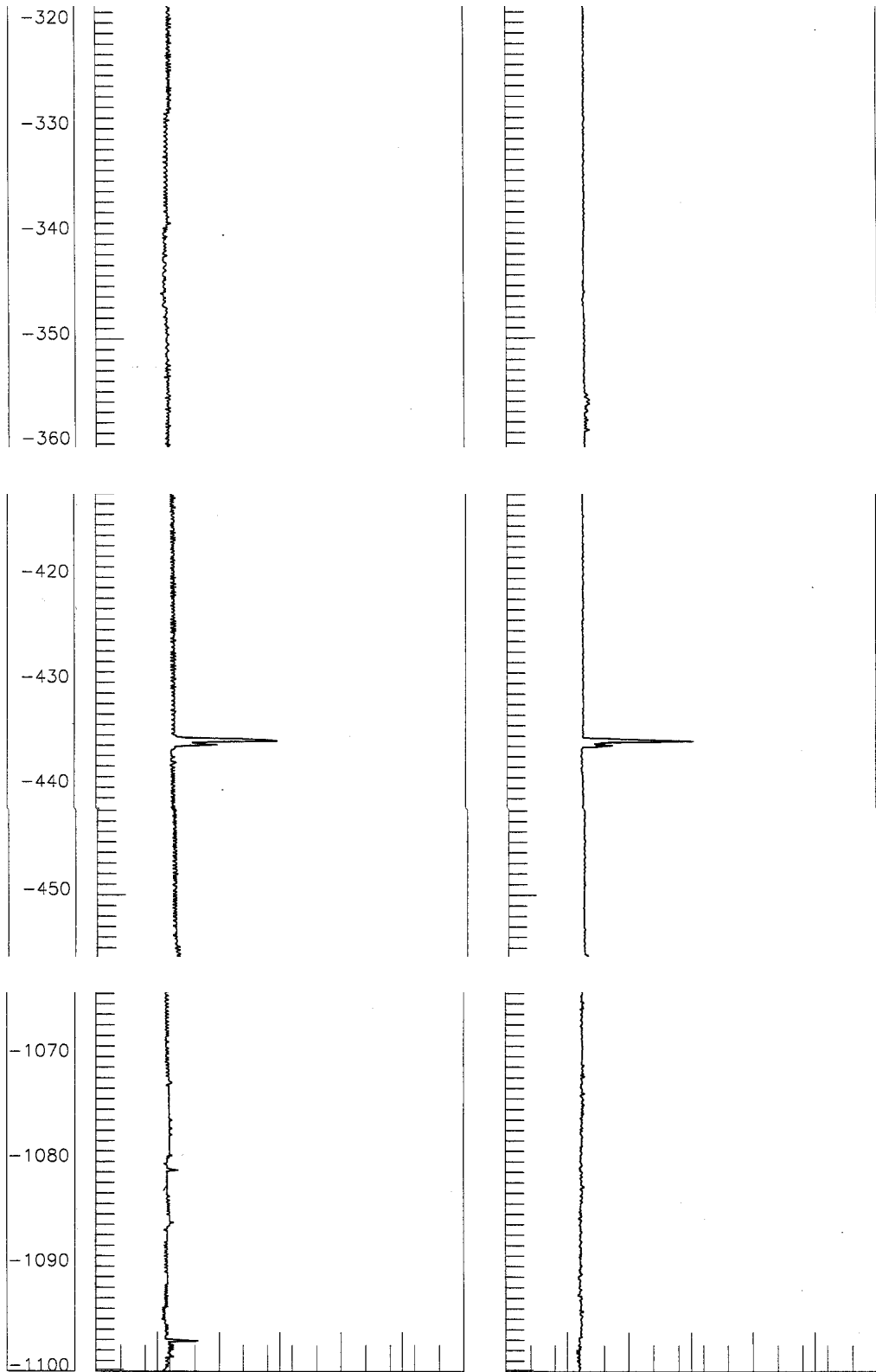


Figure 4-17. Results in selected parts of borehole KLX02 of caliper loggings performed in 1993 (left) and 1995 (right). Depth scale in metres below ground surface. From Appendix 6 in /3-15/.

None of the caliper loggings reveals any pronounced discontinuity at 339 m. At section 435–436 m, however, a caliper anomaly of about 9 mm is observed in both caliper graphs. Finally, at 1087 m the borehole wall appears as almost even. A minor anomaly is, though, observed some metre above that point in the logging from 1993.

Distribution of natural fractures

The frequency of natural fractures, i.e. the number of fractures/metre (drill induced fractures and crushed zones excluded) in boreholes KLX02, KAS02, KAS03 and KAS05 is illustrated in Figure 4-18. Borehole KLX02 exhibits sections of persistently high fracture frequencies at about 200–270 m, 430–480 m, 600–1200 m and at 1550–1700 m. Minor sections with increased frequency are encountered also between these intervals. Down-hole equipment got caught at 339 m, which corresponds to a frequency peak at 338 m of 7 fractures/m. Another hazardous spot was situated at 435–436 m. Figure 4-18 reveals a frequency top of 6 fractures/m at 434 m. The third place where equipment was jammed is situated at 1087 m. The closest frequency increase is found at 1083 m. The frequency maxima prevailing at problematic spots are by no means extreme compared to the rest of the borehole.

Comparison with the Äspö-boreholes demonstrates that all three boreholes have a fracture frequency exceeding that of KLX02 at the studied sections. Especially the fracturing in KAS03 is conspicuously high. In section 275–485 m, borehole KAS03 exhibits a significantly higher fracture frequency than borehole KLX02 at 275–485 m.

None of the Äspö-boreholes is long enough to be compared with section 1035–1135 m in borehole KLX02.

Distribution of α -angles

Figure 4-19 illustrates the frequency distribution versus depth for nine classes of α -angles (0–9°, 10–19°, ... 80–90°) in the four investigated boreholes. Each class includes all fractures – open as well as sealed – calculated as the number of fractures per m.

Borehole KLX02, section 1, 275–375 m

In this section problems with jamming of down-hole equipment occurred at 339 m.

Figure 4-19 illustrates:

- Steep α -angles were encountered at 330 m (0–9°) and at 325–345 m (10–19°).
- For α -angles flatter than 20°, a relatively even frequency distribution versus depth is prevailing.

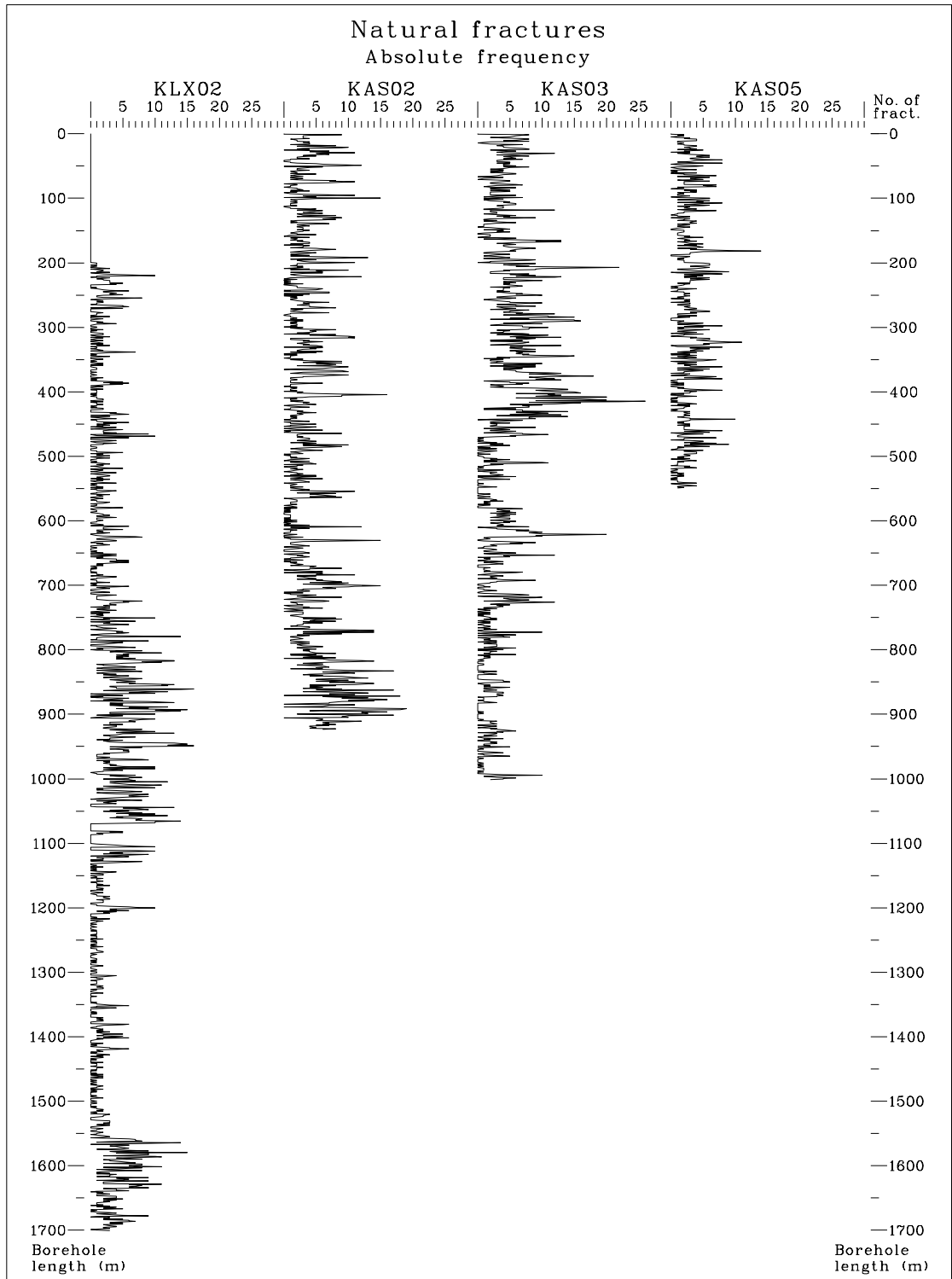


Figure 4-18. Distribution of the total number of natural fractures versus depth (induced fractures and crushed zones excluded) in boreholes KLX02, KAS02, KAS03 and KAS05. After Figure 3-1 in /4-16/.

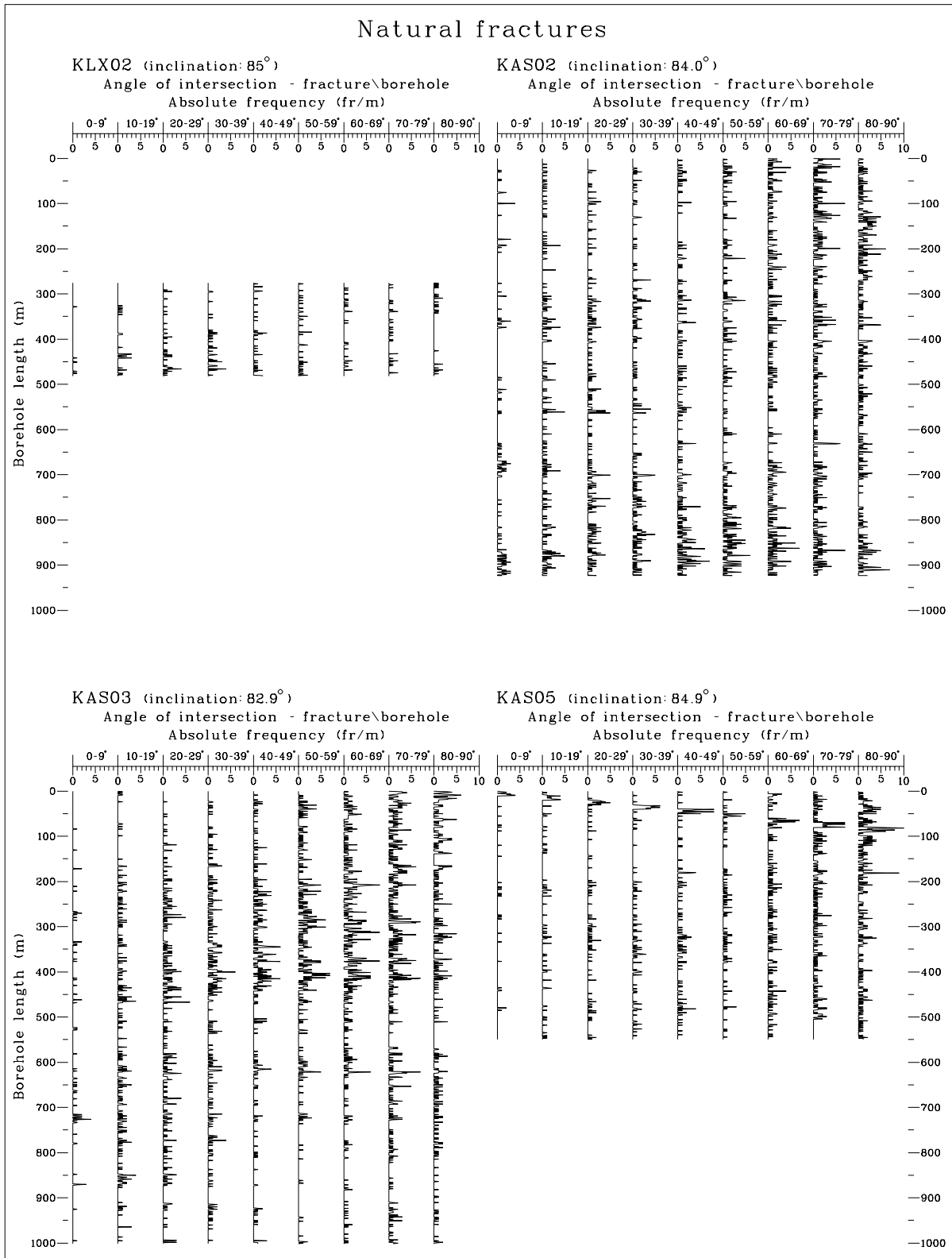


Figure 4-19. Distribution of intersection angles with (α -angles) the borehole axis versus depth in boreholes KLX02, KAS02, KAS03 and KAS05. α -angle = 0° indicates approximately vertical fracture, α -angle = 90° indicates approximately horizontal fracture. After Figure 3-2 in /4-16/.

Borehole KLX02, section 2, 375–485 m

Equipment problems occurred at 435–436 m.

Figure 4-19 shows:

- In class 0–9° increases of fracture frequency appear at 440 m, 450 m, 470 m and at 475 m.
- Class 10–19° exhibits frequency peaks at 433–441 m and at 463–478 m.
- Class 20–29° demonstrates frequency maxima at 438 m and 465 m.
- α -angles 30–39° have a high frequency in the entire section.
- Larger (flater) α -angles show a rather homogeneous distribution over all classes except in the class 80–90°, where fractures exist only in the deeper part of the section.

Borehole KLX02, section 3, 1035–1135 m

Equipment got stuck at 1087 m.

α -angles were not possible to determine with the BIPS-images in this section due to the discolouring of the borehole wall caused by chemical precipitation.

Comparison with boreholes KAS02, KAS03 and KAS05

Figure 4-19 reveals a higher frequency of steep α -angles, 0–19°, in the actual sections in KAS02 than in KLX02.

Also borehole KAS03 has a higher frequency of steep α -angles, 0–29°, than borehole KLX02. These are relatively evenly distributed in the sections in question, though peaks exist at e.g. 400 m, 440 m and 470 m. The remaining, flater, α -angles are much more frequent in borehole KAS03 than in the other investigated boreholes.

The character of the fracture distribution in borehole KAS05 is similar to that in KLX02 with a relatively low frequency of steep fractures. The share of flat fractures is, however, higher in borehole KAS05 than in borehole KLX02.

Fracture orientation

Strike/dip of a fracture set may be illustrated in a stereogram, for example a Schmidt-net with projection on the lower hemisphere. The projection of fractures with a flat dip (horizontal or sub-horizontal) will land close to the center of the stereogram, while steep fractures are projected close to the periphery. The strike decides in which sector of the stereogram the projection will appear.

Figure 4-20 illustrates plots in a Schmidt-net for section 275–485 m in boreholes KLX02, KAS02, KAS03 and KAS05, one plot for each borehole. It should be observed, that oriented fracture data is not continuous in section 275–485 m, see Table 4-6. In all plots the contour-lines 1 %, 2 %, 3 % and 5 % are assigned. In boreholes KLX02 and KAS02 also the contour-line 7 % is included.

In all boreholes the major part of the mapped natural fractures are flat, entailing a concentration towards the centre of the Schmidt-net. A significant difference between borehole KLX02 and the Äspö-boreholes is that KLX02 also exhibits a distinct concentration of steep fractures striking WNW with a dip towards NE.

BIPS-images

BIPS-images are presented in /4-16/ for borehole sections 275–485 m and 1035–1135 m. In Figure 4-21 BIPS-images from the three sections, where jamming incidents with down-hole equipment in the borehole have occurred, are selected.

The section near 339 m consists of Småland granite, between 337.3–339.3 m relatively altered. Several open fractures are observed, a couple of them displaying steep α -angles.

Also at 435–436 m with nearest surroundings the rock type is Småland granite. The rock is crushed in section 432.2–433.9 m, according to the BIPS-images (435.4–437.0 m according to the PetroCore log). Four steep fractures were encountered in this section.

Finally, the rock type at and around 1087 m likewise consists of Småland granite. The entire section is characterized by a high fracture frequency. These fractures intersect, with only a few exceptions, the borehole at a large (flat) α -angel.

4.4.3 Discussion

The first hypothesis stated at the beginning of this chapter argued, that a high frequency of fractures intersecting a borehole increases the risk of equipment getting stuck in the borehole during up- or down-hoisting. Where this problem occurred in borehole KLX02, at 339 m, 435–436 m and 1087 m, increased fracture frequencies were observed. If the investigation results from only borehole KLX02 were taken into consideration, the study therefore to some extent supported the hypothesis. This is though disapproved by the fact that still higher fracture frequencies prevail over long distances in borehole KLX02, where jamming problems have never occurred.

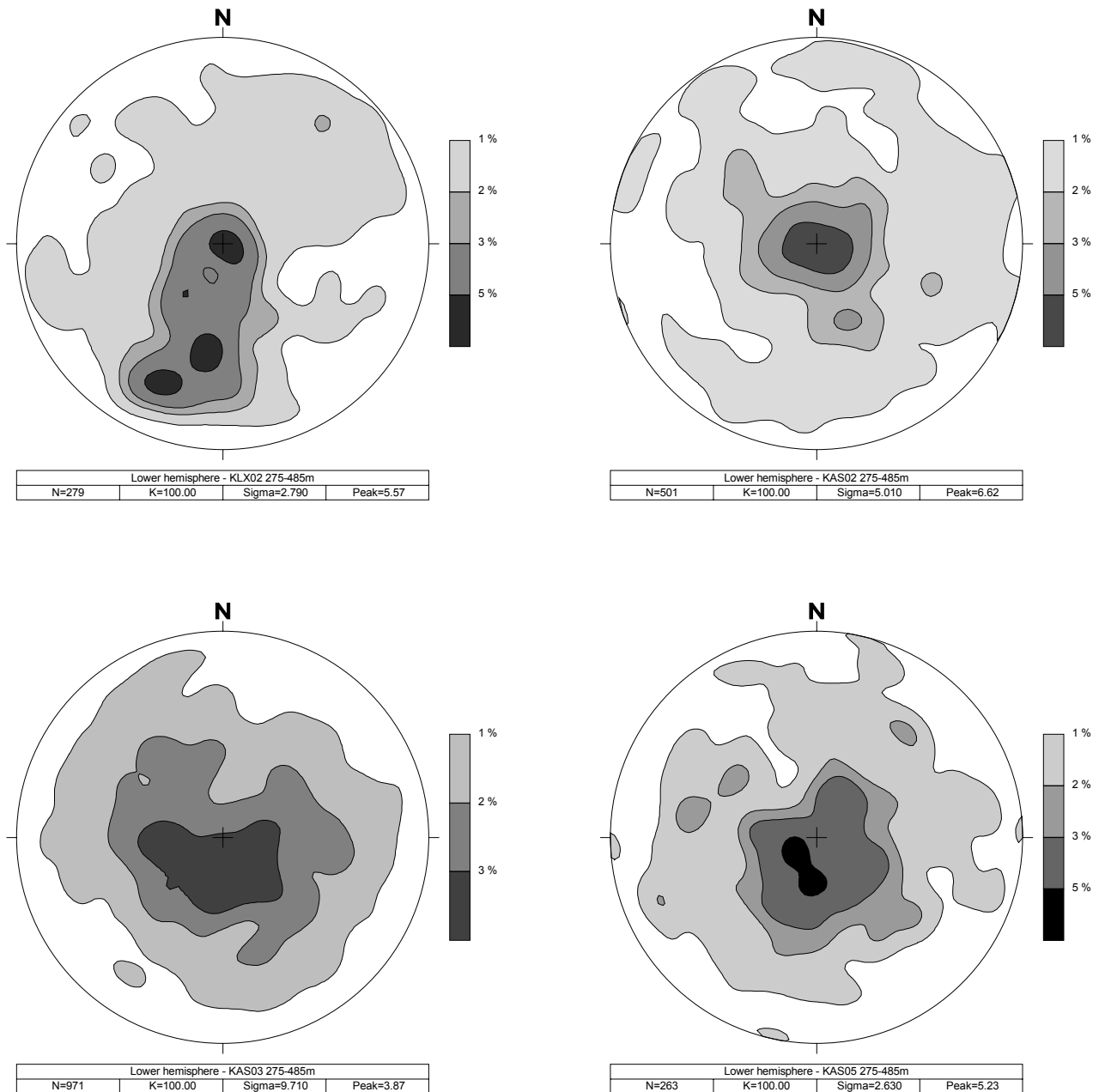


Figure 4-20. Stereogram illustrating fracture orientations for section 275–485 m in boreholes KLX02, KAS02, KAS03 and KAS05 (cf. Table 4-6). Schmidt-net, lower hemisphere, N in the small tables below the stereogram = the number of fractures included in the section for the respective boreholes. K, Sigma and Peak are calculation parameters. After Figure 3-3 in /4-16/.



Figure 4-21. BIPS-images from those parts of borehole KLX02 where incidents with equipment jamming have occurred. After Appendix in /4-16/.

When the study is extended to comparison with the conditions in boreholes KAS02, KAS03 and KAS05 at Äspö, it is quite clear that the hypothesis does not hold, because the Äspö boreholes in general exhibit higher fracture frequencies than KLX02. In spite of that, those boreholes have not been liable to equipment catching.

The second hypothesis presented in Section 4.4.1 suggested that steep fractures intersecting the borehole increases the jeopardy during down- or up-hoisting of down-hole equipment. Again, if only the fracturing in KLX02 is studied, the hypothesis appears as plausible, since moderate frequency peaks of fractures within the interval 0–40° (α -angles) are encountered at two of the problematic localities, at 339 m and 435–436 m. At 1087 m no α -angles were determined.

After comparison with the Äspö-boreholes, it is difficult to gain support for the hypothesis, because in those boreholes essentially higher frequencies of steep fractures than in KLX02 are noticed within several intervals of the drill cores.

The extent of this investigation was limited regarding the number of problematic spots investigated. General conclusions about the cause of the problem, and why some boreholes are subject to jamming more often than other boreholes, are therefore difficult to draw. The outcome of the present study was, that a high frequency of steep fractures in a borehole not necessarily implies that the borehole wall is unstable, or that borehole equipment will get stuck more easily. However, an increased risk may prevail, which in specific situations is sufficient for equipment getting stuck. However, several other factors have an influence on this problem. For example, down-hole components getting stuck in a borehole may be mainly an equipment depending problem, since it sometimes occurs also in smooth metal pipes, for example borehole casings. Other factors are related to the borehole.

Regarding borehole KLX02, the study demonstrated (possible) changes in the borehole wall at two of the problematic intervals in question: two elliptical objects at 339 m, and a caliper anomaly at 436–436 m. Furthermore, small rock fragments attached to tape balls in front of the TV-camera lens were observed, see Section 4.4.2. A certain instability of the borehole wall therefore seems to prevail, and this may well be the cause of the jamming problems in this borehole. If so, this would be a combined effect of several factors, where the character of the fracturing may be important. To connect to the initially stated hypotheses, it therefore does not seem unlikely that a high fracture frequency, inclusively fracture zones and/or a high frequency of steep fractures, *in combination with* other factors, will increase the risk of equipment jamming.

Factors of this kind may be:

- 1) A large share of open fractures.

In this study no distinction between open and closed fractures has been made. It seems reasonable to believe, that open respectively sealed fractures involve different kinds of ventures concerning equipment jamming.

- 2) The rock stress situation in combination with rock properties in the immediate vicinity of the borehole.

These factors affect the risk of borehole breakouts to occur, which indirectly may affect the jamming risk due to wedging of rock fragments between the equipment and the borehole wall (see also Section 4.4.4).

- 3) The drilling technique applied during production of the borehole.

Different drill-technical parameters may bias the number of drill induced fractures and the roughness of the borehole wall.

- 4) The inclination of the borehole.

Very inclined boreholes are probably more hazardous regarding the risk of outfall (due to gravitation) which, in turn, may increase the risk of equipment jamming.

- 5) The hydraulic conditions prevailing in the borehole.

For example, a large inflow from a fracture towards the borehole may increase the risk of rock particles to be transported into the borehole. Such risks are reinforced during artificial pressure declines, e.g. in connection with pump tests. The level of the groundwater table is also important, i.a. since this factor affects the stress situation in the borehole.

The items above are all assigned to the geological/hydrogeological conditions prevailing in the borehole. Another very important factor, although beyond the frame of this study, is:

- 6) The design of the down-hole equipment used in the borehole.

In general terms it may be concluded that sharp edges are to be avoided on down-hole equipment. The design should also be such, that loose fragments resulting from borehole washouts or other falling objects not easily can be wedged between the equipment component and the borehole wall. The size of the free space between the component and borehole wall is probably also important. During down- or up-hoisting of borehole equipment, a certain water volume must be pushed aside. If the free space is limited, the vacuum effect may be considerable, possibly increasing the risk of outfall from fractures or the borehole wall. On the other hand, a small space will prevent falling objects to wedge between the object and the borehole wall. The borehole equipment,

mainly straddle packers, which was subject to jamming in KLX02, had a large diameter, implying a free space of down to 1.5 mm. After exchanging this packer type to thinner packers, the jamming problems seem to have come to an end.

4.4.4 Borehole breakouts

In sections 4.4.1–3 above, the possibility of loose rock particles to trap borehole equipment is discussed. TV-inspection of borehole KLX02 has also revealed small loose rock fragments (Section 4.4.2).

Another method to show if rock particles may have entered the borehole is to study the borehole wall, if borehole breakouts have occurred. Borehole breakouts is a stress related phenomenon, which occurs when the tangential compressive stress around a borehole exceeds the uniaxial compressive strength of the rock material. For the depth interval discussed in this report, the probability of borehole breakouts to occur normally increases with depth, due to increasing stress magnitudes. The process is, however, time dependent. After a period of stress reorientation, the borehole wall may stabilize.

A proper study of the possible occurrence of borehole breakouts has not been performed in borehole KLX02. However, the studies focused on the stress field around borehole KLX02 reported in /4-6/ engaged the BIP-system (see Section 3.3.7) for inspection of the borehole wall. The BIPS-tool is not ideal for the study of borehole breakouts, especially not in boreholes like KLX02, where a chemical precipitation on part of the borehole wall makes inspection of the fresh rock surface difficult. However, the method may still give important indications of the breakout phenomenon. The analyses of the BIPS-images from borehole KLX02 indicated a possible borehole breakout oriented ENE-WSW at 1341–1342 m vertical depth (1346–1347 m borehole length), indicating a NNW-SSE orientation of maximum horizontal stress, cf. Section 4.2.6. This breakout has also been identified using a forward-viewing black & white TV-camera, and has a depth into the borehole wall of approximately 1–2 cm /4-6/. Another possible borehole breakout was found between 750–820 m vertical depth (753–823 m borehole length), oriented NW-S, with a maximum depth of 5 mm. The dominating elongation is in the NW direction and the less dominant in the S direction.

If these indications correspond to real borehole breakouts, several rock particles of different sizes obviously have entered the borehole and eventually reached the borehole bottom. However, the limitations of the BIP-system for this special task should again be emphasized, and the indicated breakouts must be regarded as uncertain. On the other hand, in /1-2/ core discing was reported at 863 m, 944 m, 1335 m and 1499 m vertical depth in borhole KLX02. Core discing is an indication of large deviatoric stresses, which consequently strengthens the possible occurrence of borehole breakouts.

5 Thermal properties

5.1 Introduction

Temperature and temperature distribution are fundamental parameters in the deep repository, having a direct influence on its layout /1-1/. The temperature affects the mechanical conditions, the groundwater flow and the chemical/microbiological environment, even if the influence is moderate within the temperature intervals normally regarded to predominate within a deep repository for nuclear waste. The temperature parameters include the thermal properties for the rock and prevailing temperatures.

A reliable lithological model is probably the most important basis for thermal calculations related to a deep repository. Thermal parameters (thermal conductivity and specific thermal capacity) may be derived from the mineral composition with acceptable accuracy. The distribution of different minerals must therefore be known and taken into consideration.

The ambient rock temperature is essential for the repository layout, since this is one of the factors determining the minimum distance between the canisters in the repository. The temperature at repository depth demonstrates significant regional variation from about 20°C in the southern part of the country to about 8°C in the northern part of Sweden. This temperature parameter is needed as an initial condition for modelling of the thermal development. At repository depth the temperature of the groundwater has adopted the temperature of the rock.

The thermal boundary conditions are essential for thermal modelling. At depth, the boundary conditions are determined by the geothermal gradient, whereas at the ground surface they are controlled by the mean annual temperature, which exhibits regional differences /1-1/.

5.2 Thermal investigations at Laxemar

The thermal investigations accomplished during Project Deep Drilling KLX02 – Phase 2, had not the extension necessary for a complete site characterization of a deep repository. On the other hand, if extended surveys would be considered, the already performed investigations would serve as a good platform.

5.2.1 The thermal properties of the rock

The parameters needed for characterization of the thermal properties of the rock mass are thermal conductivity, thermal capacity and thermal expansion /1-1/. These coefficients are used for repository design, thermal modelling and rock mechanical calculations. All three parameters are generically determined on core samples. This has so far not been performed on Laxemar drill cores. If required, complete drill cores from two deep boreholes, KLX01 and KLX02, are preserved.

This, together with the fact that detailed lithological documentation of both boreholes exist, would render an amplification of the thermal investigations relatively easy to accomplish.

5.2.2 Temperatures

Temperature logging, i.e. monitoring of the groundwater temperature, was conducted in February 1988 in borehole KLX01 /5-2/ and at two occasions in borehole KLX02, in January /1-2/ respectively July 1993 /3-4/. The logging surveys provided profiles of the groundwater temperature from the ground surface to about 700 m in borehole KLX01 and from 200 m to 1440 m in KLX02 (1650 m in January). As mentioned in the previous section, the groundwater temperature is at depth a good reflector of the ambient rock temperature. The temperature profiles from KLX01 and from the second logging in KLX02 are illustrated in Figure 5-1. The log from borehole KLX01 is, although the investigation was not included in the Phase 2 studies, presented for the purpose of comparison. The results from the first logging in KLX02, performed in January 1993, i.e. soon after completion of drilling, can be studied in Figure 7-1, Chapter 7. In Table 5-1 some temperature information derived from the logs in Figure 5-1 is summed up.

The temperature profiles from the two loggings in KLX02 differ in some details from each other. The temperatures appear as slightly lower (between c. 0.7 and 2.7° C lower) from the July logging than from the January logging. This may be due to different calibrations of the instrument or, possibly, to the fact that the January logging was conducted only a few weeks after drilling and subsequent test and clearance pumping. The groundwater temperature was most certainly influenced by these activities. However, it seems probable that this effect (or most of it) decayed during the period between drilling/pumping and temperature logging, although this is impossible to know for sure. Nor is it possible to decide which one of the two logging results is the most reliable.

Table 5-1. Temperature data from boreholes KLX01 and KLX02.

Parameters	KLX01 (February 1988)	KLX02 (July 1993)
Temperature at surface (15 m resp. 200 m)	7.3°C, 10.7°C	NE, 9.0°C
" at repository level (500 m)	15.2°C	13.8°C
" at 700 m	17.9°C	16.7°C
" at 1000 m	NE	21.8°C
" at 1400 m	NE	28.3°C
Temperature gradient 200– 500 m	1.500°C/100 m	1.600°C/100 m
" " 500– 700 m	1.350°C/100 m	1.450°C/100 m
" " 700–1000 m	NE	1.700°C/100 m
" " 1000–1400 m	NE	1.625°C/100 m

NE = non existing value

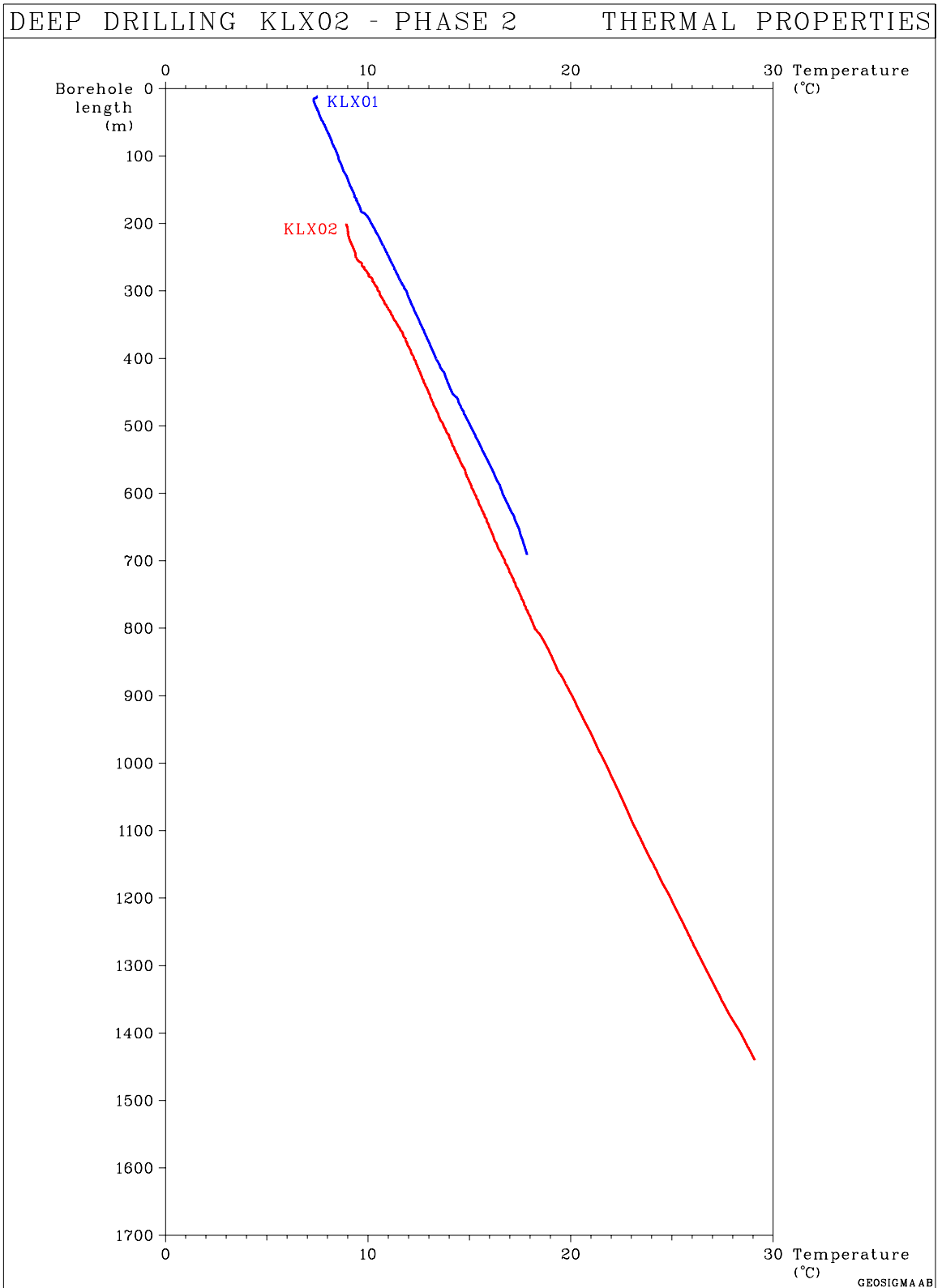


Figure 5-1. Temperature logs from boreholes KLX01 and KLX02.

Notable temperature anomalies are in borehole KLX02 observed at 250 m, 805 m and at 870 m (in the January logging also at 315 m and 1085 m). Changes of gradient are in the July logging obvious at about 220 m, 370 m, 810 m and 1340 m, in the January logging also at some other locations.

In borehole KLX01, temperature anomalies are found at 184 m, 421 m and 455 m and changes of gradient at approximately 175 m and 635 m.

6 Hydrogeology

6.1 Introduction

A solid understanding of the spatial distribution of groundwater flow is vital for the characterization of a rock mass in which a repository is planned to be constructed. Several types of hydrogeological models have to be employed for the safety analysis related to groundwater flow. A hydrogeological comprehension must also be achieved for explanation of long-term hydrogeochemical changes and of coupled hydraulic and rock mechanical phenomena. These model applications are scale dependent, and the character of the input data needed varies to some extent between the respective scales.

Hydrogeological models are, according to /1-1/, used for a large number of applications: to improve the hydrogeological understanding, for predictions of large scale groundwater chemical changes, for predictions of inflow during construction and recovery after closure, as input data for near field and far field transport models, biosphere models and for evaluation of (other) surface related environmental consequences.

Information about the following hydrogeological parameters is, according to /1-1/, regarded as necessary for the different hydrogeological models needed for the safety analysis:

- Hydraulic properties of the soil aquifer system, including meteorological and hydrogeological data, location of recharge and discharge areas, etc.
- Geometric and hydraulic properties of the rock aquifer system, in particular, deformation zones and fracture network characteristics.
- Physical properties of groundwater (density, viscosity, compressibility, salinity and temperature).
- Boundary conditions and initial conditions including historical and future development of the shoreline displacement and distribution of present-day groundwater pressure or groundwater head.
- Natural groundwater flow (measured in boreholes, e.g. by dilution technique).
- Tracer test break-through curves.

A complete supply of hydrogeological parameters demands extensive investigations in several boreholes using a wide range of methods, e.g. single-hole hydraulic tests, interference tests, large scale pumping tests, laboratory tests on drill cores, groundwater sampling, hydrogeological and hydrological mapping, studies of topography, large scale tracer tests, dilution probe tests etc. However, the hydrogeological investigations included in Project Deep Drilling KLX02 – Phase 2 were limited to single-hole tests in borehole KLX02 and to an interference test between KLX02 and the previously drilled deep borehole KLX01. These investigations are described in Section 6.2. A brief recapitulation of the hydraulic tests conducted in the Laxemar area prior to Phase 2 is also given.

6.2 Hydraulic tests in borehole KLX02

6.2.1 Background

During drilling of borehole KLX02 within Phase 1 of Project Deep Drilling KLX02, a number of hydraulic tests were performed in the borehole /3-20/. These tests were conducted as capacity tests during drilling in intervals of about 300 m length. As soon as the drilling of such an interval was completed, a borehole packer and a pressure transducer were mounted on the drill pipe string and lowered into the borehole, where the packer was expanded at the transition between the previous and the new interval. Pumping of the newly drilled borehole interval was achieved by air-lift technique. Compressed air was conducted via a plastic tubing to the bottom of the pipe string, thereby forcing water to flow upwards to the ground surface, creating a draw-down in the test interval. Flow rate and groundwater pressure in the test interval were monitored during pumping. After pumping, the pressure recovery was monitored.

Prior to drilling of borehole KLX02, single-hole hydraulic testing had been performed in borehole KLX01. Two kinds of test types were applied: 1) double-packer injection tests in 3 m- and 30 m-intervals and 2) pumping tests in long or relatively long intervals. After completed drilling of KLX02 (but still within Phase 1) also an interference test between boreholes KLX02 and KLX01 was performed. The results accomplished from these tests serve as a basis for the tests performed within Phase 2. Therefore, a compilation of the test results from the single-hole tests in boreholes KLX01 and KLX02 achieved prior to Phase 2 is given in Figure 6-1 and from the results of the interference test in Figure 6-2.

6.2.2 Objectives and Scope of Activities

As stated in Figure 6-1, the test sequence conducted during Phase 1 provided no reliable transmissivity values in the test intervals C2, C4 and C6 in KLX02 /3-20/. During Phase 2, these intervals (C2 however adjusted to 505.0–803.0 m and C4 to 1103.5–1401.5 m) were therefore re-tested by constant flow rate pumping tests using a specially designed hydraulic test container, the so called SKB Pipe String Equipment. An overview of this test system, which is thoroughly described in /4-5/, is displayed in Section 4.2.3, Figure 4-3. The system is illustrated in further detail in Figure 6-3, where also the down-hole tool can be studied. During the pumping tests, the parameters flow rate, fluid temperature and electric conductivity of the fluid from the pumped sections were registered continuously at the surface together with the pressure in the tested section /6-1/.

In addition, the interval C3 (adjusted to 805–1103 m) was re-tested by the same type of test. Subsequently this interval constituted the pumped interval in a new interference test between KLX02 and KLX01, see below. In Table 6-1 the tested intervals, flow rates, start date and duration of each test (drawdown/recovery) in KLX02 during Phase 2 are summed up.

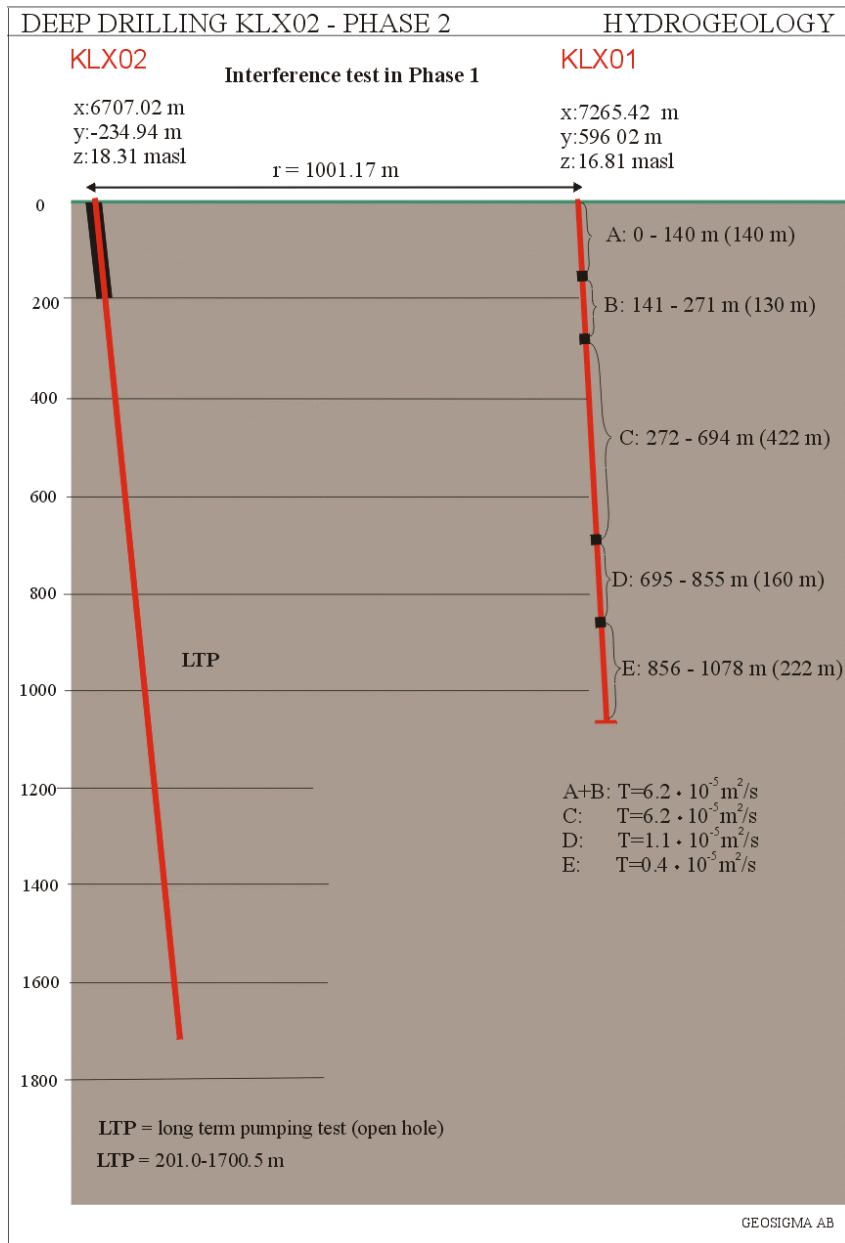


Figure 6-2. Compilation of test results from interference testing between KLX02 and KLX01 during Phase 1. Modified after Figure 1-2 in /6-1/. Co-ordinates refer to the local Äspö system.

Table 6-1. Summary of administrative data for hydraulic tests performed in KLX02 during Phase 2. Modified after Table 1-1 in /6-1/.

Section	Interval (m)	Flow rate (m ³ /s)	Start date	Duration (h)	Test type
C6	207.0– 505.0	$6.3 \cdot 10^{-4}$	1994-09-26	12 + 12	Single hole
C2	505.0– 803.0	$8.2 \cdot 10^{-5}$	1995-04-28	15 + 15	Single hole
C3	805.0–1103.0	$1.5 \cdot 10^{-4}$	1995-10-19	864 + 855	Single hole during interference
C4	1103.5–1401.5	$2.7 \cdot 10^{-5}$	1995-06-28	48 + 47	Single hole

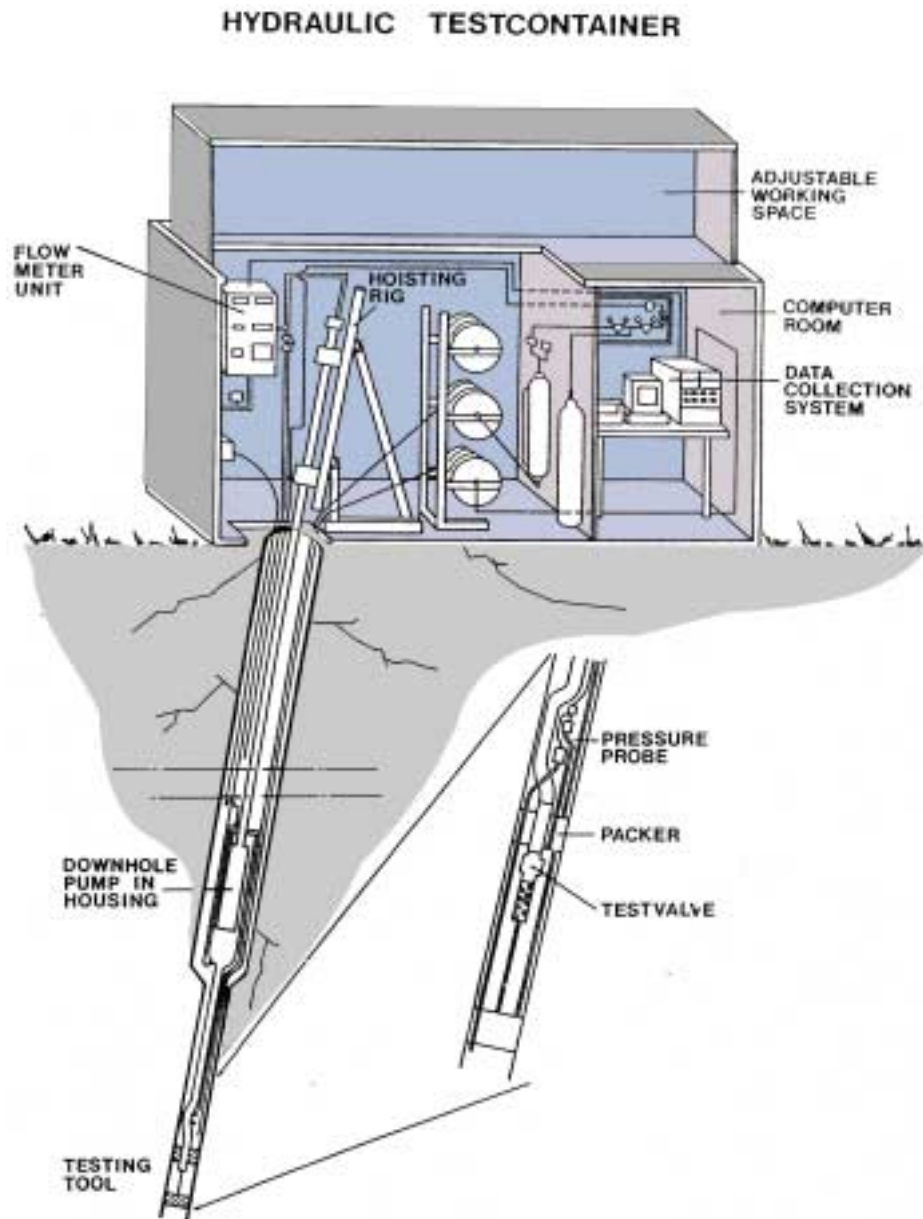


Figure 6-3. The SKB Pipe String Equipment used for hydraulic borehole tests.

The design of the new interference test between KLX02 and KLX01 during Phase 2 is illustrated in Figure 6-4. The hydraulically monitored borehole sections (1–5) in KLX01 during the interference test are in this figure visualized in relation to the radar and reflection seismic reflectors interpreted to represent possible connections between the two boreholes, /3-19, 3-33/. The monitored sections in 1–5 in KLX01 are identical to sections E-A in Figure 6-2.

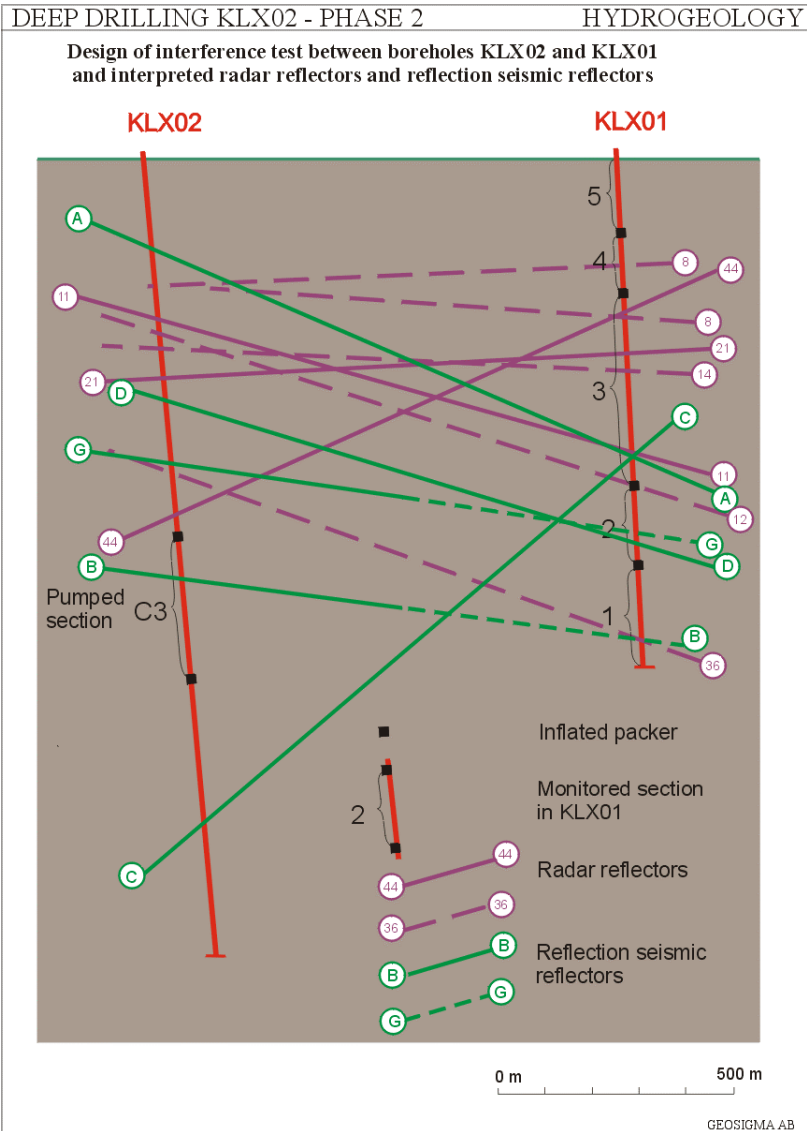


Figure 6-4. Design of the interference test between boreholes KLX02 and KLX01 during Phase 2. Solid lines correspond to radar and reflection seismic reflectors with a correlation between the boreholes considered as “good”, whereas dashed lines indicate reflectors with a correlation judged as “possible”. Modified after Figure 4-2 in /3-19/ and Figure 3-4 in /3-33/.

During the interference test, the interval C3 (805–1103 m) in KLX02 was pumped with a constant flow rate during about 36 days. The following parameters were monitored continuously in KLX02 during pumping:

- Flow rate.
- Fluid temperature.
- Electric conductivity of the fluid.
- Groundwater pressure in the test section.
- Packer inflation pressure.

The first three parameters were measured at the ground surface, whereas the pressures were monitored by down-hole pressure transducers. Besides the borehole related parameters above, the following meteorological parameters were measured:

- Barometric pressure.
- Precipitation.

Figure 6-5 A illustrates the registration of precipitation (major events), 6-5 B barometric pressure and 6-5 C flow rate from the pumped section. In Figure 6-5 A a heavy precipitation (snow) after about 40 000 minutes of pumping is observed, corresponding to a low barometric pressure displayed in Figure 6-5 B. Figure 6-5 C illustrates associated pump stops caused by interrupted power supply due to the hard weather.

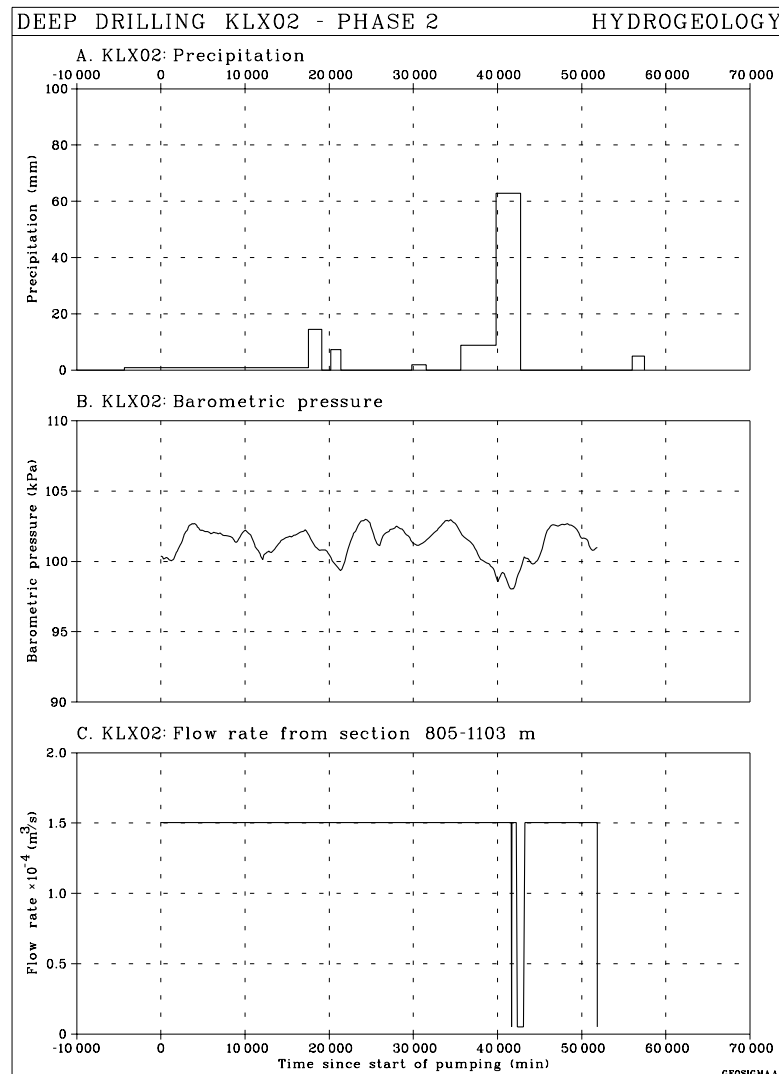


Figure 6-5. Monitored precipitation (A), barometric pressure (B), and flow rate (C) from the pumped section 805–1103 m in KLX02 during the Phase 2 interference test between KLX02 and KLX01. Modified after Appendix in /6-1/.

Simultaneously, the water levels in sections 1–5 in borehole KLX01, see Figure 6-4, were monitored by the Äspö HRL Hydro Monitoring System (HMS), /6-2/.

6.2.3 Results

Singlehole testing

An example of the decline of the pressure, P , in the tested section C4 (1103.5–1401.5 m) in borehole KLX02, together with the pressure derivative, $der(P)$, and the interpreted semi-logarithmic straight line, is presented in Figure 6-6. The transmissivity of the pumped sections was calculated using Cooper-Jacob's straight-line method from both the pumping and recovery phases. The results of the singlehole tests in KLX02 are presented in Figure 6-7 and in Table 6-2. The difference between the sum of the section transmissivities given in the table, $\Sigma T = 1.6 \cdot 10^{-4} \text{ m}^2/\text{s}$, and the open hole transmissivity, $T_{\text{open}} = 1.3 \cdot 10^{-4} \text{ m}^2/\text{s}$, determined during Phase 1 (Figure 6-1), is less than 25 %.

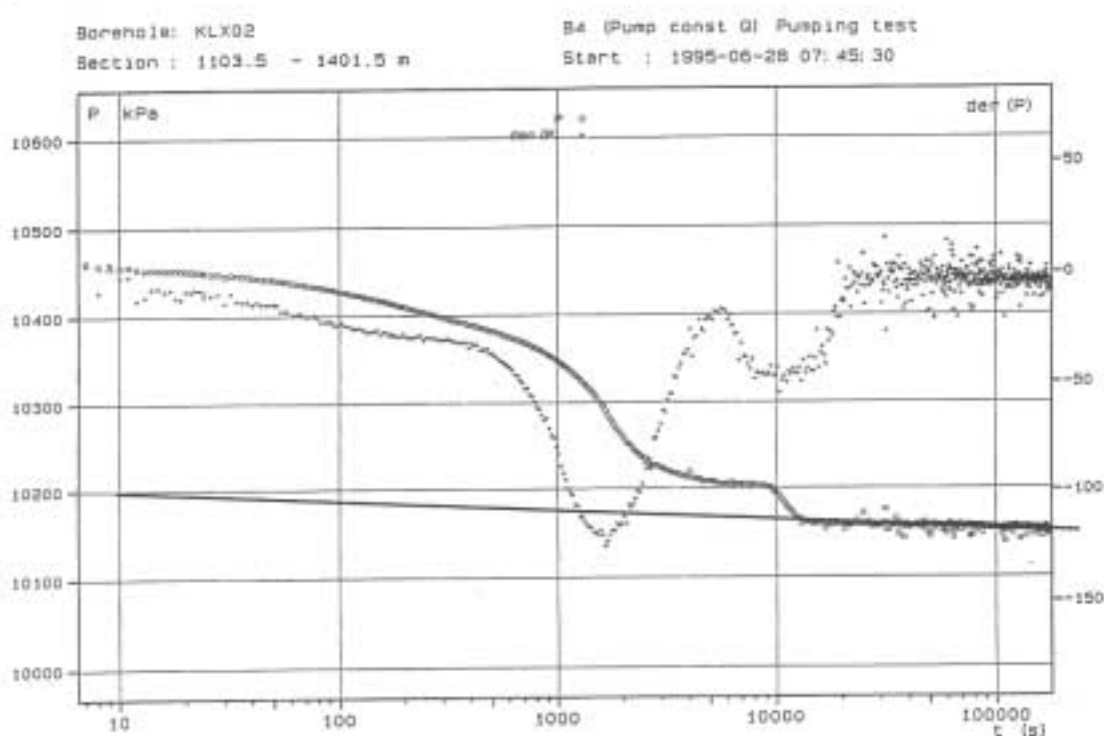


Figure 6-6. Decline of the pressure, P , in section C4 (1103.5 m–1401.5 m) in borehole KLX02 together with the pressure derivative, $der(P)$, and the interpreted straight line during the Phase 2 singlehole tests. Modified after Appendix in /6-1/.

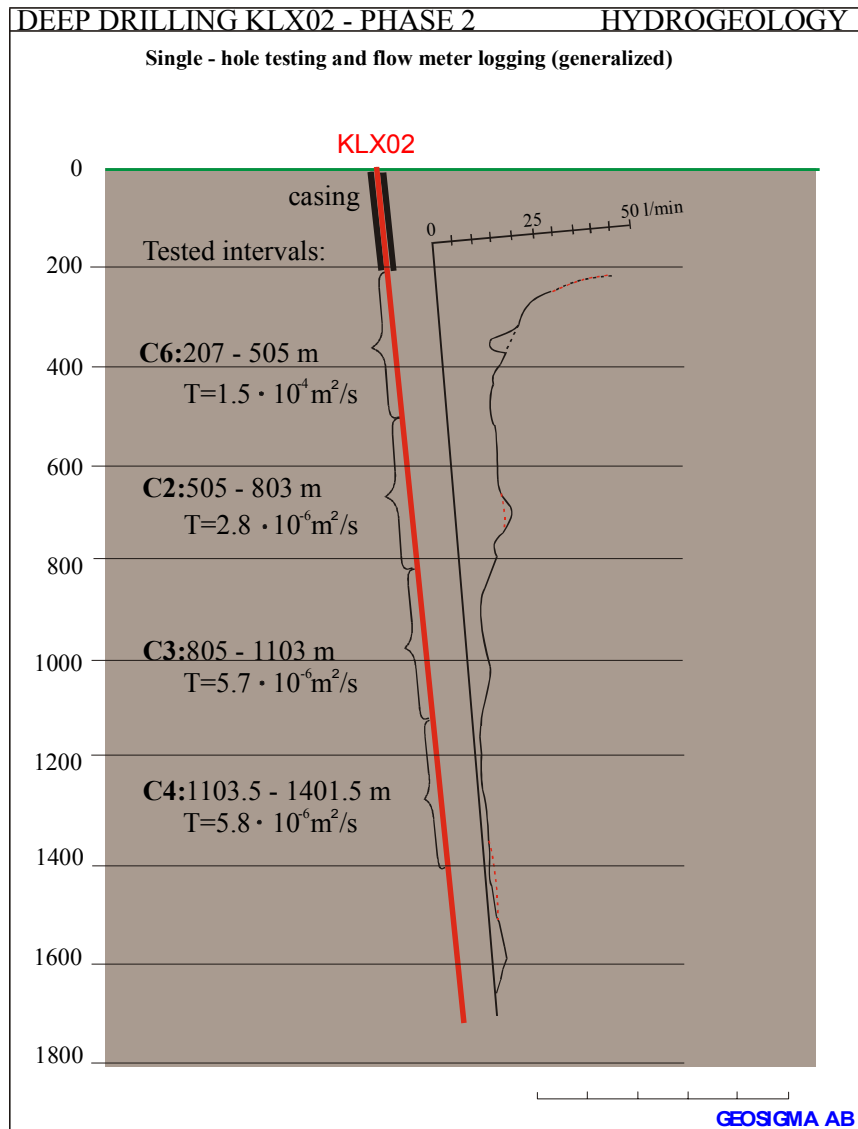


Figure 6-7. Compilation of test results from single-hole testing in KLX02 during Phase 2. To the left, results from pumping tests are presented. To the right the flow rate distribution along the borehole during flow logging is illustrated.

Table 6-2. Calculated transmissivities in sections in KLX02 tested during Phase 2. Modified after Table 2-1 in /6-1/.

Name of section	Section interval (m)	$T_{\text{pumping}} \text{ (m}^2\text{/s)}$	$T_{\text{recovery}} \text{ (m}^2\text{/s)}$
C2	505.0– 803.0	$2.8 \cdot 10^{-6}$	$2.8 \cdot 10^{-6}$
C3*	805.0–1103.0	$5.7 \cdot 10^{-6}$	$7.4 \cdot 10^{-6}$
C4	1103.5–1401.5	$5.8 \cdot 10^{-6}$	$4.8 \cdot 10^{-6}$
C6	207.0– 505.0	$1.5 \cdot 10^{-4}$	$1.5 \cdot 10^{-4}$
ΣT	207.0–1401.5	$1.6 \cdot 10^{-4}$	–

C3* = tested during interference test between KLX02 and KLX01.

Interference testing

The pressure decline in the pumped section C3 (805.0–1103.0 m) in KLX02 during interference testing, the pressure derivative, $der(P)$, and the interpreted semi-logarithmic straight line (Cooper-Jacob) are illustrated in Figure 6-8. The figure demonstrates that the total pressure drawdown in the pumped section was about 640 kPa (approximately 64 m). The transmissivity of the pumped section was calculated using Cooper-Jacob's straight-line method, both from the pumping and recovery phases, see Table 6-2.

As stated above, the groundwater level in sections 1–5 in borehole KLX01 was monitored during both the pumping and recovery phases. From this information, new plots with the observed changes of groundwater level in these sections were produced, see Figure 6-9. Start and stop of pumping are marked with arrows. The monitoring failed at the beginning of the pumping phase.

Figure 6-10 displays the observed drawdown in section 2 (695–855 m) in borehole KLX01 during the interference test (Figure 6-10 A). Also the corrected drawdown for an assumed barometric efficiency of $BE=1$ and the major events of precipitation are included in the figure, 6-10 B, (for explanation of BE , see /6-3/). The diagrams in Figure 6-10 illustrate that the total drawdown of the water table in this section exceeded 2 m during the interference test. The distance to the pumped section is approximately 1000 m, see Figure 6-4. Considering all

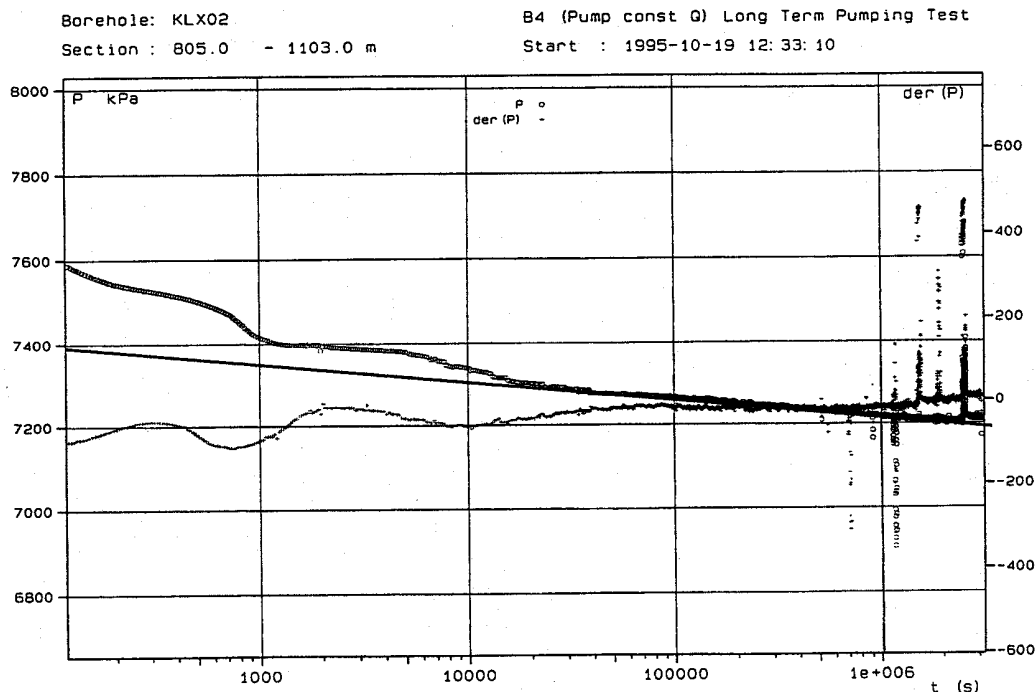


Figure 6-8. Decline of the pressure, P , in the pumped section C3 (805.0–1103.0 m) in borehole KLX02 together with the pressure derivative, $der(P)$, and the interpreted straight line during the Phase 2 interference test. Modified after Appendix in /6-1/.

information available, the observed drawdown in this section was interpreted as a combined response of the testing in KLX02, barometric changes and tidal effects, whereas the effects of precipitation were considered as small.

Table 6-3 presents a qualitative interpretation of the observed responses in all five sections of KLX01 regarding their dependence on testing, precipitation (major events), barometric changes and tidal effects.

Table 6-3. Qualitative interpretation of possible dependencies of the responses in the different observation sections in KLX01 on testing, precipitation (major events), barometric changes and tidal effects during the Phase 2 interference test between KLX02 and KLX01. After /6-1/.

Observation section (m)	Testing	Precipitation	Barometric changes	Tidal effects	Assumed aquifer type
0– 140	none	clear	Little/none	none	Phreatic
141– 271	none	clear	little/none	none	Phreatic
272– 694	clear	clear	little/none	none	Phreatic
695– 855	clear	little	clear	clear	Confined
856–1078	clear	little/none	clear	clear	Confined

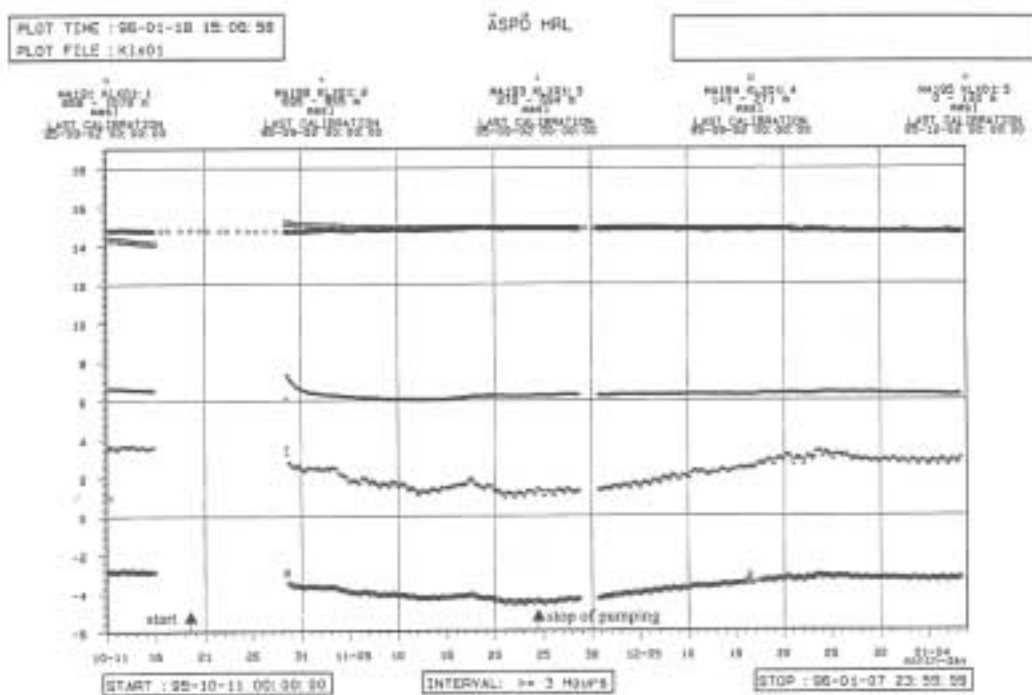
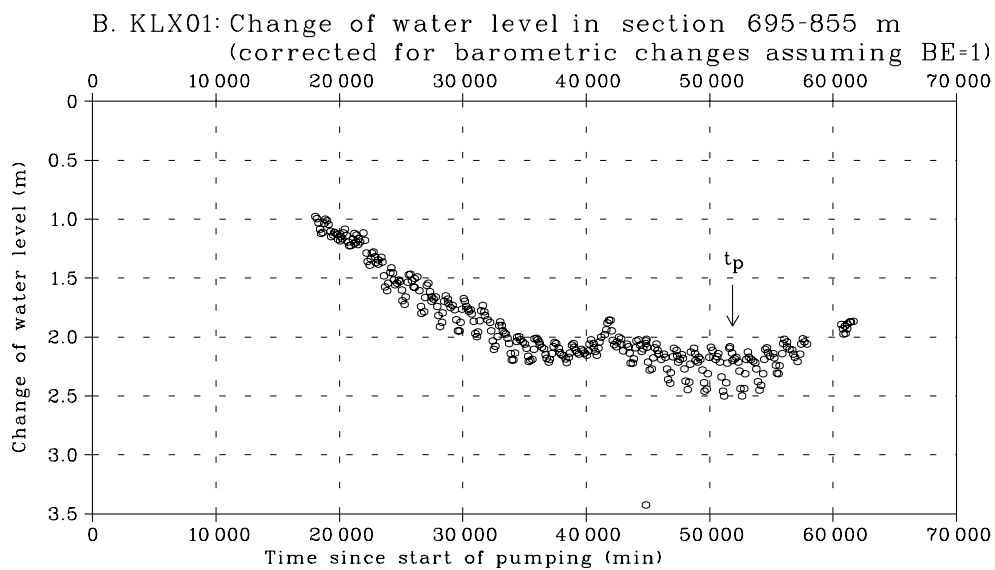
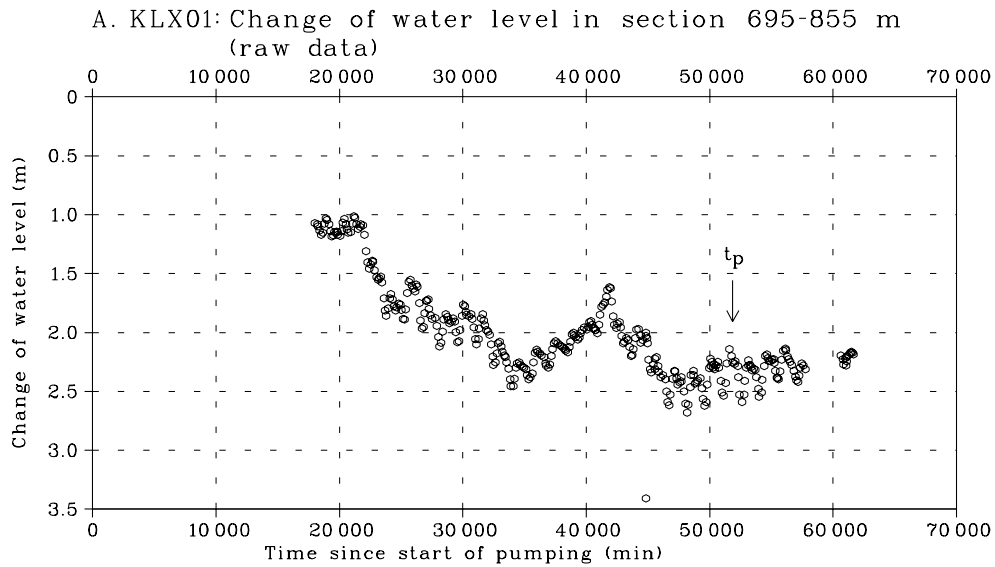


Figure 6-9. Observed changes of water levels (m.a.s.l.) in observation sections 1–5 in borehole KLX01 during the Phase 2 interference test between KLX02 and KLX01. Start and stop of pumping are indicated by arrows. Modified after Appendix in /6-1/. The sections are, from bottom to top, 1, 2, 3, 4 and 5 (after 95-11-10 sections 4 and 5 are approximately coincident).



GEOSIGMA AB

Figure 6-10. Observed (A) and corrected (B) drawdown of the water level in section 2 (695–855 m) in KLX01 during the Phase 2 interference test between KLX02 and KLX01. Modified after Appendix in /6-1/.

In /6-1/ a good hydraulic connectivity between KLX01 and KLX02 on all levels down to at least 1000 m is demonstrated. However, the transmissivities of the intervals in KLX01 could not be evaluated from the interference test during Phase 2, since the actual flow rate distribution in the rock is basically unknown. However, by application of the transmissivity values of the monitored sections in KLX01 determined earlier by independent methods, it was possible to estimate the flow rate for each affected interval in KLX01, provided that the sum of those flow rates should match the actual discharge rate at KLX02, $1.5 \cdot 10^{-4} \text{ m}^3/\text{s}$. From the results of the calculation, it was postulated that the flow rate distribution is heterogeneous in the vertical direction of the rock between KLX02 (source) and KLX01 (observation) /6-1/.

6.2.4 Hydraulic responses between KLX02 and KLX01 in relation to geological structures

From the observed drawdown in borehole KLX01 during the interference test between boreholes KLX02 and KLX01, a hydraulic connection between the two boreholes was postulated. The same conclusion was drawn from pumping tests during Phase 1. However, a quantitative interpretation of hydraulic parameters in the hydraulically monitored sections of the observation borehole, in this case borehole KLX01, requires information about the flow rate distribution in the rock mass between the boreholes during testing. The basis for such information is a good understanding of the geological structures connecting the boreholes. It is known from previous work in areas of fractured rock, that a well developed structural model with dimensions of the Laxemar site, demands an amount of geoscientific input data beyond what has been possible to extract so far from the investigations in the Laxemar area. Accordingly, at the present state, any structural model of the Laxemar site must be regarded as generalized and afflicted with a certain degree of uncertainty. Nevertheless, as described in Chapter 3, efforts have been made by several authors to, from different starting-points and different background information, establish more or less detailed structural models of the Laxemar area.

For example, an attempt was made to correlate identified radar reflectors between the two deep boreholes KLX02 and KLX01, see Section 3.4.2, /3-19/. This resulted in a simplified structural model described in Figures 3-17 and 3-18, where the radar reflectors are supposed to represent geological structures. Figure 3-18 is, together with information from Figure 3-25 /3-33/, integrated in Figure 6-4, which illustrates possible fractures and/or fracture zones with a potential of conducting fluid flow between boreholes KLX02 and KLX01, according to interpretations presented in /3-19/ and /3-33/.

Table 6-3 illustrates that hydraulic responses were observed in the three deepest sections in borehole KLX01 during pumping, but not in the upper sections 4 and 5. Figure 6-4 indicates that no direct radar indicated connections between the pumped section C3 in KLX02 and the responding sections in KLX01 were interpreted. In fact, the pumped section is not intersected by any radar reflector. However the interpreted reflector B from the reflection seismic survey connects the pumped section in KLX02 with section 1 in KLX01. Reflector B is in /3-33/

interpreted as the lower limit of an approximately 250 m wide subhorizontal zone, the upper limit of which is represented by reflector G. If this interpretation is correct, it could well explain the drawdown of sections 1 and 2 in borehole KLX01 during pumping in section C3 (805–1103 m) in KLX02. If radar reflector 44, as it appears, represents a conductive structure crossing the major interpreted subhorizontal zone limited by seismic reflectors G and B, also the observed drawdown in section 3 in KLX01 could be accounted for. No radar or seismic reflector connects the pumped section in KLX02 with sections 4 and 5 in borehole KLX01, which is in agreement with the lack of responses in those sections. It must, though, be pointed out, that the accuracy of the interpretation of the intersections of reflectors G and B with borehole KLX01 is no better than ± 150 – 200 m.

Figure 6-4 demonstrates differences between the results from the radar respectively reflection seismic survey, as well as some agreements. Although interpreted as different structures, for example the reflection seismic reflector G corresponds rather well with radar reflector 36 in KLX02. In KLX01 the radar reflector 36 instead coincides with the seismic reflector B, and radar reflector 11 intersects the borehole at the same place as the seismic reflectors A and C. A reinvestigation of radar reflectors in the light of reflection seismic data, and vice versa, could possibly explain the relations between radar and seismic survey results. Such an investigation might also give rise to modified interpretations with a better agreement between the two methods.

The interpretations of the structural conditions in the Laxemar area presented in report /3-18/, see Section 3.4.1, claims that the probability that direct, straight-forward hydraulically conductive structures exist between the two deep boreholes is low. Instead, it is inferred that a network of structures are capable of transferring hydraulic responses between the boreholes. Furthermore, it is supposed that fractures of some kind connect the pumped section with the interpreted network of fractures.

The structural model presented in Section 3.4.3 (Roy Stanfors pers. comm.), see Figures 3-19, 3-20 and 3-21, entitles more space for an interpretation involving direct responses between the boreholes. In this model, the strike and dip of the major fracture zones SFZ04 and SFZ07 are such, that the observed drawdown of the groundwater level in sections 1, 2 and 3 in borehole KLX01 could be explained as more or less direct hydraulic responses. However, the verification of this interpretation would require e.g. extended control of the geometrical properties of these zones and more information about their hydraulic behaviour.

7 Groundwater chemistry

7.1 Introduction

The purpose of groundwater chemical investigations and descriptions of groundwater composition is to give a general view of possible variations and long-term stability of the observed concentrations of elements and other properties, which are important for the construction, performance and safety assessment of a nuclear waste repository.

A hydrogeochemical model for fractured rock describes the groundwater composition in the investigated rock volume. The description is related to the water in the interconnected fracture system, consisting of major and minor water-conducting fracture zones and conductive fractures /3-1/. The origin and mixing of groundwater, the interaction between groundwater and minerals, the influence on the groundwater chemistry of micro-biological activity and the influence of the groundwater on bentonite, concrete and other materials planned to be used in a future repository are important items studied with hydrogeochemical models. The hydrogeochemical model constitutes a basis for analysis of e.g. corrosion of the canister, the function of the bentonite backfill, dissolving of the fuel and retention of radionuclides /1-1/.

According to /1-1/ the following chemical input parameters are needed in order to accomplish a geoscientific understanding of a site and to provide the necessary information for function- and safety analyses:

- Groundwater chemistry in the repository area.
- Groundwater chemistry along flow paths.
- Groundwater chemistry in the site scale.
- Mineralogic characteristics in different scales.

The methods required in order to attain the listed parameters are primarily groundwater sampling/analysis and mineralogical studies.

Far-reaching hydrogeochemical investigations were conducted within Project Deep Drilling KLX02 – Phase 2, comprising different types of groundwater sampling and analyses, also including analyses of isotopes. The investigations are reported primarily in /7-1/, /7-2/, /7-3/, /7-4/, /7-5/ and /7-6/. It should be observed, that the hydrogeochemical investigations within Phase 2 are restricted to one single borehole, KLX02. Additional hydrogeochemical information, not presented in this report, is however available from borehole KLX01, from percussion boreholes at Laxemar as well as from surface waters. The activities performed within the hydrogeochemical investigation program and the main results are described in the sections below.

7.2 Sampling of groundwater and calcite fracture fillings in borehole KLX02

7.2.1 Objectives

The objectives for the hydrogeochemical investigations in borehole KLX02 were /7-1/:

- To test new methods and equipment for sampling of deep groundwater.
- To use the data obtained to support existing hydraulic and hydrogeochemical interpretations of the Äspö site.
- To establish the composition and origin of deep basement groundwater at the Laxemar area.
- The methodology and results from a sampling campaign in 1993 is reported in /7-1/, whereas a re-sampling in borehole KLX02 with the same method, conducted in 1997, is presented in /7-2/. Results from noble gas sampling are attended to in /7-3/. Finally, /7-4/ and /7-5/ (also included in /7-3/) and part of /7-6/ treat groundwater sampling in KLX02 for analysis of stable and radiogenic isotopes together with the isotopic carbon-($\delta^{13}\text{C}$)-, oxygen-($\delta^{18}\text{O}$)- and strontium-($\delta^{87}\text{Sr}$)-composition in calcite fracture fillings.

7.2.2 Sampling in borehole KLX02

Groundwater sampling was conducted in KLX02 on four occasions using different methods /7-1/, /7-2/ and /7-3/ (a fifth sampling was performed after Phase 2, see page 130). The sampling methods and intervals are illustrated in Figure 7-1 together with background information concerning lithology, fracturing, fracture minerals and hydrogeological parameters.

The first sampling was conducted on August 3rd 1993 in the open borehole, using a so called Tube sampler /7-1/. In order to test the stability of the groundwater in an open borehole, the sampling was repeated in 1997 (the fourth sampling) /7-2/. The Tube sampler equipment is based on 50 m long sections of polyamide tubes (10 mm outer diameter) with a manually operated valve and a connector coupling attached to both ends of each tube. The lower end of the sampler involves a check valve. Several 50 m tubes are connected until the desired measuring length is achieved. In borehole KLX02 the interval 9–1681 m was sampled, see Figure 7-2. During lowering of the sampler within the borehole, the manually operated valves are kept open. After the tube strings have been filled with borehole fluid, the individual 50 m sampling intervals are isolated by closing the valves and subsequently up-lifted from the borehole. The borehole fluid contained in each 50 m tube string (1 litre) is finally poured into flasks for analysis.

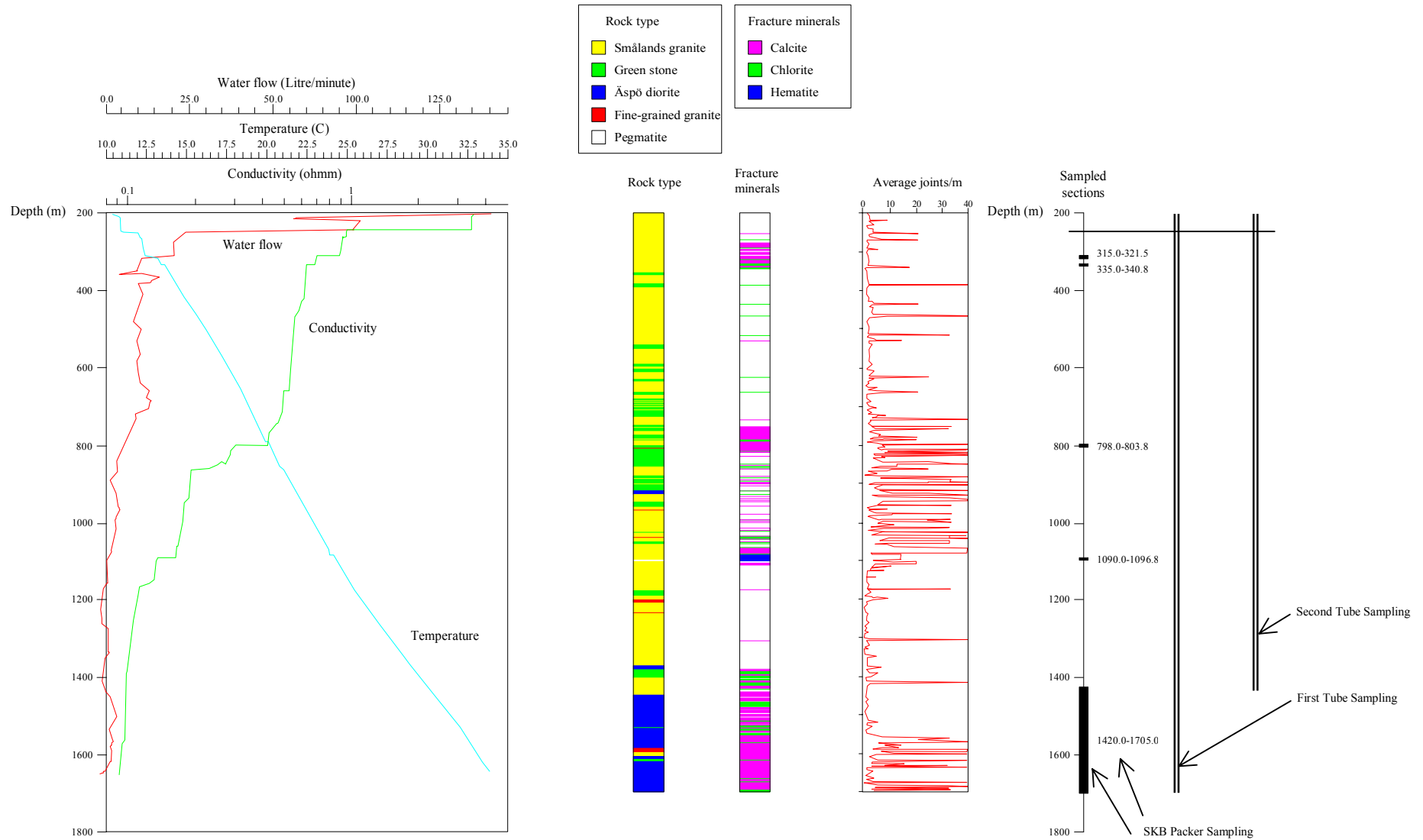


Figure 7-1. Background data for borehole KLX02 (groundwater flow, temperature and electric conductivity, rock type, fracture mineral distribution and average fracture frequency including crushed zones) and sampling intervals for different sampling campaigns. The depth scale is common for all plots. Modified after Figure 2-1 in /7-1/.

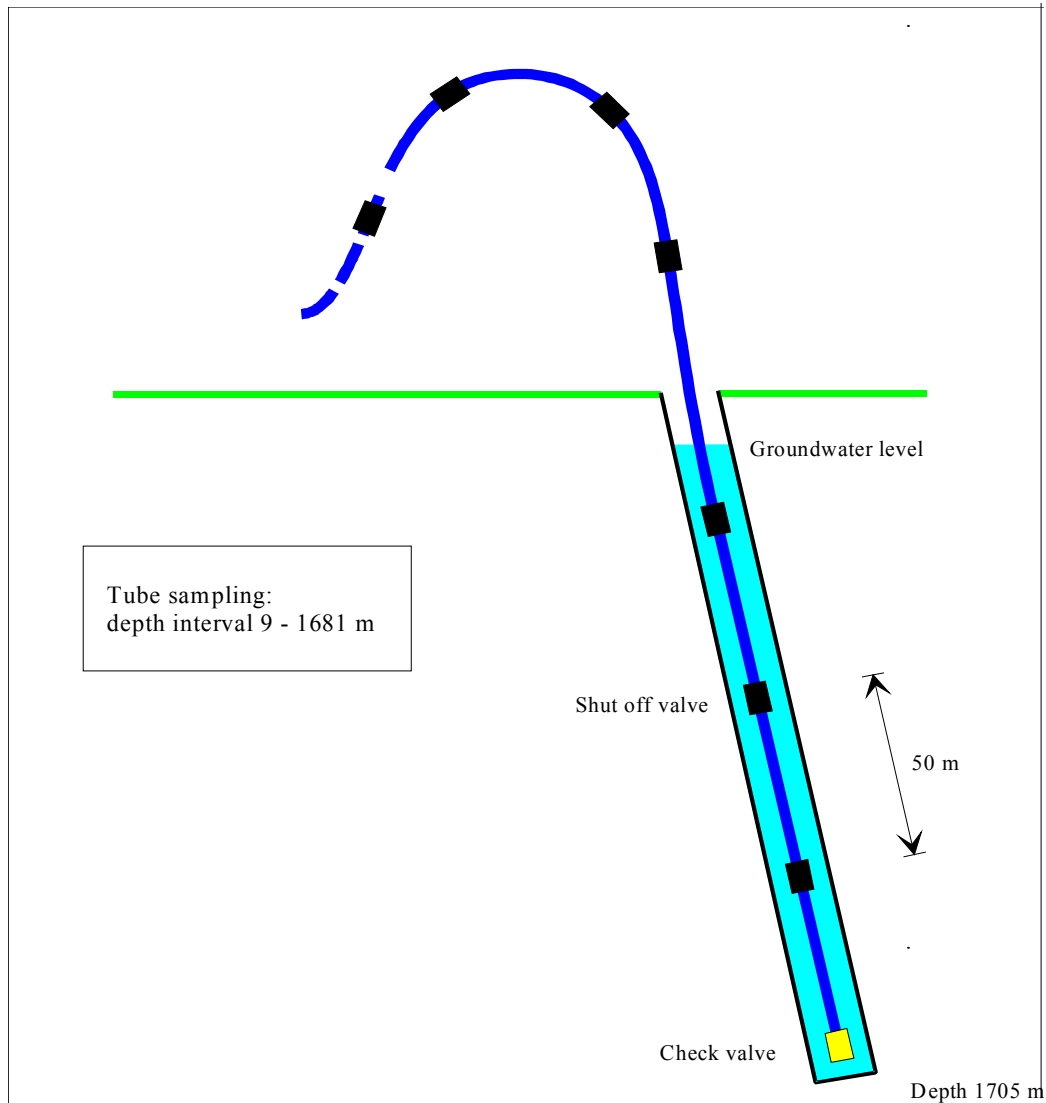


Figure 7-2. Diagrammatic representation of the Tube sampler. After Figure 3-2 in /7-1/.

The advantage of the Tube sampler technique is that the equipment is convenient as well as easy and rapid to operate, even down to considerable depths. The disadvantage is that the collected water column represents open-hole conditions. Therefore, the distribution of chemical constituents in the sample is controlled by the hydraulic properties of the fracture systems intersected by the borehole, which may not always conform to pre-drilling conditions. Furthermore, lowering the tube into the open borehole may cause perturbation and mixing of groundwater types around and inside the tube /7-1/.

The second sampling campaign was carried out during the period November 1st 1993 to January 5th 1994, /7-1/, using the SKB Mobile Field Laboratory, thoroughly described in /7-7/, and later updated to some extent /7-8/. This equipment includes a chemical laboratory unit, hose unit(s), downhole equipment including a straddle packer unit, and the CHEMMAC monitoring system, see

Figure 7-3. Prior to the sampling in KLX02, the down-hole equipment was modified to enable sampling at larger depths. In the following text activities performed with the mobile laboratory are referred to as the “SKB packer sampler”.

Using the SKB packer sampler, groundwater was extracted from selected water-conducting sections in the borehole, sealed off by inflatable rubber packers with adjustable straddle length. The (equivalent) hydraulic conductivity of these sections ranged between about $1 \cdot 10^{-8}$ m/s to $1 \cdot 10^{-6}$ m/s. The selection of sampling sections was based primarily on geological evidence (for example detailed core mapping) supported by flow meter measurements and down-hole logging of electrical conductivity and temperature. The majority of the selected sections

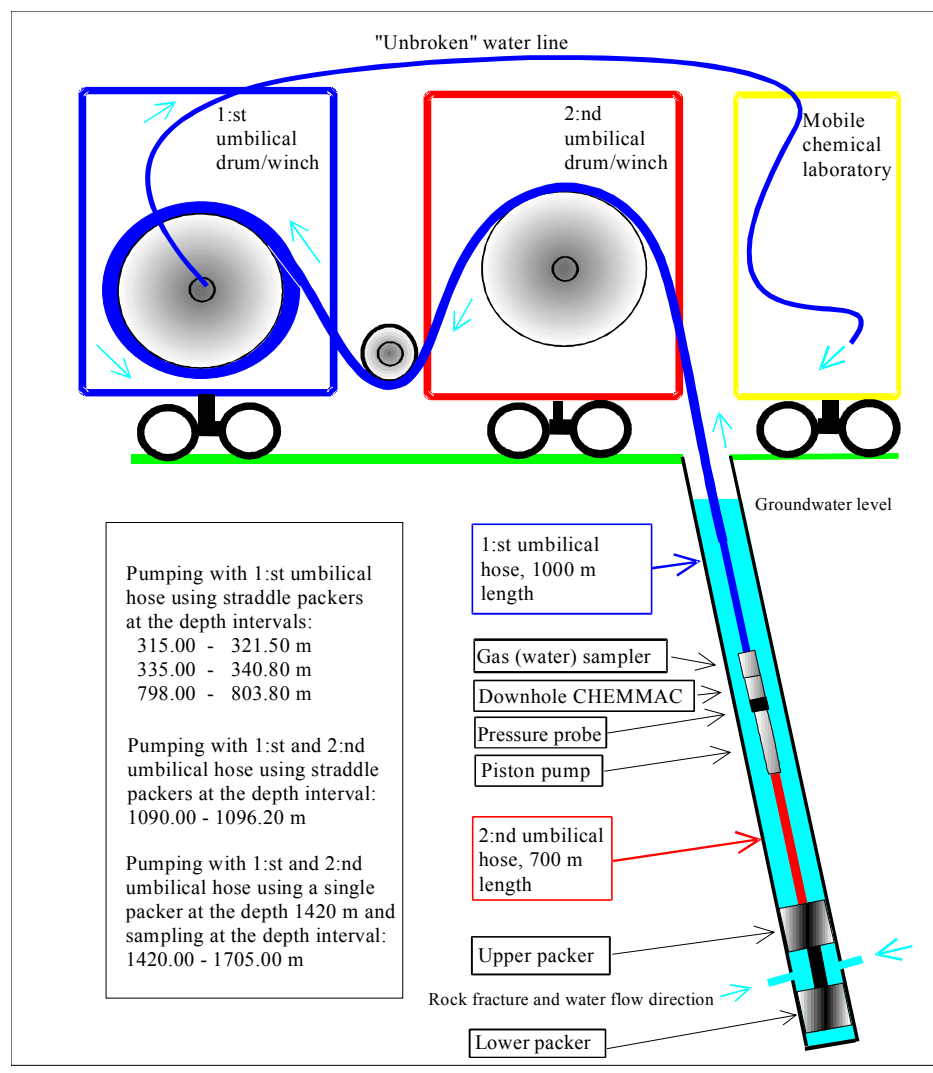


Figure 7-3. The SKB packer sampler equipment within the SKB Mobile Field Laboratory unit modified for sampling at larger depths. The down-hole CHEMMAC-probe houses Eh- and pH-electrodes. After Figure 3-3 in /7-1/.

were associated with crushed greenstone horizons or with the contact between greenstone and granite. The sampling programme is summed up in Table 7-1 and the five selected borehole sections in KLX02, together with date of sampling and the sampling activities, are shown in Table 7-2.

The parameters Eh and pH were monitored both at the surface in a flow-through cell within the mobile laboratory (surface CHEMMAC) and by a down-hole CHEMMAC-probe located within the sampling interval of the packer unit. Three different types of Eh-electrodes were used; gold, platinum and glassy carbon.

Following installation of the straddle packer and the remaining down-hole equipment, the pump was started and the capacity adjusted to give as high water flow rate as possible without exceeding a certain pressure draw-down. At KLX02 the pressure drawdown in the sampled section was generally limited to 1 bar (10 mwc). Pumping was continued until the “dead” volume of water in the tubes above the upper packer had been removed and a stable groundwater composition achieved, on average after at least two days. Stable conditions are often indicated by unchanging electrical conductivity of the groundwater. After stability had been

Table 7-1. Groundwater sampling programme carried out in KLX02 using the SKB packer sampler. After Table 3-1 in /7-1/.

Ground-water sampling activity no.	Drilling water conc.	IonChrom. Titration: Cl, HCO ₃ , Br, SO ₄	Photo-metry: Fe, HS- (NO ₂ -PO ₄)	ICP Cations	Trace elements	Isotopes: U, Th, C-13, O-18, D, Tr, Sr, S	Spec. Isotopes: 3He, 4He, Tr	Colloids	Organic matter, Gas	Gas, Isotopes and Bacteria
1									O	
2	X	X	X	X						
3	X	X								
4					O					
5							O			
6						X				
7								X		
8								O		
9										O

(X = all sampling sections; O = some sampling sections)

Table 7-2. Groundwater sampling sections with the SKB-packer sampler in KLX02 together with periods of sampling and sampling activities according to Table 7-1. After Table 3-2 in /7-1/.

Sampling interval (m)	Sampling period	Sampling activities
315.0– 322.0	94 01 27–94 02 11	1, 2, 3, 4, 5, 6, 8, 9
335.0– 340.8	93 10 28–93 11 09	2, 3, 4, 6, 7
798.0– 803.8	93 11 10–93 11 24	1, 2, 3, 4, 6, 7, 9
1090.0–1096.3	93 12 01–93 12 17	1, 2, 3, 4, 6, 7, 8, 9
1420.0–1700.5	93 12 20–94 01 18	1, 2, 3, 4, 5, 6, 7, 8, 9

attained, the duration of the sampling period was often determined by the continuous change in composition of the main constituents. At KLX02, a full monitoring programme was not possible at each sampled section due to time restrictions. In general, 1–2 weeks were allocated to each section at flow rates ranging between 117–172 ml/min. In most cases this proved to be adequate.

The third sampling was performed in 1995 in connection with the Phase 2 hydraulic tests in borehole KLX02, cf. Chapter 6. During pumping in KLX02 in different isolated borehole sections, part of the discharged groundwater was bypassed to a sampler specially constructed for collection and concentration of noble gases in groundwater /7-9/.

For the fourth sampling effort, the Tube sampler was once again engaged /7-2/. One of the main purposes with this sampling was to study possible time dependent changes in the groundwater composition and their causes. The field work was conducted on September 25th 1997. The sampler was lowered into the borehole to a depth of 1450 m.

A fifth sampling campaign, performed as a fracture specific sampling, was conducted in 1999 by using the PAVE sampling tool developed by POSIVA in Finland /7-16/. The results were not included in this report since they have not been fully evaluated. Preliminary results from the obtained groundwater data however indicate large similarities with the fracture specific sampling conducted in 1993 /7-16/.

Besides the groundwater sampling campaigns, samples of calcite fillings were taken from the drill core of KLX02 for isotope analysis. 12 samples were collected from the borehole interval c. 960–1640 m.

7.3 Analytical procedures

The groundwater samples from both Tube samplings were analysed for major components by using ICP-AES and standard titration methods /7-1/. Tritium, deuterium and oxygen-18 were also included in the analyses. Unfortunately, the tritium analyses are uncertain due to analytical problems and were therefore omitted from this evaluation. At the second Tube sampling the concentrations of the isotopes $^{87}\text{Sr}/^{86}\text{Sr}$, $^{34}\text{S}/^{32}\text{S}$ and ^{14}C were quantified /7-2/ as well. A delay of three or four days in measuring the pH and alkalinity affected the accuracy of the pH-values due to uptake or loss of CO_2 .

Using the SKB packer sampler, groundwater was continuously pumped to the laboratory unit /7-1/. Samples were taken for immediate analysis in the field as well as for external laboratory analysis. Some of the major components (anions), pH and electrical conductivity were determined daily in the field laboratory, to achieve an immediate feed-back of the groundwater composition. Ferrous and ferric iron and minor anions were also determined in the field laboratory, but not as frequent. The system enables the redox sensitive components to be determined immediately, without atmospheric contamination.

To ensure data quality, control analyses by independent laboratories were carried out on one sample from each sampled section by the SKB packer sampler. When the analytical data sets from different laboratories were considered to be in good agreement, the data was compiled and further evaluated to produce the final data set for each sample.

Isotopic analyses of fracture fillings were performed according to procedures described in /7-5/.

7.4 Representativity of groundwater samples

To ensure the quality of the field and laboratory data is a task of high priority, since the understanding of natural groundwater systems is no better than the data on which they are based. By definition, a high quality sample is considered that which best reflects the undisturbed hydrogeological and hydrogeochemical *in situ* conditions for the sampled section. A low quality, and hence low representativity of a sample, reflects errors such as excessively high or low extraction pump rates, contamination from borehole activities, complex hydrological situations, contamination from tubes of varying compositions, air contamination, losses or uptake of CO₂, long storage time prior to analysis, analytical errors etc. Some errors are easily avoided, others are difficult or impossible to circumvent /7-1/.

At KLX02 the focus was on avoiding interference from drilling, hydraulic testing and other borehole activities. Open-hole conditions, however, may have contributed to a general mixing of groundwater types in the borehole. This risk is regarded as relatively large, since the upper part of the borehole may represent active recharge, see Section 7.7 and /7-1/. Repeated lowering and raising of geophysical probes may also have caused groundwater perturbation in the boreholes, resulting in mixing of non-saline and saline groundwater types. A significant problem in deep boreholes like KLX02 is the long distance from the deeper parts of the borehole to the ground surface, entailing long transport times for the groundwater when slowly pumped to the surface. It is a known phenomenon for groundwater to undergo significant pH (and Eh) changes through degassing and oxidation etc during this transport process.

Several measures were taken to minimize contamination of the groundwater samples. Most of the samples were collected at low extraction rates (< 200 ml/min) by the SKB packer sampler. In addition, careful planning and other precautionary measures, such as long sampling times, have provided a reasonable degree of confidence in the representativeness of the groundwater samples from KLX02 /7-1/. This was supported by the on-line monitoring data with the CHEMMAC-sond. Contamination by drilling water was negligible, as uranine contents (flush-water tracer) are consistently less than 1% in the samples. Interestingly, the samples taken by the Tube sampler showed a similar character (except for the pH-values) compared to samples from the SKB packer sampler, although somewhat more dilute, i.e. less saline (lower Cl⁻ concentration).

7.5 Results

7.5.1 Scatter plots

In order to demonstrate the general trends of the analytical groundwater data, x and y scatter diagrams (Figures 7-4, 7-5, 7-6, and 7-7) for Cl, HCO₃, δ¹⁸O, and microbes were plotted against depth /7-2/. High Cl-values may be the result of influences from ancient saline water, high HCO₃ may follow from hydrogeochemical reactions in shallow waters, low δ¹⁸O-values may indicate influences from cold recharge water, such as melt water from the last glaciation.

Although sampling with the SKB-packer sampler is characterized by a better representativity including e.g. in-situ Eh and pH-measurements, the general chemistry seemed to agree well with the samples collected with the Tube sampler. In order to facilitate comparison and to illustrate depth trends, data only from 1993 and 1997 collected with the Tube sampler is compared. However, microbe data was collected merely during 1997.

Regarding general groundwater chemistry, the samples seem to reflect two distinct groupings; one shallow to intermediate *Sodium-Bicarbonate* type to a depth of 1000 m, respectively a *Calcium-Chloride* type of deep origin, occurring below 1000 m. The Cl-concentrations from 1993 appear as similar to the values obtained during the 1997 sampling campaign. The HCO₃-values from 1997 are in the upper 400 m of the borehole lower than the 1993-values. At a depth of 1000–1500 m the 1997 δ¹⁸O-values exceed those obtained at the previous campaign. Finally, the total cell counts for the microbial samples (from 1997) show a decline in the interval 500–1000 m compared to above and below. The explanation for this is unknown, but may reflect a variety of microbial populations thriving at different depths and conditions.

7.5.2 M3 groundwater modelling

The sampled groundwater was modelled by M3 (Multivariate Mixing and Mass balance calculations), /7-1/ and /7-3/. The aim of M3-modelling is to calculate how *mixing* and *reactions* affect the groundwater character. The M3-modelling starts by comparing groundwater compositions. The assumption is that waters with similar compositions have a similar origin and undergone similar mixing and reaction processes. To make this comparison with the highest possible accuracy, several groundwater constituents have to be compared. This is performed in an optimum way using multivariate techniques.

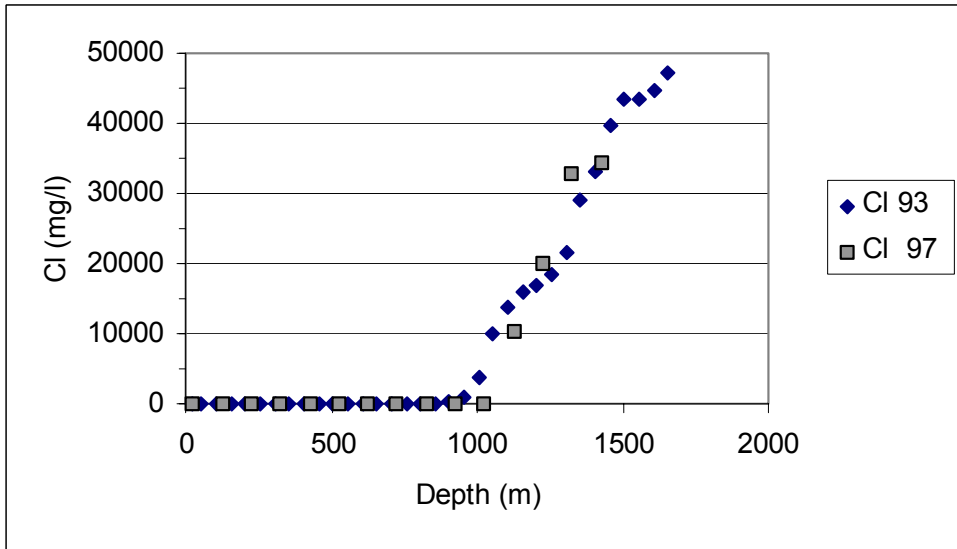


Figure 7-4. Scatter plot for data from borehole KLX02 showing Cl versus depth. Data from 1997 is compared with data from 1993.

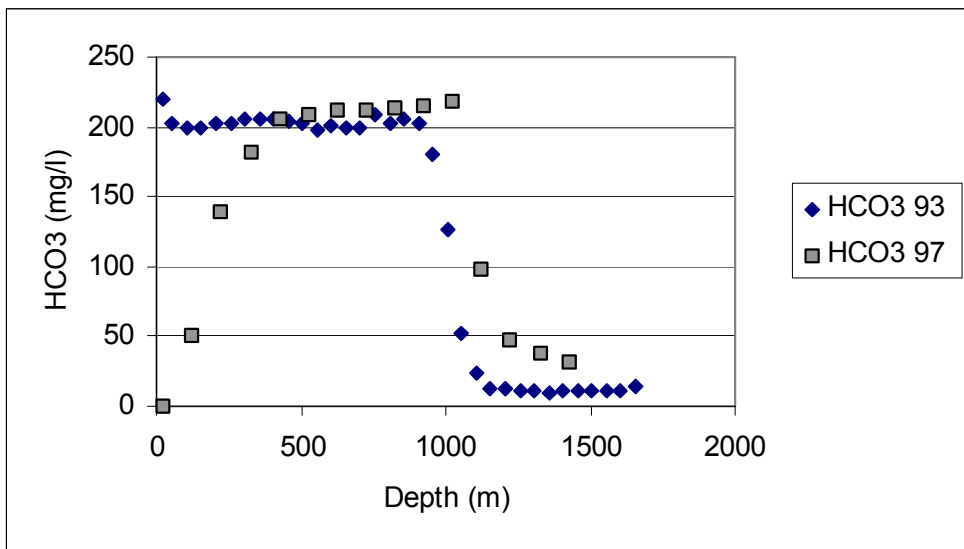


Figure 7-5. Scatter plot for data from borehole KLX02 showing HCO₃ versus depth. Data from 1997 is compared with data from 1993.

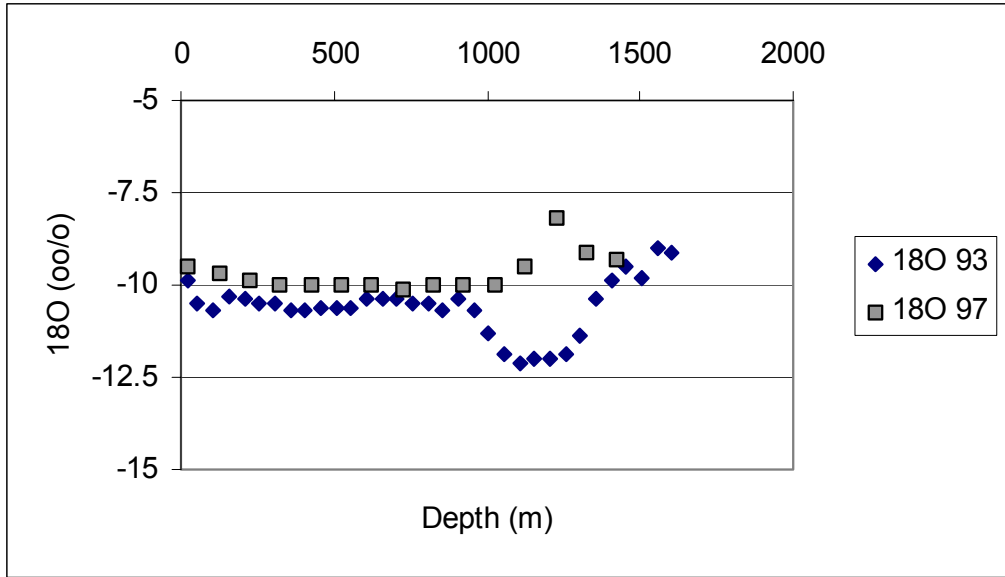


Figure 7-6. Scatter plot for data from borehole KLX02 showing $\delta^{18}O$ versus depth. Data from 1997 is compared with data from 1993.

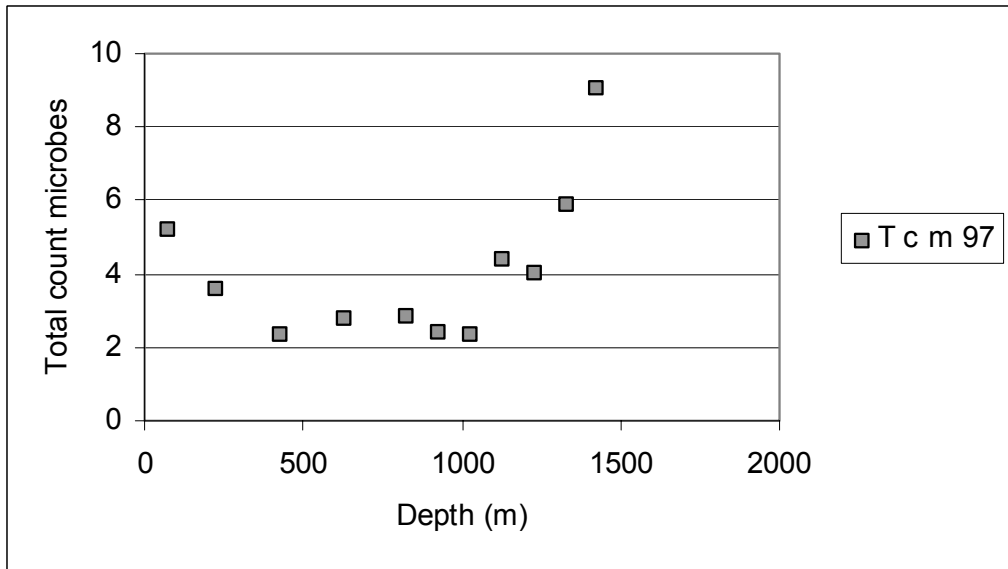


Figure 7-7. Scatter plot for data from borehole KLX02 showing total cell counts for microbes ($\cdot 10^5$) versus depth. Sampling was performed in 1997.

The result of the comparison serves to construct an *ideal mixing* model between the groundwater samples which seem to participate in the groundwater system studied. The ideal mixing model may employ different *reference waters* (selected waters of specific composition used for comparison with the sampled waters) depending on how the modeller prefers to describe the groundwater system in terms of origin, mixing and reactions. The modelling is therefore generally repeated several times to investigate alternative models, where measured and even modelled end-members (e.g. glacial meltwater or Litorina Sea water) are tested for an optimum description of the measured groundwaters.

The number of reference waters to be used in the modelling is guided by the ideal mixing model, which is dependent on the complexity of the groundwater signatures. The relevance of the selected ideal mixing model is then tested by predicting water conservative elements such as Cl and $\delta^{18}\text{O}$. If this test indicates that the model is able to predict the conservative elements fairly well, the non-conservative elements are calculated and a deviation from the ideal mixing model can be used to demonstrate the effects from reactions. A source (gain) with respect to the ideal mixing model may be the result of dissolution of a mineral; a sink (loss) often indicates precipitation of a mineral phase. The uncertainty of the model varies from case to case depending on the quality and geometrical distribution of the collected samples. In the Äspö case the uncertainty has been determined at $\pm 10\%$.

The M3-model consists of 3 steps, where the first step is a standard multivariate analysis (PCA), followed by mixing and finally by mass balance calculations. Here only the first two steps were applied, PCA- and mixing calculations. In the PCA-plot (Figure 7-8) all Äspö site data is compared with data sampled during 1993 and 1997 in borehole KLX02. Due to a known uncertainty of the tritium analyses, these were excluded from the PCA-analysis.

The following reference waters were identified in the the PCA-plot (Figure 7-8):

Brine reference water, which represents the brine type of water found in KLX02 at 1631–1681 m.

Glacial reference water demonstrates a precipitation water composition where the stable isotope values ($\delta^{18}\text{O} = -21$ SMOW and $\delta^2\text{H} = -158$ SMOW) were based on measured values of $\delta^{18}\text{O}$ in the calcite surface deposits, interpreted as sub-glacial precipitates, collected from different geological formations at the west coast of Sweden /7-10/. The water represents a possible meltwater composition from the last glaciation >13000 BP.

Litorina Sea reference water displays an ancient sea water composition (8000–2000 BP) with a Cl concentration of 6100 mg/l based on analyses of microfossils from the marine sediments in southern Finland /7-11/. A similar Cl content was suggested in /7-12/ based on measurements of interstadial water in postglacial black clays.

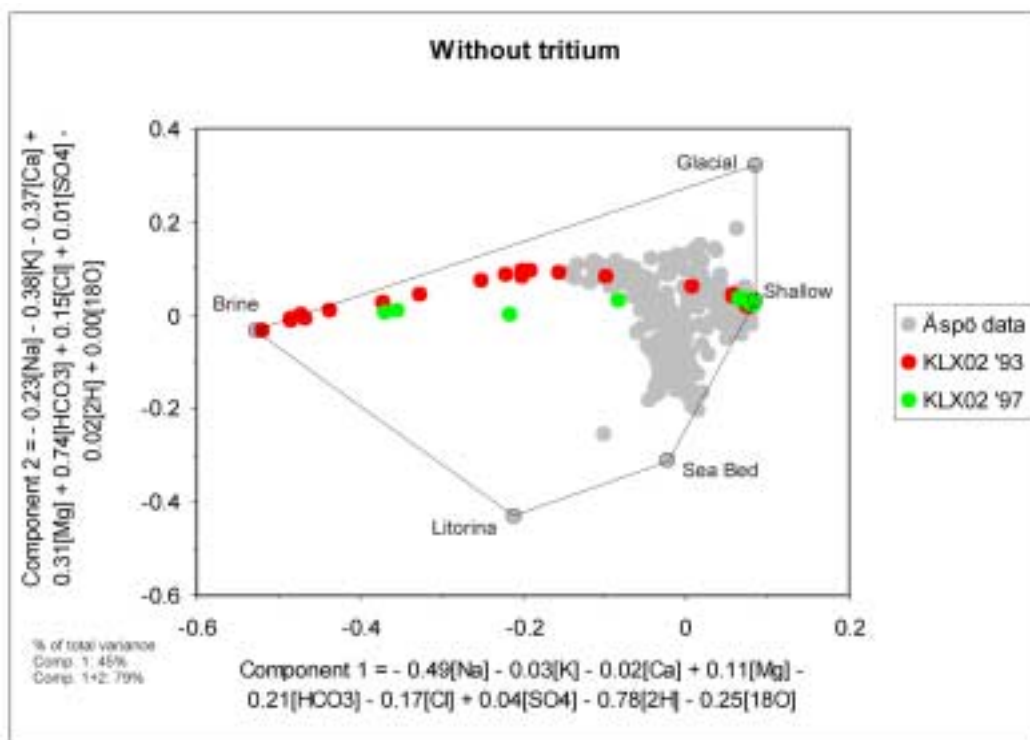


Figure 7-8. A principal component plot is used to illustrate the distribution of the Äspö site data in comparison with the data sampled during 1993 and 1997 in KLX02. In this calculation the tritium values have been excluded from the data set. The identified reference waters are named according to the discussion below. The first and second principal components together account for 79 % of the variability, or the information of the Äspö site data set. The variables Cl, HCO₃, SO₄, Na, K, Ca, Mg, δ¹⁸O and δ²H were used in the PCA-calculation. After Figure 4-15b in /7-2/.

Sea Bed reference water is extracted marine *sediment pore water*, /7-13/, with modelled values for stable isotopes. The major component chemistry in the pores resembled modern Baltic Sea values. Based on this knowledge the modern isotope values measured from the Baltic Sea water were used.

Shallow reference water represents the type of water found in borehole HLX06 (871103) at 45–100 m.

The results from the sampling campaign in 1997 differ from the results obtained in 1993 as shown in the PCA-plot (Figure 7-8). The results from 1997 include many observations associated with Meteoric water and some observations falling more or less along a straight mixing line between the Meteoric and Brine reference waters. The deviation from 1993 towards Glacial water is not obtained with the measured water composition sampled in the open borehole in 1997. The results from the M3 mixing calculations based on the data from 1993 and 1997 along the borehole are shown in Figure 7-9.

The $\delta^{18}\text{O}$ -analyses from the calcite fracture fillings indicate that the major part of the calcite was not formed from the present-day groundwater, although some of the higher $\delta^{18}\text{O}$ -values could reflect equilibrium with groundwater under current *in-situ* temperature. Similarly, the low $\delta^{18}\text{O}$ -values may have formed from groundwater, however at temperatures 30–40 °C higher than the present ambient temperature /7-5/.

The coupled variations in the oxygen, carbon and strontium isotopes at depths in excess of c. 900 m indicate the presence of different groundwaters in the past. Correlation of the $\delta^{87}\text{Sr}$ with Sr-concentrations could reflect water-rock interaction. The relatively large $\delta^{13}\text{C}$ -values for all calcite fracture fillings reflect a nonbiogenic origin, presumably a deep-seated carbon source, i.e. methane /7-5, 7-6/. Analyses of calcite fracture fillings from borehole KLX02 have been further studied within the EU project EQUIP /7-14/.

The analyses of noble gases may indicate water-rock interaction at great depth, suggested from measurements of $^{40}\text{Ar}/^{36}\text{Ar}$, ^{85}Kr and ^4He . This supports previously found indications of long residence times for the groundwater and significant water/rock interaction processes going on at these large depths /7-9/ and /7-17/.

7.6 Conclusions

From the analytical results (cf. Figures 7-4 to 7-7) and from M3-modelling (Figures 7-8 and 7-9) the following conclusions are drawn:

At a depth of 0–1050 m in borehole KLX02 the general chemistry of the groundwater seems to reflect a shallow to intermediate *Sodium-Bicarbonate* type of water. There are indications of influx of shallow groundwater in the upper part of the borehole, and the water is partly under-saturated with respect to calcite, which is reflected in the low HCO_3^- - and relatively high bacterial content. This water displays a successive evolution due to bacterial activity, calcite dissolution and mixing within the interval 0–400 m. The waters sampled at a depth of 400–1050 m are characterized by a meteoric signature with a homogenous composition both chemically, isotopically (stable isotopes and ^{14}C), and bacteriologically. This indicates that the water enters the borehole through a fracture zone of high hydraulic conductivity and is then transported along the borehole. Unexpectedly, the $\delta^{34}\text{S}$ -value is +21.5 ‰ at 400 m depth, indicating a marine signature which, however, vanishes at larger depths. These constituents have been interpreted as being leached from old marine sediments rich in sulphates residing at the surface, alternatively constituting some remnants of fossil seawater, which also may be indicated by higher Mg-values compared to the samples from 1993. The portion of meteoric water is generally 10 % larger and the penetration depth is 100 m deeper than during 1993 /7-2/.

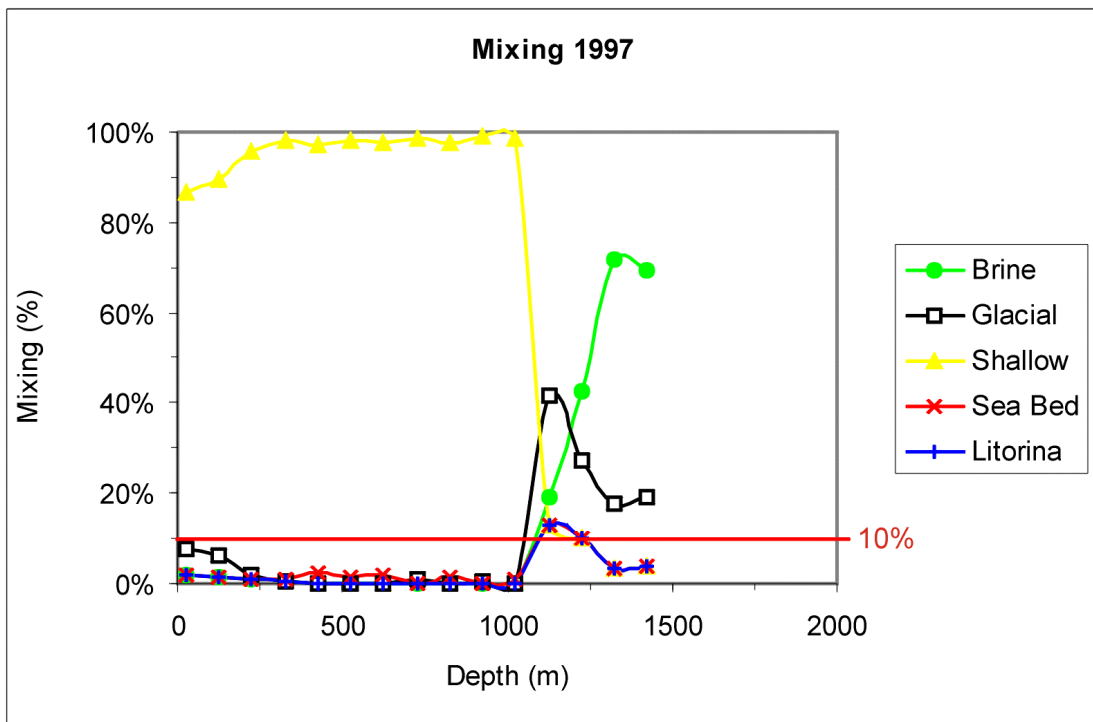
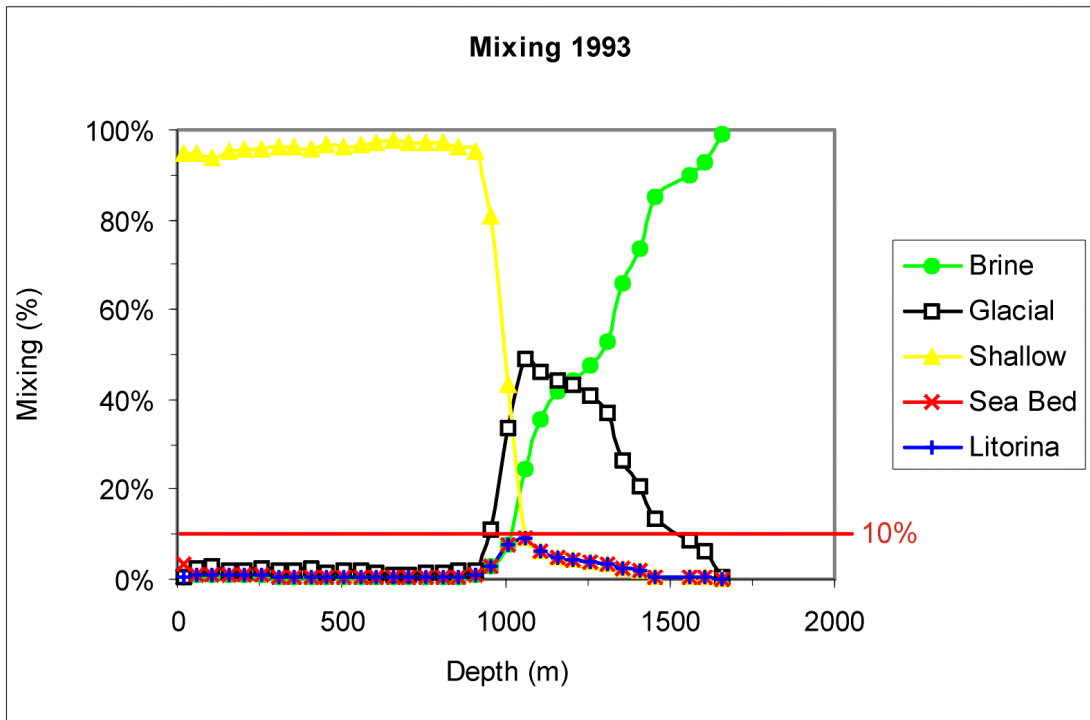


Figure 7-9. The results of M3 mixing calculations obtained on groundwater sampled during 1993 and 1997 in borehole KLX02. The calculated mixing portions of Meteoric, Brine, Glacial, Litorina and Sea Bed waters are plotted against depth. The mixing portions add up to 100 % for all the samples. A mixing portion of less than 10 % is regarded to fall below the detection limit for the M3-method and is therefore uncertain. After Figure 4-16 in /7-2/.

The non-saline/saline interface at 1050–1450 m is characterized by a change to a *Calcium-Chloride* type of brine water. The portion of such water at a depth of 1050–1450 m is larger in 1997 than during 1993. Less glacial water is obtained, which is also indicated by higher $\delta^{18}\text{O}$ -values compared to the values from 1993. There are no traces of glacial water in the sampling 1997 or a clear deviation in the $\delta^2\text{H}$ - versus $\delta^{18}\text{O}$ -signature from the MWL (Meteoric Water Line) in the brine component, as was shown in 1993 /7-2/. The deviation from MWL was used as an indicator of long contact time between groundwater and bedrock. The chloride component in brine water has been dated using the isotope ^{36}Cl to be around 1.5 m.y. (million years).

The main reason for the relatively large differences between the 1993 and 1997 sampling campaigns have been evaluated to be due to the open-hole effect, which acts like a “superconductor”, bringing about mixing of water along the borehole, thereby creating new water compositions, cf. Section 7.7 and /7-2/. Since the first sampling, the three-component mixture consisting of meteoric, glacial and brine water has been replaced by a two component mixture consisting of meteoric and brine water. Natural annual changes of 1 m water column in an open borehole may cause the interface between non-saline and saline groundwater to fluctuate up to 100 m in the borehole. This pumping effect renders changes of the water composition possible, especially of the often sensitive isotopic signature of the water. In 1997 the saline interface was situated 100 m deeper in the borehole than in 1993. The results illustrate the sensitivity of the composition of deep groundwater in open boreholes exposed to mixing and changes depending on the prevailing hydrogeological situation.

It is believed that under natural conditions the upper 1000 m of the bedrock around borehole KLX02 is located within a groundwater recharge area (Section 7.7). The sub-vertical, moderate angled and subhorizontal fracture zones (Chapter 3, Section 3.4) penetrated by the borehole facilitate groundwater circulation to considerable depths (at least to 800–1000 m), thus accounting for some of the low-saline, brackish groundwater in these water-conducting fracture zones. Below about 1100 m it is assumed that the system is hydraulically and geochemically less dynamic, such that highly saline groundwater exist in an almost stagnant environment. These Ca-Cl dominated brines represent deep regional groundwater, where long residence times and water-rock interactions have played a dominant role in determining the composition.

Since the groundwater sampled at depths below 1100 m in KLX02 has a salinity significantly higher than the most saline waters at Äspö, the analyses from KLX02 have been crucial for the understanding of the deep groundwater system. Interpretations of the large data set from Äspö and Laxemar together have demonstrated that the deep groundwaters at Äspö and Laxemar have the same origin (dominantly Ca-Cl Brine type water and Glacial melt water) although the mixing proportions are somewhat different. The stable isotope composition of the fracture calcites are in agreement with more stagnant conditions at depths below 1000 m /7-5, 7-6/.

7.7 Investigation of the flow regime in borehole KLX02

Open boreholes constitute short circuits between different fractures and fracture systems in the bedrock. If the hydrodynamic pressure prevailing in one fracture system differs from that of another fracture system, the hydraulic gradient between the two systems will result in groundwater flow along a connecting borehole. During undisturbed, pre-drilling conditions, the fracture systems may be completely or partly isolated from each other. An open borehole joining the separate systems, however, constitutes an excellent flow path. In course of time, the groundwater flow along the borehole will result in more or less extensive mixing of groundwater from different levels and, possibly, of different origin in the bedrock. One way to prevent this process is to install a multi-packer equipment in the borehole, which provides a method to isolate different fracture systems from each other.

Ever since completion of the KLX02 drilling operations, there have been speculations concerning the flow regime in the borehole and to which extent this regime reflects pre-drilling conditions. Several indications of flow along the borehole, i.e. in almost vertical direction, have been noticed. However, to determine in what parts of the borehole the flow is directed vertically-up respectively vertically-down has appeared to be quite complicated. In order to, if possible, finally settle this problem, an investigation of all indications of groundwater flow in borehole KLX02 was made after completion of Phase 2 by INTERA and GEOSIGMA (Marcus Laaksoharju and Lennart Ekman pers. comm.). Data from recently performed difference flow measurements, previous chemical sampling, geophysical borehole logging, logging with a digital colour TV-camera (BIP-system) as well as with a black & white TV-camera, hydraulic tests and structural-geological investigations were scrutinized, and comparison with data from the neighbouring deep core borehole KLX01 made. The results of this investigation are summed up below.

1. Difference flow measurements in 2 m-sections performed in borehole KLX02 during the spring 1999 by POSIVA, /7-15/, indicated several large negative flows above c. 1000 m in the borehole, see example from section 200–400 m in Figure 7-10. A negative flow is defined as a flow from the borehole into the intersecting fractures. Especially noticeable is a negative flow of c. 40 l/h at 251–252 m depth in the borehole. Below 1000 m, instead several positive flows were observed, see example in Figure 7-11. The difference flow measurements do not include the upper part of the borehole, 0–200 m, which is supplied with a casing, or the lower part, 1406.65–1700.5 m, since an obstacle at c. 1448 m prevented measurements below that level. Hence, definite conclusions regarding flow directions within the borehole cannot be drawn merely from the results of the difference flow measurements.

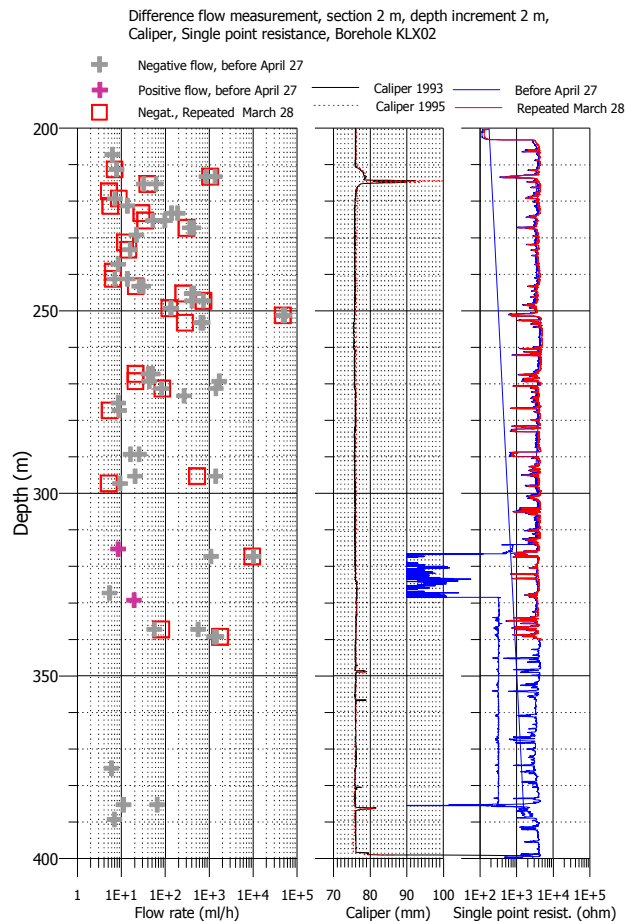


Figure 7-10. Results of difference flow measurements in short sections performed within the interval 200–400 m of borehole KLX02 during the period March-May 1999. After Appendix 1 in /7-15/.

However, a couple of complementary facts may add to the overall picture. Installation of the 200 m long borehole casing was not accompanied by grouting in order to seal the (small) gap between the casing and the borehole wall. Groundwater leakage along the casing into the borehole is therefore possible. Relatively large inflow of water was observed during drilling at e.g. 40 m, 167 m and at 185–190 m /1-2/. The flow conditions (positive or negative flow, flow rates) during undisturbed conditions are not known, however. Part of this groundwater flow may enter the borehole below the casing and render an explanation for the many observed sections with negative flow above 1000 m. A simple flow balance estimate illustrates that the outflow from the borehole within the interval 200–1000 m is not balanced by the observed inflow into section 1000–1406.65 m (plus a few sections of inflow in section 200–1000 m). A contribution of water either from section 0–200 m or from section 1406.65–1700.5 m is therefore necessary. The flow log, Figures 6-7 and 7-1, indicate a very small flow contribution during pumping from

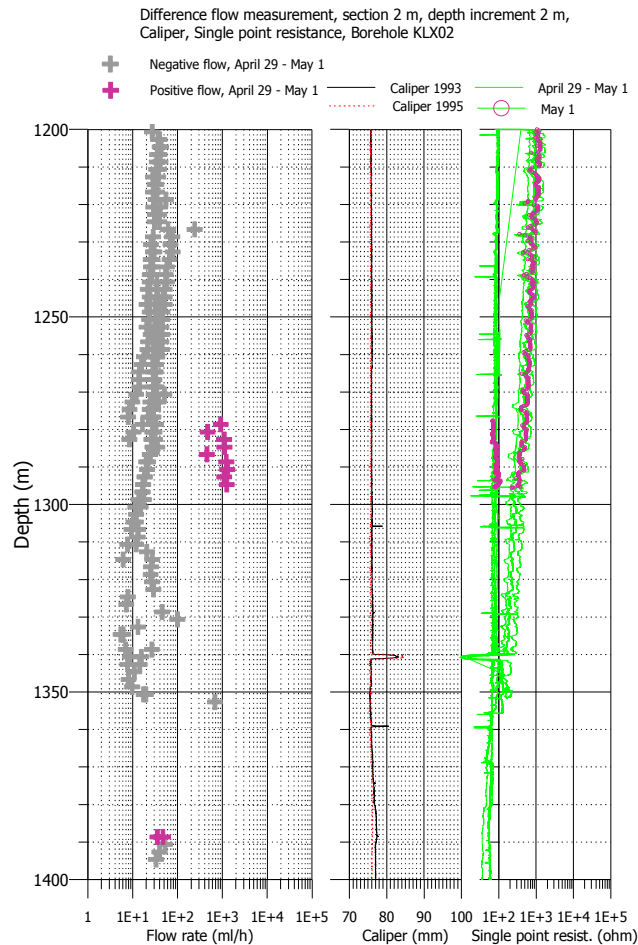


Figure 7-11. Results of difference flow measurements in short sections performed within the interval 1200–1400 m of borehole KLX02 during the period March–May 1999. After Appendix 6 in /7-15/.

section 1406.65–1700.5 m. The capacity tests during drilling demonstrated a hydraulic transmissivity $T = 3.1 \cdot 10^{-6}$ m/s in section 1427–1700.5 m, whereas in section 0–205.5 m the corresponding value was $T = 6.2 \cdot 10^{-5}$ m/s, i.e. 31 times larger per 100 m borehole length (Chapter 6). The possible flow contribution from the lower part of the borehole is hardly sufficient to explain all negative flows above 1000 m. It is therefore more likely that groundwater from section 0–200 m during undisturbed, i.e. unpumped conditions, enters the borehole below the casing, entailing groundwater flow vertically-down along the borehole. Along the downward path, more and more of the flow is lost by discharge from the borehole into fractures.

The accumulated positive flow from section 1000–1406.65 m may either be transported vertically up or vertically-down (or both). If transported upward, the groundwater flow will somewhere encounter the downward flow from the upper part of the borehole.

2. A black & white TV-logging of borehole KLX02 displays precipitated material at several levels, where the difference flow measurements recorded positive flow anomalies, e.g. at 310–330 m, 440–450 m, 730–740 m and 1000–1050 m. This phenomenon supports the results of the difference flow measurements, indicating groundwater mixing, resulting in chemical precipitation at each point where groundwater recharges into the borehole.
3. The results of the previous groundwater sampling, see Section 7.6, indicate a downward movement of about 100 m of the groundwater type dominating the upper part of the borehole, “meteoric” or “shallow” groundwater, between two sampling occasions, at 1993 and 1997 respectively. During the same period, deep groundwater of “brine”-type has moved upwards. The limit between the two systems was in 1997 situated at approximately 1000 m borehole depth.
4. At approximately 800 m borehole length, the temperature curve from borehole KLX02 exhibits an anomaly, see Figure 5-1. This may indicate either outflow of relatively cold groundwater discharging upwards or, contrary, relatively cold groundwater transported along the borehole downwards, discharging into a fracture at c. 800 m. The difference flow measurements support the latter hypothesis, see Figure 7-12 (negative flow at 800 m).
5. The electrical conductivity curve (corresponding to salinity) exhibits a rapid increase at about 800 m, see Figure 7-1. This indicates a relatively sharp limit between two groundwater systems.
6. One of the structural-geological interpretations of the Laxemar area, indicates rather steeply dipping major fracture zones penetrated by borehole KLX02 at the borehole interval 800–1100 m, see Section 3.4.3, Figures 3-19 and 3-20. If the interpretation is correct, the sub-vertical to moderate angled fracture zones SFZ04 and SFZ07 should facilitate groundwater circulation to considerable depths (at least to 800–1000 m). A similar statement can be made about the structural interpretations based on the reflection seismic survey in the Laxemar area (Section 3.4.5, Figure 3-24 and Figure 3-25), although the groundwater transport to larger depths would be less direct, partly conducted by major subhorizontal fracture zones, implying relatively long flow paths from shallow to deeper parts of the bedrock. Borehole KLX02, after completion constituting an artificial flow path from the ground surface to 1700 m depth, may speed up a natural flow regime characterized by recharge conditions down to at least 800 m.
7. Long-term groundwater level monitoring in four sections of the 1078 m deep core borehole KLX01, situated 1 km NE of KLX02, indicates recharge conditions to a depth of several hundred metres in this borehole. Figures 3-19 and 3-21 as well as Figure 3-25 indicate a structural-geological parallelism between KLX01 and KLX02, which strengthens the hypothesis of recharge conditions down to several hundred metres also in borehole KLX02.

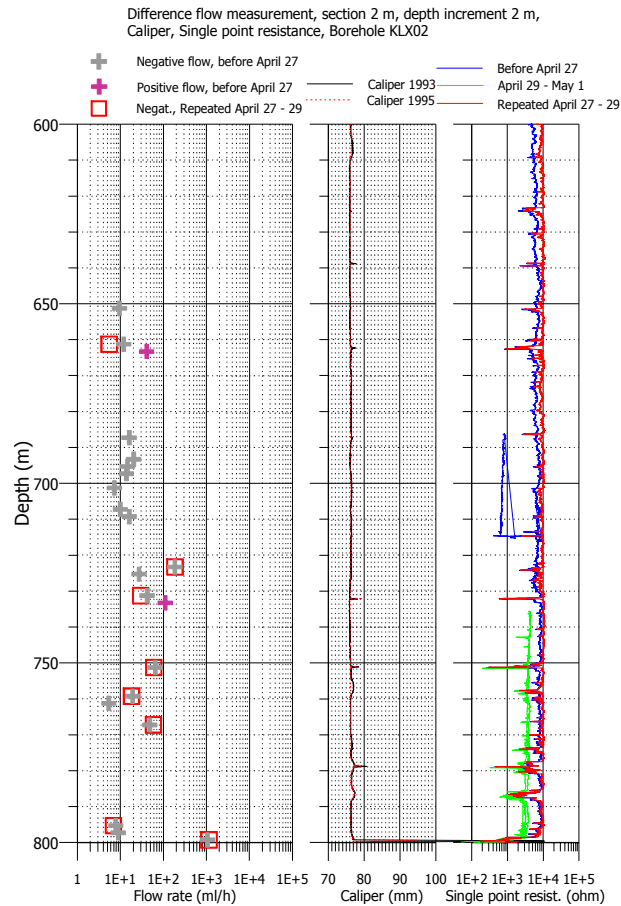


Figure 7-12. Results of difference flow measurements in short sections performed within the interval 600–800 m of borehole KLX02 during the period March–May 1999. After Appendix 3 in /7-15/.

Based on the above indications a hypothesis regarding the flow regime of borehole KLX02 was formulated (Marcus Laaksoharju and Lennart Ekman pers. comm.):

- A. The upper part of the borehole, c. 0–800 m, is more dynamic, i.e. the groundwater turnover time is shorter, than in the section 800–1700 m.
- B. Groundwater emerging from the shallow part of the bedrock recharges into the borehole, between the casing and borehole wall, above 200 m depth. This groundwater continues downwards in the borehole. Portions of this open-hole transport discharges into fractures in the borehole interval 200–800 m except in a few sections where flow recharges.
- C. At c. 800 m the downflowing groundwater encounters a minor, upwardly flowing groundwater stream from the deep parts of the borehole, i.e. 800–1700 m. The groundwater of shallow as well as that of deep origin discharges into the upper/middle part of the fracture zone, which according

to one interpretation constitutes the intersection between fracture zones SFZ04 and SFZ07, or, interpreted from the reflection seismic results, is a major subhorizontal fracture zone.

- D. The deeper parts of the groundwater aquifer, below 800 m, seem to be more stagnant than the upper part. The weak indications of groundwater flow directed upwards in the borehole may not correspond to natural flow conditions but merely represent an open-hole effect.

The above referred data support or, at least, do not contradict the hypothesis advanced. However, results from BIPS-logging (digital colour-TV), do not immediately fit into this schedule. Figures 7-13 and 7-14 are BIPS-images from the levels 363.50–363.80 m respectively 387.10–387.40 m in KLX02.

Both images show plain signs of mineral precipitation, possibly of calcite, on the borehole wall upward from distinct fractures. Several similar examples exist within the borehole interval supposed to be governed by downward groundwater movement.

Spontaneously, it would be easy to regard this fact as a convincing indication of positive flow directed upward in the borehole. The difference flow measurements, though, indicate negative flow at several of the borehole levels, where BIPS-logging indicates positive flow, e.g. around 387 m /7-15/. A plausible explanation to the observed phenomenon could be that the precipitation is a result of borehole pumping. Test pumpings, some of them with a long duration, have been performed at several occasions, see Chapter 6. During pumping, a gradient is created into the borehole at all levels. Hence, groundwater will enter the borehole through all conductive fractures, whereby groundwater from many levels and of different origin and composition will mix. This is a process which probably facilitates different types of hydrogeochemical reactions, including the observed calcite precipitation on the borehole wall.



Figure 7-13. BIPS-image from borehole KLX02, level 363.50–363.80 m.

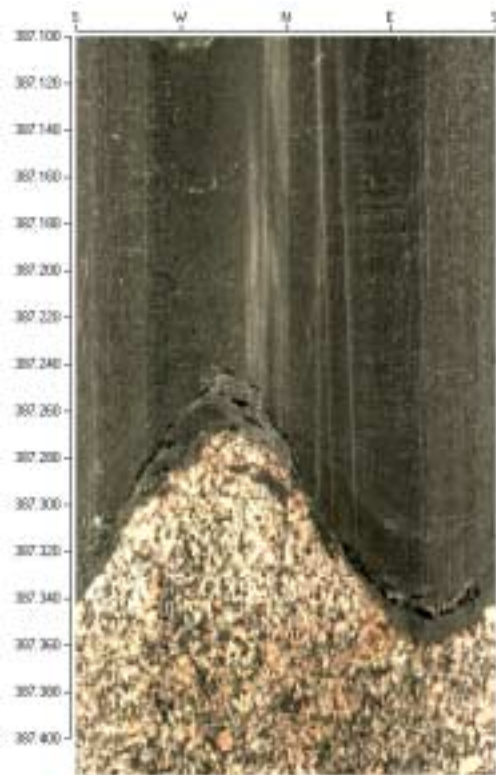


Figure 7-14. BIPS-image from borehole KLX02, level 387.10–387.40 m.

Executive summary

General

During the autumn 1992, a 1700.5 m long, subvertical \varnothing 76 mm borehole was drilled in the Laxemar area, close to the nuclear power plant at Simpevarp, south-eastern Sweden (Figure 1-1). The primary purposes of the drilling project was to test core drilling technique for \varnothing 76 mm to large depths and to enable investigations of several geoscientific parameters at larger depths than had been possible at previous geoscientific surveys conducted by SKB.

The most important aim of this report is to provide a summary of the results from all investigations performed in borehole KLX02 during the period 1993–early 1998 within a project designated Project Deep Drilling KLX02 – Phase 2. The investigation programme of Phase 2 comprised various geoscientific topics, most of them including several types of studies (cf. Figure 2-1). They were all, in one way or the other, related to what is needed for a site description of and a safety analysis for a deep bedrock sited repository. A large number of reports were produced during and after the period of field investigations. As long as the investigation results were scattered in numerous reports, a quick general view was difficult to obtain. If the present report can eliminate this problem, one important aim is fulfilled. After completion of Phase 2, i.e. during the period early 1998 to early 2001, new investigations have been performed in borehole KLX02 as well as in other parts of the Laxemar area, and a number of recent reports have been presented. Some important results from these investigations have likewise been included in this report. These results concern the regional lithological-structural setting of the Oskarshamn area as well as the local structural characteristics of the Laxemar area, the stress field around borehole KLX02 and the flow conditions prevailing in this borehole.

The report is also supposed to touch upon questions related to investigation technique for boreholes deeper than 1000 m, since investigations beyond approximately that depth had not been included in the SKB geoscientific investigation programmes until 1992/93. It is demonstrated in the report that various kinds of investigations could be conducted without problems to depths of several hundred metres below 1000 m. On the other hand, at certain occasions specific problems did reveal. For example, minor washouts, i.e. mechanically, hydrogeologically or stress induced loose rock particles emerging from the borehole wall or from fractures intersecting the borehole, were observed at different levels, and major borehole breakouts, i.e. depressions in the borehole wall from stress induced outfalls, were indicated at 1346–1347 m respectively 753–823 m borehole length /4-6/. A washout at approximately 1448 m, which possibly represents a slip on a pre-existing fault, precluded borehole investigations below that depth for a long time.

During Phase 2, problems were related especially to equipment for hydraulic testing, which got stuck in the borehole several times, possibly due to minor washouts trapping the straddle packers. Fishing out trapped or dropped components may be quite time consuming when working at large depths.

Specific procedures and, sometimes, specially applied equipment may therefore be well motivated when working in deep boreholes /4-16/.

The investigations included in Project Deep Drilling KLX02 – Phase 2 followed, on the whole, the SKB concept for site investigations. However, since primarily only one borehole was involved in the study, a fully adequate evaluation of the geoscientific conditions in the entire Laxemar area is not possible. By integrating data from other boreholes in the Laxemar area the task may be brought a bit forward, although the number of boreholes is limited. Also results from remote analysis and aerial geophysics are very important, especially in outlining the structural setting of a site. Therefore, data from previous investigations in the Laxemar area was integrated, especially borehole investigations in the deep core drilled borehole KLX01, as well as geophysical surveys. Important geophysical investigations were e.g. reflection seismics and VSP (Vertical Seismic Profiling), both studies performed after Phase 2 /3-33/. Preliminary lithological-structural models of the Laxemar area were set up by considering all available data (Chapter 3). The Laxemar area is here defined as, approximately, the area where the core drilled boreholes KLX01 and KLX02 and the percussion drilled boreholes HLX01–HLX12 are situated with nearest surroundings. For the majority of the investigations included in Phase 2, focus was, however, mainly directed towards a limited rock volume in immediate connection with borehole KLX02.

Major findings

Below, the most important results are listed and major findings summed up.

Geology

Lithological character

The main report describing lithology and fracturing of the KLX02 drill core is /3-4/. Results from borehole geophysical investigations, described mainly in /3-4/, petrological classification of drill cuttings and examination of thin sections, /3-5/, contributed substantially to the lithological interpretations.

The bedrock of the Laxemar area is dominated by different varieties of granitic rocks and greenstone of dioritic-gabbroic composition, Figure 3-2. The former are granites, granodiorites and monzonites to quartz monzodiorites belonging to the c. 1800 m.y. old Transscandinavian Igneous Belt (TIB). They are traditionally called “Småland granites” in this part of Sweden /3-2/. The different varieties are often intimately associated, and gradual transitions are common. The Småland granites in general are more or less isotropic, and large areas with rather homogeneous varieties exist.

In the drill core (and drill cuttings) from borehole KLX02 four main rock types were encountered, Figure 3-12. The classification is made according to a system developed at the Äspö HRL /3-4/:

- Småland granite (63 % of the drill core and drill cuttings).
- Äspö diorite (25 % of the drill core and drill cuttings).
- Greenstone (10 % of the drill core and drill cuttings).
- Fine-grained granite (2 % of the drill core and drill cuttings).

The Småland granite dominating in the Laxemar area is a greyish red-grey, medium-grained granitoid (granite, granodiorite), generally with 1–3 cm phenocrysts of microcline. A variety of Småland granite dominating on the island of Ävrö, and thus assigned the name Ävrö granite, also occurs e.g. in the southern part of the Laxemar area. It is very similar as the above described Småland granite, however with smaller, about 1 cm, phenocrysts. When referred to Småland granite in the Laxemar area in this report, no clear distinction is maintained between the varieties with larger or smaller phenocrysts.

Also the so called Äspö diorite is regarded as a variety, in this case of more mafic composition, of Småland granite. The Äspö diorite is a grey, medium-grained quartz monzodiorite-quartzdiorite, occasionally with red phenocrysts of microcline. Especially sections 10–70 m and 1450–1700 m are dominated by Äspö diorite.

The greenstone appears in a couple of varieties. The origin of the first, a greyish black to dark-grey, fine-grained rock, is presumably a supracrustal of volcanic derivation. The modal and chemical composition corresponds to a basalt to andesite. The exact age is unknown. The other type of greenstone comprises dark-grey, fine medium-grained diorites. The greenstone occurs in the core from top to bottom as a large number of 5–10 m wide dikes. In particular, greenstone dikes are abundant in section 540–960 m.

The fine-grained granite is a greyish red to dark red, fine-grained, often foliated or strongly fractured rock with cavities. The majority of the dikes at the ground surface are strongly deformed. This is also evident from the thin sections of fine-grained granites, which display not only parallel mylonitic structures, but also strong fracturing or crushing. The fine-grained granites may be classified as true granites rather rich in alkalifeldspar, and they appear in the core as 1–10 m wide intrusions from top to bottom.

Structural conditions

The average fracture frequency of borehole KLX02, 2.36 fractures/m, is significantly lower than the frequency, 2.57 fractures/m, observed in the second deep core drilled borehole at Laxemar, KLX01. The difference is still larger between borehole KLX02 and the two deep boreholes at Äspö, KAS02 and KAS03, in average 3.65 respectively 3.71 fractures/m, Figure 3-7.

Particularly low fracture frequencies characterize the borehole intervals 200–730 m (1–3 fractures/m in the main part), and 1130–1550 m (1–2 fractures/m over long distances). An increased fracture frequency (3–17 fractures/m) was observed in section 730–1120 m, which is dominated by greenstone and Småland granite. Also borehole interval 1550–1700.5 m displays an increased fracture frequency, see Figure 3-12.

To draw extensive conclusions of the structural character of the complete Laxemar area only from the results of Phase 2 is delicate. By combining results from Phase 2 with results from borehole investigations in the deep core borehole KLX01 as well as results from remote analysis, aerial and ground geophysics performed in the Laxemar area prior to and after Phase 2, some authors were able to present preliminary models of the structural setting of that part of the site which is situated in the vicinity of boreholes KLX01 and KLX02, /3-18, 3-19, Roy Stanfors pers. comm., 3-33/. Two of these are presented below.

One of the preliminary structural models suggests a connection between the highly fractured interval 730–1120 m in borehole KLX02 (or part of it) and two regional NE-SW-striking lineaments denominated SFZ04 and SFZ07, see Section 3.4.3, Figures 3-19 and 3-20 (Roy Stanfors pers. comm.). Lineament SFZ04 is striking NW of boreholes KLX02 and KLX01 and lineament SFZ07 SE of them. In this model the two regional lineaments are interpreted as steep to middle-steep fracture zones intersecting borehole KLX02 somewhere within the highly fractured interval at 730–1120 m. However, lineament SFZ04 is dipping towards SE, whereas lineament SFZ07 is dipping NW, and the lineaments cross each other at the fractured interval in KLX02, see Figure 3-20). Depending on the exact width and dip of the two interpreted regional fracture zones, it is assumed that the intersection with KLX02 cover the entire, or part of, the borehole interval c. 800–1500 m.

Lineaments SFZ04 and SFZ07 are in this model interpreted to intersect also borehole KLX01, from opposite directions, hence crossing each other in this borehole as well as in KLX02, probably somewhere within the interval 420–880 m (Figure 3-21). The hydraulic responses observed at depth between the two boreholes (see Chapter 6) would, according to this interpretation, be explained by lineaments SFZ04 and SFZ07.

A seismic reflection survey /3-33/ constituted the basis for a modified structural model, in which the interval c. 650–900 m in borehole KLX02 (i.e. part of the fractured interval 730–1120 m) is interpreted as a subhorizontal zone intersecting borehole KLX01 at approximately 800–1000 m depth (reflectors G and B in Figure 3-25 and Figure 6-4). No connection between the above mentioned regional lineaments SFZ04 respectively SFZ07 and borehole KLX02 was established. However, some reflection seismic reflectors intersecting borehole KLX02 were possible to extrapolate to other, less prominent lineaments in the Laxemar area. Only one of them was though intersecting borehole KLX02 at depth (at approximately 1400 m).

Rock mechanics

Rock stress

Rock stress measurements were performed in KLX02 to a depth of 1342 m applying the hydraulic fracturing method. The results are presented in /4-1/. The interpretation of the hydrofracturing measurements provided data on three stress components:

- Fracture normal stress.
- Maximum horizontal stress.
- Minimum horizontal stress.

The stress magnitudes do not follow a linear relationship with depth. Instead, all three magnitude curves are distinguished by several gradient shifts versus depth, see Figures 4-5 and 4-7. This was interpreted as a disturbance of the stress field due to a major fracture zone found in section 700–1150 m. In fact, the stress field is disturbed also several hundred metres above and below the zone.

Within the fracture zone the stress gradient (change of stress magnitude versus depth) is close to zero. Above and below the zone the stress gradient is significantly increased with depth compared to the theoretical stress gradient. Ensuing from that, the stress magnitudes have at about 1300–1350 m regained the magnitudes lost within the fracture zone. The minimum horizontal stress is between 200 m and 750 m in the same order as the theoretical vertical stress, but falls clearly below the vertical stress from 750 m to the end of the measurements at 1342 m.

The average stress increase is between 207 m and 1340 m borehole length 0.045 MPa/m for the maximum horizontal stress, respectively 0.021 MPa/m for the minimum horizontal stress. This is in good agreement with the general trend observed from a large number of stress measurements in Sweden.

A mean orientation of N29°W was in /4-1/ suggested for the maximum horizontal stress in the interval 207–1133 m borehole length, see Figure 4-6 and 4-7. Below approximately 1100 m, a reorientation of the maximum horizontal stress is indicated, and the orientation gradually changes from NW to a NE-direction at 1340 m. The start of the reorientation corresponds to the lower boundary of the major fracture zone, which further supports the previously stated suggestion that the stress field is disturbed within this zone.

Analysis of stress indicators in borehole KLX02 performed after the completion of Phase 2, /4-6/, suggested that the orientation of the maximum horizontal stress above and below the interval 700–1100 m vertical depth is NW-SE. However, within this interval an ENE-WSW orientation was proposed. These results are for the interval below 700 m contradictory to the results presented in /4-1/. Further research is necessary to provide more reliable data about the orientation of the maximum horizontal stress in connection with borehole KLX02.

Hydromechanical properties

Hydromechanical fracture properties such as aperture, roughness, stiffness and filling materials have a strong influence on the fluid flow and transport behaviour. Groundwater flow along fractures is also depending on the prevailing stress field through a sensitive aperture and flow rate relationship. A hydromechanical characterization was performed within Project Deep Drilling KLX02 – Phase 2 and the results are presented in /4-7/.

The field tests aiming at determination of hydromechanical parameters included:

- Measurements on existing fractures.
- Measurements on fractures induced by hydraulic fracturing.

The hydraulic aperture and the fracture normal stiffness were back-calculated by coupled numerical modelling of pressure injection tests. The results of the evaluation is presented as fracture transmissivity versus effective normal stress for fractures at different depths in borehole KLX02, see Figure 4-12. Two categories of fractures were identified. Some fractures displayed a low normal stiffness together with a relatively small residual aperture. The hydraulic conductivity of such fractures will decrease with increasing normal stress. The remaining fractures were relatively insensitive to normal stress. Fractures of the last category would, accordingly, even at high stresses and great depths be open and have a considerable hydraulic conductivity.

One important consequence of the results obtained is, that the hydraulic conductivity is more likely to depend on normal stress (and depth) in the upper few hundred metres of the bedrock. In this region both the mated joints and the more competent rock and fracture zones contribute to the overall hydraulic conductivity. However, at great depths, the mated joints will be closed, and the conductivity is dominated by relatively stress insensitive unmated fractures.

A relation between the fracture storativity and the effective normal stress was derived in a similar manner as for the transmissivity, see Figure 4-14. At a certain stress level the transmissivity varies widely compared to the storativity. This originates from the fact that the hydraulic aperture varies much more than the normal stiffness. The transmissivity is strongly affected by the current hydraulic aperture, which depends on the previous shear and other tectonic history as well as on the cementation and dissolution of fracture fillings. Therefore, it is not readily correlated with the present normal stress. Storativity, on the other hand, with its strong dependency on the current normal stiffness, is better correlated to the prevailing normal stress.

The results of the pulse tests performed during the hydromechanical study revealed a fracture aperture range on the induced fractures of 3–15 μm . The fractures propagated to a radius less than one metre and the fracture normal stiffness was ≤ 2000 GPa/m or less.

In /4-12/ a coupled hydromechanical modelling of a hydraulic fracturing reopening test is presented. The results of the modelling indicate that, after fracturing, the hydraulic fracture itself disturbs the stress field around the borehole, see Figure 4-15. The minimum tangential stress at the intersection of the borehole with the fracture is therefore smaller than predicted for a linear elastic, isotropic and homogeneous medium. During injection, fluid penetrates the fracture, which opens gradually as a function of the effective normal stress. At a sufficiently high flow rate, the reopening pressure and the maximum pressure become independent of the injection flow rate and equal to the minimum tangential stress at the borehole and fracture intersection, see Figure 4-16.

Borehole stability

When working with borehole investigations in KLX02, down-hole equipment got stuck at several occasions. Three borehole levels were afflicted with this problem: 339 m, 435–436 m and 1087 m. A special study was initiated to clarify the mechanisms behind the problem and especially to what extent the fracture frequency and fracture orientation had an influence. The study is reported in /4-16/.

The study focused on the fracture frequencies and orientations in the three above mentioned problematic parts of borehole KLX02, see BIPS-images in Figure 4-21. Fracture data from KLX02 was compared to corresponding data sets from approximately the same levels below the ground surface from the deep core drilled boreholes KAS02, KAS03 and KAS05 at Äspö. In these boreholes problems with equipment jamming have not occurred. Results from a black & white and a colour TV-logging (BIP-system) and from two caliper loggings in KLX02 were also analysed in the study.

The three locations in the borehole where jamming problems had occurred displayed increased fracture frequencies as well as increased frequencies of steeply oriented fractures compared to borehole sections next to the actual ones. The increases were, though, by no means extreme compared to the rest of the borehole. Comparison with the Äspö-boreholes demonstrated that all three of those have a fracture frequency exceeding that of KLX02 at the studied sections, see Figure 4-18.

Regarding fracture orientation, comparison with the three Äspö-boreholes revealed essentially higher frequencies of steep fractures in several borehole intervals in those boreholes than in borehole KLX02 (Figure 4-19).

The conclusion of the study was, that a high frequency of steep fractures in a borehole not necessarily implies that the borehole wall is unstable or that borehole equipment will get stuck more easily. However, an increased risk may prevail, which in specific situations is sufficient for borehole jamming and in other situations *in combination* with other factors may be fatal. However, several other factors have an influence on this problem, among them the rock stress situation in combination with the rock properties of the ambient rock.

Inspection of the borehole wall with a black & white TV-camera and with the BIP-system provided indications of borehole breakouts at two locations in the borehole, see Section 4.4.4. Breakouts reveal instable conditions. The process is however time dependent. After a period of stress reorientation, the borehole wall may stabilize and the outfall of rock particles cease.

Thermal properties

Temperature logging was performed in February 1988 in the 1078 m deep borehole KLX01 in the Laxemar area /5-2/ and in borehole KLX02 at two occasions, January and July 1993. The latter loggings are reported in /1-2/ respectively /3-4/.

The results, see Figure 5-1, demonstrated a temperature at repository level, i.e. at c. 500 m, of 13.8° C in KLX02 (July logging) respectively 15.2° C in KLX01. The temperature in KLX02 at 1400 m was 28.3° C (July logging) and at 1600 m 33.3° (January logging), see Figure 7-1.

A temperature gradient of 1.600° C/100 m was observed within the interval 200–500 m in KLX02 (July logging) and of 1.500° C/100 m in KLX01. At larger depths in KLX02, between 1000 m and 1400 m, the gradient appeared to be somewhat larger, 1.625° C/100 m (July logging).

Hydrogeology

The hydrogeological investigations performed during Phase 2 of Project Deep Drilling KLX02, /6-1/, may be regarded as a direct continuation of the test programme initiated during Phase 1 /3-20/. The investigations had a twofold sighting at both investigation phases. Firstly, by conducting a sequence of single-hole pumping tests in sections isolated either with a single packer or with a straddle-packer, the hydraulic transmissivity of the bedrock was determined in approximately 300 m long sections. Since the tests failed in some sections during Phase 1, the missing sections were re-tested during Phase 2, until reliable transmissivity results were obtained for the entire borehole.

Secondly, two interference tests between boreholes KLX02 and KLX01, situated at a distance of 1 km from each other, one test during Phase 1, the second during Phase 2, were aimed to reveal if hydraulic connections exist between the two deep boreholes and, if so, to study the geometrical and hydraulic character of these connections.

The duration of the single-hole tests in the 300 m long test sections (the uppermost section embraced only 0–205.5 m) was 12–48 h during Phase 2 (1–42 h during Phase 1), followed by an equally long period of pressure recovery (shorter recovery periods were applied during Phase 1). The discharge rate varied within the interval 1.6–37.8 l/min during the Phase 2 pumpings (1.5–132 l/min during Phase 1).

Transmissivity values were determined for all single-hole tested sections. The highest value obtained during the tests of both Phase 1 and Phase 2 was $T=1.5 \cdot 10^{-4} \text{ m}^2/\text{s}$, observed in section 207–505 m. Section 505–803 m displayed the lowest value, $2.8 \cdot 10^{-6} \text{ m}^2/\text{s}$, see Figures 6-1 and 6-7.

No detailed hydraulic tests, i.e. tests in short sections, were performed in borehole KLX02 and, hence, the frequency and position of individual high-conductive fractures or minor fracture zones, was unknown until a flow logging survey performed after Phase 2 was performed /7-15/. The flow logging is only briefly attended to in this report, see Section 7.7.

The Phase 1 interference tests used the entire uncased part of borehole KLX02 as the pumped section. The pumping lasted for 1986 hours and the flow rate was 180 l/min. The groundwater level in five sections in borehole KLX01 was monitored during both the pumping and recovery phases.

The pumped interval during the Phase 2 interference test was section 805–1103 m in borehole KLX02. A constant flow rate of 9 l/min was maintained during 864 hours. The groundwater level in the same five sections in borehole KLX01 as during Phase 1 were monitored during pumping and recovery.

Hydraulic responses were observed during both interference tests in the three deepest sections in borehole KLX01: 272–694 m, 695–855 m and 856–1078 m, whereas sections 0–140 m and 141–272 m were unaffected. Based on a special interpretation model, transmissivity values could be estimated from the interference test of Phase 1 for the formation between boreholes KLX02 and KLX01. They refer to, and are specified for each observation section in borehole KLX01. They vary between $T=6.2 \cdot 10^{-5} \text{ m}^2/\text{s}$ (in sections 0–140 m, 141–272 m respectively 272–694 m) and $4.0 \cdot 10^{-6} \text{ m}^2/\text{s}$ (in section 856–1078 m), see Figure 6-2.

The largest response during the Phase 2 interference test was observed in section 695–855 m, where the change of water level (corrected for barometric changes) since the start of pumping was 2.5 m, cf. Figure 6-10. The transmissivities of the observation intervals in KLX01 could not be evaluated from the interference test during Phase 2, since the actual flow rate distribution in the rock is basically unknown. However, by application of the transmissivity values of the monitored sections in KLX01 determined earlier by independent methods (single-hole tests), it was possible to estimate the flow rate for each affected interval in KLX01, provided that the sum of those flow rates should match the actual discharge rate at KLX02, $1.5 \cdot 10^{-4} \text{ m}^2/\text{s}$. From the results of the calculation, it was postulated that the flow rate distribution is heterogeneous in the vertical direction of the rock between KLX02 (source) and KLX01 (observation). 48 % of the total discharge was calculated to occur in section 695–855 m, 41 % in section 272–694 m and 11 % in section 856–1078 m.

The hydraulic responses observed during the interference test pumping of Phase 2 were tried against the geological-structural interpretations presented in Chapter 3. One of the structural models infers indirect hydraulic responses between the two deep boreholes in the Laxemar area transferred by a fracture zone network.

Another model permits more space for direct responses between KLX02 and KLX01 conducted by two regional fracture zones, SFZ04 and SFZ07, cf. Figures 3-19, 3-20 and 3-21.

Finally, the reflection seismic investigations, performed in the Laxemar area during 1999, indicate the existence of a major subhorizontal fracture zone encountered at approximately 650–900 m in KLX02, intersecting borehole KLX01 at approximately 800–1000 m, see Figures 3-25 and 6-4. This structure may explain the observed response pattern in KLX01 to the pumping in KLX02 fairly well.

Hydrogeochemistry

Groundwater chemistry

Groundwater sampling was performed in KLX02 on four occasions using different methods /7-1/, /7-2/ and /7-3/:

1. The first sampling was conducted on August 3rd 1993 within the interval 9–1681 m of the open borehole, using a so called Tube sampler /7-1/. This equipment is based on 50 m long sections of polyamide tubes (10 mm outer diameter) with a manually operated valve and a connector coupling attached to both ends of each tube. The lower end of the sampler involves a check valve. Several 50 m tubes are connected, until the desired measuring length is achieved. During lowering of the sampler within the borehole, the manually operated valves are kept open. After the tube strings have been filled with borehole fluid, the individual 50 m sampling intervals are isolated by closing the valves and subsequently up-lifted from the borehole. The borehole fluid contained in each 50 m tube string (1 litre) is finally poured into flasks for analysis.
2. The second sampling campaign was carried out during the period November 1st 1993 to January 5th 1994, /7-1/, using the SKB Mobile Field Laboratory, thoroughly described in /7-7/, later updated to some extent /7-8/. Prior to the sampling in KLX02, the down-hole equipment was modified to enable sampling at greater depths. In this report activities performed with the mobile laboratory are referred to as the “SKB packer sampler”.
3. The third sampling was performed in 1995 in connection with the Phase 2 hydraulic tests in borehole KLX02, cf. Chapter 6. During pumping in KLX02 in different isolated borehole sections, part of the discharged groundwater was by-passed to a sampler specially constructed for collection and concentration of noble gases in groundwater /7-9/.
4. For the fourth sampling effort, the Tube sampler was once again engaged /7-2/. One of the main purposes with this sampling was to study possible time dependent changes in the groundwater composition and their causes. The field work was conducted on September 25th 1997. The sampler was lowered into the borehole to a depth of 1450 m.

Besides the groundwater sampling campaigns, samples of calcite fillings were taken from the drill core of KLX02 for isotope analysis. 12 samples were collected within the borehole interval 960–1640 m.

The general chemistry of the groundwater in the bedrock horizon 0–1050 m implies a shallow to intermediate *Sodium-Bicarbonate* type of water. There are indications of influx of shallow groundwater in the upper part of the borehole, and the water is partly under-saturated with respect to calcite, which is reflected in the low HCO₃⁻ and relatively high bacterial content.

The Sodium-Bicarbonate water displays a successive evolution due to bacterial activity, calcite dissolution and mixing within the interval 0–400 m. The waters sampled at a depth of 400–1050 m are characterized by a meteoric signature with a homogenous composition both chemically, isotopically (stable isotopes and ¹⁴C), and bacteriologically. This implies that the water enters the borehole through a fracture zone of high hydraulic conductivity and is then transported along the borehole.

At about 400 m depth, the groundwater indicates a marine signature, which vanishes at larger depths. This water has been interpreted as being leached from old marine sediments, alternatively constituting some remnants of fossil seawater.

The non-saline/saline interface is situated at 1050–1450 m and is characterized by a change to a *Calcium-Chloride* type of brine water. The portion of such water at a depth of 1050–1450 m was larger in 1997 than during 1993. Less glacial water was obtained, and in the 1997 sampling there were no traces at all of such water. The chloride component in brine water has been dated using isotope ³⁶Cl to be around 1.5 m.y. (million years), indicating very long residence times.

The two samplings with the Tube sampler show relatively large differences between 1993 and 1997. Since the first sampling, the three-component mixture consisting of meteoric, glacial and brine water has been replaced by a two component mixture of meteoric and brine water, and the saline interface is situated c. 100 m deeper in the borehole 1997 than 1993. The main reason for this has been evaluated to be due to the open-hole effect, which constitutes a high-conductive short-cut between fractures at different levels, bringing about mixing of water along the borehole, thereby creating new water compositions, cf. Section 7.7 and /7-2/.

$\delta^{18}\text{O}$ -analyses from calcite fracture fillings indicate that the major part of the calcite was not formed from the present-day groundwater, although some of the higher $\delta^{18}\text{O}$ -values could reflect equilibrium with groundwater under current *in-situ* temperature. Similarly, the low $\delta^{18}\text{O}$ -values may have formed from groundwater, however at temperatures 30–40 °C higher than the present ambient temperature /7-5/.

The analyses of noble gases may indicate water-rock interaction at great depth. This supports the above mentioned indications of long residence times for the groundwater and significant water/rock interaction processes going on at large depths /7-9/ and /7-17/.

Flow regime in borehole KLX02

The chemical signature of the groundwater is the result of a very long process, where groundwater mixing and interaction with the bedrock occurs during the period of groundwater transport. Every groundwater sample therefore comprises information, which may help delineate the hydrogeochemical character and evolution of groundwater aquifers of local or even regional extension.

A borehole penetrating the bedrock from the ground surface to a certain depth, connects fractures at different levels, thereby constituting a short-cut for groundwater flow. Since the composition of the groundwater usually is different at different levels in the bedrock, a short-cutting borehole with a high flow-capacity may speed up natural mixing and evolutionary processes substantially. Depending on the direction of the pressure gradient, the groundwater flow may be directed down- or upwards along the borehole. For the study of the groundwater situation in an area, borehole effects of this kind have to be known for a correct interpretation of *in situ*-conditions.

Ever since completion of the drilling of borehole KLX02, some uncertainty about the direction of the groundwater flow at different levels in the borehole during open-hole conditions has existed. An investigation to settle this problem was therefore initiated. Results from different kinds of previously performed borehole investigations were analysed and compared with data from the second deep borehole, KLX01, in the Laxemar area. The main part of the data inquired supports the following statements about the flow regime in borehole KLX02:

1. The upper part of the borehole, about 0–800 m, is more dynamic, i.e. the groundwater turnover time is shorter than in the bottom part of the borehole, section 800–1700 m.
2. Groundwater emerging from the shallow part of the bedrock recharges into the borehole above 200 m borehole length. This groundwater continues downward in the borehole. Portions of this open-hole transport discharge into fractures in the borehole interval 200–800 m, except in a few sections, where flow recharges.
3. At about 800 m, the downward moving groundwater encounters a minor, upwardly flowing groundwater stream from the deeper parts of the borehole, i.e. from the interval 800–1700 m. The groundwater of shallow as well as of deep origin discharges into the highly fractured interval at 730–1120 m.

The conclusion is, that shallow groundwater is conducted via borehole KLX02 to larger depths, where mixing with deep groundwater occurs. With time, this process will affect increasingly large groundwater volumes around the borehole, whereby *in situ*-conditions will be concealed. This fact stresses 1) the need of early groundwater sampling, performed during drilling or shortly thereafter, and 2) if *in situ*-conditions are to be preserved, installation of a straddle packer system in the borehole as soon as borehole investigation campaigns are concluded, in order to isolate fracture systems at different levels from each other.

Acknowledgements

The investigations included in Project Deep Drilling KLX02 – Phase 2, were carried out by a large number of skilful geoscientists. To study the author names of the listed reports in “References” is the best way to recognize these people.

A group of persons were involved in the compilation of this report. I have very much appreciated the co-operation with Jan-Erik Ludvigson, GEOSIGMA, and Marcus Laaksoharju, GeoPoint (previously INTERA), who both made considerable contributions as co-authors of the report. Jan-Erik Ludvigson was head author of Chapter 6 and Marcus Laaksoharju co-author of Chapter 7.

Much work was devoted to the design of new and revision of previously existing illustrations used in the report. I am very grateful to:

Margareta Smellie, Per Askling, Allan Strähle and Seje Carlsten, all
GEOSIGMA, Uppsala,
Ingemar Markström, SYCON, Malmö,
Mikael Erlström, SGU, Lund,
Carl-Henrik Wahlgren, SGU, Uppsala.

Several colleagues contributed to the final result by reviewing the report. Special acknowledgements are directed to:

Lars O Ericson, CTH, Gothenburg (previously SKB, Stockholm),
Peter Wikberg and Bengt Leijon, SKB, Stockholm, Karl-Erik Almén and
Leif Stenberg, SKB, Äspölaboratoriet, Oskarshamn,
Roy Stanfors, Roy Stanfors Consulting, Lund,
Eva-Lena Tullborg, Terralogica, Gråbo,
Carl-Henric Wahlgren, SGU, Uppsala,
Christer Ljunggren, SwedPower, Luleå,
Daniel Ask, KTH, Stockholm,
Sven Follin, SF geologic, Solna (previously Golder Grundteknik, Solna),
Marcus Laaksoharju, GeoPoint, Sollentuna,
Bill Wallin, Geokema, Stockholm.

Finally, I like to extend special thanks to the Project Managers of Project Deep Drilling KLX02 – Phase 2, Lars O Ericson, CTH, Gothenburg (previously SKB, Stockholm), later succeeded by Peter Wikberg, SKB, Stockholm, for their enthusiastic support throughout the entire project, including compilation of this report.

Uppsala April 2001

Lennart Ekman

References

Chapter 1

/1-1/ Andersson J, Almén K-E, Ericsson L O, Fredriksson A, Karlsson F, Stanfors, R, Ström A, 1998.

Parameters of importance to determine during geoscientific site investigation. TR 98-02, Swedish Nuclear Fuel and Waste Management Co, 1998.

/1-2/ Andersson O, 1994.

Deep drilling KLX02. Drilling and documentation of a 1700 m deep borehole at Laxemar, Sweden.

TR 94-19, Swedish Nuclear Fuel and Waste Management Co, 1994.

Chapter 3

/3-1/ Rhén O, Bäckblom G, Gustafson G, Stanfors R, Wikberg P, 1997.

ÄSPÖ HRL – Geoscientific evaluation 1997/2. Results from pre-investigations and detailed site characterization. Summary report.

TR 97-03, Swedish Nuclear Fuel and Waste Management Co, 1997.

/3-2/ SKB, 2001.

Förstudie Oskarshamn. Slutrapport.

Swedish Nuclear Fuel and Waste Management Co, 2001.

/3-3/ Kornfält K-A, Wikman H, 1987.

Description of the maps of solid rocks around Simpevarp.

PR 25-87-02, Swedish Nuclear Fuel and Waste Management Co, 1987.

/3-4/ Stanfors R, 1995.

Drilling KLX02 – Phase 2. Brief geological description of the cored borehole KLX02.

AR 95-37, Swedish Nuclear Fuel and Waste Management Co, 1995.

/3-5/ Kornfält K-A, Wikman H, 1994.

Drilling KLX02 – Phase 2. Lilla Laxemar, Oskarshamn. Petrological classification of core samples and drill cuttings.

AR 94-50, Swedish Nuclear Fuel and Waste Management Co, 1994.

/3-6/ Kornfält K-A, Wikman H, 1988.

The rocks of the Äspö island. Description to the detailed maps of solid rocks including maps of 3 uncovered trenches.

PR 25-88-12, Swedish Nuclear Fuel and Waste Management Co, 1988.

/3-7/ IUGS subcommission on the systematics of igneous rocks, 1973.

Classification and Nomenclature of Plutonic Rocks. Recommendations.

N. Jb. Miner. Mh. H4, 149-164, 1973.

/3-8/ Almén K-E, Zellman O, 1991.

Field instrumentation methodology and instruments used in the pre-investigation phase, 1986-1990.

TR 91-21, Swedish Nuclear Fuel and Waste Management Co, 1991.

/3-9/ Nisca D, 1987.

Aerogeophysical interpretation.

PR 25-87-04, Swedish Nuclear Fuel and Waste Management Co, 1987.

/3-10/ Cederbom Ch, 1997.

Fission track thermochronology applied to Phanerozoic thermotectonic events in central and southern Sweden.

Licentiate thesis, Earth Science Center, Göteborg University, A 25 ISSN 1400-3813, 1997.

/3-11/ Tullborg E-L, Larson S Å, Stiberg J-P, 1996.

Subsidence and uplift of the present land surface in the southeastern part of the Fennoscandian Shield.

GFF 118, 126-128, 1996.

/3-12/ Larson, S.Å., Tullborg, E-L., Cederbom Ch., Stiberg, J-P, 1999.

Sveconorwegian and Caledonian foreland basins in the Baltic Shield revealed by fission-track thermochronology.

Terra Nova, 11, 210-215, 1999.

/3-13/ Lutz T M, Omar G, 1991.

An inverse method of modelling thermal histories from apatite fission track data.

Earth and Planetary Science Letters 104, 181-195, 1991.

/3-14/ Tullborg E-L, Larson S Å, Björklund L, Samuelsson L, Stigh J, 1995.

Thermal evidence of Caledonide foreland, molasse sedimentation in Fennoscandia.

TR 95-18, Swedish Nuclear Fuel and Waste Management Co, 1995.

/3-15/ Gustafsson C, 1995.

Djupborrning KLX02 – Etapp 2. Lilla Laxemar, Oskarshamn kommun. Loggning caliper och TV-kamera 1995-09-21 och 1995-09-28.

AR 95-38, Swedish Nuclear Fuel and Waste Management Co, 1995.

/3-16/ Stråhle A, 1996.

Borehole-TV measurements at the Kivetty site, Finland 1996. Report and appendices for K1-KR1 and K1-KR5.

POSIVA Work report PATU-96-57e, 1996.

/3-17/ Carlsten S, 1993.

Drilling KLX02 – Phase 2. Lilla Laxemar, Oskarshamn. Borehole radar measurements in KLX02.

AR 93-43, Swedish Nuclear Fuel and Waste Management Co, 1993.

/3-18/ Munier R, 1993.

Drilling KLX02 – Phase 2. Lilla Laxemar, Oskarshamn. Description of geological structures in and near boreholes KLX02 and KLX01, Laxemar.
AR 94-23, Swedish Nuclear Fuel and Waste Management Co, 1993.

/3-19/ Carlsten S, 1993.

Drilling KLX02 – Phase 2. Lilla Laxemar, Oskarshamn. Correlation of radar reflectors between boreholes KLX01 and KLX02.
AR 94-28, Swedish Nuclear Fuel and Waste Management Co, 1993.

/3-20/ Follin S, 1993.

Djupborrning KLX02 – Etapp 1. Lilla Laxemar, Oskarshamn. Evaluation of the hydraulic testing of KLX02.
AR 94-21, Swedish Nuclear Fuel and Waste Management Co, 1993.

/3-21/ Nyberg G, Jönsson S, Ekman L, 1993.

Äspö Hard Rock Laboratory. Hydromonitoring Program. Report for 1992.
PR 25-93-09, Swedish Nuclear Fuel and Waste Management Co, 1993.

/3-22/ Tirén S, Beckholmen M, 1987.

Structural analysis of contoured maps Kärsvik-Bussvik, Lilla Laxemar and Glostad areas, Simpevarp area, South-Eastern Sweden.
PR 25-87-27, Swedish Nuclear Fuel and Waste Management Co, 1987a.

/3-23/ Tirén S, Beckholmen M, 1987.

Structural analysis of contoured maps Äspö and Ävrö, Simpevarp area, South-Eastern Sweden.
PR 25-87-22, Swedish Nuclear Fuel and Waste Management Co, 1987b.

/3-24/ Tirén S, Beckholmen M, Isaksson H, 1987.

Structural analysis of digital terrain models, Simpevarp area, South-Eastern Sweden. Method study EBBA II.
PR 25-87-21, Swedish Nuclear Fuel and Waste Management Co, 1987c.

/3-25/ Niva B, Gabriel G, 1988.

Borehole radar measurements at Äspö and Laxemar – Boreholes KAS02, KAS03, KAS04, KLX01, HAS02, HAS03 and HAV07.
PR 25-88-03, Swedish Nuclear Fuel and Waste Management Co, 1988.

/3-26/ Carlsten S, 1993.

Borehole radar measurements at the Palmutto natural analogue study site, Finland.
AR 93-39, Swedish Nuclear Fuel and Waste Management Co, 1993.

/3-27/ Stenberg L, 1987.

URL. Geophysical profile measurements.
PR 25-87-01, Swedish Nuclear Fuel and Waste Management Co, 1987.

/3-28/ Stanfors R, Erlström M, 1995.

SKB Paleohydrogeological program. Extended geological modelling of the Äspö area.

AR 95-20, Swedish Nuclear Fuel and Waste Management Co, 1995.

/3-29/ Stenberg L, 1987.

Underground Research Laboratory. Geophysical profile measurements.

PR 25-87-02, Swedish Nuclear Fuel and Waste Management Co, 1987.

/3-30/ Stenberg L, Sehlstedt S, 1989.

Geophysical profile measurements on interpreted regional aeromagnetic lineaments in the Simpevarp area.

PR 25-89-13, Swedish Nuclear Fuel and Waste Management Co, 1989.

/3-31/ Eriksson L, Johansson R, Thunehed H, Triumf K-A, 1988.

Metodtester ytgeofysik 1996. Bestämning av berggrundens bulkresistivitet och djupet till salint grundvatten med halvregional resistivitetsmätning, elektrisk sondering samt transient elektromagnetisk sondering.

PR D-98-01, Swedish Nuclear Fuel and Waste Management Co, 1998.

/3-32/ Stanfors R, Olsson P, Stille H, 1997.

Äspö HRL – Geoscientific evaluation 1997/3. Results from pre-investigations and detailed site characterization. Comparison of predictions and observations. Geology and mechanical stability.

TR 97-04, Swedish Nuclear Fuel and Waste Management Co, 1997.

/3-33/ Bergman B, Juhlin C, Palm H, 2001.

Reflektionseismiska studier inom Laxemarområdet.

R-01-07, Swedish Nuclear Fuel and Waste Management Co, 2001.

/3-34/ Juhlin C, Palm H, 1997.

3-D structure below Ävrö Island from high-resolution reflection seismic studies, southeastern Sweden.

Geophysics, 64, 662-667, 1997.

Chapter 4

/4-1/ Ljunggren C, Klasson H, 1997.

Drilling KLX02 – Phase 2. Lilla Laxemar, Oskarshamn. Deep hydraulic fracturing rock stress measurements in borehole KLX02, Laxemar.

PR U-97-27. Swedish Nuclear Fuel and Waste Management Co, 1997.

/4-2/ Bjarnasson B, 1986.

Hydrofracturing Rock Stress Measurements in the Baltic Shield.

Licentiate thesis 1986:12L, Luleå University of Technology.

/4-3/ Ljunggren C, 1990.

Measurement Techniques and a Comparison to the HTPF Method.
Doctoral Thesis 1990:82D, Luleå University of Technology.

/4-4/ Bjarnasson B, Torikka A, 1989.

Field instrumentation for hydrofracturing stress measurements. Documentation of the 1000 m hydrofracturing unit at Luleå University of Technology.
TR 89-17. Swedish Nuclear Fuel and Waste Management Co, 1989.

/4-5/ Almén K-E, Zellman O, 1991.

Äspö Hard Rock Laboratory. Field investigation methodology and instruments used in the preinvestigation phase, 1986-1990.
TR 91-21. Swedish Nuclear Fuel and Waste Management Co, 1991.

/4-6/ Ask D, Stephansson O, Cornet F-H, 2001.

Integrated stress analysis of hydraulic stress data in the Äspö region. Analysis of hydraulic fracturing stress measurements and hydraulic tests on pre-existing fractures (HTPF) in boreholes KAS02, KAS03 and KLX02.
SKB-report in print. Swedish Nuclear Fuel and Waste Management Co, 2001.

/4-7/ Rutqvist J, Ekman D, Stephansson O, 1997.

High pressure hydraulic injection in deep boreholes for hydromechanical characterization of hard rocks. Field and modelling studies of coupled hydromechanical properties of fractures in borehole KLX02 at Laxemar, Sweden. (References /4-9/, /4-10/, /4-11/, /4-12/, /4-13/ and /4-14/ are included in this report.)
PR U-97-26. Swedish Nuclear Fuel and Waste Management Co, 1997.

/4-8/ Rutqvist J, 1995.

Coupled stress-flow properties of rock joints from hydraulic field testing.
Doctoral thesis. Royal Institute of Technology, 1995.

/4-9/ Ekman D, 1997.

Rock stress, hydraulic conductivity and stiffness of fracture zones in the Laxemar borehole, Småland, Sweden.
Master of Science Thesis. Royal Institute of Technology, 1997. (Included in /4-7/.)

/4-10/ Rutqvist J, Tsang C-F, Ekman D, Stephansson O, 1997.

Evaluation of in situ hydromechanical properties of rock fractures at Laxemar in Sweden.
Proceedings of the 1st Asian Rock Mechanics Symposium: ARMS'97, Seoul, Korea. A.A. Balkema publisher, pp. 619-624, 1997. (Included in /4-7/.)

/4-11/ Rutqvist J, Noorishad J, Tsang C-F, Stephansson O, 1997.

Determination of fracture storativity in hard rocks using high pressure testing.
Water Resour. Res., 34(10), pp. 2551-2560, 1998. (Included in /4-7/.)

/4-12/ Rutqvist J, Stephansson O, Tsang C-F, 1997.

Hydraulic field measurements of incompletely closed fractures in granite.
Int. J. Rock Mech. Min. Sci. & Geomech. Abstr. 34, p. 411, paper no. 267, 1997.
(Included in /4-7/.)

/4-13/ Rutqvist J, Stephansson O, 1997.

Influence of fracture aperture and normal stiffness on the reopening pressure in classical fracturing stress measurements.
Proceeding of the International Symposium on Rock Stress, Kumamoto, Japan.
A.A. Balkema publisher pp. 127-132, 1997. (Included in /4-7/.)

/4-14/ Ekman D, Rutqvist J, Stephansson O, Nilsson T, 1997.

Laboratory compliance tests of the Vattenfall Hydropower Co Multihose field unit.
(Included in /4-7/.)

/4-15/ Noorishad J, Tsang C-F, Witherspoon P A, 1992.

Theoretical and field studies of coupled hydromechanical behaviour of fractured rocks-1. Development and verification of a numerical simulator.
Int. J. Rock Mech. Min. Sci. & Geomech. Abstr., 29, pp. 401-409, 1992.

/4-16/ Askling P, 1995.

Djupborrning KLX02 – Etapp 2. Lilla Laxemar, Oskarshamns kommun.
Undersökning av sprickriktningar i valda avsnitt samt jämförelse med sprickdata från kärnborrhål på Äspö.
AR 95-44. Swedish Nuclear Fuel and Waste Management Co, 1995.

Chapter 5

/5-1/ Thunvik R, Braester C, 1980.

Hydrothermal conditions around a radio-active waste repository.
TR 80-19. Swedish Nuclear Fuel and Waste Management Co, 1980.

/5-2/ Sehlstedt S, Triumf C-A, 1988.

Interpretation of geophysical logging data from KAS02-KAS04 and HAS08-HAS12 at Äspö and KLX01 at Laxemar.
PR 25-88-15. Swedish Nuclear Fuel and Waste Management Co, 1988.

Chapter 6

/6-1/ Follin S, 1996.

Djupborrning KLX02 – Etapp 2. Lilla Laxemar, Oskars-hamns kommun.
Interpretation of the hydraulic testing of KLX02.
PR U-96-32. Swedish Nuclear Fuel and Waste Management Co, 1996.

/6-2/ Nyberg G, Jönsson S, Ekman L, 1996.

Äspö Hard Rock Laboratory. Hydro Monitoring System. Report for 1995.
PR HRL-96-17. Swedish Nuclear Fuel and Waste Management Co, 1996.

/6-3/ Bear J, 1972.

Dynamics of fluids in porous media, pp. 212.
Dover publications, Inc., New York, 1972.

Chapter 7

/7-1/ Laaksoharju M, Smellie J, Nilsson A-C, Skårman C, 1995.

Groundwater sampling and chemical characterization of the Laxemar deep borehole KLX02.

TR 95-05. Swedish Nuclear Fuel and Waste Management Co, 1995.

/7-2/ Laaksoharju M, Andersson C, Tullborg E-L, Wallin B, Ekwall K, Pedersen K, Nilsson A-C, 1999.

Re-sampling of the KLX02 deep borehole at Laxemar.

R-99-09. Swedish Nuclear Fuel and Waste Management Co, 1999.

/7-3/ Laaksoharju M, Wallin B (eds.), 1997.

Evolution of the groundwater chemistry at the Äspö Hard Rock Laboratory.

Proceedings of the second Äspö International Geochemistry Workshop, June 6-7, 1995.

ICR-97-04. Swedish Nuclear Fuel and Waste Management Co, 1997.

/7-4/ Wallin B, Peterman Z, 1997a.

Isotopic systematics of saline waters at Äspö and Laxemar, Sweden.

Paper # 11 in Appendix 1 in SKB ICR-97-04. (Included in /7-3/.)

/7-5/ Wallin B, Peterman Z, 1997b.

Calcite fracture fillings as indicators of paleohydrology at the Äspö Hard Rock Laboratory, Sweden.

Paper # 12 in Appendix 1 in SKB ICR 97-04. (Included in /7-3/.)

/7-6/ Wallin B, 1995.

Paleohydrological implications in the Baltic area and its relation to the groundwater at Äspö, south-eastern Sweden – A literature study.

TR 95-06. Swedish Nuclear Fuel and Waste Management Co, 1995.

/7-7/ Wikberg P, 1987.

The chemistry of deep groundwaters in crystalline rocks. Doctoral thesis of Inorganic Chemistry. Royal Institute of Technology, 1987.

/7-8/ SKB MD 430-434.

SKB manuals and method descriptions.

/7-9/ Kropf S, 1996.

Bestimmung der Altersverteilung Junger Grundwässer mit Hilfe des Edelgasisotopes ⁸⁵Kr und Tritium.

Diplomarbeit der Philosophisch Naturwissenschaftlichen Fakultät der Universität Bern. 1996.

/7-10/ Tullborg E-L, Larsson S-Å, 1984.

$\delta^{18}\text{O}$, tritium and $\delta^{13}\text{C}$ for limestones, calcite fissure infillings and calcite precipitates from Sweden.

Geologiska Föreningens i Stockholm Förhandlingar, Vol. 106, Pt. 2. Stockholm, Sweden.

/7-11/ Kankainen T, 1986.

Loviisa power station final disposal of reactor waste. On the age and origin of groundwater from the rapakivi granite on the island of Hästholmen.

Nuclear Waste Commission of Finnish power Companies. Report YJT-86-29.

/7-12/ Sjöberg L, Georgala D, Rickard D, 1984.

Origin of interstitial water compositions in post-glacial black clays (Northeastern Sweden).

Chemical Geology 42 (1984) 147-158.

/7-13/ Landström O, Aggeryd I, Marthiasson L, Sundblad B, 1994.

Chemical composition of sediments from the Äspö area and interaction between the biosphere and geosphere.

AR 94-03. Swedish Nuclear Fuel and Waste Management Co, 1988.

/7-14/ Walin B, Peterman Z, 1998.

Calcite Fracture Fillings as Indicators of Paleohydrology at Laxemar at the Äspö Hard Rock Laboratory, southern Sweden. Paper in Applied Geochemistry in prep.

/7-15/ Rouhiainen P, 2000. Difference flow measurements in borehole KLX02 at Laxemar.

IPR 01-06. Swedish Nuclear Fuel and Waste Management Co, 2000.

/7-16/ Laaksoharju M, 2001.

Compilation of KLX02 weekly reports and analytical results from the SKB/POSIVA joint PAVE groundwater sampling campaign of the deep KLX02 borehole at Laxemar.

TD in print. Swedish Nuclear Fuel and Waste Management Co, 2001.

/7-17/ Smellie J, Laaksoharju M, Ludin A 1995.

Isotopic and geochemical evolution of deep groundwaters from the Laxemar borehole (0–1700 m), SE Sweden. IAEA-Meeting, March 20-24, 1995. Symposium on isotopes in water resources management.

Geometrical and administrative data for the investigation boreholes at Laxemar

Table A1-1. Inclination, declination, diameter, length, length of casing and date of drilling completed for the Laxemar boreholes.

Borehole name	Inclination at ground (°)	Declination at ground (°)	Diameter (mm)	Length from to (m)	Length of casing (m)	Drilling completed
KLX01	85.3	346.0	155	0.00–101.30	101	880205 900804
			76	101.30–702.11		
			56	702.11–1077.99		
KLX02	85.0	357.0	304	0.00–3.00	2.60	921129
			215	3.00–200.80	200.80	
			165	200.80–201.00	0.20	
			92	201.0–202.95	1.95	
			76	202.95–1700.50		
HLX01	59.4	175.0	115	0.00–100.00	3.00	871021
HLX02	57.4	327.0	115	0.00–100.00	0.60	871027
				100.00–132.00		871110
HLX03	62.4	185.0	115	0.00–100.00	1.40	871104
HLX04	63.6	301.0	115	0.00–125.00	1.20	871106
HLX05	57.7	175.0	115	0.00–100.00	0.60	871105
HLX06	59.9	178.0	115	0.00–100.00	1.00	871030
HLX07	59.4	47.0	115	0.00–100.00	1.00	871103
HLX08	47.8	133	115	0.00–40	6.0	911114
HLX09	61.3	176	115	0.00–151	3.0	911121
HLX10	70		136.8	0.00–85	3.0	920930
HLX11	85		138.8	0.00–70	6.0	921001
HLX12	70		136.0	0.00–31	3.0	9210

Table A1-2. X-, Y- and Z-co-ordinates, and hydraulic capacity for the Laxemar boreholes.

Borehole name	X-co-ordinate	Y-co-ordinate	Z-co-ordinate	Capacity (l/h)	Comment
KLX01	6367485.386	1549923.198	16.81		
KLX02	6366768.597	1549224.233	18.31		
HLX01	6367353.825	1549569.853	8.93	4000	6000 l/h during pumping
HLX02	6368093.678	1549941.679	9.04	60	
HLX03	6367819.667	1549921.412	10.43	300	
HLX04	6367679.258	1549795.144	10.40	~0.5	
HLX05	6367557.447	1549968.570	15.55	~40	
HLX06	6367165.825	1549784.654	15.48	200	
HLX07	6367152.032	1550014.267	8.61	2100	
HLX08	6366588.008	1550587.233	2.27	7200	
HLX09	6367229.994	1550807.740	3.43	9000	
HLX010	6366635.49	1549140.33	11.78	10000–15000	
HLX011	6366595.43	1549092.11	13.24	100–200	
HLX012	6366590.21	1549091.35	12.69	3000–5000	

Appendix 2

Chemical analyses of thin section samples from the drill core of KLX02

Table A2-1. Chemical analyses of seven thin section samples from borehole KLX02. Major constituents.

Chemical constituents	Sample number						
	3	8	13	14	17	19	25
	weight %						
SiO ₂	47.0	69.0	50.0	51.0	47.3	71.7	57.5
TiO ₂	0.662	0.463	1.42	1.32	1.07	0.284	0.881
Al ₂ O ₃	9.49	14.5	16.1	17.5	17.1	13.4	18.9
Fe ₂ O ₃	10.8	3.53	11.3	10.4	11.1	2.36	5.92
MnO	0.178	0.066	0.179	0.168	0.174	0.037	0.105
MgO	18.5	1.23	6.17	4.43	6.52	0.50	2.24
CaO	7.42	2.40	8.23	7.97	11.2	1.29	5.81
Na ₂ O	0.446	3.34	2.95	3.18	2.80	3.27	5.17
K ₂ O	2.38	4.72	1.72	2.22	1.03	5.65	2.18
P ₂ O ₅	0.194	0.189	0.434	0.554	0.416	0.099	0.415
LOI	3.1	0.7	1.4	1.1	1.0	0.7	1.1
Total	97.1	98.5	98.5	98.7	98.7	98.6	99.1

Table A2-2. Chemical analyses of seven thin section samples from borehole KLX02. Minor constituents.

Chemical constituents	Sample number						
	3	8	13	14	17	19	25
	ppm						
Rb	181	106	47.3	70.4	15.6	168	57.9
Sr	56.2	567	598	937	632	383	1410
Ba	231	979	593	932	399	918	1430
Y	13.1	11.8	20.4	20.4	19.2	13.2	19.2
Zr	78.5	161	153	130	120	216	196
Nb	6.23	10.2	9.05	8.43	7.27	8.88	12.6
U	0.98	5.0	0.68	0.609	0.476	6.58	5.25
Th	3.72	23.0	2.22	1.89	1.35	47.0	10.2
La	17.3	61	25.7	37.9	27.4	100	57.9
Ce	38.5	112	60.8	88.3	64.9	212	129
Nd	20.9	37.4	33.6	45.0	32.2	72.6	57.6
Sm	4.05	5.14	6.27	7.59	5.84	9.14	9.12
Eu	0.89	0.20	1.38	0.85	1.48	0.31	0.21
Gd	3.15	6.97	9.78	10.3	8.38	11.6	11.2
Tb	0.41	0.70	1.07	1.16	0.97	1.10	1.16
Dy	3.19	2.73	4.53	4.63	4.23	3.40	4.49
Ho	0.63	0.53	0.89	0.90	0.82	0.67	0.86
Er	1.67	1.55	2.47	2.38	2.30	1.80	2.39
Yb	1.50	2.22	2.74	3.03	2.81	2.23	3.30
Lu	0.23	0.32	0.39	0.40	0.37	0.31	0.42

Composite log with geological and geophysical data from borehole KLX02

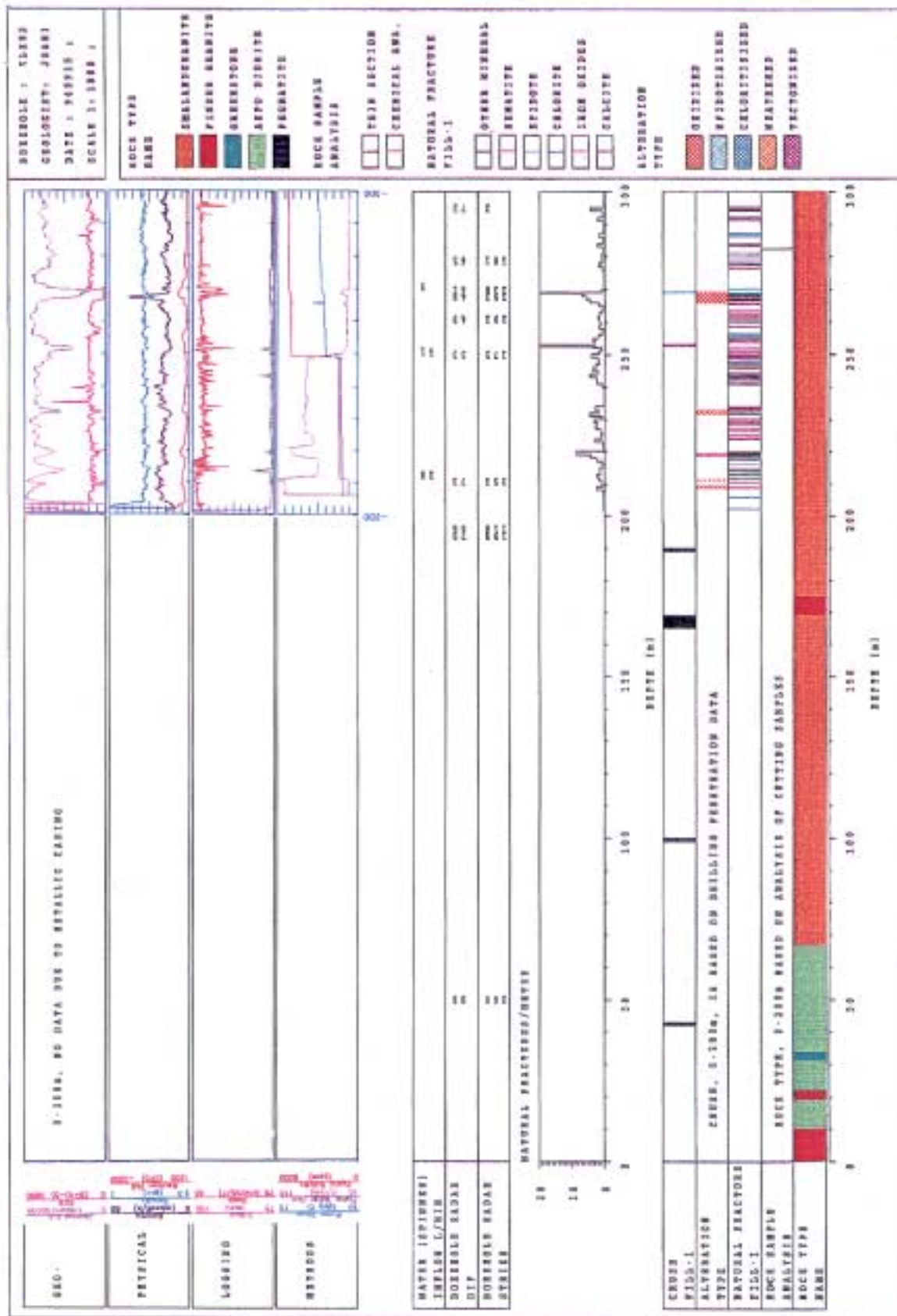


Figure A3-1. Section 0–300 m.

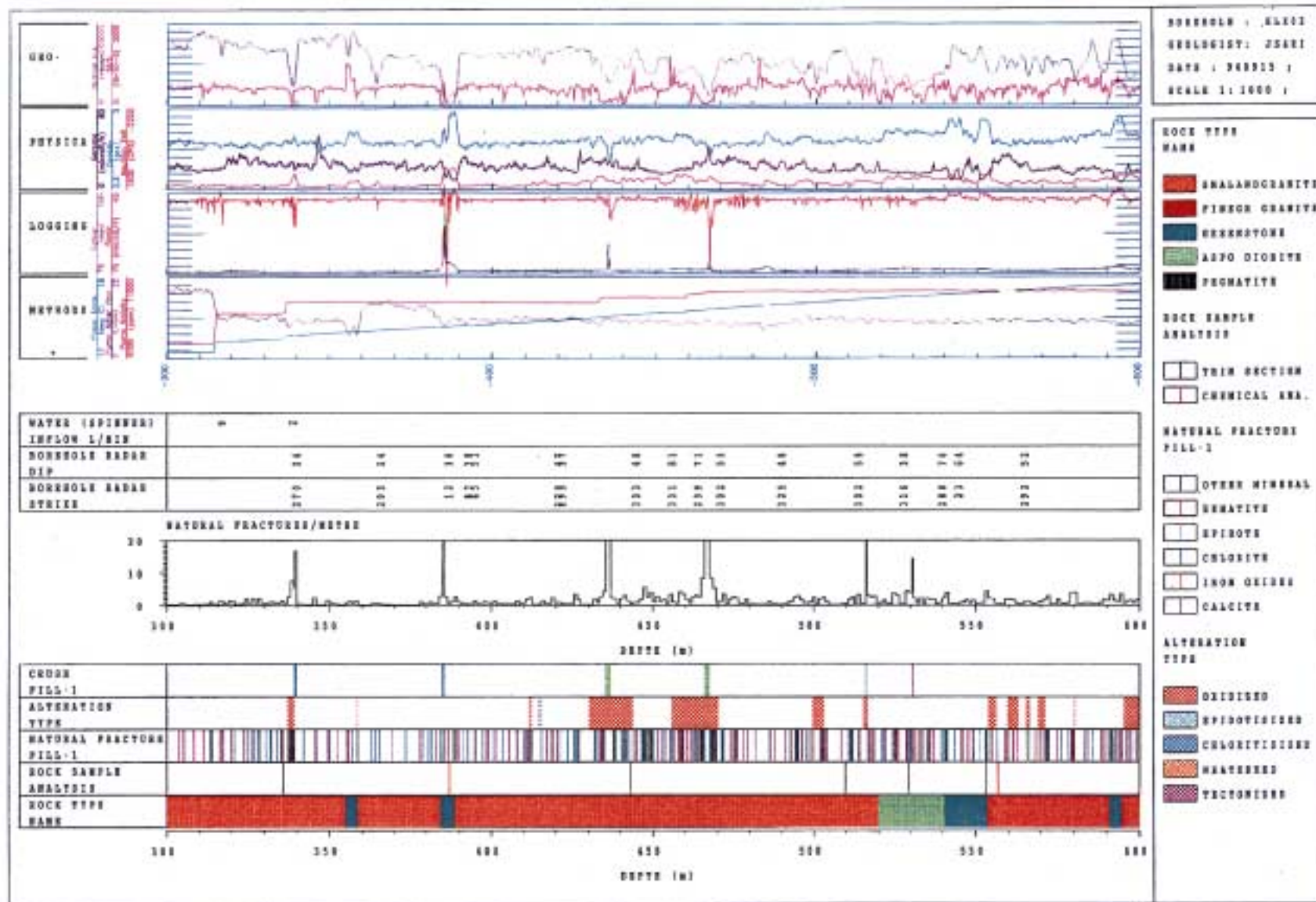


Figure A3-2. Section 300–600 m.

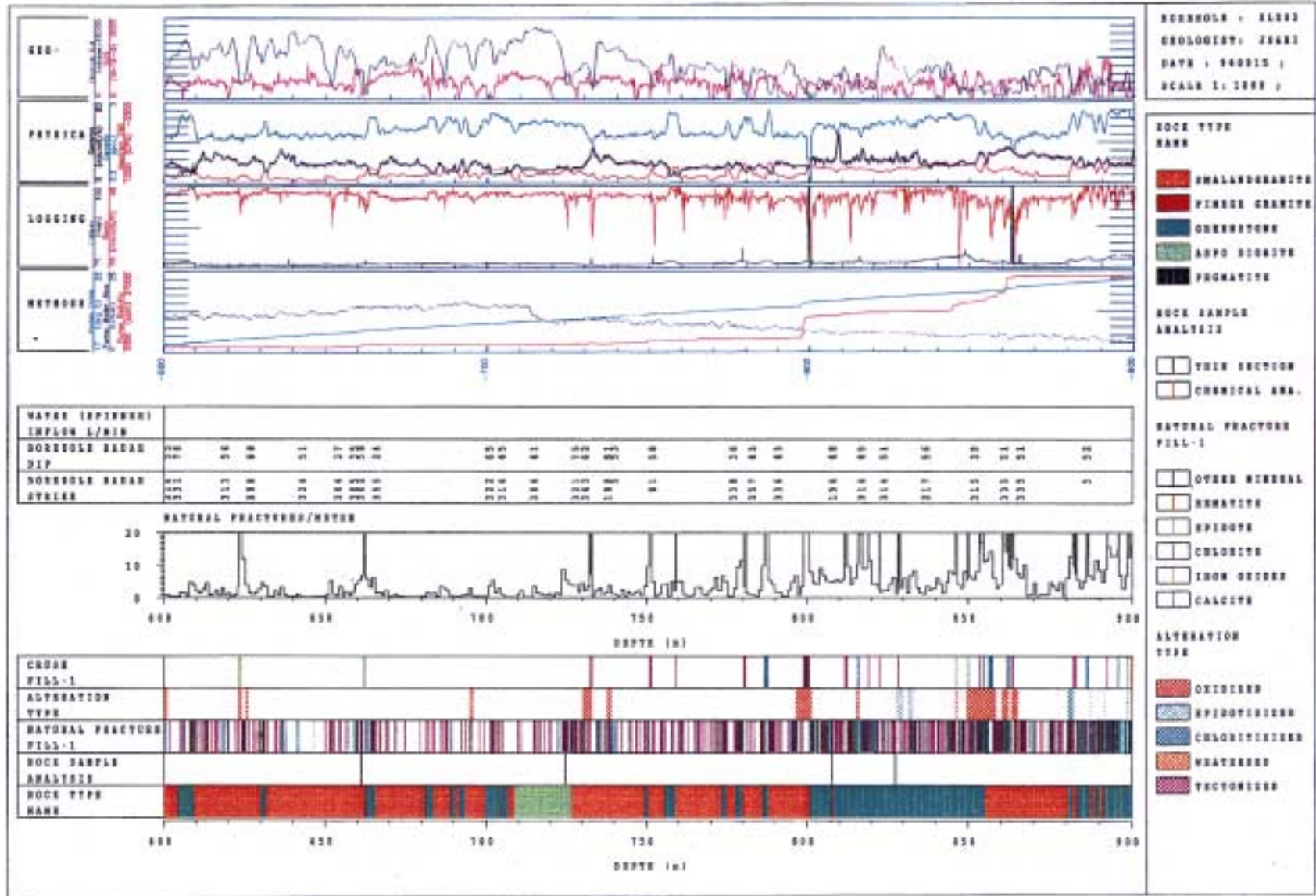


Figure A3-3. Section 600-900 m.

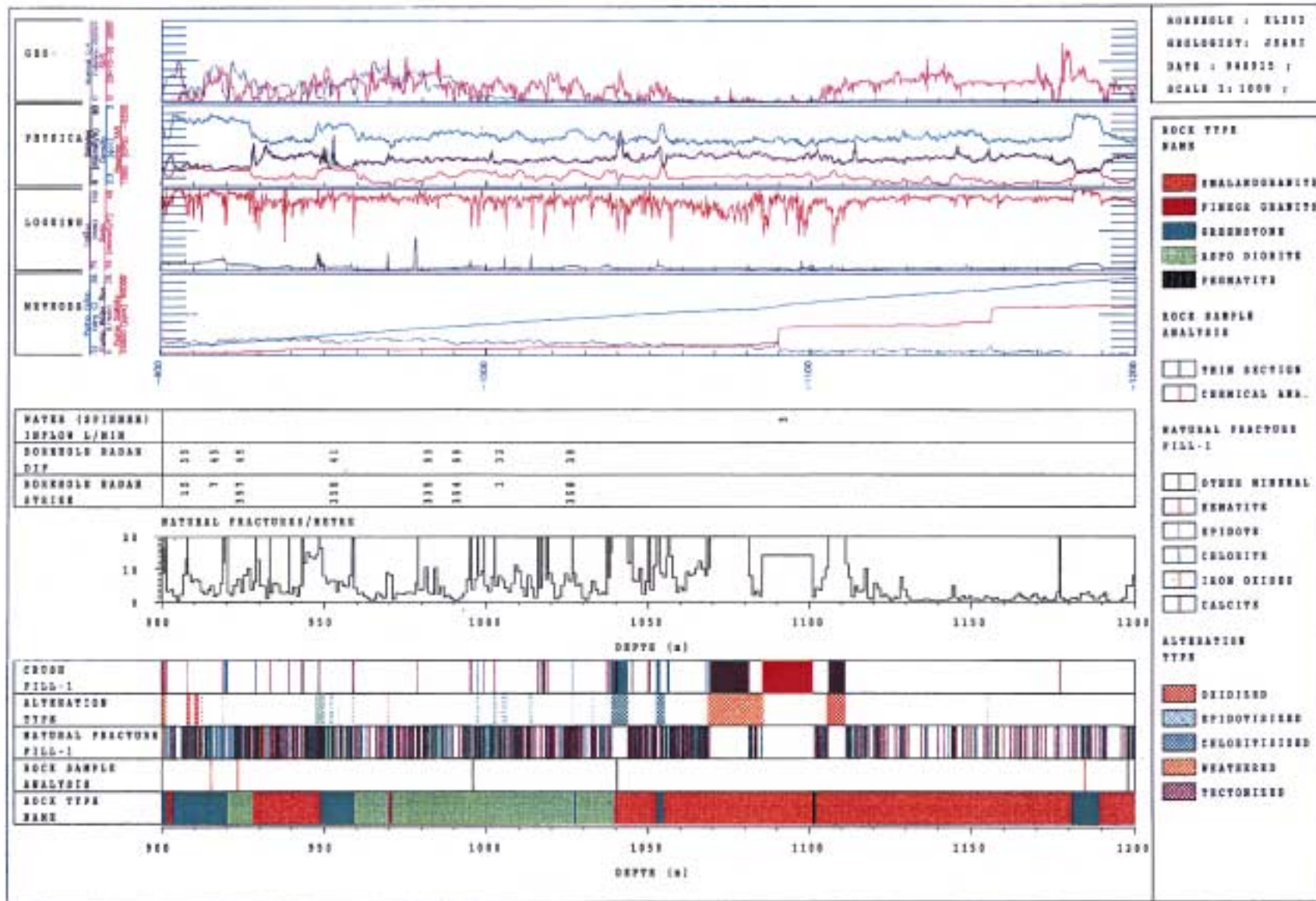


Figure A3-4. Section 900-1200 m.

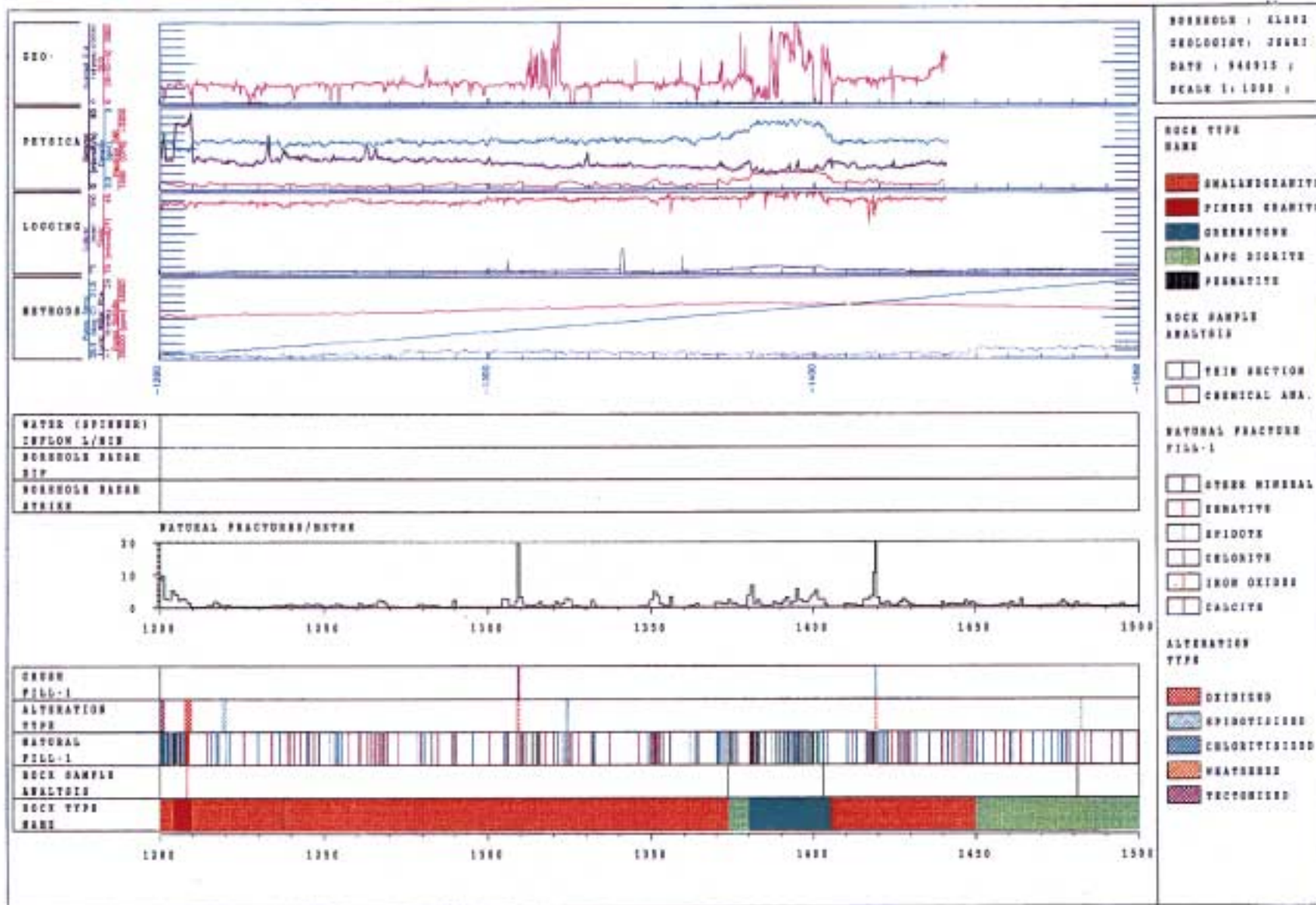


Figure A3-5. Section 1200–1500 m.

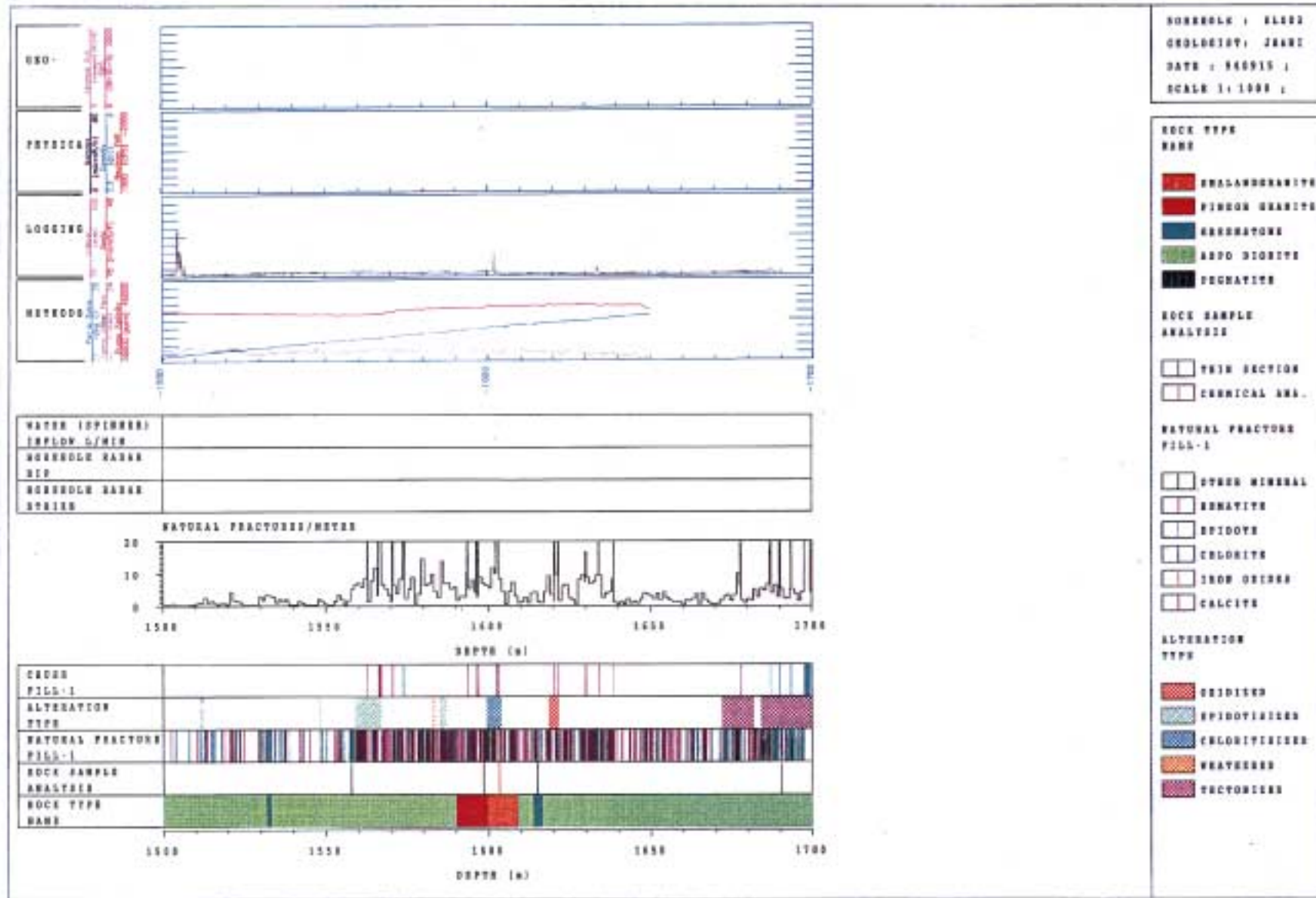


Figure A3-6. Section 1500–1700.5 m.

ISSN 1404-0344

CM Digitaltryck AB, Bromma, 2001